NOTE TO USERS

The original manuscript received by UMI contains pages with print exceeding margin guidelines. Pages were microfilmed as received.

This reproduction is the best copy available

UMI

REACTION MECHANISMS OF MAIN GROUP FLUORINATED COMPOUNDS: APPLICATION OF THE COORDINATION MODEL OF REACTION MECHANISMS

by

XIAOBO OU

A THESIS
SUBMITTED TO THE FACULTY OF GRADUATE STUDIES IN
PARTIAL FULFILLMENT OF THE REQUIREMENTS FOR THE DEGREE
OF DOCTOR OF PHILOSOPHY

DEPARTMENT OF CHEMISTRY
THE UNIVERSITY OF MANITOBA
WINNIPEG, MANITOBA

JULY 1998

National Library
of Canada

Acquisitions and
Bibliographic Services

395 Wellington Street
Ottawa ON K1A 0N4
Canada

Bibliothèque nationale
du Canada

Acquisitions et
services bibliographiques

395, rue Wellington
Ottawa ON K1A 0N4
Canada

Your file Votre référence

Our file Notre référence

The author has granted a non-exclusive licence allowing the National Library of Canada to reproduce, loan, distribute or sell copies of this thesis in microform, paper or electronic formats.

The author retains ownership of the copyright in this thesis. Neither the thesis nor substantial extracts from it may be printed or otherwise reproduced without the author's permission.

L'auteur a accordé une licence non exclusive permettant à la Bibliothèque nationale du Canada de reproduire, prêter, distribuer ou vendre des copies de cette thèse sous la forme de microfiche/film, de reproduction sur papier ou sur format électronique.

L'auteur conserve la propriété du droit d'auteur qui protège cette thèse. Ni la thèse ni des extraits substantiels de celle-ci ne doivent être imprimés ou autrement reproduits sans son autorisation.

0-612-32885-6

Canadä

THE UNIVERSITY OF MANITOBA

FACULTY OF GRADUATE STUDIES
*****
COPYRIGHT PERMISSION PAGE

REACTION MECHANISMS OF MAIN GROUP FLUORINATED COMPOUNDS: APPLICATION OF THE COORDINATION MODEL OF REACTION MECHANISMS

BY

XIAOBO OU

A Thesis/Practicum submitted to the Faculty of Graduate Studies of The University of Manitoba in partial fulfillment of the requirements of the degree

of

DOCTOR OF PHILOSOPHY

Xiaobo Ou 1997 (c)

Permission has been granted to the Library of The University of Manitoba to lend or sell copies of this thesis/practicum, to the National Library of Canada to microfilm this thesis and to lend or sell copies of the film, and to Dissertations Abstracts International to publish an abstract of this thesis/practicum.

The author reserves other publication rights, and neither this thesis/practicum nor extensive extracts from it may be printed or otherwise reproduced without the author's written permission.

ACKNOWLEDGMENTS

No words can express my appreciation to my advisor, Dr. Janzen for giving me the opportunity of working in his laboratory and for his generous support, patient guidance, continuous encouragement and insight throughout the course of this work. Other members of my advisory committee Dr. A.S. Abd-El-Aziz, Dr. J. Birchall, and Dr. R. Wallace are thanked for their help and suggestions.

I would like to thank Mr. T. Foniok and Dr. R.K. Marat for recording NMR spectra, and Mr. W. Buchannon for recording mass spectra.

I thank Dr. T. Schaefer and Mr. G. Bernard for the study of the ^{37}Cl/^{35}Cl isotope effects on ^{19}F NMR spectra of some arylsulfur halides.

To Dr. M. Sowa and Mr. R. Sebastian, I express thanks for their assistance in the use of the Gaussian programs.

Dr. R.G. Syvret (Air Products, Allentown, PA) is thanked for a sample of XeF_2.

A graduate fellowship from the University of Manitoba is very much appreciated.

Finally, I would like to thank my wife, Yun Lei, for her understanding, support and help in the progress of this work.

ABSTRACT

The Coordination Model of Reaction Mechanisms (Janzen & Jang, Can. J. Chem. 67, 71, 1989) is a topological description of the connectivity of atoms in multi-step reaction pathways which utilises directed graphs P(X,C) in which the vertex set X consists of reactants, intermediates and products, and the edge set C consists of coordination number operators +C, -C, $+C^c$ and $-C^c$. This Model provides a unified description of reaction mechanisms, and it has been tested and applied successfully in the following areas:

1. Kinetic simulations of pathways P(X,C) and comparison of the results with extensive experimental data that are available for the reaction of boron trifluoride with Lewis bases. The mechanism of reaction of boron trifluoride with amines, dialkyl ethers, and pyridine has been analyzed on the basis of the Coordination Model of Reaction Mechanisms. This model is tested mathematically by carrying out kinetic simulation of pathways P(X,C), accompanied by the calculation of structures of postulated intermediates by GAUSSIAN92 or GAUSSIAN86 methods. Analyses of reaction mechanisms, including calculation of concentration vs. time curves are carried out for the following systems: $NH_3:BF_3$, $MeNH_2:BF_3$, Me_2O-Et_2O-BF_3, Me_2O-$Et_2O:BF_3$, pyridine:BF_3, pyridine-Me_3N-BF_3, F_3B:N-N:BF_3, and (N-N)BF_2^+.

2. Molecular orbital study of silicon-fluorine and silicon-carbon bond cleavage in organofluorosilicates. The mechanism of silicon-fluorine and silicon-carbon bond cleavage in organofluorosilanes and -silicates with four-, five-, and six-coordinate silicon species is analysed with the aid of molecular orbital calculations. The optimised geometries of reactants and intermediates are calculated, and these calculations support the view that cleavage of Si-F bonds occurs by way of fluorine-bridged Si--F--Si intermediates (intermolecular). Cleavage of a Si-C bond in $PhSiF_3$ is catalysed by fluoride ion, and the calculations are in agreement with the formation of $PhSiF_4^-$ and $PhSiF_5^{2-}$, followed by oxidation to a radical anion $PhSiF_5^{-\cdot}$. The latter species, however, is predicted to decompose rapidly to give anionic SiF_5^- and phenyl radicals. These

calculations and the proposed mechanisms of bond cleavage are in agreement with experimental data, where available.

Reaction mechanisms of phosphorus fluorides are also analysed on the basis of the Coordination Model of Reaction Mechanisms. Some of the intermediates and mechanistic details arising out of such an analysis have been investigated by *ab initio* molecular orbital calculations. The rapid equilibrium between five- and six-coordinate phosphorus fluorides, and exchange of axial and equatorial fluorines in PF_5, is investigated by calculating the structures of adducts of phosphorus pentafluoride, i.e. D-PF_5 where D = NH_3, H_2O, CH_3F, HF, PF_5 and PF_6^-. Bond cleavage in phosphorus fluorides is investigated by calculating the structure of a fluorine-bridged anion $P_2F_{11}^-$. A reaction pathway is proposed for the fluoride-catalysed oxidation of phosphorus(III) to phosphorus(V) fluorides which involves the known species PF_3, PF_4^-, $PF_4\cdot$ and PF_5.

3. Oxidative fluorination of diphenyl sulfoxide and fluorine exchange in the $Ph_2S(O)F_2$-$Ph_2S(O)F^+$ system. Oxidative fluorination of diphenyl sulfoxide with xenon difluoride occurs under mild conditions in the presence of a catalytic amount of chloride ion to give $Ph_2S(O)F_2$ in essentially quantitative yield. Chloride ion appears to react with xenon difluoride to generate fluoride ion, and a mechanism of oxidative-fluorination of diaryl/diphenyl sulfoxide is proposed which involves $Ph_2S(O)F^-$ and $Ph_2S(O)F^\cdot$ intermediates. Addition of BF_3 to $Ph_2S(O)F_2$ produced the cation $Ph_2S(O)F^+$ in essentially quantitative yield. Addition of cationic $Ph_2S(O)F^+$ to $Ph_2S(O)F_2$ initiates rapid fluorine exchange, and this exchange process has been studied by ^{13}C and variable temperature ^{19}F NMR spectroscopy. In the presence of chloride ion, $Ph_2S(O)Cl_2$ is formed and can be identified by ^{13}C NMR and by its hydrolysis to Ph_2SO_2. Mechanisms are proposed for these reactions, and *ab initio* molecular orbital calculations (GAUSSIAN92) were carried out for some of the postulated intermediates.

4. Oxidative addition and isomerization reactions as illustrated by the synthesis of *cis*- and *trans*-$ArSF_4Cl$ (Ar=Ph, *p*-MeC_6H_4, *p*-$O_2NC_6H_4$) and *cis*- and *trans*-$PhTeF_4Cl$. The stereoselective synthesis and isomerization of *cis*- and *trans*-$ArSF_4Cl$ (Ar=Ph, *p*-MeC_6H_4, *p*-$O_2NC_6H_4$) is described, and this method has also been extended to the synthesis of *cis*- and *trans*-$PhTeF_4Cl$. The oxidative-fluorinating agent is a mixture of

xenon difluoride and chloride ion, and suitable sulfur reactants are Ar_2S_2 or $ArSF_3$, and Ph_2Te_2. Products were characterised by ^{19}F, ^{13}C, and ^{125}Te NMR spectroscopy, and by the $^{37}Cl/^{35}Cl$ and $^{34}S/^{32}S$ isotope effects on ^{19}F NMR chemical shifts. A mechanism of oxidative-halogenation is proposed to account for the stereoselective synthesis of *cis*- and *trans*-$ArSF_4Cl$. *Ab initio* calculations of optimised geometries of anionic and radical intermediates, *i.e.*, $PhSF_3FX^-$ and $PhSF_3X^{\cdot}$ (X=F, Cl), were carried out with the aid of the GAUSSIAN92 program.

5. Syntheses and isomerizations of *cis*- and *trans*-Ph_2SF_4, and syntheses of $PhEF_5$ (E=S, Se, Te). The synthesis and isomerization of *cis*-Ph_2SF_4 and *trans*-Ph_2SF_4 has been investigated, and the results are comparable to the synthesis of *cis*- and *trans*-Ph_2TeF_4. The catalytic syntheses of $PhSeF_5$ and $PhTeF_5$ are also described. Reaction conditions and the mechanism of oxidative-fluorination of sulfur(IV) to sulfur(VI) and isomerization of *cis* to *trans* isomers of six-coordinate sulfur compounds are discussed.

TABLE OF CONTENTS

Page

ACKNOWLEDGEMENTS....i

ABSTRACT....ii

LIST OF TABLES....ix

LIST OF FIGURES....xi

LIST OF SCHEMES....xvi

ABBREVIATIONS....xviii

GENERATION INTRODUCTION....xix

CHAPTER 1

KINETIC SIMULATIONS

1.1 Introduction....1

  1.1.1 Coordination model of reaction mechanisms....1

  1.1.2 Chemistry of Lewis acid and base reactions....4

1.2 Methods....5

1.3 Results and discussion....6

  1.3.1 The NH_3-BF_3 and $MeNH_2$-BF_3 system....6

  1.3.2 The Me_2O-Et_2O-BF_3 system....14

  1.3.3 The Me_2O and Et_2O:BF_3 system....17

  1.3.4 The Pyridine-BF_3 system....18

  1.3.5 The $(R_3N)(Py)BF_2^+$ cation and the order of addition of base....23

  1.3.6 The (N-N)BF_2^+ cation and n-centre steps....28

1.4 Conclusions....32

CHAPTER 2

REACTION MECHANISMS OF SILICON AND PHOSPHORUS FLUORIDES: *AB INITIO* MOLECULAR ORBITAL STUDIES

2.1 Silicon-fluorine and silicon-carbon bond cleavage in organofluorosilicates............34
  2.1.1 Introduction..34
  2.1.2 Molecular orbital calculation method...................................40
  2.1.3 Results and discussion..41
    2.1.3.1 Silicon-fluorine bond cleavage.....................................41
    2.1.3.2 Silicon-carbon bond cleavage.......................................51
  2.1.4 Conclusions...55

2.2 Reaction mechanisms of phosphorus fluorides...56
  2.2.1 Introduction..56
  2.2.2 Results and discussion..56
  2.2.3 Methods...64

CHAPTER 3

OXIDATIVE HALOGENATION OF SULFUR(I, II, AND IV) TO SULFUR(VI) COMPOUNDS

3.1 Introduction...66
  3.1.1 Oxidative halogenation of sulfur(I, II, IV) compounds to sulfur(VI) compounds...66
    3.1.1.1 Cobalt trifluoride, CoF_3..68
    3.1.1.2 Electrochemical fluorination.......................................68
    3.1.1.3 Silver difluoride, AgF_2...69
    3.1.1.4 Cesium fluoride and chlorine, CsF/Cl_2...........................70
    3.1.1.5 Trifluoromethyl hypofluorite, CF_3OF.............................71
    3.1.1.6 Chlorine monofluoride, ClF...72
    3.1.1.7 Elemental fluorine, F_2..73

3.1.1.8 Bromine trifluoride, BrF_3 75

3.1.2 Objective 76

3.2 Experimental 77

3.2.1 General remarks 77

3.2.1.1 Solvents and reagents 77

3.2.1.2 Instrumental 78

3.2.2 Experimental details 79

3.2.2.1 Preparation of diphenylsulfur difluoride oxide and fluorine exchange in the $Ph_2S(O)F_2$-$Ph_2S(O)F^+$ system 79

3.2.2.1.1 Preparation of $Ph_2S(O)F_2$ 79

3.2.2.1.2 Preparation of $Ph_2S(O)F^+BF_4^-$ 81

3.2.2.1.3 Fluorine exchange in the $Ph_2S(O)F_2$-$Ph_2S(O)F^+$ system 82

3.2.2.1.4 The $Ph_2S(O)F_2$ and Ph_2SO system 83

3.2.2.1.5 The $Ph_2S(O)F^+$ and Ph_2SO system 83

3.2.2.1.6 Preparation of $Ph_2S(O)Cl_2$ 83

3.2.2.1.7 Reaction of $Ph_2S(O)F_2$ with water 84

3.2.2.1.8 Reaction of $Ph_2S(O)F_2$ with aqueous HF 84

3.2.2.1.9 Reaction with the H_2O-HF-glass system 85

3.2.2.1.10 Reaction of $Ph_2S(O)F_2$ with alcohols 86

3.2.2.2 Preparation of phenyl chalcogen(VI) fluorides 86

3.2.2.2.1 Preparation of *cis*- and *trans*-Ph_2SF_4 86

3.2.2.2.2 Attempted preparation of Ph_2SeF_4 87

3.2.2.2.3 Preparation of $PhSF_5$ 88

3.2.2.2.4 Preparation of $PhSeF_5$ 88

3.2.2.2.5 Preparation of $PhTeF_5$ 90

3.2.2.2.6 Attempted preparation of Cl_2SF_4 91

3.2.2.3 Preparation of alkyl and aryl sulfur(IV) fluorides 91

3.2.2.3.1 Preparation of arylsulfur trifluoride $ArSF_3$ (Ar = Ph, *p*-MeC_6H_4, *p*-$O_2NC_6H_4$) 91

3.2.2.3.2 Preparation of Me_3CSF_3....................................93

3.2.2.3.3 Preparation of dibenzodifluorothiophene (oxidative fluorination of dibenzothiophene) 94

3.2.2.4 Preparation of aryltetrafluorosulfur(VI) chloride........................94

3.2.2.4.1 Preparation of *trans*-$ArSF_4Cl$ (Ar = Ph, *p*-MeC_6H_4, *p*-$O_2NC_6H_4$) 94

3.2.2.4.2 Preparation of *cis*-$ArSF_4Cl$.................................95

3.2.2.4.3 Preparation of *cis*- and *trans*-$PhTeF_4Cl$..................96

3.2.2.4.4 Reaction of $ArSF_4Cl$ with BF_3.............................97

3.2.2.4.5 Isomerization of *trans*-$PhSF_4Cl$ to *cis*-$PhSF_4Cl$.........97

3.2.2.4.6 Attempted isomerization of *cis*-$ArSF_4Cl$ to *trans*-$ArSF_4Cl$..99

3.2.2.4.7 $^{37}Cl/^{35}Cl$ isotope shifts on the ^{19}F NMR spectrum of *trans*-$ArSF_4Cl$..99

3.2.2.4.8 Reaction of $ArSF_4Cl$ with water...........................99

3.2.2.5 Reaction of XeF_2 with Et_4NCl..100

3.2.2.5.1 Reaction of XeF_2 with Et_4NCl in CD_2Cl_2 and CH_2Cl_2.100

3.2.2.5.2 Chlorination of 1,1-diphenylethene and cyclohexene...100

3.2.2.6 Molecular orbital calculations..101

3.3 Results and discussion..102

3.3.1 Oxidative fluorination by xenon difluoride in the presence of Et_4NCl.......102

3.3.2 Preparation of phenylfluorosulfur(VI) oxides 103

3.3.2.1 Oxidative fluorination of diphenyl sulfoxide..........................103

3.3.2.2 Proposed mechanism of oxidative-fluorination of diphenyl sulfoxide..111

3.3.2.2.1 Reaction of XeF_2 with Et_4NCl............................111

3.3.2.2.2 Proposed mechanism of oxidative-fluorination of diphenyl sulfoxide..115

3.3.2.2.3 Intermediates and molecular orbital calculations........119

3.3.2.3 Synthesis of diphenylsulfur(VI) cation, $Ph_2S(O)F^+$..................122

3.3.2.4 Fluorine exchange in the $Ph_2S(O)F_2$-$Ph_2S(O)F^+$ system and preparation of diphenyldichlorosulfur(VI) oxide 125
3.3.2.4.1 Fluorine exchange in the $Ph_2S(O)F_2$-$Ph_2S(O)F^+$ system 125
3.3.2.4.2 Preparation of diphenyldichlorosulfur(VI) oxide 135
3.3.2.5 ^{13}C NMR study of phenyl derivatives of B, Si, Sn, P, Te and S fluorides 141
3.3.2.6 $Ph_2S(O)F_2$ and the H_2O-HF-glass system 145
3.3.2.7 Reaction of $Ph_2S(O)F_2$ with alcohols 150
3.3.3 Preparation of phenylchalogen (VI) fluorides 152
3.3.3.1 Synthesis of Ph_2SF_4 152
3.3.3.2 Synthesis of $PhEF_5$ (E=S, Se, Te) 155
3.3.3.3 Proposed mechanism of oxidative-fluorination of diphenylsulfur difluoride 161
3.3.3.3.1 The intermediate diphenylsulfur(IV) trifluoride anion $Ph_2SF_3^-$ 162
3.3.3.3.2 The intermediate diphenylsulfur(V) trifluoride radical $Ph_2SF_3^{\cdot}$ 166
3.3.3.4 Proposed mechanism of isomerization of *cis*- Ph_2SF_4 and *trans*-Ph_2SF_4 170
3.3.4 Stereoselective synthesis and isomerization of *cis*- and *trans*-aryltetrafluorosulfur(VI) chloride, $ArSF_4Cl$ (Ar=Ph, *p*-MeC_6H_4, *p*-$O_2NC_6H_4$) 173
3.3.4.1 Synthesis of *cis*- and *trans*-$ArSF_4Cl$ (Ar=Ph, *p*-MeC_6H_4, *p*-$O_2NC_6H_4$) 175
3.3.4.2 Empirical correlations of NMR parameters of *cis*- and *trans*-$ArSF_4Cl$ 192
3.3.4.3 $^{37}Cl/^{35}Cl$ isotope shifts on the ^{19}F NMR spectrum of *trans*-$ArSF_4Cl$ 198
3.3.4.4 Synthesis of *cis*- and *trans*-$PhTeF_4Cl$, and $PhTeF_3Cl_2$ 201

3.3.4.5 Proposed mechanism of oxidative-halogenations.....205

3.3.4.6 *Ab initio* calculations.....209

3.3.5 Preparation of alkyl and arylchalcogen(IV) trifluorides.....212

GENERAL CONCLUSIONS.....218

REFERENCES.....221

VITA.....xxv

LIST OF TABLES

Page

1. Bond enthalpies required for calculation of rate constants................................10
2. Comparison of calculated and experimental equilibrium concentrations for the Me_2O-Et_2O-BF_3 system...15
3. Experimental and calculated Si-F bond lengths (pm), and average lengthening of bonds (%) relative to SiF_4...45
4. Experimental and calculated Si--F--Si bridging bond lengths (pm), and lengthening of bridging bond (%) relative to SiF_4...49
5. Experimental and calculated Si-C bridging bond lengths (pm), and lengthening of bridging bond (%) relative to $PhSiF_3$..53
6. ^{19}F and ^{13}C NMR chemical shifts (ppm) and C-F coupling constants (Hz) of some diphenylsulfur halides...140
7. ^{13}C NMR chemical shifts (ppm) and C-F coupling constants (in Hz, in parenthesis) of some phenyl derivatives of B, C, Si, P, Te, and S fluorides..........................143
8. ^{13}C and ^{19}F NMR data of fluorinated products of the reaction of $Ph_2S(O)F_2$ with alcohols 151
9. ^{19}F NMR data for $ClEF_5$ and $PhEF_5$ (E=S, Se, Te) 160
10. ^{13}C NMR data of *cis*- and *trans*-$ArSF_4Cl$ in CD_2Cl_2....................................181
11. Experimental conditions for the synthesis of *cis*- and *trans*-$ArSF_4Cl$ at 25 °C in CD_2Cl_2 and CD_3CN...183
12. ^{19}F NMR data of $ArSOF_3$ in CD_2Cl_2 or CD_3CN...191
13. ^{19}F NMR data of *cis*- and *trans*-$ArSF_4Cl$ in CD_2Cl_2 and chemical shifts calculated by the method of Dean and Evans...193
14. ^{19}F NMR chemical shift of *trans*-$ArSF_4Cl$ and chlorine $^{37}Cl/^{35}Cl$ and sulfur $^{34}S/^{32}S$ isotope effects...200
15. ^{19}F NMR data of $PhTeF_3Cl_2$ in CD_3CN...203
16. ^{19}F NMR data of some alkyl and arylsulfur(IV) fluorides................................217

LIST OF FIGURES

Page

1 Graphic representation of a pathway P(4,2) for the reaction of silicon tetrafluoride with bipyridine to give SiF_4(bipy)..3

2 Calculated Conc. vs. Time curves for the 1:1 reaction of BF_3 with NH_3. Input rate constants are given in eq. [2]-[4]. The concentration of $H_3N:BF_3$ after $1x10^{-8}$ s is 0.72 M..11

3. Calculated Conc. vs. Time curves for the 1:1 reaction of BF_3 with $MeNH_2$. Input rate constants are given in eq. [5]-[7]. The concentration of $MeNH_2:BF_3$ after $1x10^{-8}$ s is 0.84 M..12

4. Calculated Conc. vs. Time curves for the reaction of BF_3 with Me_2O and Et_2O. Input rate constants are given in eq. [8]-[9]..16

5. Graphic representation of a pathway P(9,4) for the proposed mechanism of reaction of pyridine with boron trifluoride..19

6. GAUSSIAN86 calculation of $H_3N:BF_2$--F--BF_3 and py:BF_2--F--BF_3 at 3-21G* level with full optimisation, except for fixed geometry of pyridine..21

7. Calculated Conc. vs. Time curves for the 1:1.5 reaction of pyridine with BF_3. Input rate constants are given in eq. [12]-[15]. The concentration of $py_2BF_2^+$ after $6x10^{-8}$ s is 0.0085 M..22

8. Calculated Log(Conc.) vs. Time curves for the 1:1 reaction of Me_3N with Py:BF_3. Input rate constants are given in eq. [16]-[20]. The concentration of (py)(Me_3N)BF_2^+ after $1x10^{-6}$ s is $2.7x10^{-16}$ M..25

9. Calculated Log(Conc.) vs. Time curves for the 1:1 reaction of pyridine with $Me_3N:BF_3$. Input rate constants are given in eq. [21]-[25]. The concentration of (py)(Me_3N)BF_2^+ after $1x10^{-6}$ s is $2.7x10^{-20}$ M..27

10. Graphic representation of a pathway P(10,5) for a suggested mechanism of reaction of BF_3 with a bidentate ligand N-N..29

11. Calculated Conc. vs. Time curves for the 2:1 reaction of BF_3 with bidentate ligand, N-N. Input rate constants are given in eq. [26]-[30]. The concentration of F_3B:N-N:BF_3 and (N-N)BF_2^+ after $1.2x10^{-8}$ s is 0.73M and 0.01 M, respectively.....31

12. Structure of $PhSiF_5^{2-}$ 36
13. Optimised (left, 6-31+G*) and experimental (right, Doppler-limited tunable diode laser spectrum) geometry for SiF_4 42
14. Optimised (left, 6-31+G*) and experimental (right, x-ray crystallography method) geometry for SiF_5^- 42
15. Optimised (left, 6-31+G*) and experimental (right, single crystal neutron diffraction method) geometry for SiF_6^{2-} 42
16. Optimised (left, 6-31G*) and experimental (right, electron diffraction method) geometry for $PhSiF_3$ 43
17. Optimised (left, 6-31G* with geometry of phenyl ring relaxed) and experimental (right, x-ray crystallography method) geometry for $PhSiF_4^-$ 43
18. Optimised (6-31G*) geometry for $PhSiF_5^{2-}$ 43
19. Optimised (6-31+G*) geometry for $\{PhSiF_5^{\cdot-}\}$ showing that $\{PhSiF_5^{\cdot-}\}$ consists essentially of a phenyl radical and SiF_5^- anion 44
20. Optimised (6-31G*) geometry for $F_4Si\text{--}F\text{--}SiF_4^-$ 46
21. Optimised (6-31G*) geometry for $MeF_3Si\text{--}F\text{--}SiF_3Me^-$ 47
22. Optimised (6-31G*) geometry for $F_5Si\text{--}F\text{--}SiF_5^{3-}$ 47
23. Optimised (6-31G*) geometry for $C_2H_2(SiMeF_2)_2F^-$ 47
24. Optimised (3-21G*) geometry for $o\text{-}C_6H_4(SiMeF_2)_2F^-$ 48
25. Experimental geometry for $o\text{-}C_6H_4(SiMeF_2)_2F^-$ 48
26. Optimised geometry for $MeSiF_5^{2-}\text{-}H_2O$ 54
27. ^{13}C NMR spectrum of reaction products of Ph_2SO with XeF_2 in the absence of catalyst. The spectrum was recorded after a two day reaction time. Integration shows only ~1/3 of Ph_2SO was converted to $Ph_2S(O)F_2$ 105
28. ^{13}C NMR spectrum of $Ph_2S(O)F_2$ 108
29. ^{19}F NMR spectrum of $Ph_2S(O)F_2$ 109
30. ^{1}H NMR spectrum of the reaction of Ph_2CCH_2 with Cl_2 113
31. ^{19}F NMR spectrum of the reaction products of Et_4NCl with XeF_2 114
32. Calculated geometries of some anionic and radical species 120
33. Experimental structural data of compound **19-21** 121

34. ^{19}F NMR spectrum of $Ph_2S(O)F^+BF_4^-$ in CD_2Cl_2.......................................123

35. ^{13}C NMR spectrum of $Ph_2S(O)F^+BF_4^-$ in CD_2Cl_2.......................................124

36. ^{19}F NMR spectrum of a 3:1 mixture of $Ph_2S(O)F_2$ and $Ph_2S(O)F^+BF_4^-$ in CD_2Cl_2 at room temperature...128

37. ^{13}C NMR spectrum of a 3:1 mixture of $Ph_2S(O)F_2$ and $Ph_2S(O)F^+BF_4^-$ in CD_2Cl_2 at room temperature.../...........129

38. ^{19}F NMR spectrum of a 6:1 mixture of $Ph_2S(O)F_2$ and $Ph_2S(O)F^+BF_4^-$ in CD_2Cl_2 at room temperature...130

39. ^{13}C NMR spectrum of a 6:1 mixture of $Ph_2S(O)F_2$ and $Ph_2S(O)F^+BF_4^-$ in CD_2Cl_2 at room temperature...131

40. Variable-temperature ^{19}F NMR spectrum of a 3:1 mixture of $Ph_2S(O)F_2$ and $Ph_2S(O)F^+BF_4^-$ in CD_2Cl_2 at room temperature......................................133

41. Variable-temperature ^{19}F NMR spectrum of a 6:1 mixture of $Ph_2S(O)F_2$ and $Ph_2S(O)F^+BF_4^-$ in CD_2Cl_2 at room temperature......................................134

42. Calculated and experimental structures for bridged S--F--S compounds..............135

43. (a) The ^{13}C NMR spectrum of a 45:55 (0.297 mmol in total) mixture of $Ph_2S(O)F^+$ and $Ph_2S(O)F_2$ in a ptfe-lined NMR tube in CD_2Cl_2 solution. (b) The same sample after addition of 18 mg (0.12 mmol) of Et_4NCl, showing that all species in solution are undergoing rapid halogen exchange. (c) The ^{13}C NMR spectrum after addition of another 50 mg (0.32 mmol) of Et_4NCl to b, showing that halogen exchange is stopped. Eight carbon peaks expected for a mixture of "rigid" $Ph_2S(O)Cl_2$ and $Ph_2S(O)F_2$ are observed. The C1-C4 peaks of the hydrolysis product Ph_2SO_2 are marked with an asterisk...137

44. Distribution of ^{13}C NMR chemical shifts of the $Ph_2S(O)F^+$ and $Ph_2S(O)F_2$ system. The 45:55 mixture of $Ph_2S(O)F^+$-$Ph_2S(O)F_2$ was prepared by adding BF_3 to a solution of $Ph_2S(O)F_2$ in CD_2Cl_2...144

45. (a)The ^{13}C NMR spectrum of $Ph_2S(O)F_2$ (0.297 mmol) in a ptfe-lined NMR tube in CD_2Cl_2 solution. The expanded C1 region shows a triplet due to C-S-F coupling. (b) The same sample after addition of a dry capillary of borosilicate glass. This spectrum was recorded after 18 hr. The expanded C1 region shows a triplet due

to C1-S-F coupling, $^2J(CSF) = 17.1$ Hz, which is identical to that in a. (c) The ^{13}C NMR spectrum after addition of a wetted capillary of borosilicate glass to b, showing loss of C1-S-F (and C2-S-F) coupling, and changes in the chemical shifts of C1-C4 peaks. The C1-C4 peaks of the hydrolysis product Ph_2SO_2 are marked with an asterisk....................147
46. Comparison of the ^{13}C NMR spectra of $Ph_2S(O)F^+$ and $Ph_2S(O)F_2$ with that of the 4:96 mixture of $Ph_2S(O)F^+$ and $Ph_2S(O)F_2$ of Figure 45c....................148
47. ^{19}F NMR spectrum of *cis*- and *trans*-Ph_2SF_4 in CD_2Cl_2....................154
48. ^{19}F NMR spectrum of $PhTeF_5$ in CD_3CN....................156
49. ^{19}F NMR spectrum of $PhSF_5$ in CD_3CN....................158
50. ^{19}F NMR spectrum of $PhSeF_5$ in CD_3CN....................159
51. Three possible isomeric structures of sulfur(IV) anion $Ph_2SF_3^-$....................162
52. Optimised geometries for three possible structure of $Ph_2SF_3^-$....................164
53. Three possible structures of sulfur(V) radical $Ph_2SF_3^{\cdot}$....................167
54. Optimised geometries for three possible structures of $Ph_2SF_3^{\cdot}$....................169
55. Optimised geometries for two possible structures of $Ph_2SF_3^+$....................172
56. Two geometrical isomers of RSF_4Cl....................173
57. ^{19}F NMR spectrum of *cis*-$ArSF_4Cl$ (Ar=*p*-MeC_6H_4) in CD_2Cl_2 showing an AB_2C spin system....................177
58. ^{13}C NMR spectrum of *cis*-$ArSF_4Cl$ (Ar = Ph) in CD_2Cl_2 showing an AB_2CX spin system....................178
59. ^{19}F NMR spectrum of *trans*-$ArSF_4Cl$ (Ar = *p*-$O_2NC_6H_4$) in CD_3CN showing an A_4 spin system....................179
60. ^{13}C NMR spectrum of *trans*-$ArSF_4Cl$ (Ar = *p*-$O_2NC_6H_4$) in CD_2Cl_2 showing an A_4X spin system....................180
61. ^{19}F NMR spectrum of a mixture of *trans*- and *cis*-$PhSF_4Cl$ on standing after Et_4NCl was added; (a) original 2:1 mixture; (b) after 16 hrs; (c) after 64 hrs; (d) after 5 days; (e) after more than two weeks....................188
62. ^{19}F NMR spectrum of *p*-$MeC_6H_4S(O)F_3$....................190
63. Two geometrical isomers of RSF_4Cl....................192

64. Structure of $PhSF_5$....................193
65. Structure of $ClSF_5$....................194
66. Structure of *cis*- and *trans*-$PhSF_4Cl$....................194
67. ^{19}F NMR spectrum at 282.363 MHz of the *trans*-$ArSF_4Cl$ in CD_3CN....................199
68. Two possible structures of $PhTeF_4Cl$....................201
69. Three possible structures of $PhTeF_3Cl_2$ with mer and fac arrangement of three fluorine substituents, and cis and trans arrangement with respect to two chlorine substituents....................201
70. ^{19}F NMR spectrum of *cis* and *trans*-$PhTeF_4Cl$ in CD_3CN....................204
71. Calculated structures of anionic and radical of some sulfur fluorides....................211
72. ^{13}C NMR spectrum of reaction product of Ph_2S_2 with XeF_2 in the absence of catalyst, Et_4NCl....................214
73. ^{13}C NMR spectrum of reaction product of Ph_2S_2 with XeF_2 in the presence of catalyst, Et_4NCl....................215
74. ^{19}F NMR spectrum of Me_3CSF_3....................216

LIST OF SCHEMES

Page

1. Proposed mechanism for the cleavage of Si-F bonds in typical fluorosilicates such as $RSiF_4^-$ and $RSiF_5^{2-}$......38
2. Proposed mechanism of fluoride-catalysed cleavage of Si-C bonds......39
3. Proposed mechanism of oxidation of P(III) to P(V) fluorides in the presence of F^-...63
4. Preparation of both *trans*- and *cis*-difluorodialkyloxy diaryl sulfur (VI) isomers by oxidatively fluorinating its corresponding stable sulfurane......75
5. Atom numbering for $Ph_2S(O)F_2$ and Ph_2SOF^+......107
6. Proposed mechanism of oxidative fluorination of Ph_2SO by XeF_2 in the presence of fluoride ion......116
7. Fluoro anions as single electron donors......117
8. Proposed mechanism of fluorine exchange in the $Ph_2S(O)F_2$-$Ph_2S(O)F^+$ system....126
9. Proposed mechanism of formation of $Ph_2S(O)Cl_2$......136
10. Atom numbering for phenyl-element fluorides......142
11. Proposed mechanism of oxidative fluorination of diphenylsulfur difluoride.........162
12. Proposed mechanism of formation of *trans*-Ph_2SF_4......170
13. Proposed mechanism of formation of *trans*-$ArSF_4Cl$ and $ArSF_5$......206

ABBREVIATIONS

N-N	Bidentate nitrogen ligand
ax	Axial substituents
eq	Equatorial substituents
TCNE	Tetracyanoethylene
NBS	*N*-bromosuccinimide
TMS	Tetramethylsilane
TBP	Trigonal bipyramid
RP	Rectangular pyramid
N-E-L	Valence electron count and cooridination number of E. For example, silicon in SiF_4 can be designed as 8-Si-4.
mer	meridian
fac	facial
d	doublet
s	singlet
t	triplet
hr	hour

GENERAL INTRODUCTION

1. The Coordination Model of Reaction Mechanisms (Janzen & Jang, Can. J. Chem. 67, 71, 1989) is a topological description of the connectivity of atoms in multi-step reaction pathways which utilises directed graphs P(X,C) in which the vertex set X consists of reactants, intermediates and products, and the edge set C consists of coordination number operators. In this model, elementary steps are described in terms of four coordination number operators: +C, -C, $+C^c$ and $-C^c$, where $+C^c$ and $-C^c$ refer to cyclic intramolecular steps, with the positive and negative signs indicating an increase or decrease in coordination number as bonds are made or broken; dashed lines refer to intermolecular steps and solid lines to intramolecular steps. This model emphasises the coordination changes of the elements during a chemical reaction. Thus it provides a unified description of reaction dynamics and it has been tested and applied successfully in this laboratory in the following areas: (1) Polytopal rearrangement reactions, e.g. mechanisms of axial-equatorial exchange in PF_5, SiF_5^- or $Fe(CO)_5$; (2) Mechanism of electron transfer reaction; (3) Stereoselective bond cleavage; (4) Mechanism of oxidation reactions; (5) 5-member rings in inorganic, organic, and biochemical systems; (6) Glass surface reaction, etc.

Until now, the Coordination Model of Reaction Mechanisms has been applied exclusive in the synthesis experiments, with emphasis on reaction dynamics and mechanisms of fluorinated compounds, we now wish to test this model mathematically by the kinetic simulation for the reaction of boron trifluoride with Lewis bases.

Lewis acid-base interactions involving boron trifluoride have been widely studied and a variety of exchange rates and mechanisms have been reported. Any mechanistic description of the BF_3-base system must accommodate the following experimental details: (a) the formation of base:BF_3 is a bimolecular process with rate constants in the range of 10^8 to 10^{10} M^{-1} s^{-1}, (b) rates of reaction of base:BF_3 are inversely proportional to gas phase enthalpies of dissociation, (c) equilibrium data for BF_3-base systems are well-established, (d) two modes of exchange in BX_3-base systems involve both halogen and base exchange, (e) excess BF_3 accelerates the rate of fluorine exchange in base:BF_3, (f) the boron cation $(amine)_2BF_2^+$ is an elusive species although, once formed, it is stable even in water, (g) some adducts such as HMPA:BF_3 and tetramethylurea:BF_3 are in equilibrium with the ionic species $(base)_2BF_2^+BF_4^-$, (h) the formation of mixed base adducts such as $(Me_3N)(pyridine)BF_2^+$ depends on the order of addition of base, and (i) formation of chelated boron cations with bidentate ligands $(N\text{-}N)BF_2^+$ occurs in some cases, but not in others.

The mechanisms of reaction of boron trifluoride with amines, dialkyl ethers, and pyridine provide a mathematical test of the Coordination Model, by comparing the calculated results with extensive experimental data that are available for the reactions of boron trifluoride with Lewis bases. These calculations differ from conventional kinetic simulations because all mechanisms and rate constants are based on the postulates of the Coordination Model.

2. However, reliable thermodynamic and kinetic data of reactive intermediates are not always available in all the reaction systems. In the absence of reliable thermodynamic and kinetic data of reactive intermediates, the calculated bond

lengths may serve as a simple criterion of bond cleavage, -C, and the generalisation, "the longer the bond, the faster it breaks" is therefore may applied to these reactive intermediates. This assumption is tested by analysis of reaction mechanisms of silicon-fluorine and silicon-carbon bond cleavage in organofluorosilicates, and the rapid equilibrium between five- and six-coordinate phosphorus fluorides, and the exchange of axial and equatorial fluorines in PF_5. First the reaction mechanisms are analyzed on the basis of the Coordination Model of Reaction Mechanisms, and then all of the intermediates and mechanistic details arising out of such an analysis have been investigated by *ab initio* molecular orbital calculations.

A large number of successful fundamental studies on the preparation and reaction of organopentafluorosilicates can be found in the literature, however, little attention has been paid to how carbon-silicon and fluorine-silicon bonds in organofluorosilicates are cleaved. On the other hand, the bond energies of Si-F and Si-C bonds are quite high, on the order of 565 and 318 kJ mol^{-1}, respectively, yet these bonds in organofluorosilanes and -silicates may be cleaved under mild conditions in the presence of fluoride ion as described in the previous section. We wondered why the addition of F^- to $PhSiF_3$ should, eventually, lead to cleavage of Si-C and Si-F bonds.

Trigonal bipyramidal molecules are among the most sensitive indicators of bond formation, +C, because of the change in symmetry and NMR spin pattern that accompanies the formation of six-coordinate adducts or intermediates, we studied the interaction of PF_5 with Lewis bases of widely differing basicity (eq 32b), and calculated the structures of adducts.

$$\mathrm{PF_5} + \mathrm{D} \underset{-\mathrm{C}}{\overset{+\mathrm{C}}{\rightleftharpoons}} \mathrm{D\text{-}PF_5}$$

$\mathrm{D} =$ NH_3 H_2O CH_3F
HF PF_5 PF_6^-

As a six-coordinate adduct such as $H_3N\text{-}PF_5$ is formed, the coordination number of phosphorus is increased from 5 to 6, and nitrogen from 3 to 4, i.e., $+C_{P(5)N(3)}$. Cleavage of a P-N bond in adduct $H_3N\text{-}PF_5$ is denoted as $-C_{P(5)N(3)}$. If the calculated structures confirm that four basal fluorines in all adducts above are essentially equivalent, then it is reasonable to assume that an equilibrium between five- and six-coordinate phosphorus species (see above equation), can provide a pathway for the exchange of axial and equatorial fluorines in PF_5. Our criterion for evaluating the equivalence of four basal $P\text{-}F^b$ bonds is based on a qualitative comparison of $P\text{-}F^b$ bond lengths and $\angle F^aPF^b$ bond angles. Other means of estimating the distortion from D_{3h} or C_{4v} symmetry in phosphorus or silicon fluorides have been proposed by Holmes.

3. The methods of analysis of reaction mechanisms are used in analysis of reaction mechanism of oxidative halogenation of sulfur compounds under mild conditions by the route of XeF_2/Et_4NCl.

Main group fluoride derivatives in high oxidation states are frequently obtained by oxidative fluorination of their corresponding lower valent compounds. For sulfur, these include sulfur tetrafluoride, bis(alkyl) sulfides, sulfurane, diperfluoroalkyl disulfides and substituted sulfur(IV) compounds. A variety of powerful fluorinating agents such as CoF_3, AgF_2, CsF, CF_3OF, ClF, F_2, BrF_3, XeF_2 and electrochemical fluorination have been used to accomplish the oxidative addition of fluorine to these lower valent sulfur compounds.

Oxidative fluorination of organosulfur compounds may produce cis and trans isomers of the corresponding organosulfur(VI) fluorides. Both cis and trans isomers of six-coordinate organosulfur(VI) fluorides are known. The outcome of the fluorination reaction is difficult to predict because of the mechanistic complexity of competing oxidative-addition, isomerization, and ligand exchange processes. Complexity also arises from the H_2O-HF-glass system because of the potential introduction of BF_3 or SiF_4: these strong Lewis acids are known to isomerize six-coordinate S(VI) and Te(VI) fluorides via cationic intermediates. Simple generalizations about the mechanisms of oxidative fluorination reactions of organosulfur fluorides are lacking in the literature, due to the difficulty of identifying and eliminating trace impurities.

There are very few reactions known that result in the formation of both cis and trans isomers of the sulfur(VI) derivatives. For example, only cis addition product, *cis*-$(R_fO)_2SF_4$ is reported when sulfur tetrafluoride is used as the starting material to react with good sources of free radicals such as peroxides, trioxides, fluoroxy compounds, and hypochlorites. Only trans addition product, *trans*-tetrafluorobis(perfluoroalkyl)sulfur, *trans*-$(R_f)_2SF_4$, was found when electrochemical fluorination method was used. Similarly, when reaction was carried out under ionic conditions, only the trans isomers were formed. A rare example of isomeric mixtures results from oxidative-addition reactions of chlorine monofluoride with bis(perfluoroalkyl)sulfides. These reactions gave a mixture of *cis*- and *trans*-tetrafluorobis(perfluoroalkyl)sulfur with the trans isomer being predominant. In contrast, alkyl perfluoroalkyl sulfide and $CF_3SCH_2SCF_3$ form only trans isomers under the same conditions. These results are identical with those for the unsymmetrically substituted R_fSCl moieties. A cis/trans isomeric mixture was formed in a ratio of 1:3 when sulfur tetrafluoride was reacted with (difluoronitridothio)imidosulfurous difluoride in the presence of CsF.

$$N{=}SF_2NSF_2 \ + \ SF_4 \xrightarrow{CsF} \textit{cis-/trans-}(F_2SN)_2SF_4$$

Both cis and trans isomers of tetrafluorobis(perfluoroalkoxy)sulfur $F_4S(OR_f)_2$ were prepared by oxidative-addition reactions between chlorine monofluoride and sulfur(IV) compounds (trifluoromethyl)imidosulfites, $CF_3N{=}S(OR_f)_2$ (R_f = CF_3CH_2, $CF_3CF_2CH_2$, and $CF_3CF_2CF_2CH_2$). Organosulfur (VI) fluorides have been prepared by a variety of methods and some representative examples are discussed below.

As the above examples illustrate, a wide range of fluorinating reagents can be chosen for oxidative fluorination of organosulfur compounds. However, when they are used to oxidize S(IV) to S(VI), they often suffer from the following problems: (1) high temperature or low temperature requirements; (2) pressure requirements; (3) long reaction times; (4) accompanying S-C bond cleavage; (5) low yields. In addition, most studies have been dominated by the preparative chemistry, consequently, their reaction mechanisms are not well understood.

Thus, searching for convenient fluorinating reagents which can cause oxidative addition of fluorine to organosulfur compounds under mild conditions, a study of the oxidative addition mechanism, and exchange processes of organosulfur(VI) halogenide compounds using the Coordination Model of Reaction Mechanisms as a guideline and applying the method developed in project 1 and 2, are the most important parts of this thesis.

`CHAPTER 1

KINETIC SIMULATIONS

1.1 Introduction

1.1.1 Coordination model of reaction mechanisms

A reaction mechanism may be analysed by breaking down the reaction into a series of reaction pathways and identifying their corresponding reaction intermediates; those intermediates and pathways that transform a reactant into a product can be further subdivided into a series of more elementary steps of bond formation and bond dissociation, and conceptually at least, into discrete changes in coordination number and electron count of individual atoms. Because of their high reactivities, studies of fluorinated compounds of the main-group elements have provided very detailed information about the identity of those highly reactive species that are involved in these elementary steps, and ^{19}F NMR spectroscopy has been particularly useful in monitoring the connectivity of chemical bonds in static and dynamic situations[1a]. Valuable mechanistic insight of reaction intermediates may also be obtained from closely related crystal structures, electron diffraction structures, from empirical bond length/bond strength relationship and from analogous reactions carried out in the gas phase.[1a,2b] Molecular orbital calculations have also shown good to excellent agreement between experimental and calculated geometries of stable main group compounds.[1b]

The Coordination Model of Reaction Mechanisms[2,3,4] is a topological description of the connectivity of atoms in multi-step reaction pathways which utilises directed graphs P(X,C) in which the vertex set X consists of reactants, intermediates and products, and the edge set C consists of coordination number operators. In this model, elementary steps are described in terms of four coordination number operators: +C, -C, $+C^c$ and $-C^c$, where $+C^c$ and $-C^c$ refer to cyclic intramolecular steps, with the positive and negative signs indicating an increase or decrease in coordination number as bonds are made or broken; dashed lines refer to intermolecular steps and solid lines to intramolecular steps. This model emphasises the coordination changes of the elements during a chemical reaction. Thus it provides a unified description of reaction dynamics and it has been tested and applied successfully in the following areas: (1) Polytopal rearrangement reactions[5,6,7] e.g. mechanisms of axial-equatorial exchange in PF_5, SiF_5^- or $Fe(CO)_5$; (2) Mechanism of electron transfer reaction;[8] (3) Stereoselective bond cleavage[9]; (4) Mechanism of oxidation reactions;[10] (5) 5-member rings in inorganic, organic, and biochemical systems;[11] (6) Glass surface reaction,[3] etc.

[1]

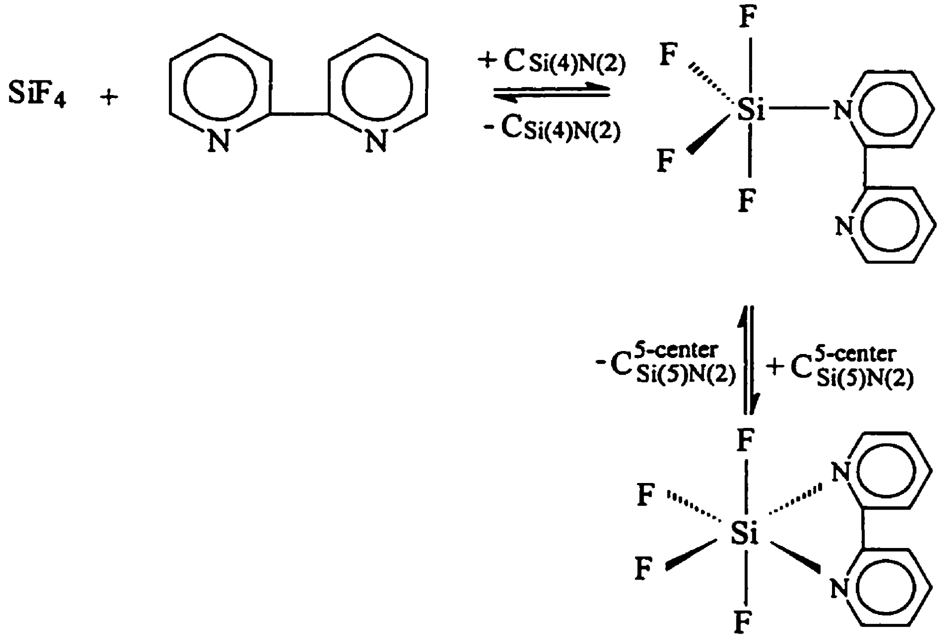

As an illustration, the reaction of silicon tetrafluoride with bipyridine to give a hexacoordinate adduct, SiF_4(bipy), is shown in eq [1]

Since the formation of SiF_4 (bipy) involves four species and two steps, a graph of 4 vertices and 2 edges is drawn, namely, pathway P(4,2), as shown in Figure 1. The first step in the forward direction is an intermolecular (bimolecular) step in which the coordination numbers of both Si and N are increased by 1, from Si(4) to Si(5), and N(2) to N(3), i.e., $+ C_{Si(4)N(2)}$, and the second step is a cyclic intramolecular step, $+ C^{5\text{-center}}_{Si(5)N(2)}$ Reverse steps are drawn below the edges of the graph, and dashed and solid lines refer to intermolecular and intramolecular steps, respectively.

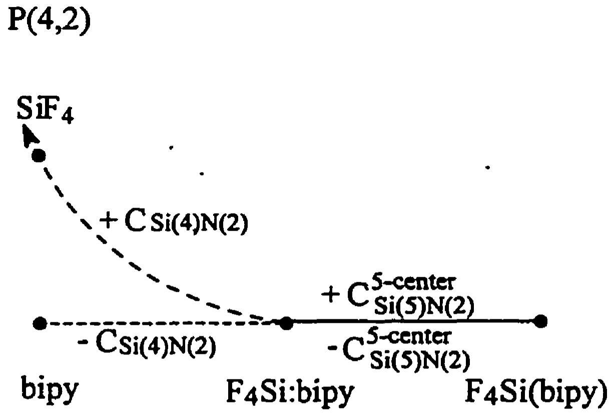

Figure 1. Graphic representation of a pathway P(4,2) for the reaction of silicon tetrafluoride with bipyridine to give SiF_4(bipy)

1.1.2 Chemistry of Lewis acid and base reactions

The chemistry of boron trifluoride has been extensively studied. This compound is a strong Lewis acid and forms a wide range of simple 1:1 adducts with most amines and ethers. These adducts serve as model compounds for the study of Lewis acid-base interactions. It has also been reported that in some cases complexes of the type $R_3N{:}2BF_3$ are formed both in solid state and in solution. Because the 2:1 complexes might be the nitrogen analogue of the reactive intermediates in certain Friedel-Crafts catalysed isomerizations, examination of these systems has been widely studied by techniques such as ^{19}F NMR spectroscopy.[13]

Lewis acid-base interactions involving boron trifluoride have been widely studied and a variety of exchange rates and mechanisms have been reported.[13-20] Any mechanistic description of the BF_3-base system must accommodate the following experimental detailss: (a) the formation of base:BF_3 is a bimolecular process with rate constants in the range of 10^8 to 10^{10} M^{-1} s^{-1},[12] (b) rates of reaction of base:BF_3 are inversely proportional to gas phase enthalpies of dissociation,[14,17] (c) equilibrium data for BF_3-base systems are well-established,[13] (d) two modes of exchange in BX_3-base systems involve both halogen and base exchange,[14,17] (e) excess BF_3 accelerates the rate of fluorine exchange in base:BF_3,[14] (f) the boron cation (amine)$_2BF_2^+$ is an elusive species although, once formed, it is stable even in water,[15] (g) some adducts such as HMPA:BF_3 and tetramethylurea:BF_3 are in equilibrium with the ionic species (base)$_2BF_2^+BF_4^-$,[18] (h) the formation of mixed base adducts such as (Me_3N)(pyridine)BF_2^+ depends on the order of addition of base,[15] and (i) formation of chelated boron cations with bidentate ligands (N-N)BF_2^+ occurs in some cases,[19] but not in others.[20]

The mechanisms of reaction of boron trifluoride with amines, dialkyl ethers, and pyridine provide a mathematical test of the Coordination Model, by comparing the calculated results with extensive experimental data that are available for the reactions of boron trifluoride with Lewis bases. These calculations differ from conventional kinetic simulations because all mechanisms and rate constants are based on the postulates of the Coordination Model.

1.2 Methods

For the kinetic simulation of a reaction pathway, elementary rate constants must be associated with the four coordination operators. Intermolecular steps, +C, are assigned rate constants equal to the diffusion-controlled value of about 10^9 M^{-1} s^{-1}, while rate constants associated with bond cleavage, -C, are estimated from bond enthalpy data. If experimental bond enthalpies are not available for the bridged intermediate, then *ab initio* molecular orbital calculations are used in estimating the relative bond length/strength of the two bridging bonds. Once rate constants have been assigned to all reactions, then the kinetic simulation of the pathway is a straightforward task and gives the concentration vs. time curves on which further analysis and predictions are based.

The assumption that intermolecular (bimolecular) steps, +C, are diffusion controlled with rate constants of about 10^9 M^{-1} s^{-1} places severe restrictions on any mechanism; however, the dilemma of slow reactions is resolved by taking into account the presence or absence of reactive intermediates. If these intermediates are present in exceedingly small amounts, then the importance of impurities and catalysts is greatly magnified. However, if all essential intermediates are readily available in multistep equilibria, as in a catalytic or enzymatic system, then chemical reactions are expected to display their intrinsically rapid rates.

The kinetic simulations were carried out by means of the standard fourth-order Runge-Kutta algorithm[21] here implemented in terms of MathCad software.[22] Difficulties associated with the fact that rate constants varied over a wide range, i.e. "stiffness" of the equations, were dealt with by partitioning the time interval into sections and by choosing as large a time interval within each section as was consistent with obtaining an accurate solution. All calculations were carried out on a 386PC using the MathCad 3.1 program, and a typical kinetic simulation of a four-step, nine-species system required 30 min of computational time per time interval.

Ab initio geometries were calculated for intermediate $H_3N{:}BF_2\text{-}F\text{-}BF_3$ and py:BF_2-F-BF_3 using the GAUSSIAN86 or GAUSSIAN92 programs at the 3-21G* level with full optimisation, except for pyridine where a fixed geometry was chosen.[32]

1.3 Results and discussion

1.3.1 The NH_3-BF_3 and $MeNH_2$-BF_3 systems

The analysis of the NH_3-BF_3 system by the coordination model begins by considering all possible interactions between the atoms of ammonia and boron trifluoride, of which the strongest will most likely involve B-N, H--N and H--F bonds. The model is tolerant of higher coordination numbers as these reflect interactions between reactants and intermediates, but weakly bound intermediates will decompose rapidly and consequently their effect can be neglected, unless they are a prerequisite for further reaction along a multi-step pathway. Pathways P(X,C) are constructed after choosing a minimum set of coordination numbers for the NH_3-BF_3 system, i.e., B(3) B(4) N(3) N(4) F(1) F(2) H(1) H(2). This minimum set of coordination numbers is used for all base-BF_3 systems, with the exception of pyridine, where N(2) N(3) is more appropriate, and dialkyl ether, where O(2) O(3) is used. The formation of B-N, H--N and H--F bonds in the NH_3-BF_3 system is an example of Pathway P(3,1), as illustrated in eq [2]-[4].

[2]

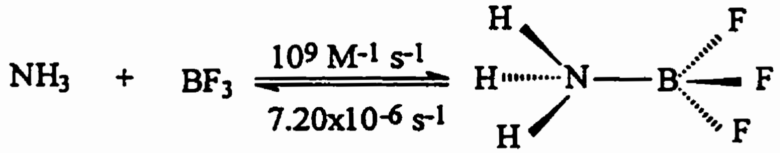

X1 X2 X3

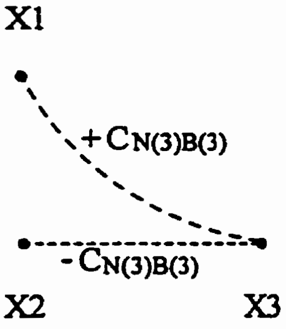

P(3,1)

[2]

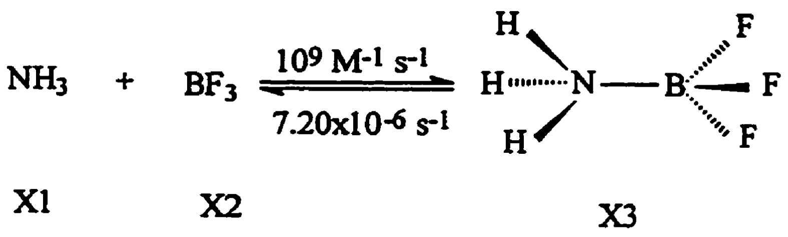
NH3
+
BF3
10^9 M^-1 s^-1
7.20x10^-6 s^-1
H
H
H
N
B
F
F
F
X1
X2
X3

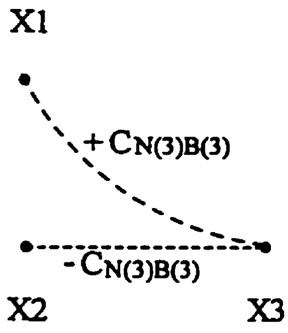
X1
+ CN(3)B(3)
- CN(3)B(3)
X2
X3

P(3,1)

[3]

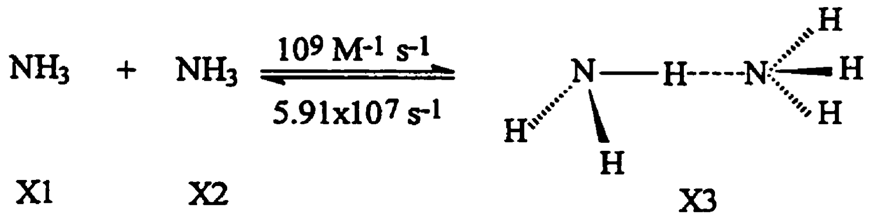
NH3
+
NH3
10^9 M^-1 s^-1
5.91x10^7 s^-1
N
H
N
H
H
H
H
H
X1
X2
X3

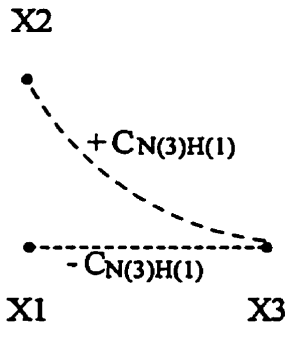
X2
+ CN(3)H(1)
- CN(3)H(1)
X1
X3

P(3,1)

For the testing of the coordination model, each +C and -C must be associated with elementary rate constants and these are selected as follows: intermolecular steps, +C, are assigned rate constants equal to the diffusion-controlled value of about 10^9 M^{-1} s^{-1}, while rate constants associated with bond cleavage, -C, are calculated with the aid of equation $k = Ae^{-\Delta H/RT}$, where $A = 10^{11}$, $T = 298$ K, and ΔH is the bond enthalpy associated with a specific -C, as listed in Table 1. The rate constants are shown in eq [2]-[4], and by selecting rate constants in this way, without any further modification, ΔH becomes the only adjustable parameter of our mechanistic analysis, and a semi-quantitative but stringent test of the coordination model is now possible, even for multi-step processes.

Kinetic simulations were carried out by means of Runge-Kutta algorithm[21] on a 386PC using the MathCad 3.1 program[22] and the calculated Concentration vs. Time curves for the reaction of NH_3 and BF_3 in a 1:1 molar ratio using the rate constants of eq [2]-[4] are shown in Figure 2. Identical pathways P(3,1) are assumed for the reaction of BF_3 with $MeNH_2$ and the kinetic simulation of a 1:1 reaction using the bond enthalpies of Table 1 and the rate constants of eq [5]-[7], are displayed in Figure 3.

$$[5]\quad MeNH_2 + BF_3 \underset{8.36\text{x}10^{-9}\ s^{-1}}{\overset{10^9\ M^{-1}\ s^{-1}}{\rightleftharpoons}} MeNH_2{:}BF_3$$

$$[6]\quad MeNH_2 + MeNH_2 \underset{3.20\text{x}10^{8}\ s^{-1}}{\overset{10^9\ M^{-1}\ s^{-1}}{\rightleftharpoons}} MeHN\text{-}H\text{--}NH_2Me$$

$$[7]\quad MeNH_2 + BF_3 \underset{9.23\text{x}10^{9}\ s^{-1}}{\overset{10^9\ M^{-1}\ s^{-1}}{\rightleftharpoons}} MeHN\text{—}H\text{--}F\text{—}BF_2$$

TABLE 1. Bond enthalpies required for calculation of rate constants.

Species	Bond	$-\Delta H$ (kJ/mol)[a]	Comment
$Me_2O:BF_3$	O-B	54.81	gas phase[14]
$Et_2O:BF_3$	O-B	44.35	gas phase[33]
$H_3N:BF_3$	N-B	92.05	gas phase[28]
$MeNH_2:BF_3$	N-B	108.8	gas phase[28]
$Me_3N:BF_3$	N-B	129.3	gas phase[34]
$Py:BF_3$	N-B	104.6	solution[34]
$Py_2BF_2^+$, $Py:BF_2$--F—BF_3	N-B	104.6	est., same as $py:BF_3$
N-N:BF_3, (N-N)BF_2^+	N-B	129.3	est., same as $Me_3N:BF_3$
H_2NH--NH_3	N--H	18.4	gas phase[35]
MeHNH--NH_2Me	N--H	14.2	gas phase[35]
H_2NH--FBF_2, MeHNH--F-BF_2	H--F	5.9	est. [36]
base:BF_2--F—BF_3	B--F--B	15.0 - 25.0	est., see text

[a] Converted from literature values in kcal/mol.

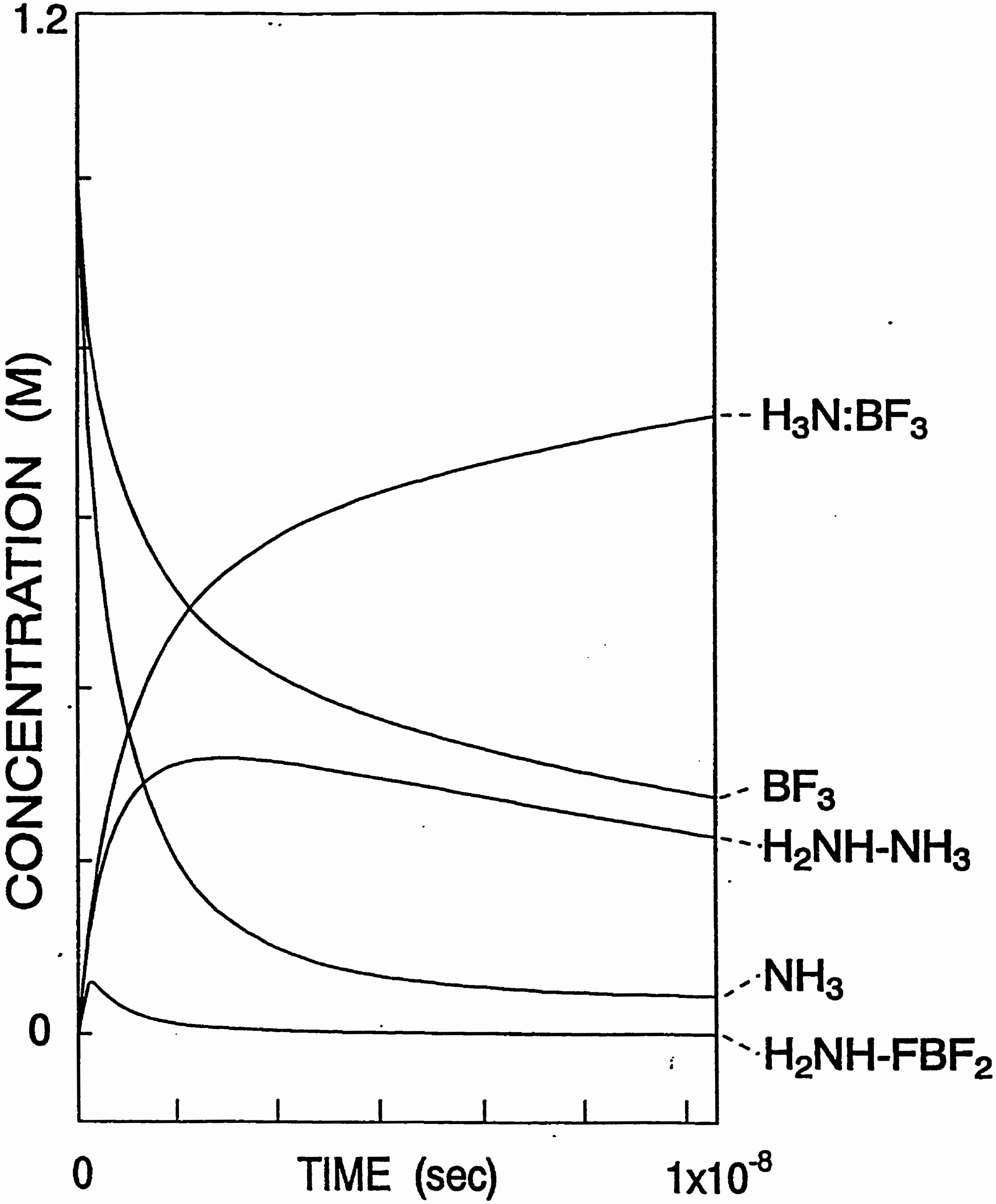

Figure 2. Calculated Concn. vs. Time curves for the 1:1 reaction of BF_3 with NH_3. Input rate constants are given in eq [2]-[4]. The concentration of $H_3N:BF_3$ after $1x10^{-8}$ s is 0.72 M.

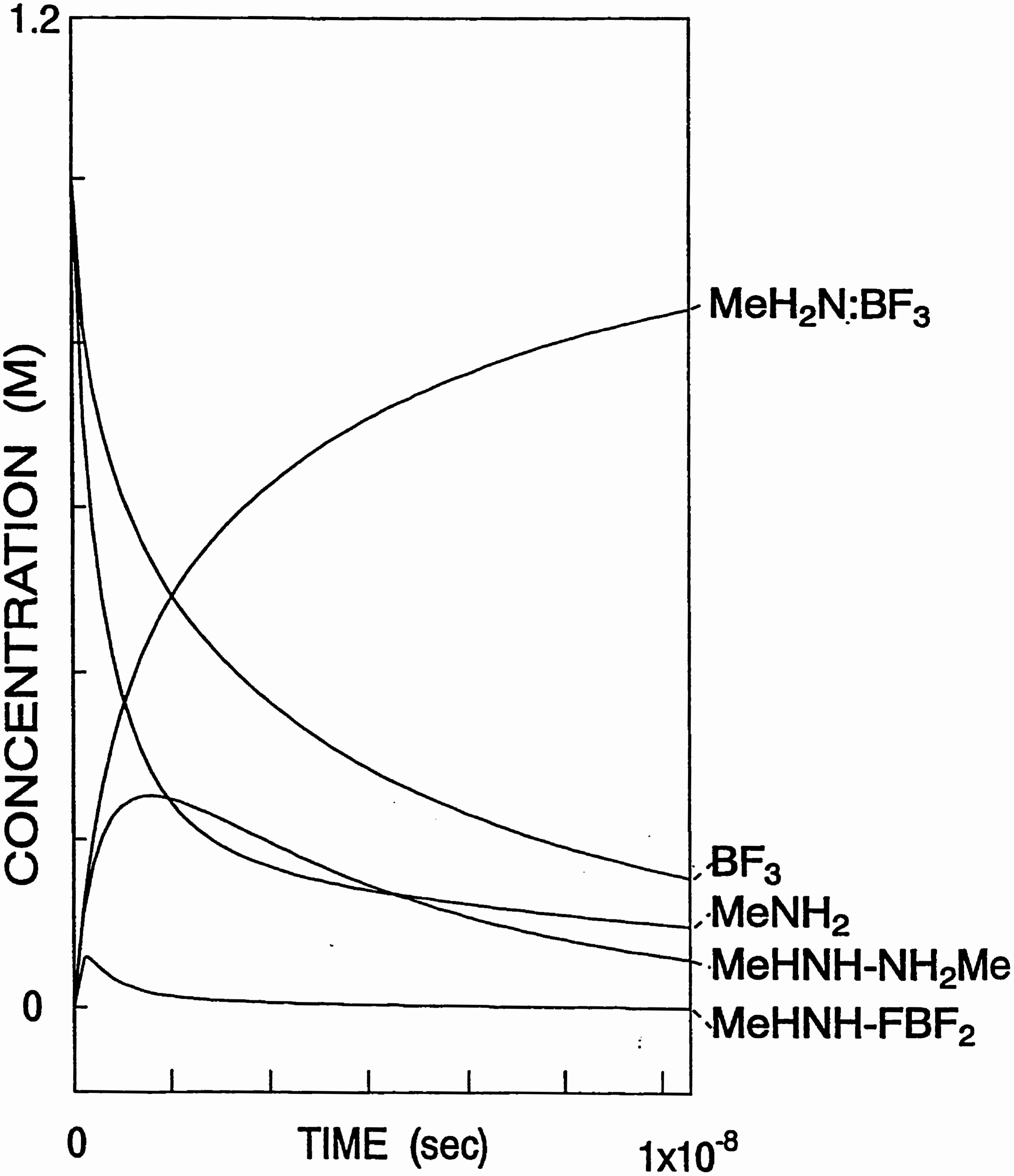

Figure 3. Calculated Concn. vs. Time curves for the 1:1 reaction of BF_3 with $MeNH_2$. Input rate constants are given in eq [5]-[7]. The concentration of $MeNH_2{:}BF_3$ after 1×10^{-8} s is 0.84 M.

The experimental rate constants for reaction of boron trifluoride with ammonia and methylamine were determined by Kistiakowsky and Williams,[12] k(NH_3) = 2.7x10^8 and k($MeNH_2$) = 6.7x10^8 M^{-1} s^{-1} at 25 °C. The slower reaction with ammonia was attributed to an activation energy ranging from 8 kJ for ammonia to near zero for heavier amines; however, the activation energies could not be confirmed experimentally. The coordination model does not assume an activation energy for +C, and a theoretical CNDO study has concluded that no activation energy is necessary for the formation of $H_3N{:}BF_3$. Our model suggests that he slower reaction of ammonia as compared to methylamine, which is displayed in Figure 2 as a lower yield of $H_3N{:}BF_3$ (0.72 M) as compared to $MeNH_2$ (0.84 M) after 10^{-8} s, must arise from a weaker B-N and a stronger N--H bond for the ammonia reaction because the rate constants, +C, are fixed at 10^9 M^{-1} s^{-1} and N--F bond enthalpies were estimated to be equal (Table 1). The weaker B-N bond of $H_3N{:}BF_3$ results in a slightly greater dissociation of the ammonia adduct, eq [2], while greater hydrogen-bonding between ammonia molecules increases the concentration of hydrogen-bonded intermediate, eq [3], and thereby reduces slightly the overall rate of formation of $H_3N{:}BF_3$, as compared to $MeNH_2{:}BF_3$. Statistical factors[24] related to the number of equivalent pathways by which H--N or H--F bonds can be formed were not included in our calculation, but would also favour the ammonia intermediates and further reduce the overall rate formation of the ammonia adduct, as compared to methylamine adduct, in agreement with experiment.

1.3.2 The Me_2O-Et_2O-BF_3 system

This system was studied by Rutenberg, Palko and Drury[13] by means of ^{19}F NMR spectroscopy and their reported equilibrium composition of three mixtures of Et_2O, Me_2O and BF_3 are shown in Table 2. We have calculated Concentration vs. Time curves for the same mixture using bond enthalpies of Table 1 and rate constants of eq [8]-[9], and Figure 4. shows the results for an initial mixture of $Et_2O:Me_2O:BF_3 = 7.51:2.27:3.06$. As seen in Figure 4, equilibrium is reached rapidly, within about 10^{-9} s, and a comparison of calculated and experimental equilibrium concentrations for three sets of initial conditions, Table 2, shows moderately good agreement. An exact agreement is not expected because all the data in Table 2 are based on simplifications: the ^{19}F NMR spectral results of Rutenberg *et al.* neglect the effect of ionic species such as base:BF_2^+ and $(base)_2:BF_2^+$ on the chemical shift and line-width, while our calculations neglect entropy effects and assume a uniform rate constant for the formation, +C, of base:BF_3 adducts.

$$[8] \quad Me_2O + BF_3 \underset{26.3\ s^{-1}}{\overset{10^9\ M^{-1}\ s^{-1}}{\rightleftharpoons}} Me_2O{:}BF_3$$

$$[9] \quad Et_2O + BF_3 \underset{1.77\times10^3\ s^{-1}}{\overset{10^9\ M^{-1}\ s^{-1}}{\rightleftharpoons}} Et_2O{:}BF_3$$

TABLE 2. Comparison of calculated and experimental equilibrium concentrations for the Me_2O-Et_2O-BF_3 system.

Compound	Initial concn.[13] (M)	Equil. conc.[13] at 26 °C (M)	Calcd[a]. conc. after $2x10^{-8}$ s (M)
Experiment 1			
Et_2O	7.51	5.73	5.14
Me_2O	2.27	0.99	1.54
BF_3	3.06	0.0	$5.8x10^{-7}$
$Et_2O:BF_3$	0.0	1.78	2.37
$Me_2O:BF_3$	0.0	1.28	0.71
Experiment 2			
Et_2O	5.77	2.21	2.15
Me_2O	3.98	1.42	1.48
BF_3	6.12	0.0	$1.63x10^{-6}$
$Et_2O:BF_3$	0.0	3.56	3.62
$Me_2O:BF_3$	0.0	2.56	2.50
Experiment 3			
Et_2O	4.59	0.0	0.02
Me_2O	4.59	0.0	0.02
BF_3	9.18	0.0	0.05
$Et_2O:BF_3$	0.0	4.59	4.57
$Me_2O:BF_3$	0.0	4.59	4.57

[a] Calculations are based on the initial conditions of column 2 and rate constants of eq [8]-[9].

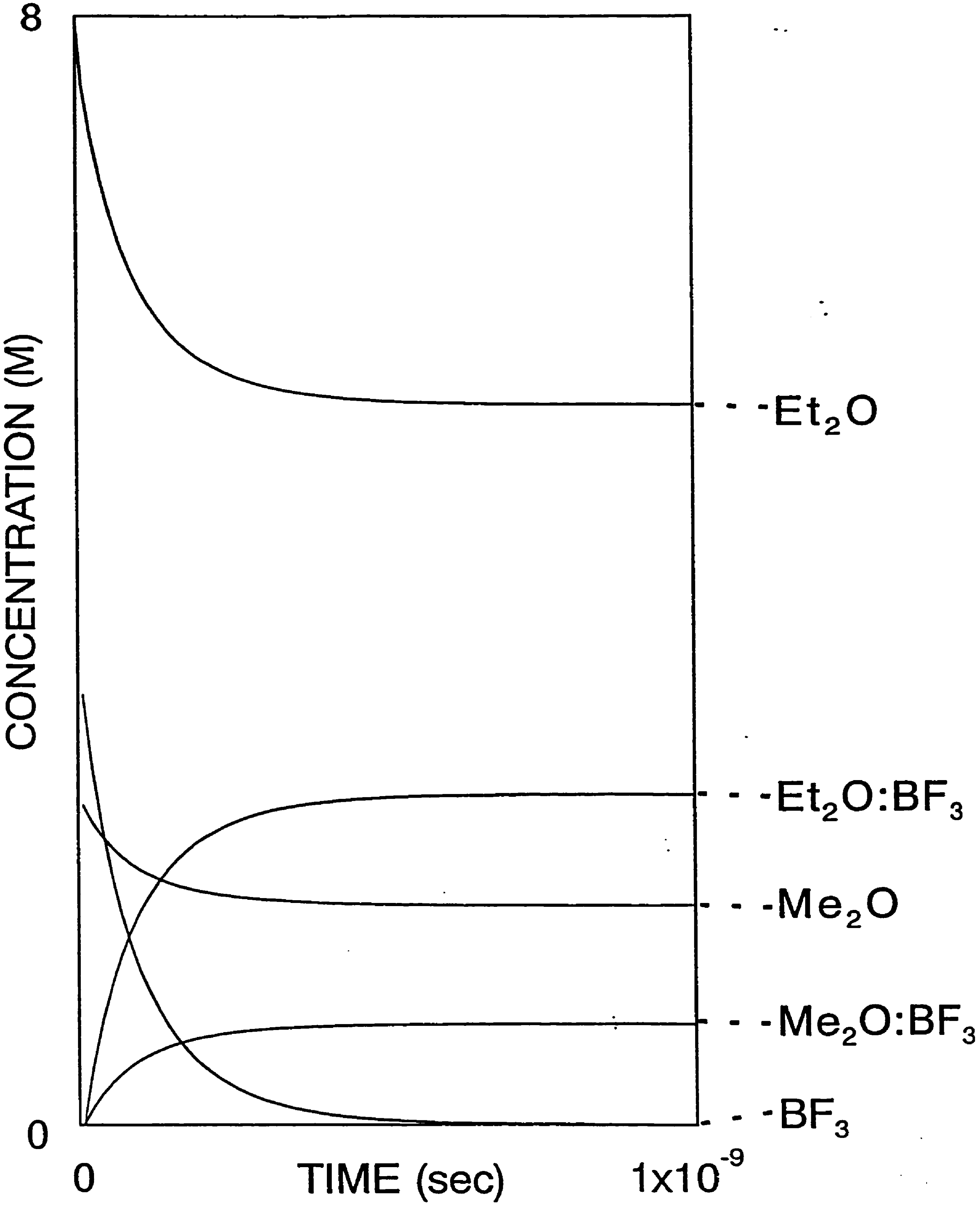

Figure 4. Calculated Concn. vs. Time curves for the reaction of BF_3 with Me_2O and Et_2O. Input rate constants are given in eq [8]-[9].

1.3.3 The Me_2O and $Et_2O{:}BF_3$ system

If rapid diffusion-controlled steps, +C, have rate constants of about 10^9 M^{-1} s^{-1}, then slow reactions must depend on -C, or on ratios of C's, and the concentration of reactive intermediates in slow reactions must be exceedingly low. A slow reaction may be analysed by calculating the outcome of the reaction of $Et_2O{:}BF_3$ with Me_2O, in a 4.00:2.76 ratio, using identical rate constants, eqs [10]-[11], as for the previous Me_2O-Et_2O-BF_3 system which reached equilibrium within 10^{-9} s. The calculations show that after 6×10^{-6} s the concentration of

$$[10] \quad Et_2O{\cdot}BF_3 \quad \underset{10^9\ M^{-1}\ s^{-1}}{\overset{1.77\text{x}10^3\ s^{-1}}{\rightleftharpoons}} \quad Et_2O + BF_3$$

$$[11] \quad Me_2O + BF_3 \quad \underset{26.3\ s^{-1}}{\overset{10^9\ M^{-1}\ s^{-1}}{\rightleftharpoons}} \quad Me_2O{\cdot}BF_3$$

$Et_2O{:}BF_3$ (3.96 M) and Me_2O (2.72 M) decreased slightly while the concentration of $Me_2O{:}BF_3$ (0.041 M) slowly increased, but the concentration of the reactive intermediate BF_3 was maintained at a low concentration of about 10^{-6} M. Synthetic reactions utilising $R_2O{:}BF_3$ are often carried out in the presence of excess dialkyl ether, and this calculation illustrates a common role of solvent as stabiliser and dispenser of reactive intermediates.

1.3.4 The pyridine-BF_3 system

The behaviour of the base-BF_3 systems discussed above is largely determined by the cleavage of B-N and B-O bonds and all calculations point to a small or negligible concentration of uncomplexed BF_3. However, the existence of two modes of exchange in these systems[14,17] has been known for a long time and exchange is particularly influenced by an excess of BF_3. The most likely role of excess BF_3 is to form fluorine-bridged intermediates, and we therefore associate the two modes of exchange with the cleavage, -C, of two types of bonds, namely, bridging B--F--B bonds, as well as B-N or B-O bonds. Our proposed mechanism of reaction of pyridine with boron trifluoride is summarised as pathway P(9,4) as shown in Figure 5.

A systematic study of $(base)_2BF_2^+$ cations has been reported by Hartman and co-workers[15]. Fluorine-bridged adducts such as base:BF_2--F-BF_3 have been postulated before[25], furthermore, F_3B--F--BF_3^- is stable at low temperature but undergoes rapid bond cleavage at ambient temperature[26]. In order to simplify the analysis of the pyridine-BF_3 system, we have considered only one fluorine-bridged intermediate in pathway P(9,4) although it is implicitly assumed that BF_3 can interact with all fluorine-containing species to generate other intermediates such as py_2BF--F--BF_3^+. Inclusion of the latter cation in the kinetic analysis of a larger pathway would be a straightforward task and would be necessary if the analysis were extended to species such as $Py_2BF_2^+$or Py_3BF^{2+}.

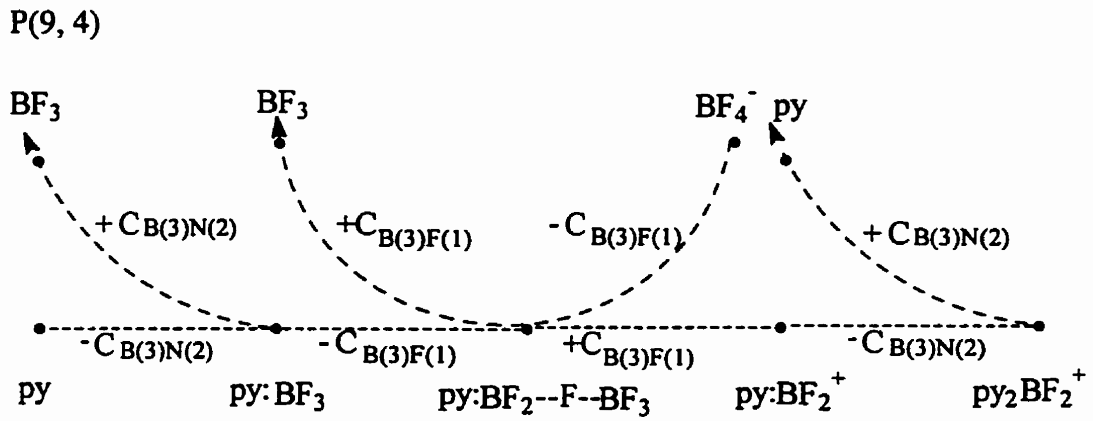
P(9, 4)
BF₃
BF₃
BF₄⁻
py
+C B(3)N(2)
+C B(3)F(1)
-C B(3)F(1)
+C B(3)N(2)
-C B(3)N(2)
-C B(3)F(1)
+C B(3)F(1)
-C B(3)N(2)
py
py:BF₃
py:BF₂--F--BF₃
py:BF₂⁺
py₂BF₂⁺

Figure 5. Graphic representation of a pathway P(9,4) for the proposed mechanism of reaction of pyridine with boron trifluoride.

Our calculations require an estimate of the strength of these bridging B--F--B bonds for which experimental data are not available, but, since NMR studies of fluorine exchange show "activation energies" in the range of about 15-25 kJ for boron fluorides[27], we assume that bond enthalpies are of about this magnitude. We have carried out GAUSSIAN86 and GAUSSIAN92 calculations on two possible fluorine-bridged intermediates and, as shown in Figure 6. The structures show significant differences in relative bond lengths. We therefore assign, somewhat crudely, a bond strength of 25 kJ for the shorter bridging bond and 15 kJ for the longer bridging bond. An experimental B-N bond energy is not available for $py_2BF_2^+$, thus we assume the same value as for $py{:}BF_3$, and with these approximations it is possible to assign the rate constants of eq [12]-[15] and calculate a Concentration vs. Time curve for a 1:1.5 reaction of pyridine and BF_3, as shown in Figure 7

$$[12]\quad py \quad + \quad BF_3 \xrightleftharpoons[4.53\text{x}10^{-8}\ s^{-1}]{10^{9}\ M^{-1}\ s^{-1}} py{:}BF_3$$

$$[13]\quad py{:}BF_3 \quad + \quad BF_3 \xrightleftharpoons[2.34\text{x}10^{8}\ s^{-1}]{10^{9}\ M^{-1}\ s^{-1}} py{:}BF_2\text{--}F\text{--}BF_3$$

$$[14]\quad py{:}BF_2\text{--}F\text{--}BF_3 \xrightleftharpoons[10^{9}\ M^{-1}\ s^{-1}]{4.13\text{x}10^{6}\ s^{-1}} py{:}BF_2^+ \quad + \quad BF_4^-$$

$$[15]\quad py{:}BF_2^+ \quad + \quad Py \xrightleftharpoons[4.53\text{x}10^{-8}\ s^{-1}]{10^{9}\ M^{-1}\ s^{-1}} py_2{:}BF_2^+$$

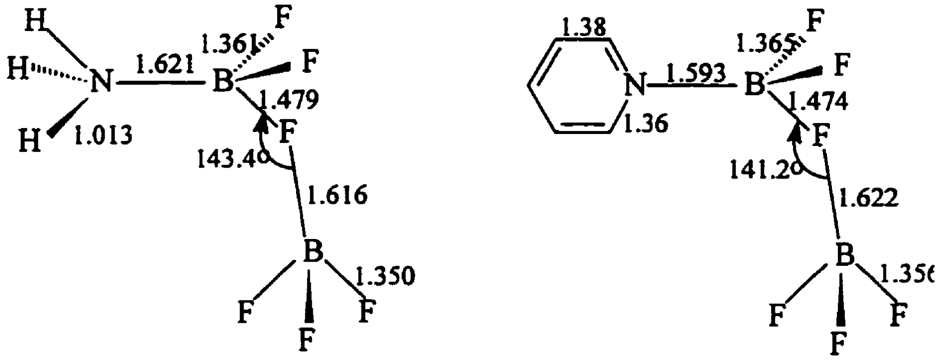
H
H
H
N
1.621
B
1.361
F
F
1.479
F
1.013
143.4°
1.616
B
1.350
F
F
F
1.38
N
1.593
B
1.365
F
F
1.474
F
1.36
141.2°
1.622
B
1.35
F
F
F

Figure 6. Ab initio calculation of $H_3N:BF_2$--F--BF_3 and py:BF_2--F--BF_3 at 3-21G* level with full optimisation, except for fixed geometry of pyridine.

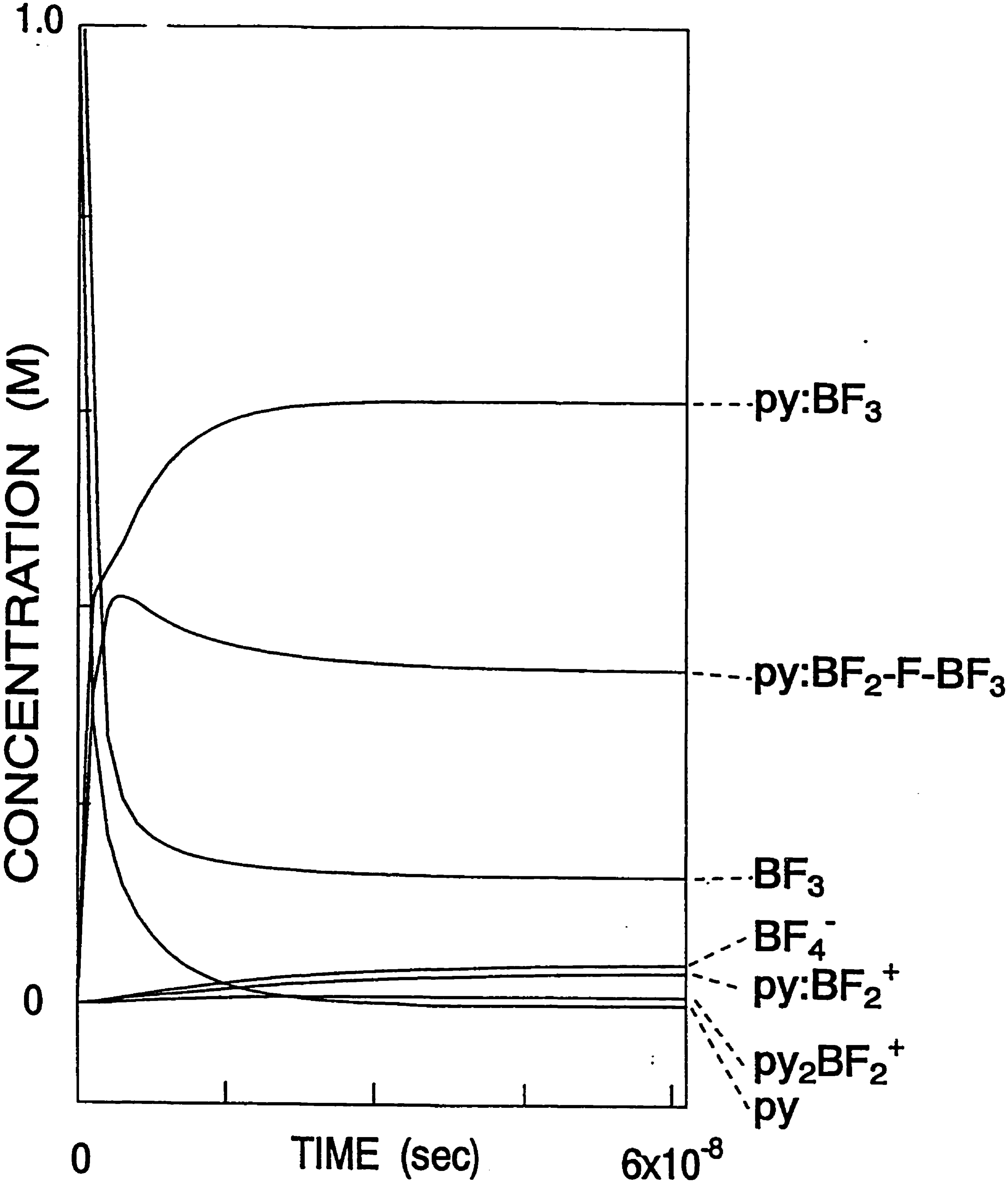

Figure 7. Calculated Concn. vs. Time curves for the 1:1.5 reaction of pyridine with BF_3. Input rate constants are given in eq [12]-[15]. The concentration of $py_2BF_2^+$ after $6x10^{-8}$ s is 0.0085 M.

Figure 7 reveals that species py:BF_2--F--BF_3, py:BF_2^+, and $py_2BF_2^+$ are present in relatively modest concentrations. Since the rate constants for cleavage of B--F--B bonds are large it is not surprising that previous attempts to identify individual species in solution by NMR spectroscopy have been met with difficulty. The acceleration of fluorine exchange by excess BF_3 is readily explained by eq [13]-[14], and the stability of $(base)_2BF_2^+$, once isolated,[15] is consistent with the estimated rate constants of eq [15], which predict a large and favourable equilibrium constant.

Pathway P(9,4) is in agreement with previous mechanisms that require dissociation of boron-base bonds or halogen-bridge bonds, but it differs significantly in its suggestion that base exchange occurs via intermediates $(base)_2BF_2^+$ or (base)(base')BF_2^+, rather than exchange by collision or S_N2 processes. The latter mechanisms, if correct, would require a change in the minimum set of coordination numbers to include either B(5) or N(5), but pathway P(9,4) makes such proposals unnecessary.

1.3.5 The $(R_3N)(py)BF_2^+$ cation and the order of addition of base

Hartman and co-workers found that $(R_3N)(py)BF_2^+$ is formed more rapidly when R_3N is added to py:BF_2Br than when pyridine is added to $R_3N:BF_2Br$.[15] We have considered the order of addition of base by analyzing the addition of trimethylamine to py:BF_3, eq [16]-[12], as compared to adding pyridine to $Me_3N:BF_3$, eq [21]-[25], using the bond enthalpies of Table 1 and the assumption that B-N bond strengths in $(Me_3N)_2BF_2^+$, $(Me_3N)(py)BF_2^+$, and $py_2BF_2^+$ are the same as in $Me_3N{:}BF_3$ and $py{:}BF_3$.

An abbreviated mechanism for the 1:1 reaction of Me_3N with $py{:}BF_3$, which includes the essential features of cleavage of B-N and B--F--B bonds, but omits other possible fluorine-bridged intermediates such as $Me_3N{:}BF_2\text{--}F\text{--}BF_3$, is shown in eq [16]-[20], and the calculated Log(concn) vs. Time curve is shown in Figure 8.

$$\text{[16]}\qquad py{:}BF_3 \xrightleftharpoons[10^{9}\ M^{-1}\ s^{-1}]{4.53x10^{-8}\ s^{-1}} py + BF_3$$

$$\text{[17]}\qquad Me_3N + BF_3 \xrightleftharpoons[2.12x10^{-12}\ s^{-1}]{10^{9}\ M^{-1}\ s^{-1}} Me_3N{:}BF_3$$

$$\text{[18]}\qquad py{:}BF_3 + BF_3 \xrightleftharpoons[2.34x10^{8}\ s^{-1}]{10^{9}\ M^{-1}\ s^{-1}} py{:}BF_2\text{--}F\text{--}BF_3$$

$$\text{[19]}\qquad py{:}BF_2\text{--}F\text{--}BF_3 \xrightleftharpoons[10^{9}\ M^{-1}\ s^{-1}]{4.13x10^{6}\ s^{-1}} py{:}BF_2^+ + BF_4^-$$

$$\text{[20]}\qquad py{:}BF_2^+ + Me_3N \xrightleftharpoons[2.12x10^{-12}\ s^{-1}]{10^{9}\ M^{-1}\ s^{-1}} (Me_3N)(py)BF_2^+$$

The reverse reaction of pyridine with $Me_3N{:}BF_3$ is summarized in eq [21]-[25] and the Log(concn) vs. Time curve is shown in Figure 9.

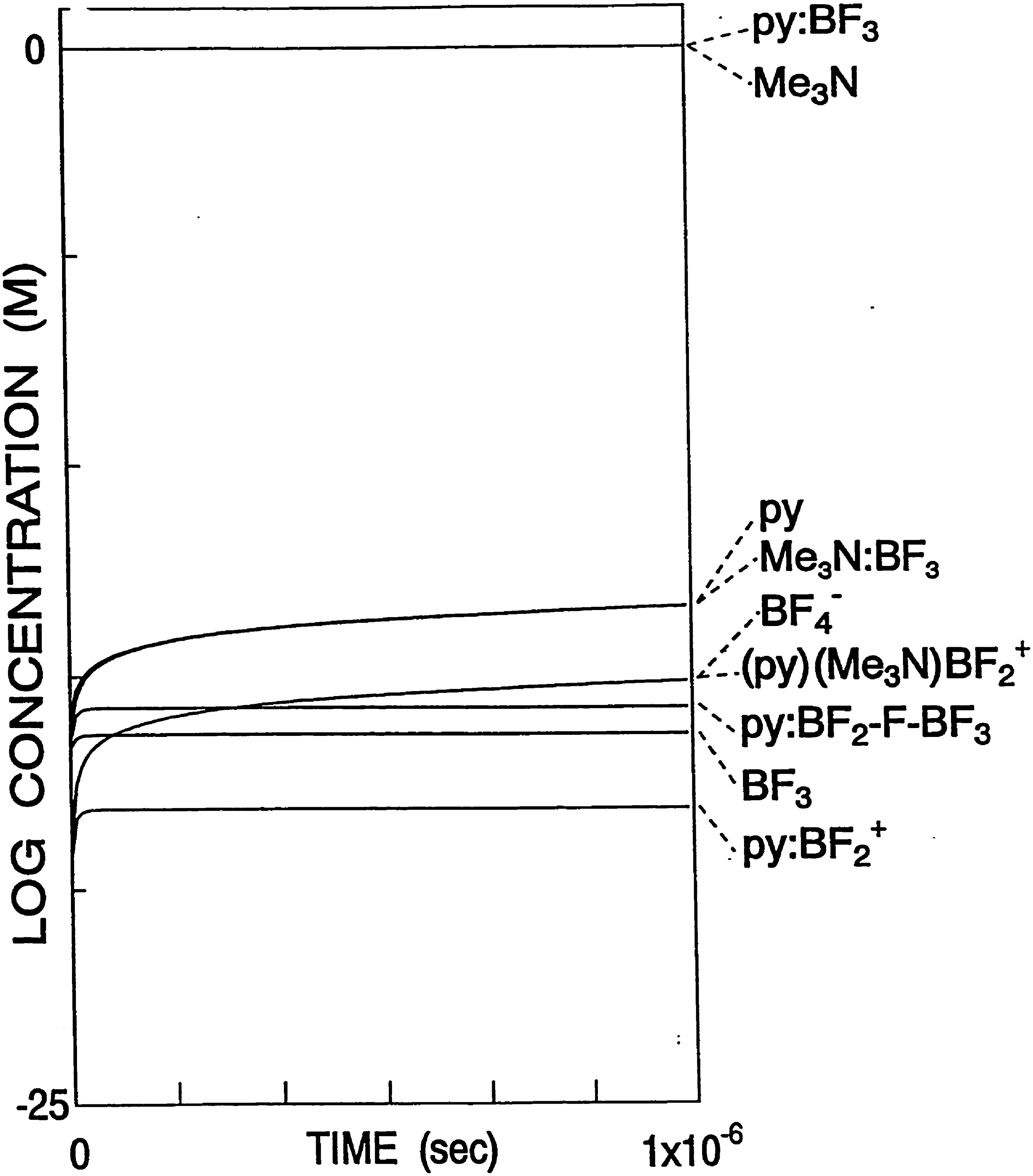

Figure 8. Calculated Log(Concn.) vs. Time curves for the 1:1 reaction of Me_3N with $py:BF_3$. Input rate constants are given in eq [16]-[20]. The concentration of $(py)(Me_3N)BF_2^+$ after 1×10^{-6} s is 2.7×10^{-16} M.

[21] $$\mathrm{Me_3N{:}BF_3} \underset{10^{9}\ \mathrm{M^{-1}\ s^{-1}}}{\overset{2.12\mathrm{x}10^{-12}\ \mathrm{s^{-1}}}{\rightleftharpoons}} \mathrm{Me_3N} + \mathrm{BF_3}$$

[22] $$\mathrm{py} + \mathrm{BF_3} \underset{10^{9}\ \mathrm{M^{-1}\ s^{-1}}}{\overset{4.53\mathrm{x}10^{-8}\ \mathrm{s^{-1}}}{\rightleftharpoons}} \mathrm{py{:}BF_3}$$

[23] $$\mathrm{Me_3N{:}BF_3} + \mathrm{BF_3} \underset{2.34\mathrm{x}10^{8}\ \mathrm{s^{-1}}}{\overset{10^{9}\ \mathrm{M^{-1}\ s^{-1}}}{\rightleftharpoons}} \mathrm{Me_3N{:}BF_2\text{--}F\text{--}BF_3}$$

[24] $$\mathrm{Me_3N{:}BF_2\text{--}F\text{--}BF_3} \underset{10^{9}\ \mathrm{M^{-1}\ s^{-1}}}{\overset{4.13\mathrm{x}10^{6}\ \mathrm{s^{-1}}}{\rightleftharpoons}} \mathrm{Me_3N{:}BF_2^{+}} + \mathrm{BF_4^{-}}$$

[25] $$\mathrm{Me_3N{:}BF_2^{+}} + \mathrm{py} \underset{4.53\mathrm{x}10^{-6}\ \mathrm{s^{-1}}}{\overset{10^{9}\ \mathrm{M^{-1}\ s^{-1}}}{\rightleftharpoons}} \mathrm{(Me_3N)(py)BF_2^{+}}$$

Figure 8 and 9 show the concentrations after 1.0x10^{-6} s. Although the equilibrium is far from established, the results do show that the initial concentration of $(Me_3N)(py)BF_2^+$ depends markedly on the order of addition of base, being 2.7x10^{-16} M for addition of trimethylamine, Me_3N, versus 1.7x10^{-20} M for addition of pyridine, and this increases to 5.6x10^{-14} M and 2.6x10^{-18} M, respectively, after 7.2x10^{-5} s. Longer times were impractical because of the limitation of our kinetic simulation program. An inspection of the rate constants of eq [16] to [25] shows clearly that the effect can be attributed mainly to the smaller N-B bond strength of the $Py{:}BF_3$ adduct, which favours dissociation and eventual production of $Py{:}BF_2^+$ and $(Me_3N)(Py)BF_2^+$. This dissociation of base:BF_3 to

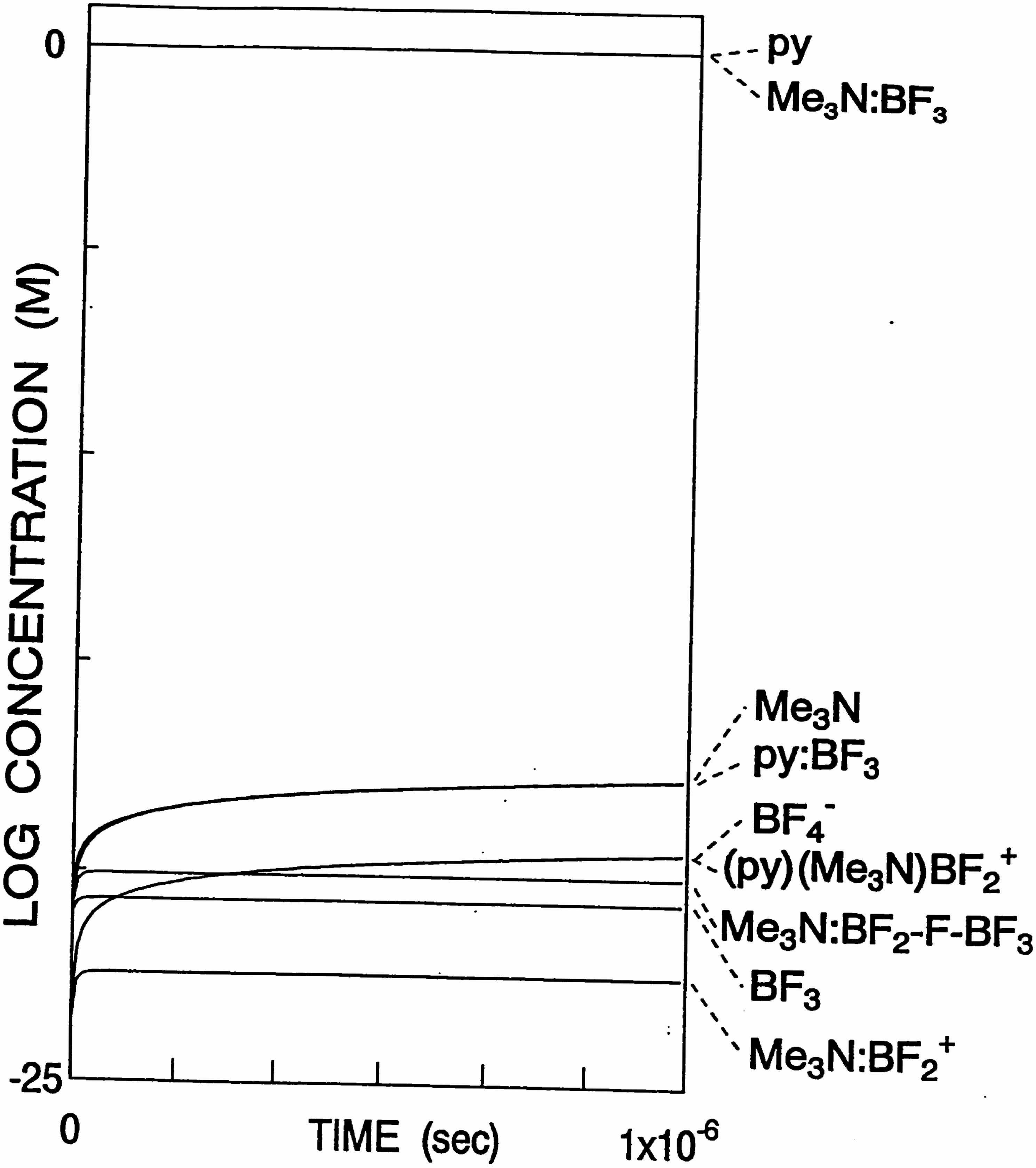

Figure 9. Calculated Log(Concn.) vs. Time curves for the 1:1 reaction of pyridine with $Me_3N:BF_3$. Input rate constants are given in eq [21]-[25]. The concentration of $(py)(Me_3N)BF_2^+$ after $1x10^{-6}$ s is $2.7x10^{-20}$ M.

produce free BF_3 is required in eq [18] and [23] for the cleavage of boron-fluorine bonds. Another effect may also be important, namely, the relative strength of bridging bonds B--F--B, but the lack of experimental bond strength data prevents a realistic test of this suggestion, although selective cleavage of fluorine-bridging bonds has been described for related systems.[2,3,11]

1.3.6 The (N-N)BF_2^+ cation and n-center steps

Entropy effects have been neglected in the analysis of the base-BF_3 systems discussed above, but cyclic n-center steps, $+C^{n\text{-center}}$, are strongly favoured by entropy, particularly 3- to 6-center steps where interacting atoms are in close proximity.[2] This introduces the possibility that changes in the ratio of $+C^{n\text{-center}}/+C$ may affect the outcome of a chemical reaction. In order to estimate a rate constant for ring closure, it may be noted that the entropies of gas-phase reactions of BF_3 with acyclic amines are generally negative with $\Delta S^o = -202 \pm 8$ J mol^{-1} deg^{-1} at 0 °C.[28] It is also known that formation of a five-membered ring (chelate effect) in a multi-step reaction of, say, Cd^{2+}(aq) with ethylenediamine rather than with acyclic $MeNH_2$ leads to enhanced stability[29] because of a change in ΔS^o from -67.3 to +14.1 J mol^{-1} deg^{-1}. Moreover, the five-membered ring in phosphate esters also accelerates the rate of hydrolysis by factors[30] of 10^6 to 10^8. It is therefore reasonable to assume that ring closure, $+C^{5\text{-center}}$, involves a more positive entropy change than reaction with acyclic bases, +C, and we crudely estimate that entropy

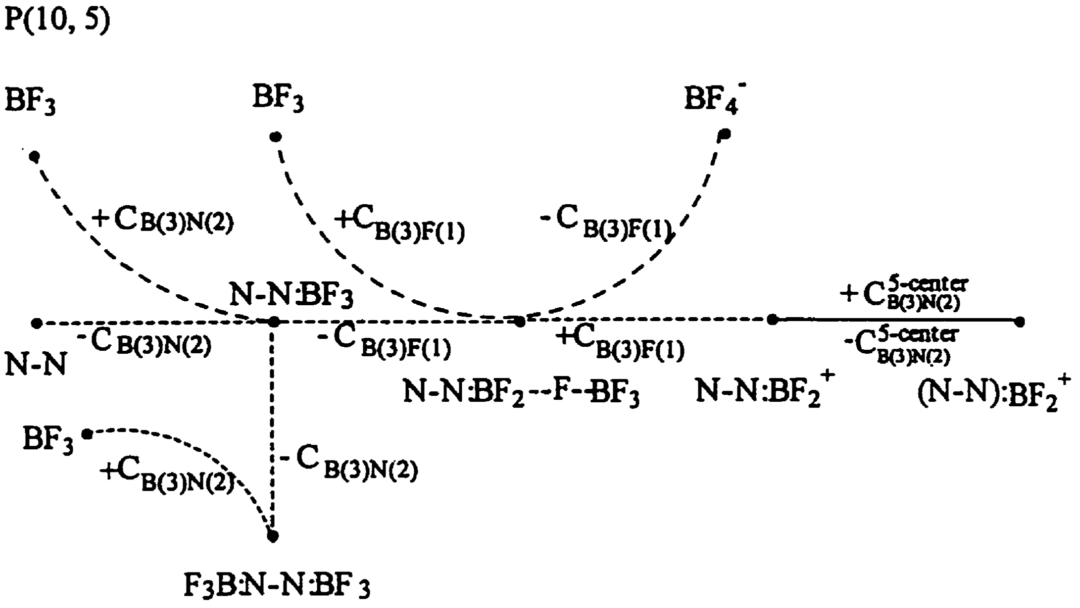
P(10, 5)
BF_3
BF_3
BF_4^-
$+C_{B(3)N(2)}$
$+C_{B(3)F(1)}$
$-C_{B(3)F(1)}$
$N\text{-}N{:}BF_3$
$+C^{5\text{-center}}_{B(3)N(2)}$
N-N
$-C_{B(3)N(2)}$
$-C_{B(3)F(1)}$
$+C_{B(3)F(1)}$
$-C^{5\text{-center}}_{B(3)N(2)}$
$N\text{-}N{:}BF_2\text{--}F\text{--}BF_3$
$N\text{-}N{:}BF_2^+$
$(N\text{-}N){:}BF_2^+$
BF_3
$+C_{B(3)N(2)}$
$-C_{B(3)N(2)}$
$F_3B{:}N\text{-}N{:}BF_3$

Figure 10. Graphic representation of a pathway P(10,5) for a suggested mechanism of reaction of BF_3 with a bidentate ligand N-N.

changes lead to an increase in the ratio $+C^{5\text{-center}}/+C$ of about 100, thus $k = 10^{11}\ s^{-1}$ for the ring-closure step of eq [30].

Pathway P(10,5), as shown in Figure 10, and eq [26]-[30] may be suggested as a mechanism for the reaction of BF_3 with a bidentate ligand N-N.

$$[26] \quad N\text{-}N + BF_3 \underset{8.36x10^{-9}\ s^{-1}}{\overset{10^{9}\ M^{-1}\ s^{-1}}{\rightleftharpoons}} N\text{-}N{:}BF_3$$

$$[27] \quad N\text{-}N{:}BF_3 + BF_3 \underset{8.36x10^{-9}\ s^{-1}}{\overset{10^{9}\ M^{-1}\ s^{-1}}{\rightleftharpoons}} F_3B{:}N\text{-}N{:}BF_3$$

$$[28] \quad N\text{-}N{:}BF_3 + BF_3 \underset{2.34x10^{8}\ s^{-1}}{\overset{10^{9}\ M^{-1}\ s^{-1}}{\rightleftharpoons}} N\text{-}N{:}BF_2\text{--}F\text{--}BF_3$$

$$[29] \quad N\text{-}N{:}BF_2\text{--}F\text{--}BF_3 \underset{10^{9}\ M^{-1}\ s^{-1}}{\overset{4.16x10^{6}\ s^{-1}}{\rightleftharpoons}} N\text{-}N{:}BF_2^{+} + BF_4^{-}$$

$$[30] \quad N\text{-}N{:}BF_2^{+} \underset{8.36x10^{-9}\ s^{-1}}{\overset{1x10^{11}\ s^{-1}}{\rightleftharpoons}} (N\text{-}N)BF_2^{+}$$

The question of interest is the relative yield of acyclic $F_3B{:}N\text{-}N{:}BF_3$ versus cyclic $(N\text{-}N)BF_2^{+}$ because the experimental evidence is not clear on this point: some authors have found only acyclic product,[20] while others found cyclic cation in high yield.[19] If we assume that typical B-N and B--F--B bond strengths of Table 1 apply to this system, with the B-N bond strength equal to that of $Me_3N{:}BF_3$, then the rate constants of eq [26]-[30] can be used to calculate the Concentration vs. Time curve shown in Figure 11 for a 2:1 reaction of BF_3 and N-N. The results of Figure 11 clearly show that $F_3B{:}N\text{-}N{:}BF_3$ (0.73 M) is favoured over $(N\text{-}N)BF_2^{+}$(0.01 M) after $1.2x10^{-8}$ s. These initial concentrations are

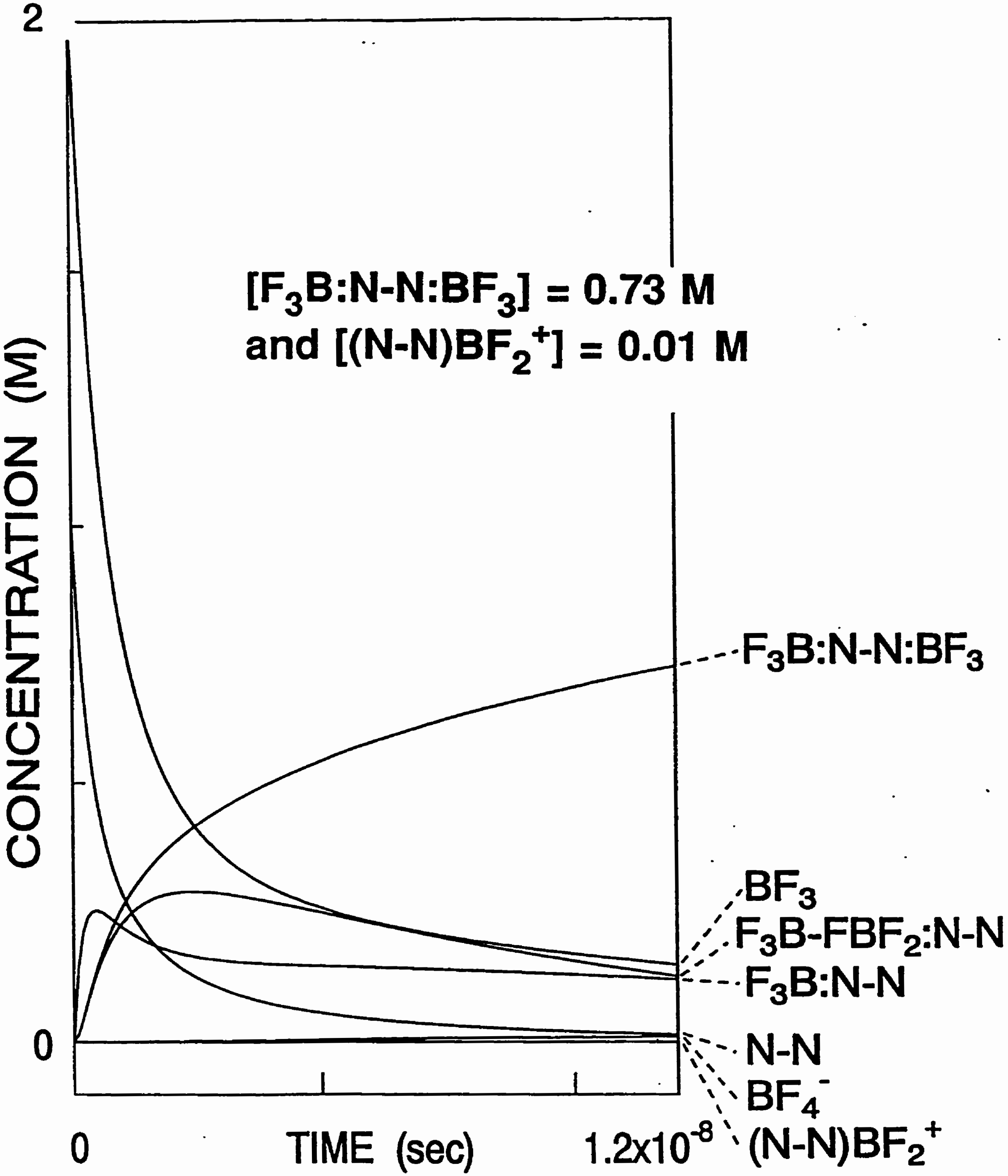

Figure 11. Calculated Concn. vs. Time curves for the 2:1 reaction of BF_3 with bidentate ligand, N-N. Input rate constants are given in eq [26]-[30]. The concentration of $F_3B:N\text{-}N:BF_3$ and $(N\text{-}N)BF_2^+$ after $1.2x10^{-8}$ s is 0.73 M and 0.01 M, respectively.

in agreement with the results of Brown and Singaram[20] who found only $F_3B:NH_2CH_2CH_2NH_2:BF_3$ in their 2:1 reaction of BF_3 with ethylenediamine. An inspection of the rate constants of eq [27] confirms that F_3B:N-N:BF_3 will always be favoured over any competitive reaction with BF_3.

Contrary to these calculations, however, are the observations of Wiberg and Bucher[19] who reported high yield (66%) of (N-N)$BF_2^+BF_4^-$ in their reaction of BF_3 with the bidentate ligands tetrakis(dimethylamino)ethene and *o*-bis(dimethylamino)benzene. These authors also reported an appreciable amount (13-26%) of $[HN\text{-}NH]^{2+}2BF_4^-$ among the reaction products, and the latter result leads us to suggest that an additional mechanistic feature may be responsible for the formation of cyclic products, namely a protected species F_3B:N-N-H^+. This species cannot react with BF_3, as in eq.[27]. The synthesis of a related cyclic cation (N-N)PF_6^- is also accompanied by the formation of N-$NH^+PF_6^-$, where N-N is bipyridine, 4-fluorobipyridine and phenanthroline.[3] The simulation of a more complex pathway which includes protonation and deprotonation steps is beyond the capacity of our kinetic simulation program, although analogous system have been studied by NMR in which protonation-deprotonation is coupled to a rapid ring closure step, e.g., the base-$R_2P(O)OC(CF_3)_2C(CF_3)_2OH$ system.[31]

1.4 Conclusions

In conclusion, the coordination model of reaction mechanisms has been tested mathematically by comparing calculated with experimental results for the reactions of boron trifluoride with amines and ethers, and the model appears to account satisfactorily for all experimental details, at least in a semi-quantitative manner. This model allows chemical reactions to be analysed in three stages: firstly, by the construction of a pathway P(X,C) which specifies the connectivity of all atoms of that pathway, secondly, by the application of molecular orbital calculations to the postulated intermediates to assist in the task of estimating relative bond strengths and selecting individual steps of multi-step pathways, and, thirdly, by carrying out kinetic simulations of all possible pathways P(X,C) and obtain the Concentration vs. Time curves on which further analysis and prediction is based.

The Coordination Model provides a novel way of looking at reaction systems. It is extensively used in this laboratory, and the good agreement between experimental results and calculated results is convincing evidence of the usefulness of the model in its simplified and most straightforward form.

CHAPTER 2

REACTION MECHANISMS OF SILICON AND PHOSPHORUS FLUORIDES:

AB INITIO MOLECULAR ORBITAL STUDIES

2.1 Silicon-fluorine and silicon-carbon bond cleavage in organofluorosilicates

2.1.1 Introduction

Six-coordinate silicon compounds were first observed independently by Gay-Lussac[37] and J. Davy[38] at the beginning of this century, in the formation of the SiF_6^{2-} ion and of the adduct of SiF_4 with ammonia. In the past 30 years there has been growing interest in the chemistry of pentacoordinate and hexacoordinate silicon compounds because of their interesting electronic structures and their distinctive reactivity. They find widespread use in nucleophilic activation and catalytic process in organic synthesis, and are invoked to explain stereochemical studies and as reaction intermediates in many reactions of silicon.[40,43] Another intriguing aspect of hypervalent silicon compounds comes from the studies of the formation and reactivity of organopentafluorosilicates, which have been shown to be especially useful intermediates in the transformation of, in particular, olefins to primary alkyl halides and alcohols as shown in the following eq [31].

$$[31] \quad \text{Olefin or acetylene} \xrightarrow{HSiCl_3} RSiCl_3 \xrightarrow[H_2O]{KF} K_2[RSiF_5] \xrightarrow{CuX_2} RX \quad (X{=}Cl, Br)$$

Organopentafluorosilicates, $RSiF_5^{2-}$, have been known for thirty years. The first compounds of this class was prepared by Tansjoe[39] in 1961 who synthesised $(RNH_3)_2[PhSiF_5]$ by the reaction of phenyltriamine silanes with anhydrous hydrogen fluoride in ether solution.

$$[32] \quad PhSi(NHR)_3 + 6HF \xrightarrow{\text{ether}} (RNH_3)_2[PhSiF_5] + RNH_3F$$

Since then, the syntheses, reactions, and structural studies of $RSiF_5^{2-}$ continue to be of lively interest and have been studied by several research groups.

Because penta- and hexa-coordinate organopentafluorosilicates are either monoanions or dianions, their reactivities are expected to be quite different from those of neutral, coordinatively unsaturated tetracoordinate organosilicon compounds. In fact, some known representative examples of facile silicon-carbon and silicon-fluorine bond cleavage reactions have been recorded in the literature:

(1) Muller and collaborators[40] found that alkyl carbon-silicon bonds in hexacoordinate organopentafluorosilicates, $RSiF_5^{2-}$, are readily cleaved by the action of various oxidizing agents which do not affect neutral tetracoordinate silanes, i.e., one electron oxidizing agents such as Cu(I), Ag(I), Pd(II), Bi(III), Hg(I), Hg_2(II), NBS, etc, caused rapid Si-C bond cleavage in organofluorosilicates $RSiF_5^{2-}$, and these studies on the reactivity of organopentafluorosilicates, were further developed by Kumada and Tamao and co-workers.[41]

(2) In 1977, Janzen *et al.*[42] reported the first NMR spectrum of a six-coordinated organosilicon fluoride, $PhSiF_5^{2-}$. The hexa-coordination around the silicon, as shown in Figure 12 was confirmed by its unique AB_4 spin system in the ^{19}F NMR spectrum. They also found that $PhSiF_5^{2-}$ decomposes to C_6H_6 and SiF_5^- on standing in CH_2Cl_2 at room temperature.

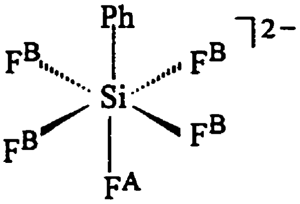

Figure 12. Structure of $PhSiF_5^{2-}$

(3) Tamao and co-workers[43] found that the organopentafluorosilicates readily undergo silicon-carbon cleavage by halogen (chlorine, bromine, and iodine), copper(II) halides, and *N*-bromosuccinimide (NBS) in organic solvents to give the corresponding organic halides, and by 3-chloroperbenzoic acid (MCPBA) to give the corresponding organic alcohol.

(4) In 1980, Kumada *et al*[44] confirmed by ESR that tetracyanoethylene, TCNE, accepts an electron from $RSiF_5^{2-}$.

(5) Previous NMR studies of ligand exchange in tetra-, penta- and hexa-coordinate silicon fluorides carried out in this laboratory[5] have shown that intermolecular fluorine exchange is rapid in systems such as $MeSiF_3$-$MeSiF_4^-$ and SiF_5^--SiF_6^{2-}.

(6) *Ab initio* calculations on a variety of pentavalent organofluorosilicates were reported by Dixon and co-workers[45], and good agreement with the experimental data was found.

In spite of a large number of successful fundamental studies on the preparation and reaction of organopentafluorosilicates, little attention has been paid to how carbon-silicon and fluorine-silicon bonds in organofluorosilicates are cleaved. On the other hand, the bond energies of Si-F and Si-C bonds are quite high, on the order of 565 and 318 kJ mol^{-1}, respectively,[46] yet these bonds in organofluorosilanes and -silicates may be cleaved under mild conditions in the presence of fluoride ion as described in the previous section. We wondered why the addition of F^- to $PhSiF_3$ should, eventually, lead to cleavage of Si-C and Si-F bonds.

Our Coordination Model,[2,47] as described in Section 1.1 of this chapter, prompts us to ask the key mechanistic question in the following way: what coordination number and electron count of silicon leads to a cleavage Si-C and Si-F bonds that allow spontaneous Si-C and Si-F bond cleavage under mild conditions?

A mechanism that accounts for the cleavage of Si-F bonds in typical fluorosilicates such as $RSiF_4^-$and $RSiF_5^{2-}$, and involves a fluorine-bridged intermediate, is shown in Scheme 1. In this mechanism, the N-X-L notation of Perkins *et al.*[48] is used to specify the valence electron count (N) and coordination number (L) of elements (X) silicon and fluorine.

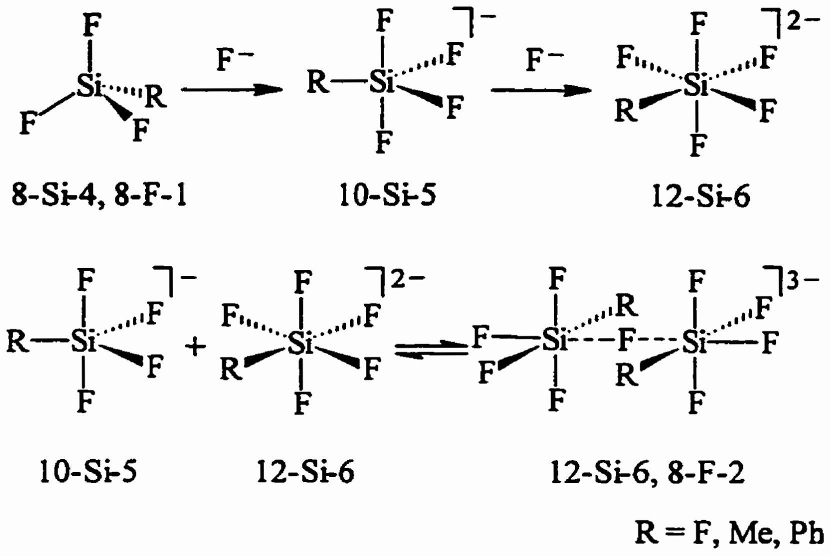

Scheme 1. Proposed mechanism for the cleavage of Si-F bonds in typical fluorosilicates such as $RSiF_4^-$and $RSiF_5^{2-}$.

Evidence that fluorine-bridged intermediates are involved in the cleavage of Si-F bonds is based on NMR studies of rapid fluorine exchange in four-, five- and six-coordinate silicon fluorides,[5] synthesis of new fluorosilicates, and the X-ray crystallographic structural determination of three fluorine-bridged silicate anions, *o*-$C_6H_4(SiPhF_2)_2F^-$, *o*-$C_6H_4(SiPh_2F)(SiF_3)F^-$ and *o*-$C_6H_4(SiPh_2F)(SiPhF_2)F^-$.[49,50]

The fluoride-catalysed cleavage of Si-C bonds is a more complex process, and a possible mechanism is given in Scheme 2. The first step of the reaction mechanism is the addition of two moles of fluoride anion F^- to form a six-coordinate silicon compound, then a one electron transfer may occur from $RSiF_5^{2-}$ to an oxidizing agent to form a radical anion. In the next step, cleavage of the carbon-silicon bond takes place to give an aryl radical and SiF_5^-. This mechanism agrees with the proposal of Kumada and co-workers,[5] however, details of the electron-transfer step are not specified since they depend on the choice of oxidizing agent.

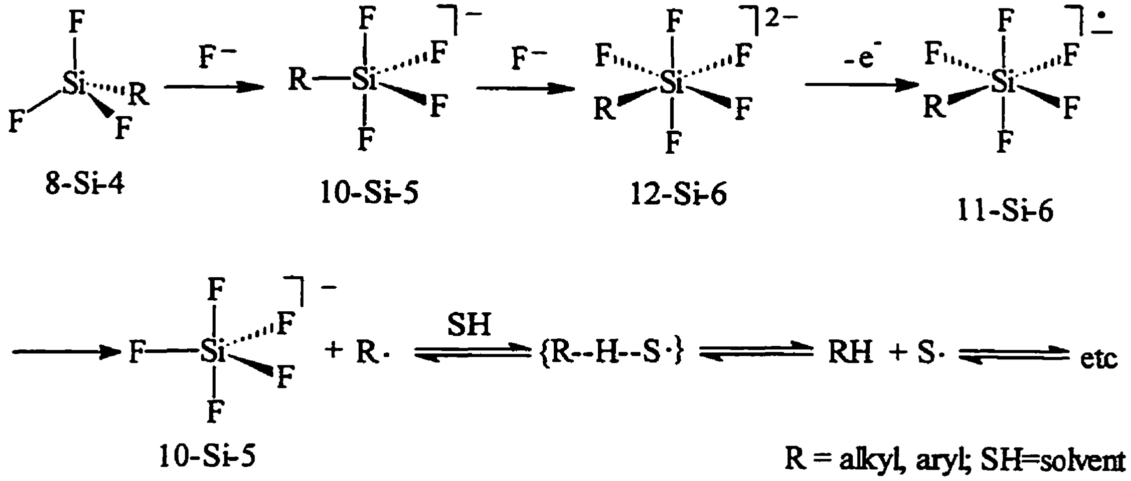

Scheme 2. Proposed mechanism of fluoride-catalysed cleavage of Si-C bonds.

Experimental evidence supporting a radical anion intermediate in Scheme 2 includes the finding that typical one-electron oxidizing agents such as Hg(I/II), Sb(III), Pb(IV), Bi(III), Ag(I), Cu(I/II), Pd(II), NBS, halogens, etc., bring about rapid cleavage of Si-C bonds in $RSiF_5^{2-}$. Furthermore, if an electron acceptor such as tetracyanoethylene (TCNE) is added to $RSiF_5^{2-}$, the radical anion $TCNE^{\cdot-}$ can be observed by EPR spectroscopy, and TCNE is alkylated.[5] Spin trapping of alkyl radical intermediates has been reported and electron transfer from $RSiF_5^{2-}$ to TCNE also occurs in the solid state.[44] Electrolysis of $PhSiF_5^{2-}$ gives benzene, while $MeSiF_5^{2-}$ gives methane. Benzene is also detected in a sample of $PhSiF_5^{2-}$ after several weeks in dichloromethane solution.[42] In the presence of fluoride ion, the bond in hexacoordinate diorgano(phthalocyaninato)silicon compounds is cleaved by NBS, halogens and Cu(II). Radical anions have been observed in silicon catecholates.[51]

The possibility that the pentacoordinate anion $RSiF_4^-$, rather than the hexacoordinate dianion $RSiF_5^{2-}$, is responsible for Si-C bond cleavage is unlikely in view of the finding that $MeSiF_4^-$ reacts with Ag(I) salt only in the presence of added fluoride ion. In the absence of oxidizing agents, organopentafluorosilicates $RSiF_5^{2-}$ are stable,[44,52] even in aqueous solution, and can be conveniently identified by their AB_4 fluorine NMR spectra.

2.1.2 Molecular orbital calculation method

All *ab initio* molecular orbital calculations were performed with the GAUSSIAN86 and GAUSSIAN92 system of programs, and geometrical parameters were fully optimized with analytical gradients by the Hartree-Fock method. Interacting molecules and ions were treated as one large system.[54] Standard literature values were used for the geometries of methyl and phenyl substituents, except for some calculations in Table 4 and 5, where the geometry of the phenyl group was relaxed. The basis sets STO-3G*, 3-21G*, 6-31G*, and 6-31+G* were used in the calculations, and the optimized geometries compared with experimental data, where available. Second derivative calculations were carried out for structures **1-5** in Figure 20-25, and polarization functions (6-31G*) were used for the hydrogen-bonded structure **7**.

2.1 3 Results and Discussion

2.1.3.1 Silicon-fluorine bond cleavage

The optimized geometries of silicon fluorides were calculated with the aid of GAUSSIAN86 and GAUSSIAN92 programs to determine the nature of stationary points found by geometry optimization. Frequency calculations were carried out for all fluorine-bridged intermediates, i.e., structures **1-5** in Figure 20-25, and it was found that all of the frequencies are real from second derivative calculations. Therefore, these final structures correspond to minima on their potential surfaces. Several basis sets were used for the calculations and the results are compared with experimental data, where available, in Tables 1-3. Structural data for related four-, five-, and six-coordinate silicon fluorides are available, and silicon fluorides have previously been the subject of theoretical analysis[64].

For the series SiF_4, SiF_5^- and SiF_6^{2-}, there is an increase in the experimental Si-F bond length of 5.21% in SiF_5^- and 9.37% in SiF_6^{2-}, relative to SiF_4, as shown in Table 3. This experimental trend is reproduced quite satisfactorily by the higher level calculations. i.e., 5.3% (SiF_5^-) and 9.6% (SiF_6^{2-}) with the 6-31+G* basis set, and 5.0% (SiF_5^-) and 9.2% (SiF_6^{2-}) with the 6-31G* basis set. Agreement with the 3-21G* calculation of 4.5% (SiF_5^-) and 7.9% (SiF_6^{2-}) is less satisfactory, but even the STO-3G* calculation, although underestimating the Si-F bond lengths, nevertheless provides a useful estimate of the relative lengthening of Si-F bonds of 4.7% (SiF_5^-) and 8.2% (SiF_6^{2-}).

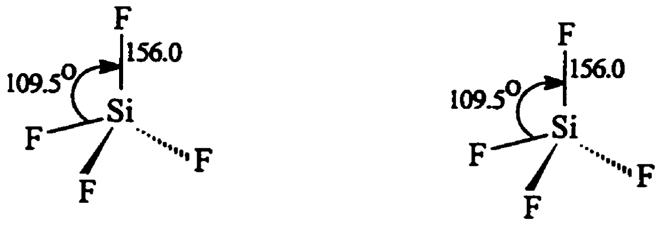
F
156.0
109.5°
Si
F
F
F
F
156.0
109.5°
Si
F
F
F

Figure 13. Optimised (left, 6-31+G*) and experimental (right, Ref 55) geometry for SiF_4.

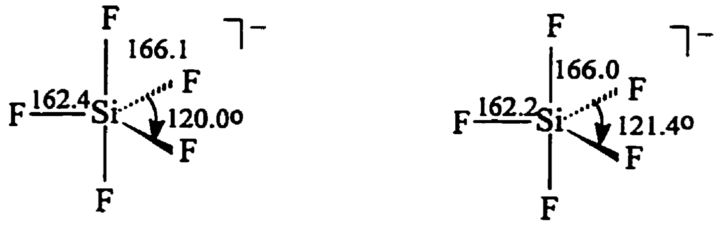
]⁻
F
166.1
F
162.4
Si
120.00
F
F
F
]⁻
F
166.0
F
162.2
Si
121.4°
F
F
F

Figure 14. Optimised (left, 6-31+G*) and experimental (right, Ref 56) geometry for SiF_5^-.

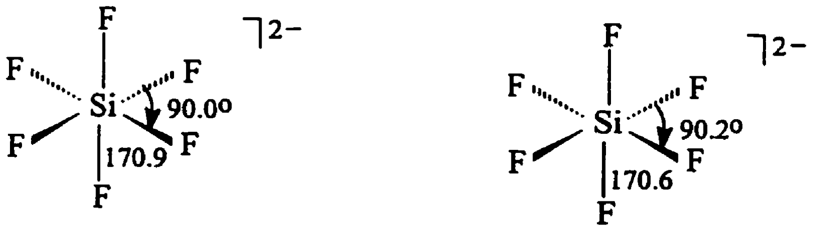
]2−
F
F
F
Si
90.0°
F
F
170.9
F
]2−
F
F
F
Si
90.2°
F
F
170.6
F

Figure 15. Optimised (left, 6-31+G*) and experimental (right, Ref 57) geometry for SiF_6^{2-}.

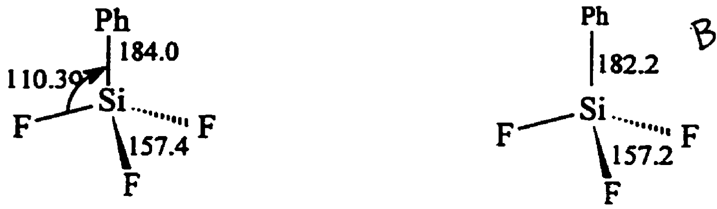
Ph
184.0
110.39
Si
F
F
157.4
F
Ph
182.2
Si
F
F
157.2
F

Bond angles missing

Figure 16. Optimised (left, 6-31G*) and experimental (right, Ref 56) geometry for $PhSiF_3$.

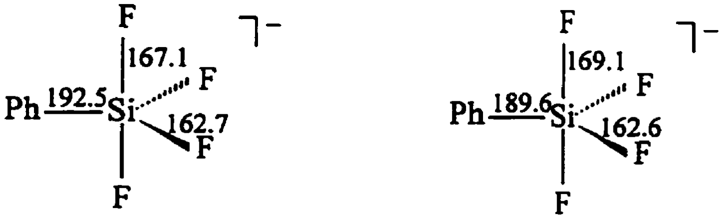
F
167.1
F
Ph
192.5
Si
162.7
F
F
]-
F
169.1
F
Ph
189.6
Si
162.6
F
F
]-

Figure 17. Optimised (left, 6-31G* with geometry of phenyl ring relaxed) and experimental (right, Ref 56) geometry for $PhSiF_4^-$.

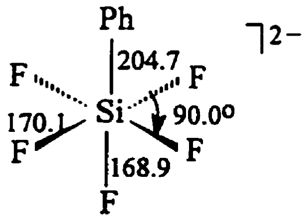
Ph
204.7
F
F
170.1
Si
90.0°
F
F
168.9
F
]2-

Figure 18. Optimised (6-31G*) geometry for $PhSiF_5^{2-}$. Experimental data not available.

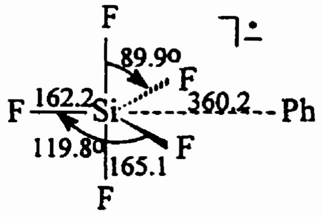
F
89.9o
F
162.2
Si
360.2
Ph
119.8o
F
165.1
F

Figure 19. Optimised (6-31+G*) geometry for $\{PhSiF_5^{\cdot-}\}$ showing that $\{PhSiF_5^{\cdot-}\}$ consists essentially of a phenyl radical and SiF_5^- anion.

Table 3. Experimental and calculated Si-F bond lengths (pm), and average lengthening[a] of bonds (%) relative to SiF_4.

	Experimental	6-31 +G*	6-31G*	3-21G*	STO-3G*
SiF_4	155.98[55]	156.0	155.7	155.7	152.1
SiF_5^-	166.0 ax 162.2 eq[56] (5.21%)	166.1 ax 162.4 eq (5.3%)	165.3 ax 161.8 eq (5.0%)	164.2 ax 161.2 eq (4.5%)	160.8 ax 157.6 eq (4.7%)
SiF_6^{2-}	170.6[57] (9.4%)	170.9 (9.6%)	170.0 (9.2%)	168.0 (7.9%)	164.6 (8.2%)
$PhSiF_3$	157[56]		157.4	157.2	152.4
$PhSiF_4^-$	169.1 ax 162.6 eq[56] (6.3%)		167.1 ax 162.7 eq (4.8%)	165.9 ax 161.8 eq (4.2%)	159.8 ax 157.3eq (4.0%)
$PhSiF_5^{2-}$			168.9 ax 170.1 eq (7.8%)	166.6 ax 168.0 eq (6.6%)	162.0 ax 162.3 eq (6.4%)
$Ph\text{--}SiF_5^{\cdot -}$			165.1 ax 162.2eq[b]	163.8 ax 162.1 eq[b]	160.7 ax 157.6 eq[b]

[a] For compounds having non-equivalent fluorines, an average of the axial and equatorial bond length is used for estimating % lengthening of bonds; ax = axial, eq = equatorial fluorines.

[b] Note similarity to SiF_5^- in third row.

For the series of $PhSiF_3$, $PhSiF_4^-$ and $PhSiF_5^{2-}$, experimental information is only available for $PhSiF_3$ and $PhSiF_4^-$. The experimental lengthening of the Si-F bond is 6.3% in $PhSiF_4^-$, relative to SiF_4, and this may be compared with the calculated lengthening of 4.0-4.8%. These calculations assume a fixed phenyl ring of standard geometry. The calculations also show bond lengthening of 6.4-7.8% in $PhSiF_5^{2-}$, relative to SiF_4 (Table 3).

Since it is known from NMR studies of fluorine exchange that no Si-F bond cleavage occurs in purified samples of $RSiF_3$, $RSiF_4^-$, or $RSiF_5^{2-}$ (R = F, Me, Ph), we must conclude that a bond lengthening of about 4-9% is insufficient to cause Si-F bond cleavage in these compounds under mild thermal conditions.

In order to establish that fluorine bridging leads to more substantial bond lengthening/weakening, the structures of five Si--F--Si bridged anions **1-5** were calculated and the results, along with the experimental data of **6**, are summarised in the diagrams below in figure 20-25 and in Table 4.

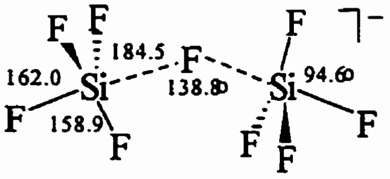

1 (6-31G*)

Figure 20. Optimised (6-31G*) geometry for $F_4Si\text{--}F\text{--}SiF_4^-$ **1**.

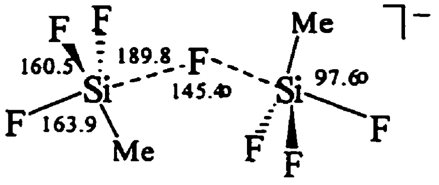

F
F
160.5
189.8
F
145.40
Me
97.60
Si
Si
F
163.9
Me
F
F
F

2 (6-31G*)

Figure 21. Optimised (6-31G*) geometry for MeF$_3$Si--F--SiF$_3$Me$^-$ **2**.

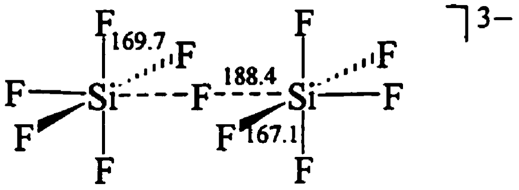

F
169.7
F
F
F
188.4
F
Si
F
Si
F
F
F
167.1
F
F

3 (6-31G*)

Figure 22. Optimised (6-31G*) geometry for F$_5$Si--F--SiF$_5^{3-}$ **3**.

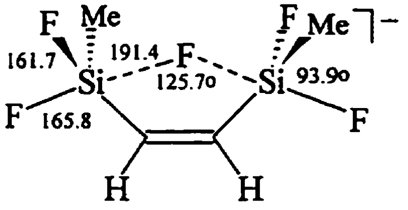

F
Me
F
Me
161.7
191.4
F
125.70
Si
Si
93.90
F
165.8
F
H
H

4 (6-31G*)

Figure 23. Optimised (6-31G*) geometry for C$_2$H$_2$(SiMeF$_2$)$_2$F$^-$ **4**.

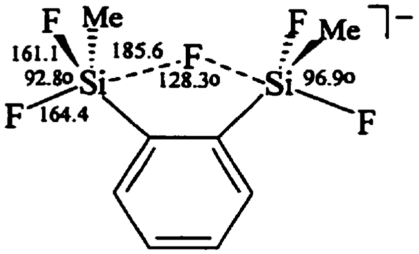
F
Me
161.1
185.6
F
92.8°
Si
128.3°
Si
96.9°
F
164.4
F
Me
]−

5 (3-21G*)

Figure 24. Optimised (3-21G*) geometry for *o*-$C_6H_4(SiMeF_2)_2F^-$ **5**.

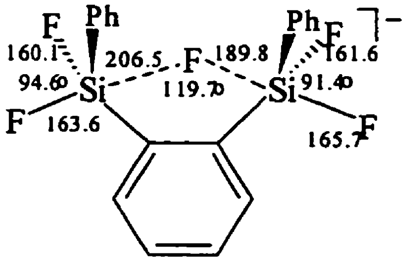
F
Ph
160.1
206.5
F
189.8
Ph
F
161.6
94.6°
Si
119.7°
Si
91.4°
F
163.6
165.7
F
]−

6 (exp[63])

Figure 25. Experimental geometry for *o*-$C_6H_4(SiPhF_2)_2F^-$ **6**.

Table 4. Experimental and calculated Si--F--Si bridging bond lengths (pm), and lengthening[a] of bridging bond (%) relative to SiF_4

	Experimental	6-31G*	3-21G*	STO-3G*
SiF_4 Si-F	156.0[55]	155.7	155.7	152.1
$F_4Si{-}{-}F{-}{-}SiF_4^-$ **1**		184.5[g]	180.5	175.1
Si--F--Si		(18.3%)	(15.7%)	(12.3%)
$MeF_3Si{-}{-}F{-}{-}SiF_3Me^-$ **2**		189.8[g]	184.2	174.9
Si--F--Si		(21.7%)	(18.1%)	(12.3%)
$F_5Si{-}{-}F{-}{-}SiF_5^{3-}$ **3**		188.4[g]	182.6	176.5
Si--F--Si		(20.8%)	(17.1%)	(13.2%)
$C_2H_2(SiPhF_2)_2F^-$ **4**		191.4[b,e,g] 190.0[c]	185.1[b,f], 185.3[c]	174.6[b]
Si--F--Si		(22.7%)	(18.7%)	(11.9%)
o-$C_6H_4(SiMeF_2)_2F^-$ **5**			184.9[b,d,g],184.4[c]	174.1[b]
Si--F--Si			(18.5%)	(11.6%)
o-$C_6H_4(SiPhF_2)_2F^-$ **6**	189.8-206.5[15,16]			
Si--F--Si	(21.7%-32.4%)			

[a] For compounds having non-equivalent fluorines, an average of the axial and equatorial bond lengths is used for estimating % lengthening of bonds. [b] Methyl groups have *trans* configuration. [c] Methyl groups have *cis* configuration. [d] *Trans* isomer is more stable than *cis* isomer by 1.7 kJ mol^{-1}. [e] *Trans* isomer is more stable than *cis* isomer by 1.9 kJ mol^{-1}. [f] *Trans* isomer is more stable than *cis* isomer by 2.4 kJ mol^{-1}. [g] With second derivative calculations.

Two of the anions **4** and **5** contain five-membered rings, and these were chosen so that calculations could be compared with the experimental result that is available for the bridged anion *o*-$C_6H_4(SiPhF_2)_2F^-$ **6**, which, in the solid state, has an unsymmetrical Si--F--Si bridge and a *cis* arrangement of phenyl substituents. Calculations of both the *cis* and *trans* isomers of **4** and **5** were carried out, and a slightly lower energy of 1.8-1.9 kJ mol^{-1} was found for the *trans* isomer. On the other hand, all calculations show symmetrical Si--F--Si bridges in anions **4** and **5**. The synthesis and stability of the cyclic Si--F--Si bridged anion **6** is undoubtedly favoured by a 5-center step, and bridging bonds in related systems, e.g. S--F--S[58] and B--F--B[59], are also part of four- and five-membered ring structures. The experimental Si--F bridging bond length in **6** varies between 189.8 pm and 206.5 pm in the solid state, which corresponds to a bond lengthening of 21.7-32.5%, relative to SiF_4. The calculated Si--F bond lengthening in **4-5** is 18-22%, using the 3-21G* and 6-31G* basis sets, and 15% according to STO-3G* calculations.

The calculations of the linearly-bridged anions **1-3**, show a lengthening of 18-22% (6-31G*) and 15-19% (3-21G* and STO-3G*), which is nearly identical to that of the cyclic anions **4-5**. Anion **3** has an eclipsed (D_{4h}) geometry, with a lengthening of 21% (6-31G*) or 17-16% (3-21G* and STO-3G*) for the bridge bond, relative to SiF_4. For the isoelectronic anion $P_2F_{11}^-$, the calculated lengthening of the bridging bond is 18%, relative to PF_5, and the energy of the staggered (D_{4d}) conformation is only 0.59 kJ mol^{-1} lower than the eclipsed (D_{4h}), implying virtually free rotation about the bridging bond. The calculations therefore support the view that substantial bond lengthening/weakening occurs as a consequence of the formation of Si--F--Si intermediates, hence, these bridged intermediates can provide a pathway for rapid cleavage of silicon-fluorine bonds in fluorosilanes and -silicates, as well as related fluoro compounds. Although the experimental and calculated Si--F bridging bonds of **1-6** are in the range 174-207 pm, they are still less than the sum of the van der Waals radii of 360-370 pm.

A crude estimate of the experimentally determined strength of these silicon-fluorine bridging bonds may be obtained from dynamic NMR studies of fluorine exchange, which show energy barriers of about 21 kJ mol^{-1} for the SiF_5^--SiF_6^{2-} system, 23 kJ mol^{-1} for the $MeSiF_3$-$MeSiF_4^-$ system,[5] and 38 kJ mol^{-1} for **6**.[49]

2.1.3.2 Silicon-carbon bond cleavage

NMR studies of fluorine exchange in organosilicon fluorides, and in related main group compounds of tin, phosphorus and tellurium, have demonstrated that rapid cleavage of element-fluorine bonds is not accompanied by cleavage of element-carbon bonds. Therefore, the pathway by which Si-C bonds are weakened must differ significantly from that of Si-F bonds, as postulated in Scheme 2.

The calculated Si-C bond lengths for the series $PhSiF_3$, $PhSiF_4^-$, and $PhSiF_5^{2-}$ are shown in Table 5, and these values are compared with experimental data for $PhSiF_3$ and $PhSiF_4^-$. For some of the calculations shown in Table 5, the geometry of the phenyl ring was relaxed, and this reduced the Si-C bond length slightly. There is a moderate lengthening/weakening of the Si-C bond with increasing fluorine content, for example, the experimental lengthening of the Si-C bond is 4.1% in $PhSiF_4^-$, relative to $PhSiF_3$, and this may be compared with the calculated bond lengthening of 4.4-6.9%. The calculations show greater bond lengthening of 11-14% in $PhSiF_5^{2-}$ (3-21G* and 6-31G*), relative to $PhSiF_3$. These calculations are in agreement with IR studies which indicate that the force constant of the Si-C bond in $PhSiF_5^{2-}$, as well as of the Si-C bond, in $MeSiF_5^{2-}$ is smaller than in $MeSiF_3$[60]. Since NMR studies have shown that Si-C bond cleavage does not occur in these purified compounds under mild thermal conditions, therefore, we may conclude that a bond lengthening of about 4-14% is insufficient to cause Si-C bond cleavage in $PhSiF_4^-$ or $PhSiF_5^{2-}$ under these conditions.

Table 5. Experimental and calculated Si-C bridging bond lengths (pm), and lengthening of bridging bond (%) relative to $PhSiF_3$.

	Experimental	6-31G*	3-21G*	STO-3G*
$PhSiF_3$	182.2[56]	180.0	182.5	184.3
$PhSiF_4^-$	189.6[56] (4.1%)	192.5,[a] 193.2 (6.9%)	190.6,[a] 191.3 (4.4%)	196.1,[a] 196.6 (6.4%)
$PhSiF_5^{2-}$		204.7 (13.7%)	202.0,[a] 203.1 (10.7%)	217.3 (17.9%)
$\{Ph\text{--}SiF5^{\cdot -}\}$		360.2 (200%)	312.6,[a] 312.6 (171%)	336.2 (182%)

[a] Geometry of phenyl ring relaxed.

Substantially greater changes in Si-C bond lengths accompany a formal change in electron count, as $PhSiF_5^{2-}$ is oxidized to $\{Ph\text{--}SiF_5^{\cdot-}\}$. The calculated Si-C bond in $\{Ph\text{--}SiF_5^{\cdot-}\}$ is in the range 313-360 pm, which corresponds to a lengthening of 171-200%, relative to $PhSiF_3$. These calculated bond lengths of 313-360 pm approach the sum of the van der Waals radii of 375 pm,[61] implying that $\{Ph\text{--}SiF_5^{\cdot-}\}$ consists essentially of a phenyl radical and anionic SiF_5^-. Such a view is supported by the calculated Si-F bond lengths of $\{Ph\text{--}SiF_5^{\cdot-}\}$ in Table 4, which are those of anionic SiF_5^-. We conclude that oxidation of $PhSiF_5^{2-}$ to $\{Ph\text{--}SiF_5^{\cdot-}\}$ must be followed by the rapid appearance of phenyl radical and SiF_5^-. The experimental result of Kumada and co-workers, who found complete loss of stereospecificity in the Cu(II) cleavage of Si-C bonds in norbornylpentafluorosilicates,[62] is in agreement with the formation of alkyl radicals after an oxidation step.

Organopentafluorosilicates $RSiF_5^{2-}$ are known to be stable in aqueous solution,[5] and we carried out calculations, with full optimization and polarization functions (6-31G**), of three water-bonded intermediates. In one intermediate, $MeSiF_5^{2-}$-H_2O as shown in Figure 26, water was hydrogen-bonded to two fluorines of $MeSiF_5^{2-}$.

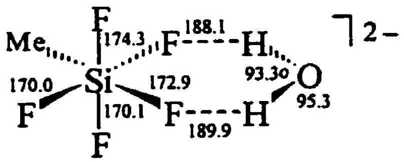

(6-31G**)

Figure 26. Optimised geometry for $MeSiF_5^{2-}$-H_2O.

In another calculation, only one hydrogen-bond between water and $MeSiF_5^{2-}$ was initially assumed, but the optimised geometry of this calculation was essentially that of $MeSiF_5^{2-}$-H_2O shown in Figure 26. In a third calculation, water was treated as a seventh ligand and placed along a pseudo-C_3 axis of octahedral $MeSiF_5^{2-}$, but this calculation also converged towards the geometry of $MeSiF_5^{2-}$-H_2O shown in Figure 26. Since the hydrogen bonds in $MeSiF_5^{2-}$-H_2O remain relatively long, 189.1 pm (av), while the bridging Si-F bond in $MeSiF_5^{2-}$-H_2O, 173.6 pm (av), is lengthened only 11% relative SiF_4, we conclude that $MeSiF_5^{2-}$ is likely to be stable in water, in agreement with experiment. On the other hand, $RSiF_5^{2-}$ is expected to decompose slowly in the H_2O-HF-glass system because of the release of boron and silicon-containing Lewis acids from glass in this system.[53]

2.1.4 Conclusions

1. The *ab initio* calculations of organosilanes and -silicates support the view that cleavage of Si-F bonds occurs by way of a Si--F--Si bridged intermediate, while cleavage of Si-C bonds occurs by way of a radical anion $RSiF_5^{\cdot-}$. These intermediates contain, formally, 8-F-2 fluorine and 11-Si-6 silicon, respectively, and the discrete variables of coordination number and electron count, combined with the classification of elementary steps, i.e. +C, -C, $+C^c$, $-C^c$, proved helpful in our detailed analysis of multi-step reaction pathways. Calculated bond lengths in cyclic and linear Si--F--Si intermediates are very similar, but the preference of cyclic intermediates is ascribed to a favourable ratio of $+C^c/+C$, where $+C^c$ refers to an intramolecular step, and +C to a diffusion-controlled intermolecular step.[2] In the absence of reliable thermodynamic and kinetic data of

reactive intermediates, the calculated bond lengths may serve as a simple criterion of bond cleavage, -C, and the generalisation, "the longer the bond, the faster it breaks"[169] is therefore applied to these reactive intermediates.

2. The *ab initio* calculations are in general agreement with the stability of organopentafluorosilicates $RSiF_5^{2-}$ in aqueous solution.

3. Synthetic, mechanistic, and theoretical studies of organofluorosilanes and silicates agree that fluoride ion in aqueous solution, in combination with common oxidizing agents, can transform organometallic compounds into sources of aryl and alkyl free radicals. This finding may have important implications for synthetic, as well as environmental[64] aspects of fluorine and organometallic chemistry.

2.2 Reaction mechanisms of phosphorus fluorides: an *ab* initio study

2.2.1 Introduction

Calculations have been carried out for phosphorus fluorides, and these results are related to mechanistic details such as rapid equilibria between five- and six-coordinate phosphorus compounds, exchange of axial and equatorial fluorines in PF_5, the cleavage of P-F bonds in phosphorus compounds, and the mechanism of oxidation of phosphorus(III) to phosphorus(V) fluorides.

2.2.2. Results and discussion

In order to test the statement that trigonal bipyramidal molecules are among the most sensitive indicators of bond formation, +C, because of the change in symmetry and

NMR spin pattern that accompanies the formation of six-coordinate adducts or intermediates,[53] we studied the interaction of PF_5 with Lewis bases of widely differing basicity (eq 32b), and calculated the structures of adducts **7-12**.

$$[32b] \qquad PF_5 + D \xrightleftharpoons[-C]{+C} D\text{-}PF_5$$

$$D = \mathbf{7}\ NH_3 \quad \mathbf{8}\ H_2O \quad \mathbf{9}\ CH_3F$$

$$\mathbf{10}\ HF \quad \mathbf{11}\ PF_5 \quad \mathbf{12}\ PF_6^-$$

As a six-coordinate adduct such as $H_3N\text{-}PF_5$ **7** is formed, the coordination number of phosphorus is increased from 5 to 6, and nitrogen from 3 to 4, i.e., $+C_{P(5)N(3)}$. Cleavage of a P-N bond in adduct **7** is denoted as $-C_{P(5)N(3)}$. If the calculated structures confirm that four basal fluorines in adducts **7-12** are essentially equivalent, then it is reasonable to assume that an equilibrium between five- and six-coordinate phosphorus species (see eq 32b), can provide a pathway for the exchange of axial and equatorial fluorines in PF_5. Our criterion for evaluating the equivalence of four basal $P\text{-}F^b$ bonds is based on a qualitative comparison of $P\text{-}F^b$ bond lengths and $\angle F^aPF^b$ bond angles. Other means of estimating the distortion from D_{3h} or C_{4v} symmetry in phosphorus or silicon fluorides have been proposed by Holmes.[68]

Of adducts **7-12**, only **7** is sufficiently inert to allow characterization by NMR spectroscopy and X-ray crystallography,[69] but some indirect evidence supports the existence of **8-12**. For example, adduct **8** has not been characterized, but the closely related adduct $Et_2O\text{-}PF_5$ is stable below -65°C.[70] Furthermore, the deprotonated anion F_5PO^{2-},[71] and related species F_5AsOH^-[72] and $H_2O\text{-}GeF_5^-$,[73] have been described in the literature. The adducts H_3N-PF_5 **7** and H_2O-PF_5 **8** are reasonable intermediates of ammonolysis and hydrolysis reactions, respectively.[69,70] Adducts CH_3F-PF_5 **9** and HF-PF_5 **10** are unknown, but related adducts with somewhat stronger Lewis acids have been identified by NMR at low temperature, e.g., CH_3F-AsF_5 and CH_3F-SbF_5.[74] Suggestions have been made that dimeric PF_5 **11**,[75] or dimeric SiF_5^-,[5] might contribute to axial-equatorial ligand exchange. NMR studies on the PF_5-PF_6^- [76] and $PhPF_4$-$PhPF_5^-$ [7] systems confirm that rapid P-F bond cleavage occurs in these systems, and a bridged intermediate, e.g., $P_2F_{11}^-$ **12**, can account for the NMR results.

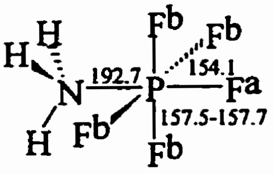
H
H
N
H
192.7
P
Fb
Fb
154.1
Fa
Fb
157.5-157.7
Fb

∠FaPFb = 93.3°

7 [6-311G*(2d,2p)]

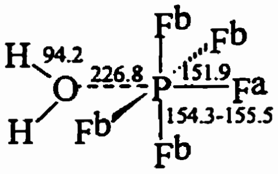
H
94.2
O
H
226.8
P
Fb
Fb
151.9
Fa
Fb
154.3-155.5
Fb

∠FaPFb = 97.7-99.6°

8 [6-311G*(2d,2p)]

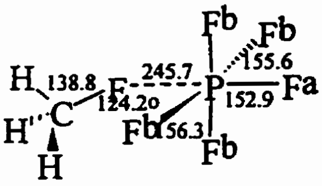
H
138.8
C
H
H
124.2°
F
245.7
P
Fb
Fb
155.6
Fa
152.9
Fb
156.3
Fb

∠FaPFb = 100.6-101.2°

9 (6-31G**)

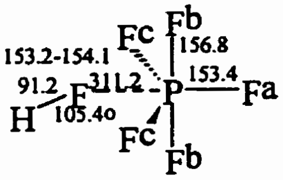
153.2-154.1
Fc
Fb
156.8
91.2
F
311.2
P
153.4
Fa
H
105.4°
Fc
Fb

∠ FaPFb = 91.0°

∠ FaPFc = 116.8-117.0

10 (6-31G**)

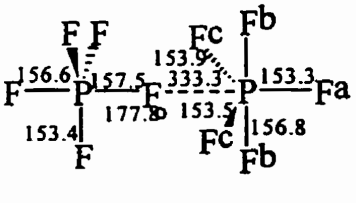
F F
F
156.6
P
157.5
F
333.3
P
153.3
Fa
153.9
Fc
Fb
153.4
F
177.8°
153.5
Fc
156.8
Fb

∠ FaPFb = 90.4 °

∠FaPFc = 118.8-118.9 °

11 (6-31G*)

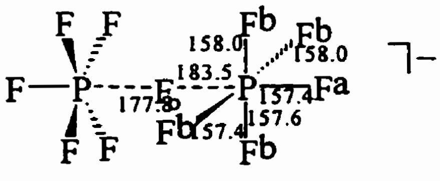
F F
F
P
F F
177.8°
F
183.5
P
158.0
Fb
Fb
158.0
157.4
Fa
Fb
157.4
157.6
Fb
1-

∠FaPFb = 94.0-94.3 °

12 (6-31G*)

Calculations were carried out with several basis sets, and they confirm that the four basal fluorines in adduct H_3N-PF_5 **7** are essentially equivalent. With the 6-311G*(2d,2p) basis set, the four basal P-F^b bond lengths in 7 are in the range 157.5-157.7 pm, and the four angles between the apical and basal fluorines, $\angle F^aPF^b$, are all 93.3°. With the 3-21G* basis set, very similar results were obtained, namely, four basal P-F^b bond lengths in the range 158.1-158.2 pm, and four angles $\angle F^aPF^b$ in the range 94.5-94.6°. Calculations therefore show that all basal P-F^b bonds in adduct **7** are essentially equivalent. These results may be compared with experimental P-F^b bond lengths in the solid state, which are in the range 158.9-160.0 pm, and $\angle F^aPF^b$ in the range 90.8-92.3°.[69]

The calculated lengths of the P-N bond in **7** are 192.7 pm [6-311G*(2d,2p)], 193.1 pm (3-21G*), and 195.1 pm (MINI-1). In the solid state, the experimental P-N bond length is 184.2 pm.[68]

Calculations with the 6-311G*(2d,2p) basis set also show that adduct H_2O-PF_5 8 has four essentially equivalent basal fluorines, with P-F^b bond lengths in the range 154.3-155.5 pm, and bond angles $\angle F^aPF^b$ in the range 97.7-99.6 °. It was suggested some time ago that the rapid formation and dissociation of adduct **8** can lead to exchange of axial and equatorial fluorines in PF_5[70].

Adduct CH_3F-PF_5 **9** was selected to test the hypothesis that "inert" solvents may bring about axial-equatorial ligand exchange in PF_5 without participating in further chemical reactions [53]. Calculations with the 6-31G* basis set show four basal P-F^b bond lengths in the range 155.6-156.3 pm, and $\angle F^aPF^b$ in the range 100.6-101.2°. These results strongly imply that axial and equatorial fluorines in PF_5 can be exchanged as a result of interaction with a solvent such as CH_3F. A similar conclusion is reached on the basis of 3-21G* calculations, which show four basal $P\text{-}F^b$ bond lengths in the range 155.9-157.4 pm, and four bond angles $\angle F^aPF^b$ in the range 97.0-98.0°.

It is uncertain from our calculation of **10** or **11** whether interaction with HF, or with another PF_5 molecule, leads to exchange of axial and equatorial fluorines in PF_5. Adduct **10** (6-31G**) shows a relatively large variation in $P\text{-}F^b$ and $P\text{-}F^c$ bond lengths in the range of 153.2-156.8 pm, and bond angles $\angle F^aPF^b$ and $\angle F^aPF^c$ in the range 91.0-117.0°. The long bond between HF and PF_5, namely, 311.2 pm (6-31G**), or 211.1 pm (3-21G*), implies that **10** is a very weakly bound adduct in which the PF_5 moiety is only slightly distorted. Similar comments can be made about the PF_5 dimer **11**, where calculation (6-31G*) shows relatively large variation in basal P-F bond lengths, 153.3-156.8 pm, and $\angle F^aPF^b$ and $\angle F^aPF^c$ bond angles, 90.4-118.9°.

Calculation (6-31G*) of the fluorine-bridged anion $P_2F_{11}^-$ **12** shows four basal $P\text{-}F^b$ bond lengths in the range 157.4-158.0 pm, and $\angle F^aPF^b$ in the range 94.0-94.3°, indicating that **12** has essentially equivalent basal fluorines.

In summary, the calculations described above are in agreement with the view that axial and equatorial fluorines in PF_5 undergo intramolecular ligand exchange as a result of bond formation, +C, whenever PF_5 interacts with a donor molecule such as NH_3, OH_2, CH_3F and PF_6^-, to give adducts **7-9,12** (eq 32b). The calculated structures of adducts **10-11**, however, suggest that the interaction with HF, or with another PF_5 molecule, probably does not bring about exchange of axial and equatorial fluorines in PF_5.

NMR studies show clearly that rapid bond cleavage occurs in the PF_5-PF_6^-[76] and $PhPF_4$-$PhPF_5^-$[7] systems. The calculated structure of intermediate **12** shows a substantially longer/weaker P--F bridging bond of 183.5 pm, as compared to the terminal P-F bond lengths of 157.4-158.0 pm. This calculated (6-31G*) bridge bond of 183.5 pm may be compared with a previous calculation of 183.1 pm.[77] An analogously bridged intermediate $Si_2F_{11}^{3-}$ can account for rapid intermolecular fluorine exchange in the SiF_5^--SiF_6^{2-} system[5] as discussed above. As the strength of the bridging bond increases in related anions such as $As_2F_{11}^-$ or $Sb_2F_{11}^-$, the bridged species can be identified in solution, or isolated.[78]

NMR experiments show that P-F coupling is retained in purified samples of PF_5, or when PF_5 is dissolved in solvents such as CH_3F.[53] Furthermore, PF_5 is a nonelectrolyte and has a small solubility in hydrogen fluoride.[79] Based on the calculated structures of **9-11**, only cleavage of the weakest/longest P--F bridge bond in **9-11** is expected, which leaves the original PF_5 molecule intact. For example, the calculated long/weak bridging P--F bond in **9**, namely, 245.7 pm (6-31G*) or 196.5 (3-21G*), may be compared to the shorter/stronger terminal P-F bonds of 152.9-156.3 pm (6-31G*), or 154.1-157.4 pm (3-21G*). Only a simple dissociation of adduct CH_3F-PF_5 **9** is thus expected, with no further chemical reaction, and this result is consistent with the known stability of PF_5 in hydrocarbon and halogenated solvents.

Similar arguments can be applied to **10** and **11** to account for the chemical stability of PF_5 in the presence of HF, or in the presence of other PF_5 molecules.

To test for the possibility that hydrogen bonding might lead to P-F bond cleavage, the calculation (6-31G**) of **13** and **14** was carried out. However, other than a small lengthening of the axial or equatorial P-F bond, no significant changes are evident in the PF_5 moiety. The trigonal bipyramidal geometry of PF_5 is not significantly distorted; therefore, neither chemical reaction nor axial-equatorial fluorine exchange is expected as a result of the formation of hydrogen-bridged intermediates **13-14**.

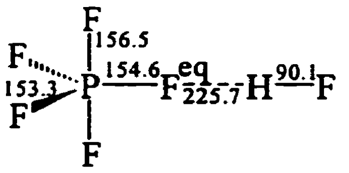

13 (6-31G**)

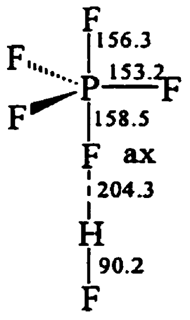

14 (6-31G**)

Finally, a mechanism of oxidation of phosphorus(III) to phosphorus(V) fluorides is proposed (Scheme 3) which is based on the mechanism of oxidation of sulfur(IV) to sulfur(VI) fluorides in the presence of fluoride ion.[67] The latter mechanism postulates initial attack of F^- on sulfur(IV) compounds, followed by oxidation to a fluorosulfur radical and, lastly, reaction with a suitable fluorine atom donor to give the sulfur(VI) product. Again, the N-X-L notation of Perkins *et al.*[48] is used in Scheme 3 to specify the valence electron count (N) and coordination number (L) of phosphorus (X). Calculations for **15-18** were not carried out in this study because both calculated and experimental results have been reported by others.[80-83]

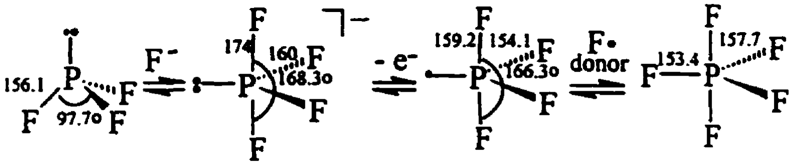

8-P-3 10-P-4 9-P-4 10-P-5

15 **16** **17** **18**

Scheme 3. Proposed mechanism of oxidation of P(III) to P(V) fluorides in the presence of F^-.

The fact that F^- adds readily to PF_3 to give anion PF_4^-, in solution[81] or in the gas phase,[84] is in agreement with the first step of the proposed mechanism (Scheme 3). In the absence of F^- (and PF_4^-), the mechanism of oxidation is presumably simplified to $PF_3 \rightarrow PF_4\cdot \rightarrow PF_5$, as suggested for the free-radical addition of fluorine atoms to PF_3[85]. In principle, a sharp distinction exists between an oxidation that occurs in the presence of F^-, and a free-radical oxidation that occurs in the absence of F^-, but this distinction may be difficult to observe in practice because of the inadvertent introduction of fluoride ion during the course of typical oxidative-fluorinations. The finding that the rate of oxidative-chlorination of PF_3 is photosensitive, but also catalysed by glass surfaces,[86] hints at these experimental difficulties.

Scheme 3 does not identify the electron acceptor that converts anion PF_4^- **16** to radical $PF_4\cdot$ **17**. However, for the related anion-to-radical oxidation of $PhSiF_5^{2-}$ to $PhSiF_5^{-}\cdot$, numerous one-electron acceptors can be used, including metal ions, halogen compounds, tetracyanoethylene, etc..[87]

The last step of Scheme 3 involves the interaction of $PF_4\cdot$ with a fluorine atom donor to give the product PF_5. For typical oxidative-fluorinating agents such as F_2, ClF or XeF_2, we postulate that rapid bond cleavage occurs as a result of the formation of intermediates $F_4P\text{-}F\text{--}F\cdot$, $F_4P\text{-}F\text{--}Cl\cdot$ or $F_4P\text{-}F\text{--}XeF\cdot$, respectively. An explanation for the catalytic role of F^- is then apparent, because the presence of F^- allows bond cleavage of very weakly bound intermediates, e.g., $F_4P\text{-}F\text{--}F\cdot \rightarrow PF_5 + F\cdot$, however, in the absence of F^- the oxidizing agents themselves must undergo bond cleavage to give radical intermediates, e.g. $F\text{-}F \rightarrow 2\ F\cdot$.

It is interesting to speculate whether the catalytic role of F^- (Scheme 3) applies to less electronegative anions such as Cl^-, and the X-ray structure of the anion PCl_4^- provides some insight into this question. There are nonequivalent axial P-Cl bonds in PCl_4^-, 211.8 and 285.0 pm,[88] and the substantial lengthening of one of the axial P-Cl bonds (285.0 pm) raises the possibility that the lifetime of anion PCl_4^- in solution might be relatively short, as compared to that of anion PF_4^-. This suggests that electronegative anions such as F^-, and perhaps HO^-, are suitable catalysts for oxidation of phosphorus(III) compounds, whereas larger and less electronegative anions such as Cl^- or Br^- are less effective. Without a catalyst, oxidation may follow a free-radical pathway and, indeed, radical $PCl_4\cdot$ is a known species.[89]

2.2.3 Methods

The GAUSSIAN92 system of programs[90] was used for all ab initio molecular orbital calculations. Interacting molecules and ions were treated as one large system and were fully optimized with analytical gradient method at restricted Hartree-Fock level, using basis sets 3-21* and 6-31G*. Polarization basis sets, 6-31G**, with p orbitals for each hydrogen, were used for hydrogen-bond structures **10**, **13**, and **14**, and triple split-valence orbital basis set 6-311G*(2d,2p) were used for structures **7** and **8**.

For the MINI-1 calculations, Huzinaga's minimal basis set[91] was used with the atomic scaling factors of Deisz.[92] Binding energies were determined by the supermolecule approach with the full counterpoise correction of Boys and Bernardi.[93]

CHAPTER 3

OXIDATIVE HALOGENATION OF SULFUR TO SULFUR (VI) COMPOUNDS

3.1. Introduction

3.1.1 Oxidative halogenation of sulfur compounds to sulfur(VI) compounds

Main group fluoride derivatives in high oxidation states are frequently obtained by oxidative fluorination of their corresponding lower valent compounds. For sulfur, these include sulfur tetrafluoride, bis(alkyl) sulfides, sulfurane, diperfluoroalkyl disulfides and substituted sulfur(IV) compounds[94-118]. A variety of powerful fluorinating agents such as CoF_3, AgF_2, CsF, CF_3OF, ClF, F_2, BrF_3, XeF_2 and electrochemical fluorination have been used to accomplish the oxidative addition of fluorine to these lower valent sulfur compounds.

Oxidative fluorination of organosulfur compounds may produce cis and trans isomers of the corresponding organosulfur(VI) fluorides. Both cis and trans isomers of six-coordinate organosulfur(VI) fluorides are known. The outcome of the fluorination reaction is difficult to predict because of the mechanistic complexity of competing oxidative-addition, isomerization, and ligand exchange processes. Complexity also arises from the H_2O-HF-glass system because of the potential introduction of BF_3 or SiF_4:[54] these strong Lewis acids are known to isomerize six-coordinate S(VI) and Te(VI) fluorides via cationic intermediates.[110,151] Simple generalizations about the mechanisms of oxidative fluorination reactions of organosulfur fluorides are lacking in the literature, due to the difficulty of identifying and eliminating trace impurities.

There are very few reactions known that result in the formation of both cis and trans isomers of the sulfur(VI) derivatives. For example, only cis addition product, *cis*-$(R_fO)_2SF_4$ is reported when sulfur tetrafluoride is used as the starting material to react with good sources of free radicals such as peroxides,[94,95,160a] trioxides,[96] fluoroxy compounds,[95] and hypochlorites.[97] Only trans addition product, *trans*-tetrafluorobis(perfluoroalkyl)sulfur, *trans*-$(R_f)_2SF_4$, was found when electrochemical fluorination method was used.[98] Similarly, when reaction was carried out under ionic conditions, only the trans isomers were formed.[103,109] A rare example of isomeric mixtures results from oxidative-addition reactions of chlorine monofluoride with bis(perfluoroalkyl)sulfides. These reactions gave a mixture of *cis*- and *trans*-tetrafluorobis(perfluoroalkyl)sulfur with the trans isomer being predominant. In contrast, alkyl perfluoroalkyl sulfide and $CF_3SCH_2SCF_3$ form only trans isomers under the same conditions. These results are identical with those for the unsymmetrically substituted R_fSCl moieties.[110] A cis/trans isomeric mixture was formed in a ratio of 1:3 when sulfur tetrafluoride was reacted with (difluoronitridothio)imidosulfurous difluoride in the presence of CsF.[111]

$$N{=}SF_2NSF_2 \ + \ SF_4 \xrightarrow{CsF} \mathit{cis\text{-}/trans\text{-}}(F_2SN)_2SF_4$$

Both cis and trans isomers of tetrafluorobis(perfluoroalkoxy)sulfur $F_4S(OR_f)_2$ were prepared by oxidative-addition reactions between chlorine monofluoride and sulfur(IV) compounds (trifluoromethyl)imidosulfites, $CF_3N{=}S(OR_f)_2$ ($R_f = CF_3CH_2$, $CF_3CF_2CH_2$, and $CF_3CF_2CF_2CH_2$).[153] Organosulfur (VI) fluorides have been prepared by a variety of methods and some representative examples are discussed below.

3.1.1.1 Cobalt trifluoride, CoF_3

One of the very first fluorinating reagents used to oxidatively fluorinate organosulfur (I and II) compounds was cobalt trifluoride. In 1950, Silvey and Cady[100] studied the reaction of methyl mercaptan with cobalt trifluoride. The yield of CF_3SF_5 resulting from this reaction at 200 °C was about 15% based on the quantity of mercaptan used. They also found that CF_3SF_5 did not react with NaOH for 2.5 months at room temperature.

$$[33] \quad CF_3SH + CoF_3 \longrightarrow \underset{\text{yield: 15\%}}{CF_3SF_5}$$

3.1.1.2 Electrochemical fluorination

Electrochemical fluorination of dimethyl sulfide in anhydrous hydrogen fluoride was carried out by Emeleus and co-workers[98] in 1953. Conversion of the low valent organosulfur into six valent organosulfur occurred at an early stage in the electrolysis. In this reaction, 20% CF_3SF_5 and 2% $(CF_3)_2SF_4$ were obtained. However, attempts to fluorinate the corresponding selenium compounds were unsuccessful.

$$[34]\quad CF_3SCF_3 \xrightarrow[\text{in anhydrous HF}]{\text{Electrochemical fluorination}} CF_3SF_5 + (CF_3)_2SF_4$$

Dialkyl sulfides were found to yield the corresponding di-perfluoroalkylsulfur tetrafluoride, $(R_f)_2SF_4$, together with degradation products.

3.1.1.3 Silver difluoride, AgF_2

Many (partially) fluorinated compounds were first prepared by the reaction of silver difluoride with the corresponding low valent organosulfur compounds. For example, Martin and co-workers[99] accomplished the oxidative fluorination of sultene with silver difluoride to generate the corresponding difluorosulfurane, as shown in eq.35.

[35]

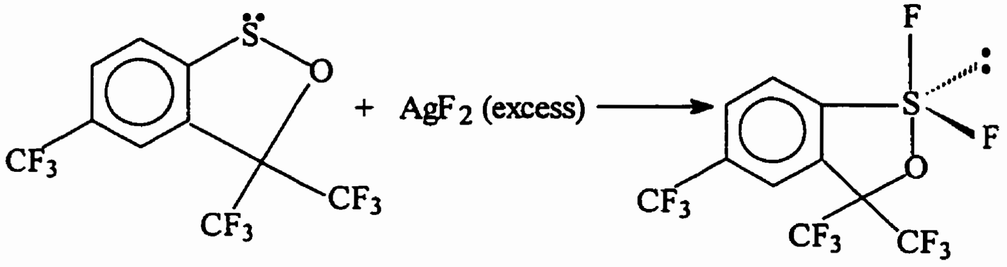

The interesting structural feature about this difluorosulfurane is that, in contrast to $RR'SF_2$, it contains non-equivalent fluorine atoms bonded to sulfur, as its ^{19}F NMR spectrum shows nonequivalent trifluoromethyl groups and non-equivalent fluorines bonded to sulfur.

The first general synthesis of arylsulfur trifluoride and the first synthesis of arylsulfur pentafluoride was also achieved by the reaction of ArSSAr with AgF_2 in 1962 by Sheppard,[102] as shown in eq [36]-[37].

$$[36]\quad Ar_2S_2 + 6AgF_2 \longrightarrow 2ArSF_3 + 6AgF$$

$$[37]\quad ArSF_3 + 2AgF_2 \xrightarrow{130\,^{o}C} ArSF_5 + 2AgF$$

Phenylsulfur trifluoride is obtained in 50 to 60% yield by the exothermic reaction of silver difluoride with a solution of phenyldisulfur in a Freon solvent, 1,1,2-trichloro-1,2,2,-trifluoroethane. When phenylsulfur trifluoride is heated gradually to 130 °C with silver difluoride in a reactor made of copper or ptfe (polytetrafluoroethylene), phenylsulfur pentafluoride is obtained in about 10% yield.

3.1.1.4 Cesium fluoride and chlorine, CsF/Cl_2

CsF, used with chlorine, is a useful oxidative fluorinating agent for organosulfur compounds. Muetterties and co-workers[101] prepared $ClSF_5$ in high yield from sulfur tetrafluoride by the reaction of chlorine in the presence of cesium fluoride as shown in eq [38].

$$[38]\quad SF_4 + CsF + Cl_2 \longrightarrow SF_5Cl + CsCl$$

They suggested that the role of cesium fluoride is to react with sulfur tetrafluoride to yield the cesium salt $Cs^+SF_5^-$, which could be the intermediate in the synthesis of $ClSF_5$.

The synthesis of substituted derivatives of $ClSF_5$ resulting from the corresponding reaction using substituted derivatives of SF_4 was carried out by Darragh and Sharp.[103] For example, chlorine reacts with trifluoromethylsulfur trifluoride in the presence of CsF at room temperature to give *trans*-trifluoromethylsulfur(VI) chloride tetrafluoride, *trans*-CF_3SF_4Cl.

$$[39]\quad CF_3SF_3 + CsF + Cl_2 \longrightarrow CF_3SF_4Cl + CsCl$$

Trans-$CF_3SF_4^-$ was postulated as an intermediate, and this reaction, shown in eq [40], was later proved by Minkwitz and Werner.[104]

$$[40]\quad CF_3SF_3 + CsF \xrightarrow{400\text{-}500^{o}C} Cs^+CF_3SF_4^-$$

CF_3SF_4Cl reacts in Pyrex apparatus with olefins and acetylenes, when U.V. irradiated, to give products resulting from addition of *trans*-CF_3SF_4Cl across the multiple C-C bond.[106]

[41]

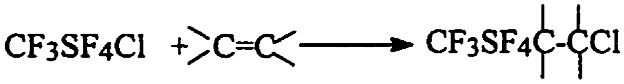

$$CF_3SF_4Cl + {>}C{=}C{<} \longrightarrow CF_3SF_4\overset{|}{\underset{|}{C}}-\overset{|}{\underset{|}{C}}Cl$$

3.1.1.5 Trifluoromethyl hypofluorite, CF_3OF

Trifluoromethyl hypofluorite, CF_3OF, has been used for oxidative fluorination of SF_4 and R'SR.[107] Trifluoromethyl hypofluorite reacts with sulfur tetrafluoride to form CF_3OSF_5 and $(CF_3O)_2SF_4$ as seen in eq [42].

$$[42]\quad SF_4 + CF_3OF \longrightarrow CF_3OSF_5 + (CF_3O)_2SF_4$$

When CF_3OF and SF_4 were allowed to react in the presence of N_2F_4, the ^{19}F NMR spectrum indicated the formation[111] of *cis*-$CF_3SF_4NF_2$.

$$[43]\ SF_4 + CF_3OF + N_2F_4 \longrightarrow CF_3OSF_5 + \textit{cis}\text{-}CF_3SF_4NF_2$$

Denny and co-workers[108] reported that dialkyl and diaryl sulfides react with trifluoromethyl hypofluorite very easily to yield dialkyl- and diaryl sulfur difluoride at -78 °C. If excess CF_3OF was used, the oxidative fluorination may go further, but the conversion of difluorosulfurane was quite slow and a large excess of CF_3OF was required.

$$[44]\quad CF_3OF + RSR' \longrightarrow RR'SF_2 \xrightarrow[\text{large excess}]{CF_3OF} \textit{trans}\text{-}RR'SF_4$$

3.1.1.6 Chlorine monofluoride, ClF

Chlorine monofluoride, ClF, is one of the most reactive halogen fluorides. Extensive studies by Shreeve *et al*[109,110] have shown that ClF is a very useful oxidative fluorination reagent for preparation of perfluoroalkyl sulfur (VI) fluoride and chloride compounds.

When ClF is used in reactions with perfluoroalkylsulfenyl chlorides (R_fSCl) and perfluoroalkyl disulfides (R_fSSR_f) at 25 °C, chlorine monofluoride acts primarily as a chlorinating and fluorinating reagent to give R_fSF_4Cl, in modest yields. However, small amounts of perfluoroalkylsulfur pentafluoride, R_fSF_5, are also obtained as shown in eq [45].

$$[45]\quad R_fSCl \text{ or } R_fSSR_f + ClF \longrightarrow \textit{trans}\text{-}R_fSF_4Cl + R_fSF_5$$

Oxidative additions of excess ClF with bis(perfluoroalkyl)sulfides can also occur readily according to eq [46].

$$[46]\quad R_fSSR_f' + ClF \longrightarrow \begin{array}{ll} \textit{cis-}\text{ and }\textit{trans-}R_fSF_4R_f' & \\ R_f{=}R_f'{=}CF_3 & \text{yield: } 42\% \\ R_f{=}CF_3,\ R_f'{=}C_2F_5 & \text{yield: } 13\% \end{array}$$

A mixture of both *cis* and *trans* isomers of bis(perfluoroalkyl)sulfur tetrafluoride forms. A family of cis-/trans-sulfur hexafluoride derivatives, tetrafluoro-bis(polyfluoroalkoxy)sulfur, $F_4S(OR_f)_2$ are obtained when chlorine monofluoride reacted with (trifluoromethyl)imidosulfites,[153] $CF_3N{=}S(OR_f)_2$, ($R_f = CF_3CH_2$, $CF_3CF_2CH_2$, and $CF_3\,CF_2CF_2CH_2$).

$$[47]\quad CF_3N{=}S(OR_f)_2 + ClF \xrightarrow[10\ h]{-78\ ^{o}} \textit{cis-/trans-}(R_fO)_2SF_4 + Cl_2$$

Chlorine monofluoride also reacts with dialkyl sulfoxide $R_fS(O)R_f'$ to give bis(perfluoroalkyl)sulfur oxydifluorides[112].

$$[48]\quad R_fS(O)R_f' + ClF \longrightarrow R_fS(O)F_2R_f'$$

3.1.1.7 Elemental fluorine, F_2

Direct liquid-phase fluorination (with dilution of substrate and fluorine) can, to some extent, be successful in introducing fluorine while still controlling the reaction as competing CH-substitution or cleavage of the aryl moiety can be largely suppressed.

However, the direct reaction of fluorine with organic compounds usually gives extensive degradation and fragmentation of the starting materials and not simple reaction products. Special techniques are required to give moderately selective fluorination.

Ruppert[113] reported the direct oxidative liquid-phase fluorination of Ph_2S at -78 °C in CF_3Cl to give 1:2 *cis*- and *trans*-diphenyl sulfur (VI) tetrafluoride via isolable Ph_2SF_2. Both *cis*- and *trans*-Ph_2SF_4 were uniformly hydrolyzed in $CHCl_3$, with a little NEt_3, to give Ph_2SO_2.

$$[49]\quad Ph_2S + F_2 \longrightarrow Ph_2SF_2 \xrightarrow{F_2} \textit{cis-}\text{ and }\textit{trans-}Ph_2SF_4 \xrightarrow{H_2O} Ph_2SO_2$$

Using the same technique (oxidative liquid-phase fluorination), Ruppert also prepared diarylsulfur (VI) oxide difluorides,[112] along with the product resulting from the cleavage of the aryl moiety, $ArS(O)F_3$, by the reaction of diarylsulfoxide with elemental fluorine, as shown in eq [50].

$$[50]\quad Ar_2SO + F_2 \longrightarrow Ar_2S(O)F_2 + ArS(O)F_3$$

Lagow and co-workers studied the reaction of *neo*-$C_5H_{11}SH$ with elemental fluorine at -120 °C, and a yield of 24.5% of *neo*-$C_5H_{11}SF_5$, was obtained.[117]

$$[51]\quad \textit{neo-}C_5H_{11}SH + F_2 \xrightarrow{-120\ ^oC} \textit{trans-}(\textit{neo-}C_5H_{11})_2SF_5$$

3.1.1.8 Bromine trifluoride, BrF_3

Bromine trifluoride is less reactive than chlorine monofluoride. Martin and Michalak[118] prepared both *trans*- and *cis*-difluorodialkyloxy diaryl sulfur (VI) isomers by oxidatively fluorinating its corresponding stable sulfurane with two bidentate ligands, using varying amounts of bromine trifluoride, as shown in Scheme 4.

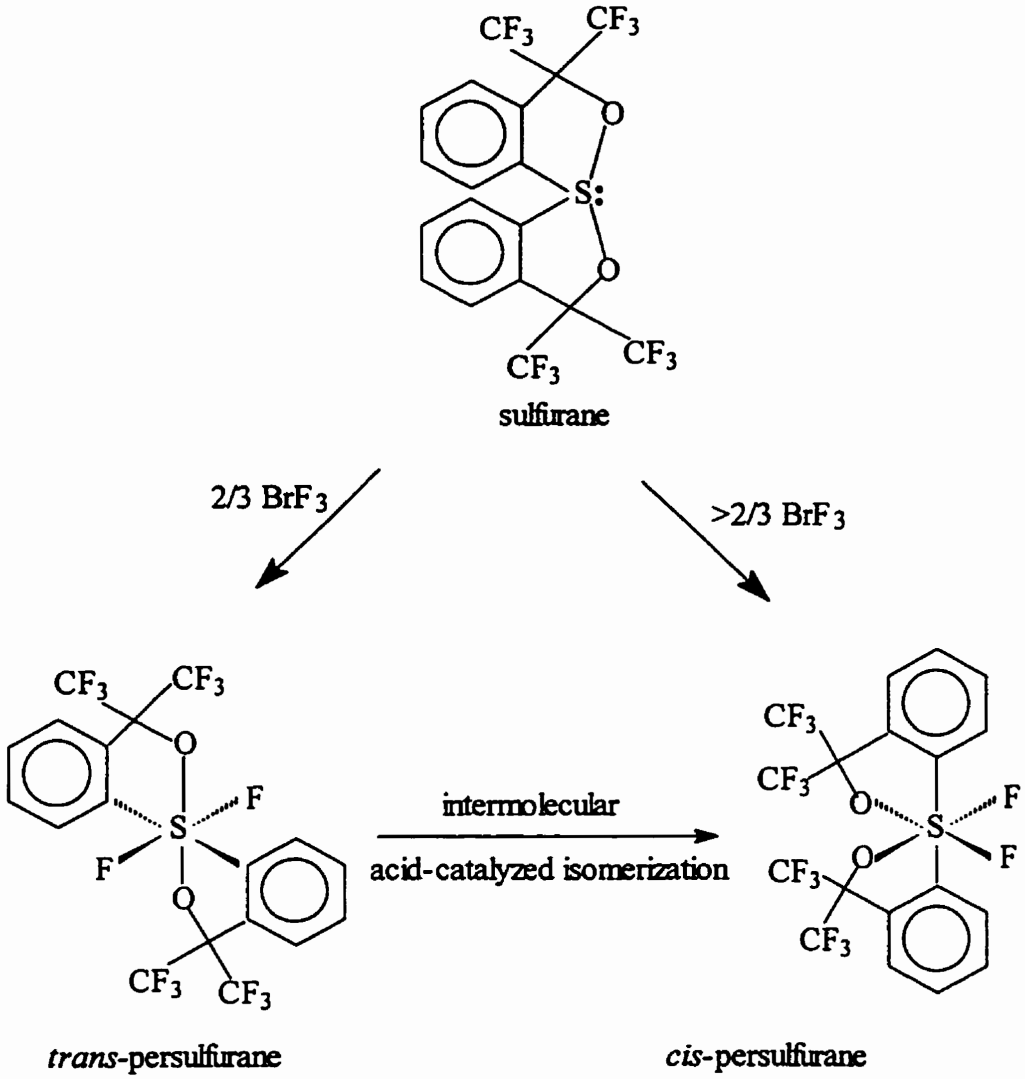

CF3
CF3
O
S:
O
CF3
CF3
sulfurane
2/3 BrF3
>2/3 BrF3
CF3
CF3
O
F
S
F
O
CF3
CF3
intermolecular
acid-catalyzed isomerization
CF3
CF3
O
S
F
O
F
CF3
CF3
trans-persulfurane
cis-persulfurane

Scheme 4. Preparation of both *trans*- and *cis*-difluorodialkyloxy diaryl sulfur (VI) isomers by oxidatively fluorinating its corresponding stable sulfurane.

With a ratio of BrF_3 to sulfurane of 2/3, the kinetically favoured *trans* isomer was obtained, and if the ratio is greater than 2/3, gives thermodynamically stable *cis* isomer. The structures of these two isomers were determined by X-ray crystallography. In addition, thermodynamic studies indicate that the *cis* isomer is slightly more energetically favoured at 25 °C, with acid-catalysed isomerization of *trans* to *cis* occurring via a dissociative mechanism.

3.1.2 Objectives

As above examples illustrate, a wide range of fluorinating reagents can be chosen for oxidative fluorination of organosulfur compounds. However, when they are used to oxidize S(IV) to S(VI), most of them often suffer from the following problems: (1) high temperature or low temperature requirements; (2) pressure requirements; (3) long reaction times; (4) accompanying S-C bond cleavage of; (5) low yields. In addition, most studies have been dominated by the preparative chemistry, consequently, their reaction mechanisms are not well understood.

Thus, searching for convenient fluorinating reagents which can cause oxidative addition of fluorine to organosulfur compounds under mild conditions, a study of the oxidative addition mechanism, and exchange processes of organosulfur(VI) halogenide compounds, are the most important parts of this thesis.

3.2 Experimental

3.2.1 General remarks

Xenon difluoride is a very powerful oxidizing agent. All operations involving xenon difluoride were conducted as much as possible under a dry nitrogen atmosphere. Small quantities of xenon difluoride were used for all related reactions. Due to the moisture and glass sensitivity of some of the reactants and products, all reactions were carried out in dry polytetrafluoroethylene (ptfe) apparatus unless otherwise specified. Reactions were also carried out in NMR tubes, with and without ptfe liners. All ptfe and glass equipment was dried at 110 °C for several days prior to use. Although no violent reactions occurred with CD_2Cl_2, $CDCl_3$ and CD_3CN as the solvents, suitable shielding was employed at all times. All gases were handled according to standard procedures.

3.2.1.1 Solvents and reagents

Dichloromethane, chloroform and acetonitrile solvents (Fisher reagent grade) were distilled and stored over 5 Angstrom molecular sieves. Deuterium solvents CD_2Cl_2, $CDCl_3$, and CD_3CN were purchased from Aldrich Chemical Company and were used without further purification or drying.

Tetraethylammonium chloride (Eastman Organic Chemicals) and tetraethylammonium bromide (Matheson, Coleman and Bell) were recrystallized from dry CH_3CN and stored over P_2O_5 (Allied Chemicals) in a vacuum desiccator. Sodium fluoride (Fisher Scientific Company) was dried in an oven at 150 °C for two days.

Diphenyltellurium dichloride and diphenyl ditelluride (K and K Laboratories), diphenylselenium dichloride (Alfa, Ventron Division), and phenylselenol (PCR Research Chemicals, Inc.) were stored in the dark to prevent decomposition by light.

The following reagents were used as received from commercial suppliers: xenon difluoride (Air Products or PCR Research Chemical Inc.), boron trifluoride (Matheson), phenyl sulfide and tetramethylammonium fluoride hydrate (Eastman Organic Chemicals), diphenyl sulfoxide and dibenzothiophene (Matheson Coleman and Bell), diphenyl disulfide, 4-nitrophenyl disulfide, sulfur dichloride, p-thiocresol, and 2,5-dimethylthiophene (Aldrich Chemical Company), triphenylmethyl chloride and hexafluorobenzene (Pfaltz and Bauer, Inc.), and tert-butyl disulfide (J.T. Baker Chemical Co.).

3.2.1.2 Instrumental

All ^{19}F, ^{13}C, and ^{125}Te nuclear magnetic resonance spectra were recorded on a Bruker AM-300 NMR spectrometer with operating frequencies at 282.4 MHz, 75.47 MHz, and 94.76 MHz, respectively. Chemical shifts were measured relative to internal hexafluorobenzene, C_6F_6 (-162.9 ppm with respect to $CFCl_3$) for fluorine NMR spectra. Internal CD_2Cl_2 (53.1 ppm with respect to TMS, quintet $J_{C\text{-}D} = 27$ Hz) and CD_3CN (1.3 ppm with respect to TMS, septet, $J_{C\text{-}D} = 21$ Hz) were used as references for proton decoupled and proton coupled ^{13}C NMR spectra. Ph_2Te (692.3 ppm with respect to

Me_2Te) was used as external reference for ^{125}Te NMR spectra. Ptfe inserts were used inside the standard 5 mm NMR tubes for the reactive compounds.

All NMR chemical shifts are reported following the IUPAC convention, i.e. positive values in high frequency (low field) direction. The yields of products was estimated by ^{19}F or ^{13}C peak integration, based on the known amount of C_6F_6 or internal compounds. Mass spectra were run on a VG7070E instrument.

3.2.2 Experimental details

3.2.2.1 Preparation of phenylsulfur fluoride oxide and fluorine exchange in the $Ph_2S(O)F_2$-$Ph_2S(O)F^+$ system

3.2.2.1.1 Preparation of $Ph_2S(O)F_2$

a. Without catalyst

Solid XeF_2 (44 mg, 0.26 mmol) and Ph_2SO (50 mg, 0.25 mmol) were dissolved in CD_2Cl_2 (0.3 mL) in a ptfe-lined NMR tube. No immediate reaction, as judged by the absence of xenon gas evolution and confirmed by ^{19}F NMR spectroscopy. After two days, a mixture of Ph_2SO (33%) and $Ph_2S(O)F_2$ (67%) in a 1:2 molar ratio was found based on ^{13}C NMR spectroscopy. After a period of 6 days, all Ph_2SO was converted to $Ph_2S(O)F_2$, but the C1 peak was exchange broadened and C1-F coupling was not observed in this sample.

b. With catalyst Et_4NCl (tetraethylammmonium chloride)

In a typical reaction, solid Ph_2SO (60 mg, 0.30 mmol) was added to a solution of XeF_2 (54 mg, 0.32 mmol) in CD_2Cl_2 (0.3 mL) at room temperature in an NMR tube with a ptfe insert. Ph_2SO dissolves completely in CD_2Cl_2, but negligible reaction occurred within 30 minutes, as judged by exceedingly slow xenon gas evolution. Et_4NCl (2.0 mg, 0.012 mmol) was then added to the mixture of Ph_2SO and XeF_2, and a rapid reaction occurred with vigorous evolution of xenon gas. The solution mixture was constantly shaken, and the reaction was completed within 5 minutes. A slightly yellow colour was observed, then the colour went back to colourless very quickly during the reaction period. The ^{13}C (triplets) and ^{19}F (singlet) NMR of the solution confirmed the formation of $Ph_2S(O)F_2$ in a yield close to 100%, as almost no impurity was found from either ^{13}C or ^{19}F NMR spectra. ^{13}C NMR of $Ph_2S(O)F_2$: δC1 147.8 ppm, J(C1, F) = 17.1 Hz δC2 124.9, J(C2, F) = 6.1 Hz δC3 129.2 δC4 132.9 ^{19}F NMR: $\delta F=99.0$ ppm.

For a similar amount of Ph_2SO and XeF_2, the amount of Et_4NCl catalyst could be reduced to 0.5 mg, without reducing the yield of $Ph_2S(O)F_2$.

c. With Et_4NBr (tetraethylammmonium bromide)

A very similar reaction was carried out according to the procedure above except that Et_4NBr (5 mg, 0.024 mmol) was used, instead of Et_4NCl. The solution was yellow when Et_4NBr was added to the reaction mixture of Ph_2SO and XeF_2, and the reaction was slower than when Et_4NCl was used, as judged by the rate of xenon gas evolution. After the reaction was complete, the solution turned back to colourless. Yield of $Ph_2S(O)F_2$: ~100%.

d. With Ph_3CCl

In order to investigate the function of chloride ion in this reaction, Ph_3CCl was used as a catalyst. In this reaction, 20 mg (0.072 mmol) of Ph_3CCl was added to a mixture of solid XeF_2 (60 mg, 0.35 mmol) and Ph_2SO (60 mg, 0.30 mmol) in CD_2Cl_2 (0.3 mL) at room temperature in a ptfe-lined NMR tube. The solution turned yellow immediately with a small amount of xenon gas evolution. Examination by ^{13}C NMR after 24 hours revealed that Ph_2SO remained unreacted, and no oxidation products such as $Ph_2S(O)F_2$, Ph_2SO_2 and other sulfur (VI) compounds formed.

3.2.2.1.2 Preparation of $Ph_2S(O)F^+BF_4^-$

A small amount of BF_3 was bubbled into a freshly prepared solution of $Ph_2S(O)F_2$ (72 mg, 0.30 mmol) in CD_2Cl_2 (0.5 mL) at room temperature in a ptfe-lined NMR tube. Changes in chemical shifts, and loss of C-F coupling and line broadening occurred immediately, as confirmed by the ^{13}C NMR spectrum. The addition of excess BF_3 gave $Ph_2S(O)F^+BF_4^-$ in essentially quantitative yield as confirmed by both ^{13}C and ^{13}F NMR spectroscopy. Excess BF_3 was then removed under vacuum. ^{13}C NMR of $Ph_2S(O)F^+$: δC1 126.3 ppm, J(C1, F) = 10.9 Hz δC2 129.8, J(C2, F) = 1.3 Hz δC3 132.2 δC4 141.5 J(C4, F)= 1.2 Hz. ^{19}F NMR: $\delta F = 29.5$ ppm.

The identity of $Ph_2S(O)F^+$ was also confirmed by its chemical reactions. Addition of a large excess of NaF to the solution of $Ph_2S(O)F^+$ in CD_2Cl_2 gave $Ph_2S(O)F_2$. Addition of a large excess of Et_4NCl to the solution of $Ph_2S(O)F^+$ gave $Ph_2S(O)F_2$ and $Ph_2S(O)Cl_2$.

3.2.2.1.3 Fluorine exchange in the $Ph_2S(O)F_2$-$Ph_2S(O)F^+$ system

Several variable-temperature experiments were carried out on a mixture of $Ph_2S(O)F_2$ and $Ph_2S(O)F^+$ with two different concentrations. $Ph_2S(O)F_2$ is too reactive to be separated and isolated. The typical experimental details are as follows: a sample of $Ph_2S(O)F_2$ in CD_2Cl_2 was freshly prepared, and the ^{19}F NMR revealed a sharp singlet at 99.0 ppm due to $Ph_2S(O)F_2$, (or the ^{13}C NMR revealed two triplets at 147.8 and 124.9 ppm). Various amounts of BF_3 were then bubbled into this solution at room temperature to generate a mixture of $Ph_2S(O)F_2$ and $Ph_2S(O)F^+$. After the ^{13}C and ^{19}F NMR spectra of the mixture were recorded at ambient temperature (300 K), the ratio of $Ph_2S(O)F_2$ and $Ph_2S(O)F^+$ was determined by ^{13}C or ^{19}F NMR as described later in the text, and the following results were obtained:

(1) The ^{19}F NMR peaks of both $Ph_2S(O)F_2$ and $Ph_2S(O)F^+$ disappeared, and only one broadened peak between δF [$Ph_2S(O)F_2$] and δF [$Ph_2S(O)F^+$] was observed.

(2) The separate ^{13}C NMR phenyl peaks of both $Ph_2S(O)F_2$ and $Ph_2S(O)F^+$ were not observed anymore, and only the average broadened peaks, C1 to C4 of the phenyl ring, were seen.

The sample was then cooled to 280 K and its ^{19}F NMR spectrum was recorded. The low temperature ^{19}F NMR experiments were continued with 20 K temperature decrements until 200 K. The total experimental time required was approximately 3 hours.

During the course of the synthesis of $Ph_2S(O)F_2$, in some cases, excess XeF_2 was used. Sharp peaks of XeF_2 were also observed at the end of the reaction, indicating that fluoride donor ability of $Ph_2S(O)F_2$ towards $Ph_2S(O)F^+$ is greater than that of XeF_2.

3.2.2.1.4 The $Ph_2S(O)F_2$ and Ph_2SO system

Ph_2SO (30 mg, 0.15 mmol) was added to a freshly prepared sample of $Ph_2S(O)F_2$ (75 mg, 0.31 mmol) in CD_2Cl_2 at room temperature. After standing for 24 hours, eight separate ^{13}C NMR signals were observed for $Ph_2S(O)F_2$ and Ph_2SO, however, C1-F and C2-F coupling was not observed for $Ph_2S(O)F_2$ in this sample.

3.2.2.1.5 The $Ph_2S(O)F^+$ and Ph_2SO system

Ph_2SO (15 mg, 0.075 mmol) was added to a solution of $Ph_2S(O)F^+BF_4^-$ (72 mg, 0.32 mmol) in CD_2Cl_2 at room temperature. Separate ^{13}C NMR signals were observed for $Ph_2S(O)F^+$ and Ph_2SO. The ^{13}C NMR chemical shifts and coupling constants for $Ph_2S(O)F^+$ remained unchanged. There was no evidence of intermolecular fluorine exchange from the ^{13}C NMR spectra.

3.2.2.1.6 Preparation of $Ph_2S(O)Cl_2$

To a 45:55 molar mixture of $Ph_2S(O)F_2$ and $Ph_2S(O)F^+$, prepared from $Ph_2S(O)F_2$ (60 mg, 0.25 mmol) and BF_3 as described previously, was added Et_4NCl (18 mg, 0.12 mmol), and the ^{13}C NMR spectrum was recorded. An excess of Et_4NCl (50 mg, 0.32 mmol) was then added, and the ^{13}C NMR spectrum was recorded and integrated. The ^{13}C NMR of $Ph_2S(O)Cl_2$: δC1 145.9 ppm, δC2 124.4 ppm, δC3 129.4 ppm, δC4 131.1 ppm.

The mixture of $Ph_2S(O)F_2$ and $Ph_2S(O)Cl_2$ was hydrolyzed by addition of H_2O (25 ml, 1.4 mmol) to give only sulfone Ph_2SO_2.

3.2.2.1.7 Reaction of $Ph_2S(O)F_2$ with water

An excess amount of H_2O (10 ml 0.56 mmol) was added to a solution of $Ph_2S(O)F_2$ (72 mg, 0.30 mmol) in CD_2Cl_2 (0.3 mL) at 25 °C, and a rapid exothermic reaction occurred. The ^{13}C NMR spectrum revealed that all $Ph_2S(O)F_2$ was hydrolyzed to Ph_2SO_2. Yield of Ph_2SO_2: ~100%

3.2.2.1.8 Reaction of $Ph_2S(O)F_2$ with aqueous HF

Various controlled small amounts of H_2O (usually ~1 to 3 ml) were added to a solution of freshly prepared $Ph_2S(O)F_2$ (72 mg, 0.30 mmol) in CD_2Cl_2 (0.3 mL) at room temperature in a NMR tube with a ptfe insert. ^{13}C NMR spectrum showed four sharp singlets for Ph_2SO_2 and four broadened peaks for $Ph_2S(O)F_2$-$Ph_2S(O)F^+$. As more small amounts of H_2O were added, more Ph_2SO_2 was obtained, and the chemical shifts of the four broadened peaks shifted toward the cationic species, $Ph_2S(O)F^+$, suggesting the percentage of $Ph_2S(O)F^+$ increased as more H_2O was added. In one sample, the ^{19}F NMR spectrum gave no signal for $Ph_2S(O)F_2$, $Ph_2S(O)F^+$, HF, or HF_2^-. Instead only a flat baseline was observed, implying a rapid exchange reaction involving these four species. When a further 2.5 ml of H_2O was added, only resolved sharp ^{13}C NMR peaks for Ph_2SO_2 and $Ph_2S(O)F^+$ were observed, however, the C1-F and C2-F coupling was not observed for $Ph_2S(O)F^+$ in this sample.

3.2.2.1.9. Reaction with the H_2O-HF-glass system

A standard Pyrex test tube was drawn into a capillary, and a small segment of dimensions 4mm x 1mm was removed and dried overnight at 110 °C. Typical concentration (weight percent) of Pyrex glass is:18% SiO_2, 13% B_2O_3, 4% Na_2O, 2% Al_2O_3.

$Ph_2S(O)F_2$ was prepared as described previously. A small dried capillary of borosilicate glass was added to $Ph_2S(O)F_2$ in a ptfe-lined NMR tube in CD_2Cl_2 solution. The ^{13}C NMR spectrum was recorded immediately, and again after several hours. The ^{13}C NMR spectrum recorded after 18 hr is identical to that of unreacted $Ph_2S(O)F_2$. Coupling of C1-S-F, as well as C2-S-F is retained, and this demonstrates that dry glass does not react with $Ph_2S(O)F_2$ within 18 hr. However, when a small capillary of borosilicate glass was dipped into water and then added to the above sample, the ^{13}C NMR showed four new C1-C4 peaks of the hydrolysis product Ph_2SO_2. This hydrolysis product does not participate in any exchange process. There is a significant change in the C1-C4 chemical shifts of $Ph_2S(O)F_2$, and the C1 triplet (and C2 triplet) have been replaced by a single average broad peak due to the equilibrium between $Ph_2S(O)F_2$ and $Ph_2S(O)F^+$. On standing, the relative percentage of $Ph_2S(O)F^+$ in $Ph_2S(O)F_2$-$Ph_2S(O)F^+$ increased, and more hydrolysis product Ph_2SO_2 was found.

3.2.2.1.10 Reaction of $Ph_2S(O)F_2$ with alcohols

$Ph_2S(O)F_2$ was prepared as described previously. In a typical reaction, solid Ph_2SO (60 mg, 0.30 mmol) was added to a solution of XeF_2 (52 mg, 0.31 mmol) and Et_4NCl (2 mg, 0.012 mmol) in CD_2Cl_2 (0.3 mL) at 25 °C in a NMR tube with a ptfe insert. Equivalent molar amounts of reacting alcohol (e.g. 52 mg, 0.3 mmol of $Ph(CF_3)CHOH$) were then added to this freshly made $Ph_2S(O)F_2$. ^{13}C NMR spectra confirmed the formation of the corresponding fluorinated compounds in high yield.

3.2.2.2 Preparation of phenyl chalcogen(VI) fluorides

3.2.2.2.1 Preparation of *cis*- and *trans*-Ph_2SF_4

Diphenyl sulfide (40 µl, 0.24 mmol) in a microsyringe was added to a solution of XeF_2 (120 mg, 0.71 mmol) in CD_2Cl_2 at -30 °C in a pfte-lined NMR tube. Reaction occurred on warming to about -5 °C with vigorous evolution of xenon gas. The solution mixture was constantly shaken. The reaction was finished within 10 minutes. No colour change was observed in this reaction. The ^{13}C and ^{19}F NMR confirmed the formation of Ph_2SF_2 in essentially quantitative yield without any phenylsulfur (VI) compounds present.

Adding Et_4NCl (40 mg, 0.24 mmol) to this freshly made diphenylsulfur difluoride caused rapid gas evolution and the solution turned yellow. The reaction mixture was shaken for 30 minutes and the solution became very faintly yellow (almost colourless), and ^{19}F NMR confirmed the formation of *cis*-Ph_2SF_4, *trans*-Ph_2SF_4 and *trans*-$PhSF_4Cl$. The latter product was formed by loss of one aromatic substituent.

Large amounts of fluoride impurities such as FDF^-, CD_2F_2, and CDF_3 were produced along with phenylsulfur(VI) fluorides.

On standing, the *cis* isomer slowly undergoes *cis*-to-*trans* isomerization in solution to give more trans isomer.

3.2.2.2.2 Attempted preparation of Ph_2SeF_4

Solid XeF_2 (100 mg, 0.59 mmol) was added to a solution of Ph_2SeCl_2 (70 mg, 0.23 mmol) in CD_2Cl_2 (0.3 mL) in a ptfe bottle. The reaction mixture was stirred for half an hour, but no reaction occurred, as judged by the absence of colour change and the absence of xenon gas evolution. When tetraethylammonium chloride, Et_4NCl (8 mg, 0.048 mmol) was added to the reaction mixture, the colourless solution rapidly turned yellow with gas evolution. When gas evolution ceased, the solution turned colourless within 10 minutes. Both ^{19}F and ^{13}C NMR spectra of this solution only confirmed the formation of Ph_2SeF_2. No Ph_2SeF_4, $PhSeF_4Cl$ or other selenium (VI) compounds were found. Keeping the solution for 2 weeks at room temperature did not change the result.

3.2.2.2.3 Preparation of $PhSF_5$

To Ph_2S_2 (17 mg, 0.078 mmol) in 0.3 mL CD_2Cl_2 in a ptfe-lined NMR tube was added Et_4NCl (2 mg, 0.012 mmol) at room temperature, but no reaction occurred as judged from the colour change. Solid XeF_2 (82 mg, 0.48 mmol) was then added slowly into the reaction mixture. The colourless solution rapidly turned yellow with slow gas evolution. After 30 minutes, another portion of Et_4NCl (6 mg, 0.036 mmol) was added to the solution. A large amount of gas evolved vigorously, and the deep yellow solution quickly turned back to colourless. Analysis of the ^{19}F NMR spectra revealed the formation of $PhSF_5$ (25%), along with *trans*-$PhSF_4Cl$.

3.2.2.2.4 Preparation of $PhSeF_5$

a. Synthesis of Ph_2Se_2

Ph_2Se_2 was prepared with slight modification according to the method of synthesis of the corresponding disulfide by Drabowicz and Mikolajczyk.[121]

Solid phenylselenol (1.58 g, 10 mmol) was added to a stirred solution of dichloromethane (10 mL) and 10% aqueous potassium hydrogen carbonate in a round bottom flask. The flask was immersed in a water bath and a solution of bromine (0.8 g, 5 mmol) was added slowly to the well-stirred mixture. During the addition of bromine, the colour disappeared quickly. After addition was completed, the CD_2Cl_2 phase was separated and the aqueous phase extracted with CD_2Cl_2 (10 mL). The CD_2Cl_2 phases were combined and dried with magnesium sulfate. Evaporation of the solvent CD_2Cl_2 gave virtually pure deep yellow solid Ph_2Se_2. The product was characterised by its known ^{13}C NMR spectrum.

b. Preparation of $PhSeF_3$

Maxwell and Wynne[120] used a method of oxidative fluorination of diselenide, RSeSeR, with silver difluoride to generate the corresponding arylselenium trifluoride.

The reaction mixture was gently refluxed for a period of 4 hours at 47 °C in Freon 113 with stirring under a slow stream of nitrogen, and gave only a modest yield of $PhSeF_3$, 32%.

Using XeF_2 as the fluorinating reagent in the presence of chloride ion, a much more rapid and higher yield reaction can occur under mild conditions. Solid XeF_2 (35 mg, 0.21 mmol) was added to a solution of Ph_2Se_2 (28 mg, 0.12 mmol) in CD_2Cl_2 at room temperature in a NMR tube with ptfe insert. There was negligible conversion to product after 30 minutes. Et_4NCl (2 mg, 0.012 mmol) was then added to the reaction mixture of Ph_2Se_2 and XeF_2, and a rapid reaction occurred with vigorous evolution of xenon gas. The reaction was completed within 15 minutes. The colourless solution turned yellow during the reaction period, but then turned to colourless at the end of the reaction. The ^{19}F NMR spectrum of this solution confirmed the formation of $PhSeF_3$ by its known broad peak, which indicates rapid fluorine exchange of equatorial and apical fluorines. The yield of $PhSeF_3$ was ~90% based on ^{19}F NMR spectrum.

c. Synthesis of $PhSeF_5$

Adding another batch of Et_4NCl (25 mg, 0.18 mmol) to the freshly prepared solution of $PhSeF_3$ caused rapid gas evolution, and the solution turned yellow, then back to colourless, and the reaction was complete within 15 minutes. ^{19}F NMR showed the formation of $PhSeF_5$ (25%). ^{19}F NMR of $PhSeF_5$: δFax 86.9 ppm, δFeq 4.6 ppm, $J_{Fax\text{-}Feq}$ 191.2 Hz.

3.2.2.2.5 Preparation of $PhTeF_5$

a. Without catalyst

K. Alam in this laboratory prepared pentafluorophenyltellurium(VI), $PhTeF_5$, by oxidative fluorination of diphenylditelluride Ph_2Te_2, or phenyltellurium trifluoride $PhTeF_3$ with XeF_2 without the use of catalyst. This reaction required about 4 hours, and only a modest yield ~50% was achieved. This reaction was modified by the use of catalytic amount of Et_4NCl.

b. With catalyst Et_4NCl

Solid XeF_2 (50 mg, 0.30 mmol) was added to a suspension of red orange Ph_2Te_2 (24 mg, 0.06 mmol) in CD_3CN (0.5 mL) in a 5 mL ptfe bottle (Ph_2Te_2 is insoluble in CD_3CN solvent) at -10 °C. Reaction occurred after a few minutes, as judged by xenon gas evolution, and the solution quickly turned yellow. In addition, it was also noticed that the solid particles gradually disappeared. At this stage, Et_4NCl (2 mg, 0.012 mmol) was dropped into the reaction mixture, more xenon gas was evolved, and the solution turned light yellow. After another 15 minutes, the solution became faint yellow to colourless. The ^{19}F NMR showed the formation of $PhTeF_5$ with a yield greater than 90%.

3.2.2.2.6. Attempted preparation of Cl_2SF_4

Dark red sulfur dichloride (10 μl, 0.16 mmol) in a microsyringe was added to a solution of XeF_2 (56 mg, 0.33 mmol) in CD_2Cl_2 at room temperature in a pfte-lined NMR tube. A rapid exothermic reaction occurred with vigorous evolution of xenon gas after Et_4NCl (2 mg, 0.012 mmol) was added to the reaction mixture. The solution mixture was constantly shaken. The reaction was completed within 10 minutes. The colour of the solution became much lighter when the reaction was completed. The ^{19}F NMR at room temperature identified two broad peaks characteristic of SF_4. A small amount of DF/FDF^- was also present, but no Cl_2SF_4 was formed.

3.2.2.3 Preparation of alkyl and aryl sulfur(IV) fluoride

3.2.2.3.1 Preparation of arylsulfur trifluoride $ArSF_3$ (Ar = Ph, *p*-MeC_6H_4, *p*-$O_2NC_6H_4$)

a. Synthesis of (*p*-$MeC_6H_4)_2S_2$

(*p*-$MeC_6H_4)_2S_2$ was prepared according to the method of synthesis of diphenyl disulfide by Drabowicz and Mikolajczyk with slight modification.[121]

Solid *p*-thiocresol (1.24 g, 10.0 mmol) was added to a stirred solution of dichloromethane (10 mL) and 10% aqueous potassium hydrogen carbonate in a round bottomed flask. The flask was immersed in a water bath and a solution of bromine (0.8 mg, 5 mmol) was added slowly to the well-stirred mixture. During the addition of bromine, the colour disappears quickly. After addition was completed, the CD_2Cl_2 phase was separated and the aqueous phase extracted with CD_2Cl_2 (10 mL). The CD_2Cl_2 phases were combined and dried with magnesium sulfate. Evaporation of the solvent CD_2Cl_2 gave virtually pure light yellow solid (*p*-$MeC_6H_4)_2S_2$. The product was characterised by its known ^{13}C and ^1H NMR spectra.

b. Reaction of Ar_2S_2 with XeF_2 (without Et_4NCl)

In a typical reaction, solid XeF_2 (70 mg, 0.42 mmol) was added to a solution of Ph_2S_2 (30 mg, 0.14 mmol) in CD_2Cl_2 in a ptfe-lined NMR tube at room temperature. Gas slowly evolved. A ^{13}C NMR spectrum of this sample after 24 hours showed only ~60% of $PhSF_3$ along with some other unidentified products.

c. Synthesis of arylsulfur trifluoride, $ArSF_3$, with catalyst

Solid XeF_2 (115 mg, 0.68 mmol) was added to a mixture of $(p\text{-}MeC_6H_4)_2S_2$ (50 mg, 0.20 mmol) and Et_4NCl (4 mg, 0.024 mmol) in CD_2Cl_2 (0.3 mL) in a ptfe lined NMR tube. The solution rapidly turned yellow with gas evolution. When gas evolution ceased, the solution turned light yellow within 10 minutes. ^{19}F and ^{13}C NMR confirmed the formation of $p\text{-}MeC_6H_4SF_3$ with a yield greater than 95%. The total reaction time was about 30 minutes.

3.2.2.3.2 Preparation of Me_3CSF_3

a. Without Cl^-

Tert-butyl sulfide (10 mL, 0.052 mmol) was syringed into a solution of XeF_2 (45 mg, 0.26 mmol) in CD_2Cl_2 (0.3 mL) in a ptfe lined NMR tube. Gas evolution took place after shaking for a few minutes and the solution turned yellow. A deep blue viscous solution was finally obtained. The ^{19}F and ^{13}C NMR spectra of this sample indicated that $(Me_3C)_2S_2$ decomposed to various unidentified compounds, but no Me_3CSF_3 was found.

b. With catalyst Et_4NCl

Solid XeF_2 (70 mg, 0.41 mmol) was added to a reaction mixture of *tert*-butyl sulfide (10 mL, 0.052 mmol) and Et_4NCl (10 mg, 0.06 mmol) in CD_2Cl_2 (0.3 mL) in a ptfe lined NMR tube at room temperature. Gas evolved and the solution turned deep yellow immediately. Upon tapping the ptfe lined NMR tube, gas evolution ceased within 10 minutes and the solution turned back to colourless. ^{19}F NMR showed the formation of Me_3CSF_3 with a yield ~95%. Adding excess amounts of Et_4NCl and XeF_2 further oxidized all Me_3CSF_3 to the sulfur(VI) compound, which upon loss of the *tert*-butyl substituent gave SF_5Cl, as confirmed by ^{19}F NMR.

3.2.2.3.3 Preparation of dibenzodifluorothiophene (oxidative fluorination of dibenzothiophene)

Dibenzothiophene (22 mg, 0.12 mmol) was added to a solution of XeF_2 (40 mg, 0.24 mmol) in CD_2Cl_2. There was no reaction within 30 minutes, as judged by the absence of colour change and xenon gas evolution. Gas was evolved and the solution turned yellow immediately after Et_4NCl (2 mg, 0.012 mmol) was added to the reaction mixture. The solution went back to colourless at the end of reaction. The reaction was complete within 30 minutes. Both ^{13}C and ^{19}F NMR spectra confirmed the formation of dibenzodifluorothiophene in essentially quantitative yield. Further attempts to oxide this dibenzodifluorothiophene to a S(VI) compound with the use of excess Et_4NCl and XeF_2 failed. The dibenzodifluorothiophene remained unchanged when another 20 mg of Et_4NCl was added to this solution which contained excess XeF_2.

3.2.2.4 Preparation of aryltetrafluorosulfur(VI) chloride

3.2.2.4.1 Preparation of *trans*-$ArSF_4Cl$ (Ar = Ph, *p*-MeC_6H_4, *p*-$O_2NC_6H_4$)

Method A) *Trans*-Aryltetrafluorosulfur(VI) chloride in a one step method.

In a typical reaction, to a mixture solution of (*p*-$MeC_6H_4)_2S_2$ (14.5 mg, 0.06 mmol) and Et_4NCl (20 mg, 0.12 mmol) in CD_3CN (0.3 mL) in a ptfe lined NMR tube was added XeF_2 (80 mg, 0.48 mmol). An exothermic rapid reaction occurred with vigorous evolution of gas and the solution turned yellow. When the evolution of gas ceased, the solution turned back to colourless within 10 minutes. The total reaction took about 25 minutes. Analysis of the ^{19}F NMR spectrum of this solution revealed the formation of 84% of *trans*-(*p*-$MeC_6H_4)SF_4Cl$, and ~13% of (*p*-$MeC_6H_4)SOF_3$ (because the reaction is carried out on such a small scale, the trace amount of moisture in the solvent could easily cause hydrolysis). A modest amount of DF/FDF$^-$, CD_2F_2, CD_2FCl and excess unreacted XeF_2 were also found. After several days, the ^{13}C NMR of this sample again confirmed the presence of *trans*-(*p*-MeC_6H_4)SF_4Cl in a very high yield.

Method B) *Trans*-aryltetrafluorosulfur(VI) chloride in greater than ~80% yield from arylsulfur (IV) trifluoride.

Et_4NCl (20 mg, 0.12 mmol) was added to a freshly prepared solution of $PhSF_3$ (~0.12 mmol) and XeF_2 (40 mg, 0.24 mmol) in CD_2Cl_2 in a ptfe lined NMR tube. A rapid reaction occurred with gas evolution, and the solution turned yellow. The reaction mixture was tapped for 20 minutes, the mixture turned colourless, and the product, *trans*-aryltetrafluorosulfur(VI) chloride, *trans*-$ArSF_4Cl$, was characterised as described above in method A.

3.2.2.4.2 Preparation of *cis*-$ArSF_4Cl$

Cis-$ArSF_4Cl$ can also be synthesised by a method similar to the preparation of *trans*-$ArSF_4Cl$, except that the amount of XeF_2 has to be reduced.

Method A)

Solid XeF_2 (60 mg, 0.36 mmol) was used to react with Ph_2S_2 (13 mg, 0.06 mmol) and Et_4NCl (20 mg, 0.12 mmol) in CD_2Cl_2 at room temperature in a NMR tube with a ptfe-insert according to the procedure described in method A for *trans*-$ArSF_4Cl$. The ^{19}F NMR of the solution showed an AB_2C spin system for the reaction product, *cis*-$PhSF_4Cl$ (about 80%), *trans*-$PhSF_4Cl$ (about 10%), and $PhSOF_3$ (about 10%). Modest amounts of DF/FDF^-, CD_2F_2, CD_2FCl were also observed, but no excess XeF_2 was found.

Method B)

Cis-$ArSF_4Cl$ can also be prepared from the reaction of XeF_2 and $ArSF_3$ in the presence of Et_4NCl.

Et_4NCl (20 mg, 0.12 mmol) was added to a freshly prepared solution of $PhSF_3$ (~0.12 mmol) and XeF_2 (20 mg, 0.12 mmol) in CD_2Cl_2 at room temperature in a ptfe lined NMR tube according to the procedure described in Method B for *trans*-$ArSF_4Cl$. The analysis of the ^{19}F NMR spectrum of this sample after the reaction showed the formation of *cis*-$PhSF_4Cl$ in 79%, *trans*-$PhSF_4Cl$ in 13% and $PhSOF_3$ in 6% yield.

3.2.2.4.3 Preparation of *cis*- and *trans*-$PhTeF_4Cl$

The method of synthesis of *cis*- and *trans*-$ArSF_4Cl$ has been extended to the preparation of *cis*- and *trans*-$PhTeF_4Cl$.

Ph_2Te_2 (24 mg (0.06 mmol) was added into CD_3CN in a 100 mL ptfe bottle. Ph_2Te_2 is not soluble in CD_3CN (0.5 mL). Then 30 mg (0.18 mmol) of XeF_2 was added slowly to this suspension. During each aliquot addition of XeF_2, an exothermic reaction occurred with the evolution of xenon gas. Solid Ph_2Te_2 disappeared gradually with xenon gas evolution, but the reddish orange colour remained. 20 mg (0.12 mmol) of Et_4NCl was then added to the reaction mixture, but there was no colour change whatsoever. Another 19 mg (0.11 mmol) of XeF_2 was dropped into the solution in small portions. After the final addition, the orange colour of the solution became much lighter within 5 minutes, when gas evolution ceased. ^{19}F NMR of this solution indicated the formation of *cis*- and *trans*-$PhTeF_4Cl$, as well as $PhTeF_3Cl_2$. No DF/FDF^-, CD_2F_2 and CD_2FCl were detected.

3.2.2.4.4 Reaction of $ArSF_4Cl$ with BF_3

An excess of BF_3 was bubbled into a solution of *cis*- and *trans*-$PhSF_4Cl$ in CD_2Cl_2 in a NMR tube with a ptfe insert at room temperature in small portions. The reaction mixture was shaken constantly and monitored by ^{19}F NMR. As shown from the spectra, the relative areas of the peaks for *cis*- and *trans*-$PhSF_4Cl$ were gradually decreasing, whereas the relative integration of $PhSF_5$ was increasing, and finally all *cis*- and *trans*-$PhSF_4Cl$ were converted to $PhSF_5$.

3.2.2.4.5 Isomerization of *trans*-$PhSF_4Cl$ to *cis*-$PhSF_4Cl$

a. With XeF_2 and Et_4NCl

A ptfe-lined NMR tube containing a solution of *trans*-$PhSF_4Cl$ (13.5 mg, 0.061 mmol) and *cis*-$PhSF_4Cl$ (7.5 mg, 0.034 mmol) in a ~2:1 ratio. XeF_2 (3 mg, 0.018 mmol) in 0.3 mL CD_3CN was treated with Et_4NCl (15 mg, 0.091 mmol), and the colourless solution turned yellow immediately with a small amount of gas evolution. The ^{19}F NMR spectrum revealed that:

(1) after 16 hours reaction time

a) the single sharp peak of *trans*-$PhSF_4Cl$ became very broad, and its relative integration decreased dramatically

(b) the position of all peaks from *cis*-$PhSF_4Cl$ remained unchanged, but their relative intensity increased

(c) the ratio of *trans*-$PhSF_4Cl$ to *cis*-$PhSF_4Cl$ changed from ~2:1 to ~1:2

(2) after 48 hours, more *trans* isomer was converted to the *cis* isomer, and the molar ratio *trans/cis* was about 1:4

(3) after 5 days, more *trans* isomer was converted to the *cis* isomer, and the molar ratio *trans/cis* was about 1:8

(4) finally, after 2 weeks, all *trans*-$PhSF_4Cl$ was converted to *cis*-$PhSF_4Cl$

b. On Standing

On standing, *trans*-$ArSF_4Cl$ can be also isomerized to *cis*-$ArSF_4Cl$, but the rate was much slower, especially in the presence of XeF_2. Once all the XeF_2 was used up, then the isomerization could be a little faster, but it still took about 2 months for all the *trans* isomer to be converted to the *cis* isomer.

3.2.2.4.6 Attempted isomerization of *cis*-$ArSF_4Cl$ to *trans*-$ArSF_4Cl$

A ptfe-lined NMR tube with only *cis*-$PhSF_4Cl$ (20 mg, 0.09mmol) in CD_3CN (0.3 mL) was treated with XeF_2 (22mg, 0.12 mmol) and Et_4NCl (15mg, 0.09 mmol). ^{19}F NMR of this solution showed only the presence of *cis*-$PhSF_4Cl$, and no *trans*-$PhSF_4Cl$ was detected.

3.2.2.4.7 $^{37}Cl/^{35}Cl$ isotope shifts on the ^{19}F NMR spectrum of *trans*-$ArSF_4Cl$

All *trans*-$ArSF_4Cl$ compounds were prepared in NMR tubes with ptfe inserts according to the methods described above. All these tubes, except the one with *trans*-$PhSF_4Cl$, were not degassed. Spectra were recorded by Guy Bernard on a Bruker AM 300 spectrometer at 282.363 MHz (^{19}F). All spectra were acquired at 300 K with spectral width of 200-300 Hz.

3.2.2.4.8 Reaction of $ArSF_4Cl$ with water

Hydrolysis of $ArSF_4Cl$ by water is slow. Water (1:1 molar ratio) was added to a solution of *trans*-$PhSF_4Cl$ and *cis*-$PhSF_4Cl$ in CD_3CN and mixed by shaking the reaction tube. All $PhSF_4Cl$ was hydrolyzed to $PhSOF_3$ after 2 days as revealed by ^{19}F NMR. Another 1:1 molar ratio of H_2O was added to this solution and all $PhSOF_3$ was further hydrolyzed to $PhSO_2F$.

3.2.2.5 Reaction of XeF_2 with Et_4NCl

In order to get further information about the catalytic role of chloride ion in oxidative fluorination of organosulfur compounds, we studied the reaction of XeF_2 with Et_4NCl separately.

3.2.2.5.1 Reaction of XeF_2 with Et_4NCl in CD_2Cl_2 and CH_2Cl_2

Solid XeF_2 (15 mg, 0.09 mmol) was added to a solution of Et_4NCl (20 mg, 0.12 mmol) in a mixture of CD_2Cl_2 and CH_2Cl_2 in a ptfe-lined tube at room temperature. Gas evolved at a modest rate and the solution turned pale yellow. The ^{19}F NMR spectrum of this solution after 20 minutes revealed the formation of FDF^- (the coupling between deuterium and fluorine was observed), FHF^-, CD_2F_2, and CD_2FCl. No ClF was detected. On standing, the ^{19}F NMR peaks of FDF^- and FHF^- broadened and became overlapped with the DF/HF peaks.

3.2.2.5.2 Chlorination of 1,1-diphenylethene and cyclohexene

The pale yellow colour disappeared immediately on addition of 1,1-diphenylethene or cyclohexene to the above solution.

1,1-Diphenylethene $Ph_2C=CH_2$ (30 ml, 0.17 mmol), in CD_2Cl_2 (0.2 mL) was added to the reaction mixture of XeF_2 and Et_4NCl. The characteristic colour of chlorine disappeared immediately. The ^1H NMR spectrum confirmed the known reaction of chlorine with 1,1-diphenylethene to give 1,2-dichloro-1,1-diphenylpropane and 2-chloro-1,1-diphenylethene.

3.2.2.6. Molecular orbital calculations

The mechanism of oxidative-addition of fluorine to organosulfur compounds was studied. Molecular orbital calculations were performed to obtain the structures of intermediates that are too labile for direct experimental observation.

All *ab initio* molecular orbital calculations were performed with the GAUSSIAN86 and GAUSIAN92 system of programs on the Unix system and Amdahl 5870 system. The geometrical parameters were fully optimised with the analytical gradient method by the Hartree-Fock method. Standard literature values were used for the geometries of phenyl substituents. Only basis sets STO-3G*, 3-21G* and 6-31G* were used in the calculation of these fairly large molecules in this chapter.

3.3 Results and discussion

3.3.1 Oxidative fluorination by xenon difluoride in the presence of Et_4NCl

Since its discovery in 1962, xenon difluoride, XeF_2, has been a particular attractive as an oxidative fluorination agent both in main group chemistry and in organic fluorine chemistry for the following reasons:

(1) Stable solid xenon difluoride is available commercially and is inert to nickel monel, thoroughly dried glass or Teflon equipment at room temperature.

(2) It readily oxidizes the central element of main group compounds under mild conditions, very smoothly and efficiently, more or less at room temperature without destruction of other bonds, which makes it especially favourable for controllable selective oxidative fluorination.

(3) The very inert xenon gas is the only side product in the oxidative fluorination by XeF_2, allowing very clean reactions.

Specific instances of oxidative fluorination of main group compounds by XeF_2 have been reported from this and other laboratories[171]. Some typical examples of fluorination or oxidative fluorination (eq 52-59) by xenon difluoride are given below:

[52] $C_6H_5(CH_3)SiCl(H) + XeF_2 \longrightarrow C_6H_5(CH_3)SiF_2 + Xe + HCl$

[53] $(CH_3)_3SiCl + XeF_2 \longrightarrow (CH_3)_3SiF + Xe + Cl_2$

[54] $Ph_2PCl + XeF_2 \longrightarrow Ph_2PF_3 + Xe + Cl_2$

[55] $Ph_2PH + XeF_2 \longrightarrow$ 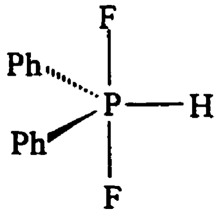 $+ Xe$

[56] $Ph_2S + XeF_2 \longrightarrow Ph_2SF_2 + Xe$

[57] $Ph_2Te_2 + XeF_2 \longrightarrow PhTeF_5 + Xe$

[58] $Ph_2TeCl_2 + XeF_2 \longrightarrow \textit{trans}\text{-}Ph_2TeF_4 + Xe$

[59] $MeI + XeF_2 \longrightarrow MeIF_2 + Xe$

These reactions demonstrate that XeF_2 is a very powerful oxidative fluorination agent. However, in some cases, oxidative fluorination of higher oxidation state main group compounds with xenon difluoride is a slow process, giving products in low yield. In some other cases, there is no reaction at all.

$Ph_2SF_2 + XeF_2 \not\longrightarrow$ No reaction for a month

$Ph_2SO + XeF_2 \not\longrightarrow$ No reaction for 12 hours

Therefore, a modified and enhanced method of oxidative fluorination of organosulfur(IV) to organosulfur(VI) by xenon difluoride in the presence of tetraethylammonium chloride, Et_4NCl, will be discussed.

3.3.2 Preparation of phenylfluorosulfur(VI) oxides

3.3.2.1 Oxidative fluorination of diphenyl sulfoxide

Aryl derivatives of sulfur oxide fluoride cannot be obtained by arylation of SOF_4. Sauer and Shreeve[112] synthesized bis(perfluoroalkyl)sulfur oxydifluoride, $R_fR_f'S(O)F_2$ by the reaction of chloride monofluoride (ClF) with perfluoroalkyl sulfoxide, $R_fR_f'SO$. Wilson[120] carried out the oxidation of SO_2 with XeF_2 in the presence of fluoride and chloride ions. Zupan and Zajc[119] carried out the oxidation of Ph_2SO by XeF_2, and postulated that $Ph_2S(O)F_2$ was formed as an intermediate which hydrolyzed rapidly to the sulfone, Ph_2SO_2. The direct oxidative fluorination of diorganyl sulfoxide by the method of Ruppert,[113] who first prepared $Ar_2S(O)F_2$ using elemental fluorine, F_2, did give a modest yield, but during the fluorination process, one aromatic substituent was lost and $ArS(O)F_3$ was also one of the final products. Hence, a convenient high yield synthetic method of organo-sulfur(VI) oxide fluoride compounds, without loss of the aromatic substituent, will be discussed in this section.

Diphenyl sulfoxide, Ph_2SO, reacts with XeF_2 very slowly when no catalyst was used, as shown in Figure 27. After 2 days, only about 2/3 of the starting material Ph_2SO was oxidized to $Ph_2S(O)F_2$. Therefore, an alternative synthesis was necessary for the reaction of Ph_2SO with XeF_2.

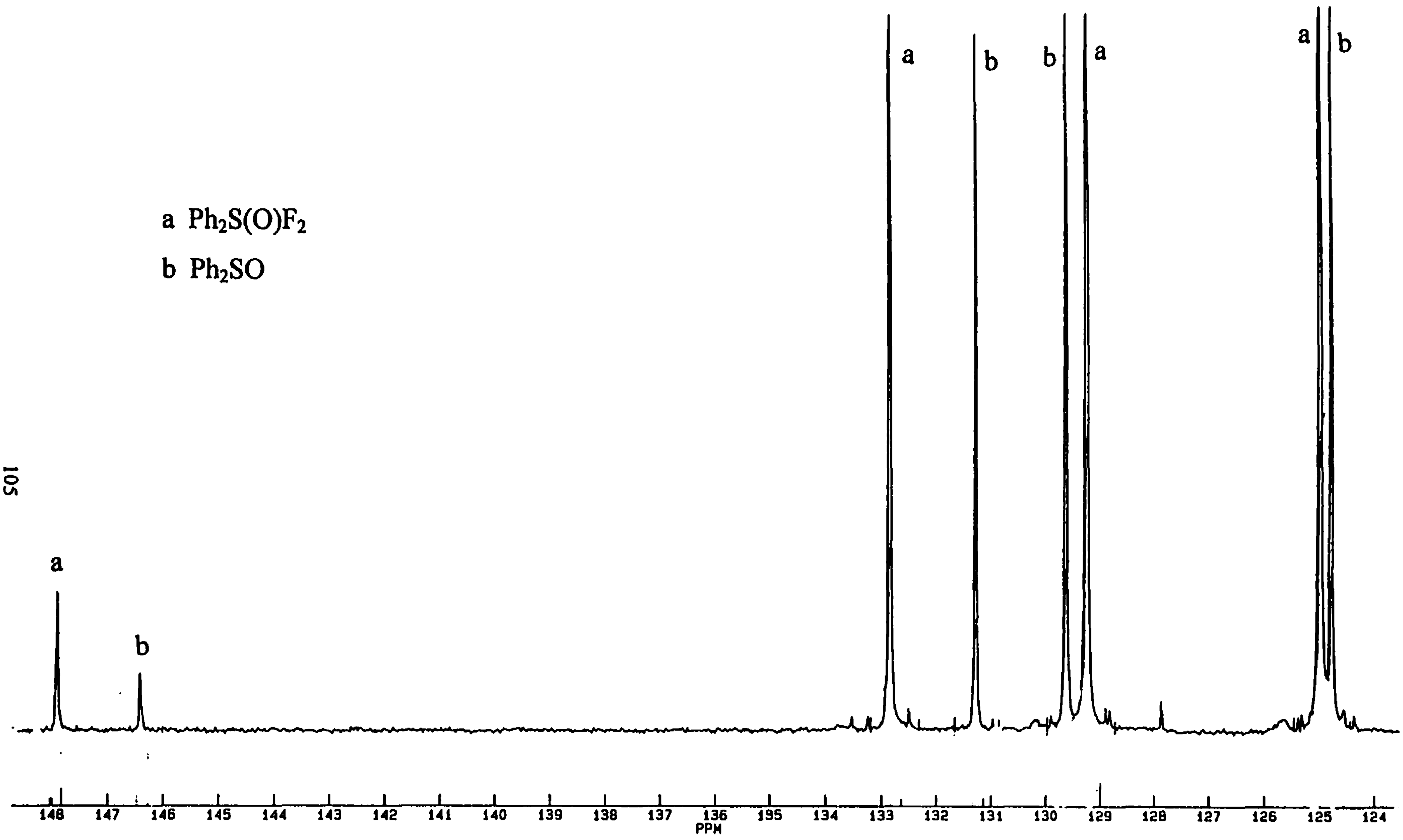

Figure 27. ^{13}C NMR spectrum of reaction products of Ph_2SO with XeF_2 in the absence of catalyst. The spectrum was recorded after a two day reaction time. Integration shows only ~2/3 of Ph_2SO (peaks b) was converted to $Ph_2S(O)F_2$ (peaks a)

Oxidative fluorination is very fast when a catalytic amount of tetraethylammonium chloride, Et_4NCl, is used, as shown in eq [60].

[60]

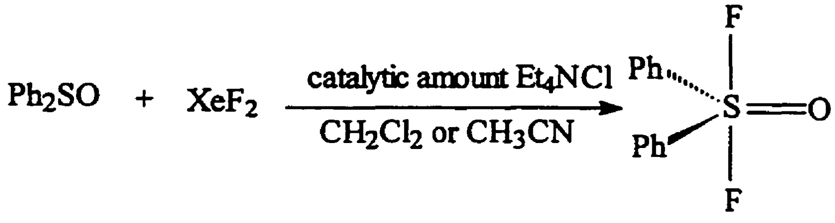

The synthesis of $Ph_2S(O)F_2$ was carried out by adding XeF_2 and ~1% tetraethylammonium chloride, Et_4NCl, to diphenyl sulfoxide, Ph_2SO, in dichloromethane or acetonitrile at ambient temperature, eq [60]. The reaction was completed within 5 minutes and the yield was greater than 95%, as judged by the ^{13}C and ^{19}F NMR spectra.

All reactions were monitored by ^{13}C rather than ^{19}F NMR because the starting material Ph_2SO and the hydrolysis product Ph_2SO_2 cannot be observed by the latter technique. Traces of moisture rapidly hydrolyzed $Ph_2S(O)F_2$ to Ph_2SO_2, and the same result was found by Zupan and his co-workers.[119] This hydrolysis reaction provided a useful criterion for judging whether reagents and solvent were adequately dried.

The ^{13}C and ^{19}F NMR spectra of $Ph_2S(O)F_2$ are shown in Figures 28 and 29, respectively.

The structures of $Ph_2S(O)F_2$ and $Ph_2S(O)F^+$, with atom numbering, are shown in scheme 5.

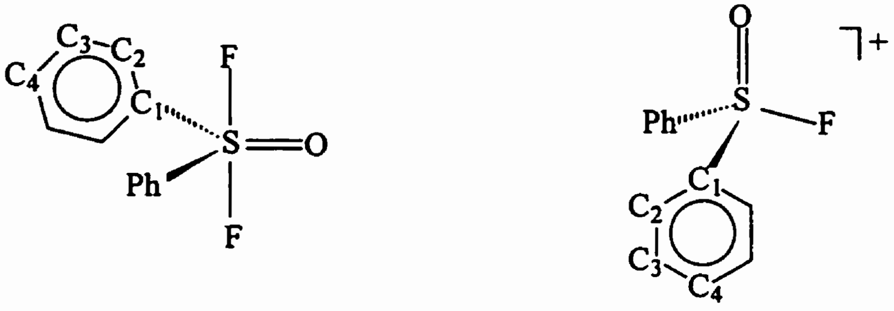
C3
C2
C4
C1
F
S
O
Ph
F
O
]+
Ph
S
F
C1
C2
C3
C4

Scheme 5. Atomic numbering for $Ph_2S(O)F_2$ and Ph_2SOF^+.

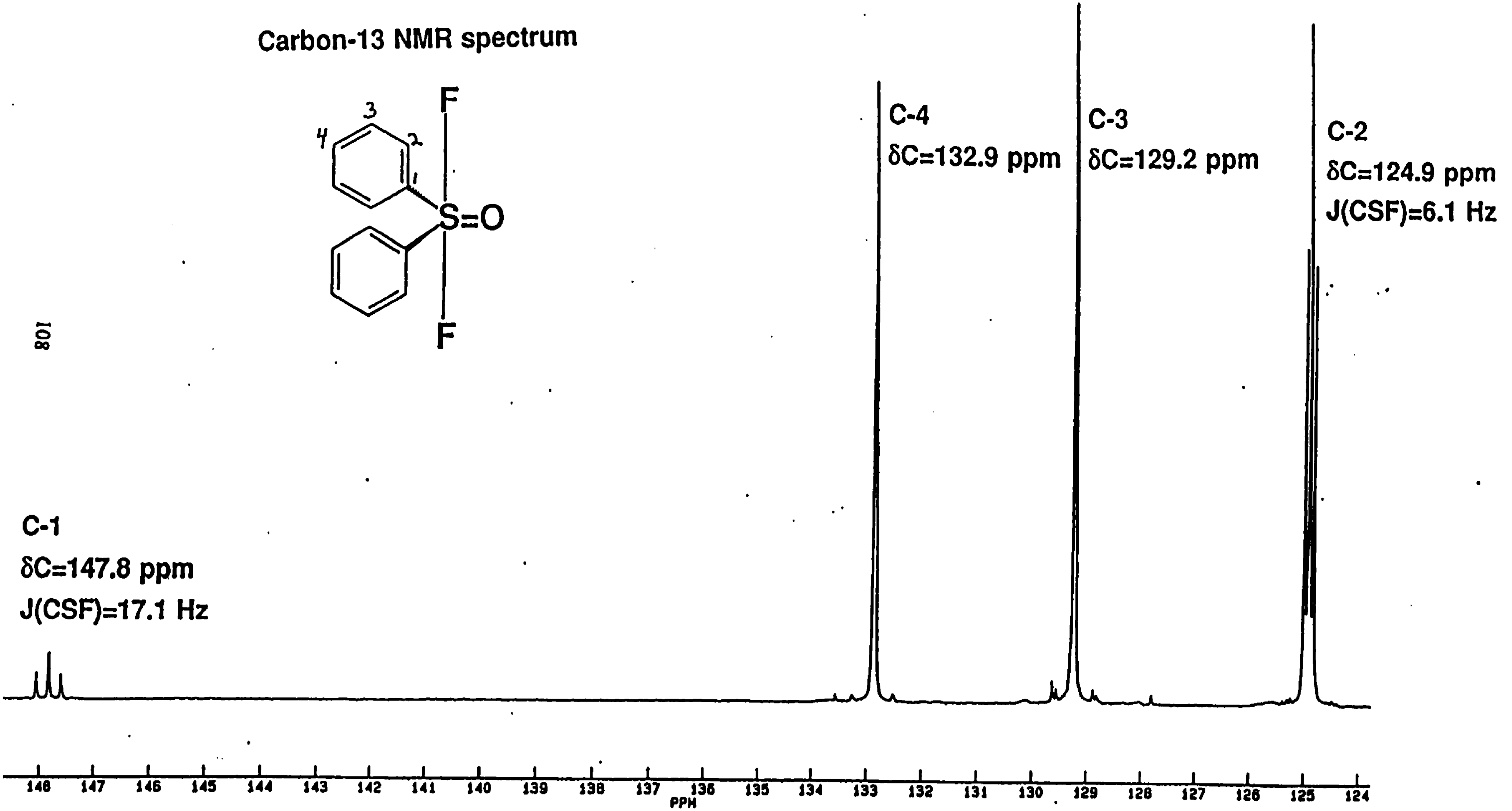

Figure 28. ^{13}C NMR spectrum of $Ph_2S(O)F_2$.

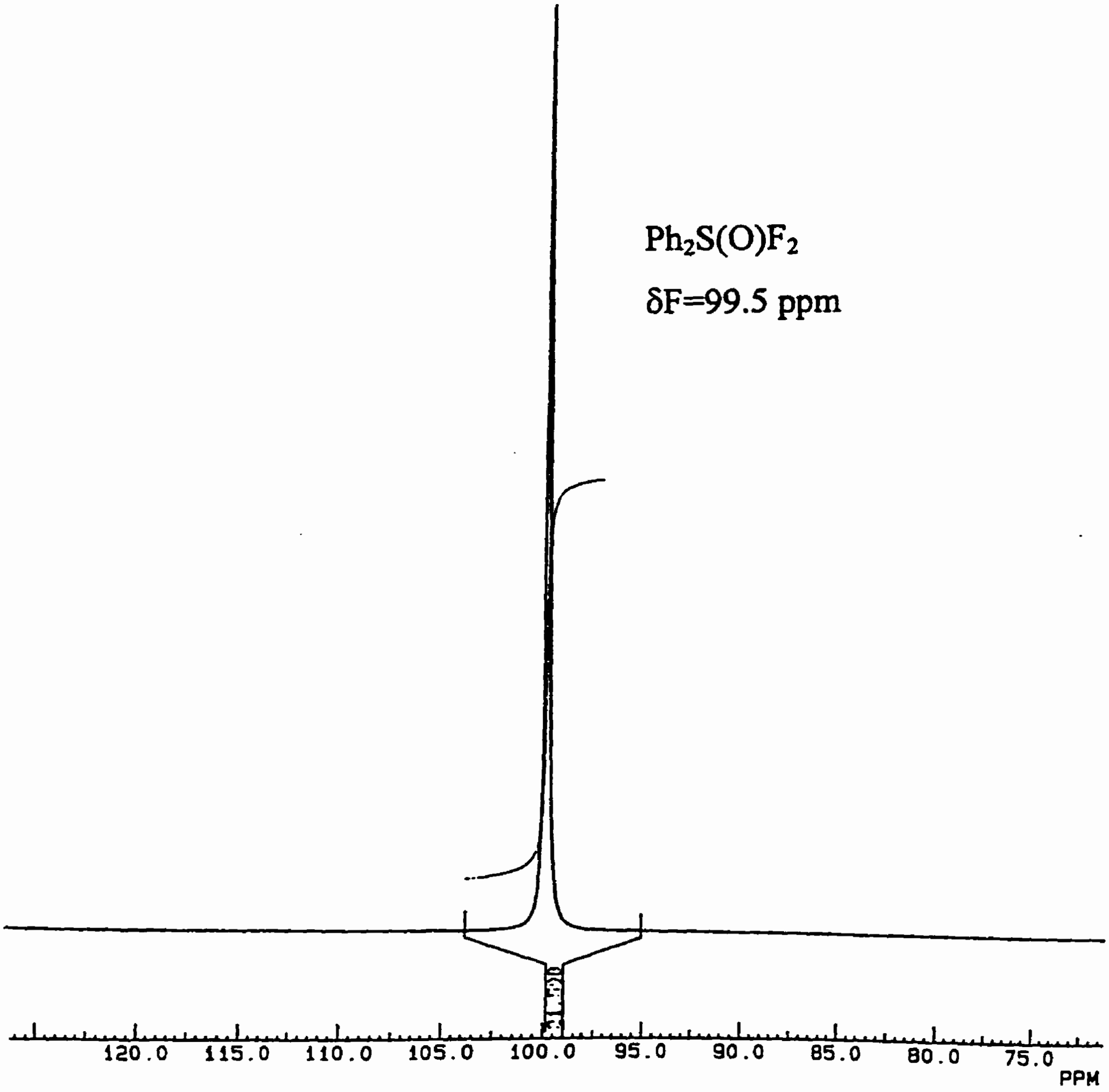

Figure 29. ^{19}F NMR spectrum of $Ph_2S(O)F_2$

The ^{19}F NMR spectrum gives a single fluorine resonance at 99.5 ppm because the two fluorines are equivalent. The ^{13}C NMR spectrum of $Ph_2S(O)F_2$ is also very simple since the two phenyl substituents are equivalent. Carbon nuclei in the phenyl substituents are coupled to two equivalent fluorines and this gives a triplet resonance for the two carbons closest to sulfur. Coupling over 4 bonds or more is not seen.

The assignments of C1-C4 peaks in the ^{13}C NMR spectra of $Ph_2S(O)F_2$ are based on the integrated peak intensities and the multiplicity of carbon-fluorine coupling, and related NMR spectra in the literature. The ipso-carbon, C1, is a triplet with large $J_{C\text{-}F}$ coupling (17.1 Hz) and has the smallest integrated intensity because it lacks a NOE. It is also the most deshielded (downfield) as shown in Figure 28. The integrated intensity of the para-carbon C4 resonance is about half that of C2 and C3 peaks because it has only one carbon. Assignment of ortho- and meta- carbon resonances is based on the magnitude of carbon-fluorine coupling constants. C2 is a triplet with a $^{3}J_{C\text{-}F}$ 6.1 Hz, while C3 is a singlet because it is too far away from the fluorine atoms (4 bonds). All ^{13}C and ^{19}F NMR spectral data for Ph_2SOF_2 (Figure 28-29 and Table 6) are in agreement with that reported by Ruppert.[113]

Addition of a catalytic amount of tetraethylammonium bromide, Et_4NBr, also accelerates the oxidative fluorination of Ph_2SO with XeF_2 and the detailed reaction mechanism (pathway) will be discussed shortly.

3.3.2.2 Proposed mechanism of oxidative-fluorination of diphenyl sulfoxide

3.3.2.2.1 Reaction of XeF_2 with Et_4NCl

Experimental results from this laboratory have demonstrated that the oxidative fluorination of organochalcogen(IV) to organochalcogen(VI) by XeF_2 is very slow or does not take place at all, except in the presence of Et_4NCl. The oxidative fluorination and/or chlorination of sulfur, selenium and tellurium compounds such as diphenyl sulfoxide, diphenylsulfur difluoride, diaryl disulfide, diphenyl diselenium, and diphenyl ditellurium etc., occurs very rapidly and smoothly under mild conditions on addition of xenon difluoride and Et_4NCl. In most cases, the sulfur(VI) and tellurium(VI) products are formed in essentially quantitative yield within a few minutes at room temperature.

What is the (catalytic) role of chloride ion? In order to obtain further information about the chloride ion in the oxidative addition of fluorine and/or chlorine to organochalcogen compounds, we studied the reaction of xenon difluoride with Et_4NCl separately, and we propose that chloride ion, when reacted with XeF_2, is a convenient source of a chlorine radical, and anhydrous and HF-free fluoride ion F^-, according to eq [61].

$$[61] \quad 2Cl^- + XeF_2 \longrightarrow 2F^- + 2Cl\cdot + Xe$$

In support of eq [61], it was found that a pale yellow solution was obtained when XeF_2 was added to a solution of Et_4NCl, and that colour disappeared on addition of cyclohexene or Ph_2CCH_2. ^1H NMR spectra confirmed the reaction [62], as shown in Figure 30.

[62]

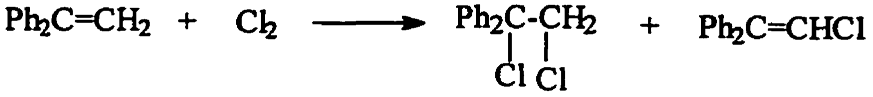

$$\mathrm{Ph_2C{=}CH_2 + Cl_2 \longrightarrow Ph_2\underset{Cl}{\underset{|}{C}}{-}\underset{Cl}{\underset{|}{CH_2}} + Ph_2C{=}CHCl}$$

Identification of F^-, along with DF, FDF^-, CD_2FCl and CD_2F_2, was confirmed by ^{19}F NMR spectroscopy as seen for example in Figure 31. Anhydrous F^- reacts with organic solvents to produce DF, FDF^- and fluorinated solvents, and this is a known reaction.[124] Hydrogen/halogen exchange to give DF and other fluorinated solvents is believed to occur via a radical process.[125]

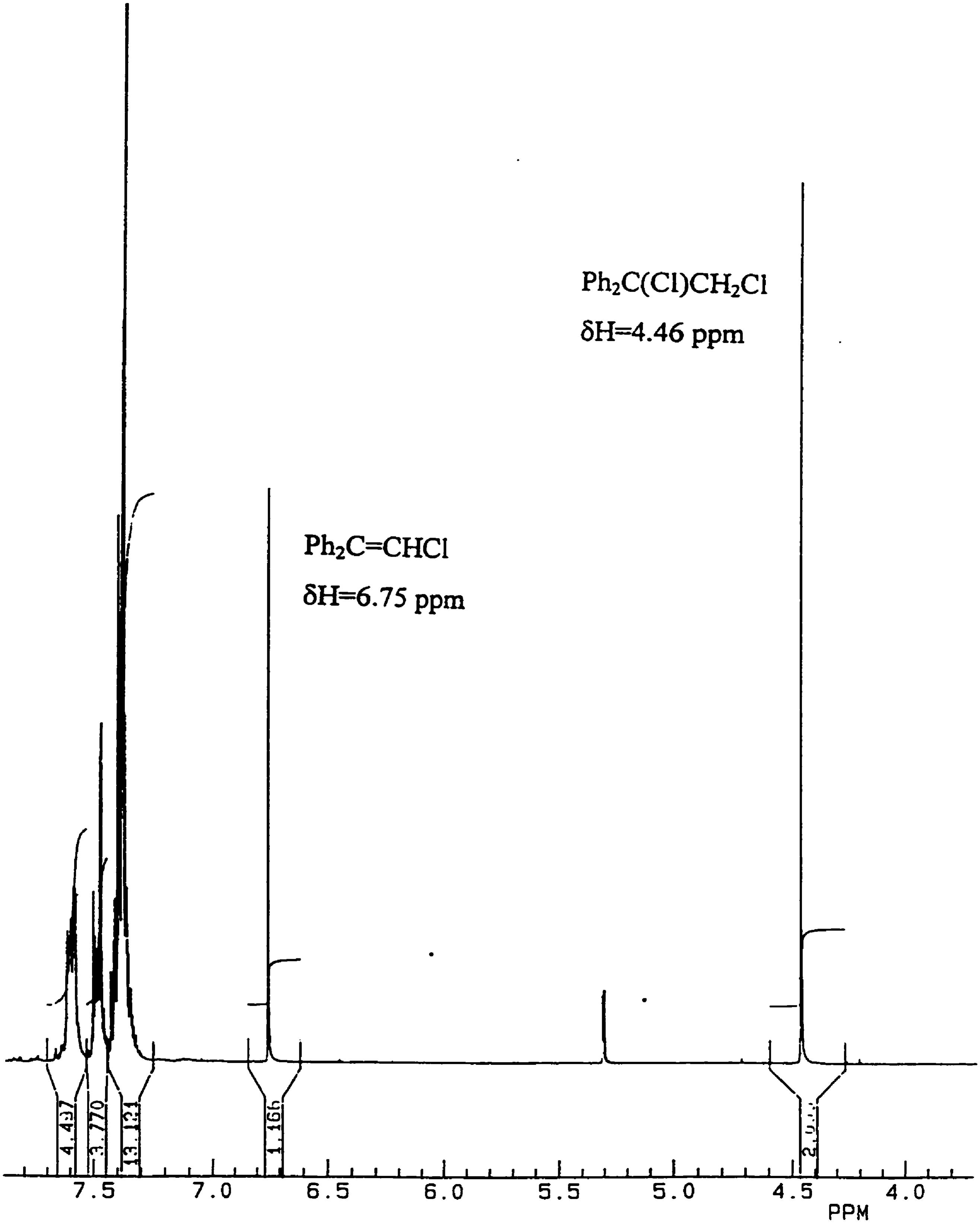

Figure 30. ^1H NMR spectrum of the products of the reaction of Ph_2CCH_2 with Cl_2

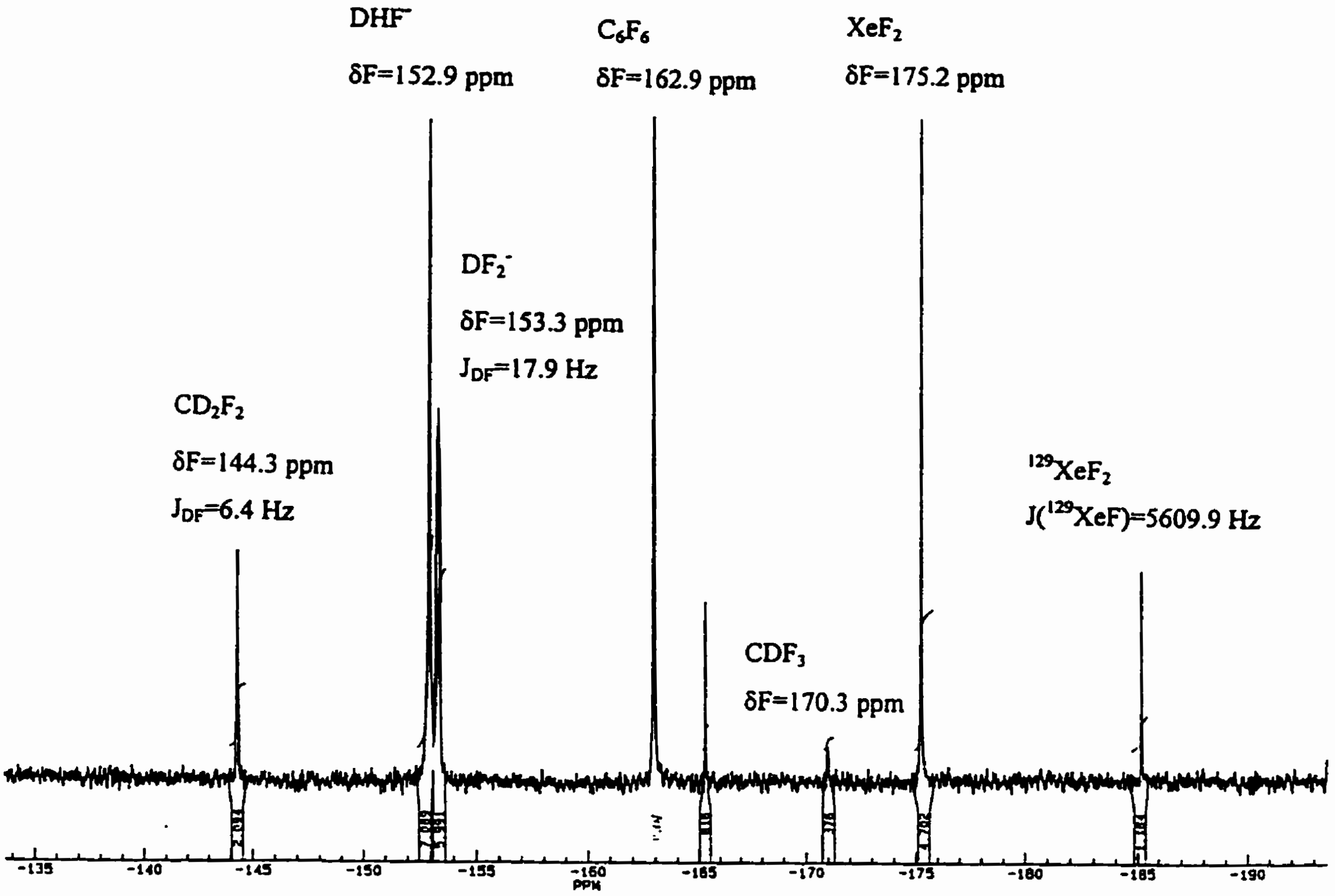

Figure 31. ^{19}F NMR spectrum of the reaction products of Et_4NCl with XeF_2

It has been shown previously in the literature that XeF_2 oxidizes HCl to Cl_2,[126] and alkaline solutions of XeF_2 liberate fluoride ion.[113,114] Fluoride ion is also liberated during the oxidation of iodide ion by XeF_4.[127]

3.3.2.2.2 Proposed mechanism of oxidative-fluorination of diphenyl sulfoxide

The synthesis of $Ph_2S(O)F_2$ was carried out in an NMR tube with a polytetrafluoroethylene (ptfe) insert by adding equivalent amount of XeF_2 and ~1% tetraethylammonium chloride, Et_4NCl, to 0.3~0.6 mmol of diphenyl sulfoxide, Ph_2SO, in dichloromethane or acetonitrile at ambient temperature, eq [60]. The reaction was completed rapidly, within 5 minutes, and $Ph_2S(O)F_2$ was formed in essentially quantitative yield.

During the reaction, the pale green colour of Cl_2 was visible, and traces of the solvent fluorination reaction products such as CD_2F_2 and CD_2FCl were detected by ^{19}F NMR, which is in agreement with eq [61]. Traces of the hydrolysis product, Ph_2SO_2, were sometimes detected by ^{13}C NMR, but hydrolysis could be completely eliminated by further drying of solvent and reagents.

In the absence of chloride ion, the formation of diphenyldifluorosulfoxide $Ph_2S(O)F_2$ proceeds sluggishly over a period of 2-6 days, but the addition of catalytic amount (~1% molar) of chloride ion (Et_4NCl) or bromide ion (Et_4NBr) brings about a smooth reaction in high yield. Evidently, chloride ion is an effective catalyst, and we propose that chloride ion, as a result of its oxidation by XeF_2, is a convenient source of anhydrous and HF-free fluoride ion F^- and chlorine radical $Cl^{\cdot}$. Hence, we propose that in the presence of fluoride ion and chlorine radical, oxidative fluorination proceeds according to the mechanism of Scheme 6.

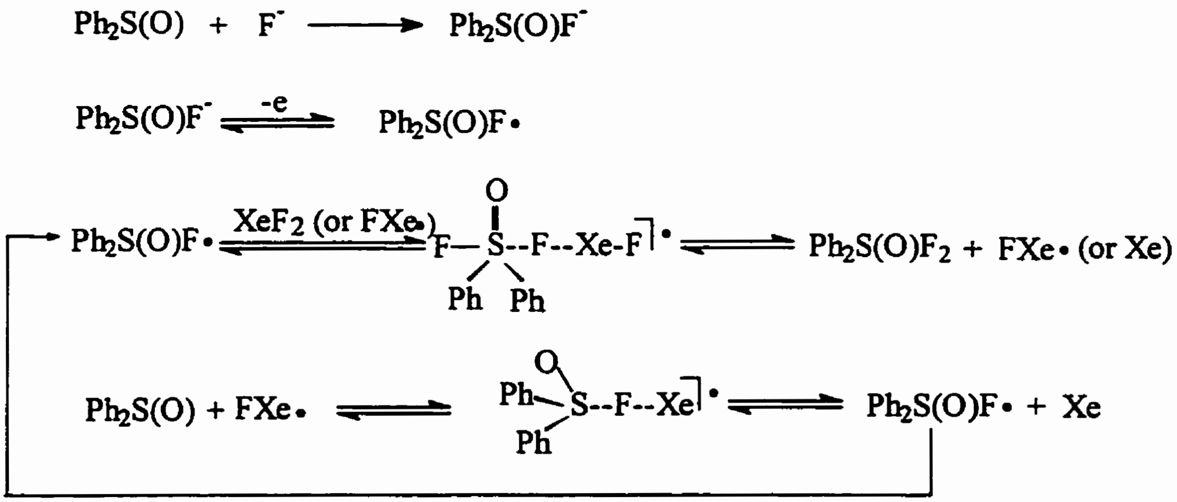

Scheme 6. Proposed mechanism of oxidative fluorination of Ph_2SO by XeF_2 in the presence of fluoride ion.

The first step of the reaction mechanism is the addition of a fluoride ion to the starting compound, Ph_2SO, then fluoroanion $Ph_2S(O)F^-$ is oxidized to the phenylsulfur(V) radical intermediate $Ph_2S(O)F^{\cdot}$, followed by cleavage of weak $[S\text{--}F\text{--}Xe]^{\cdot}$ bridging bonds. The radical intermediate further reacts with XeF_2 or $XeF^{\cdot}$ to give the final product and regenerates the $XeF^{\cdot}$ radical.

There is support in the literature for the mechanism of Scheme 6. For instance, the addition of fluoride ion to sulfur (IV) compounds produces stable anions such as SO_2F^-, SF_5^-, $CF_3SF_4^-$, etc.,[128] as shown in the following reactions, eq [63-65].

$$[63] \quad Me_4NF + SF_4 \longrightarrow Me_4N^+SF_5^-$$

$$[64] \quad (Me_3N)_3S^+Me_3SiF_2^- + R_fSF_3 \longrightarrow (Me_3N)_3S^+R_fSF_4^- + Me_3SiF$$

$$[65] \quad Me_4NF + SO_2 \longrightarrow Me_4N^+SO_2F^-$$

The intermediary of a sulfur(V) radical appears reasonable in view of known related sulfur(V) radicals[129] such as $SOF_3^{\cdot}$, $CF_3OSF_4^{\cdot}$, and $ROSF_4^{\cdot}$. Fluoro anions are often good electron donors. Anion-to-radical oxidation, as proposed in Scheme 6, is also known for other fluorinated species, e.g. oxidation of $PhSiF_5^{2-}$ to $PhSiF_5^{-\cdot}$ in the presence of electron acceptors.[66] (See the following Scheme 7 and the previous discussion of the *ab initio* MO study of silicon-fluorine and silicon-carbon bond cleavage in organofluorosilicates in Chapter 2).

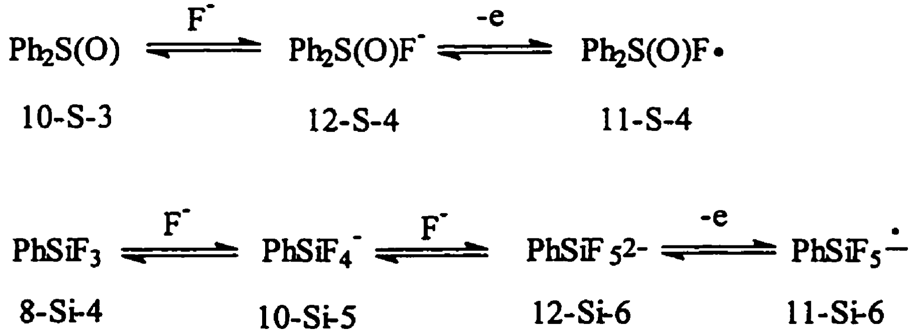
$Ph_2S(O) \xrightleftharpoons{F^-} Ph_2S(O)F^- \xrightleftharpoons{-e} Ph_2S(O)F\bullet$
10-S-3
12-S-4
11-S-4
$PhSiF_3 \xrightleftharpoons{F^-} PhSiF_4^- \xrightleftharpoons{F^-} PhSiF_5^{2-} \xrightleftharpoons{-e} PhSiF_5^{\dot{-}}$
8-Si-4
10-Si-5
12-Si-6
11-Si-6

Scheme 7. Fluoro anions as single electron donors

Our experiments do not allow us to identify the oxidizing agent that converts $Ph_2S(O)F^-$ to $Ph_2S(O)F^\bullet$, although Cl_2 or XeF_2 are possibilities. In the case of oxidation of $PhSiF_5^{2-}$ to $PhSiF_5^\bullet$, numerous one-electron acceptors can be used[87], including metal ions, halogen compounds, tetracyanoethylene, etc.. The intermediacy of $XeF^\bullet$ has been proposed before,[130] and its spectrum is known.[131]

It is conceivable that the end product $Ph_2S(O)F_2$ can be formed by the addition of F^+ to anionic $Ph_2S(O)F^-$, and arguments against,[53] and in favour,[132] of a role for positive fluorine have been discussed. We consider the direct transfer of F^+ from a cationic species such as XeF^+ or $FXeFXeF^+$ to be problematic because of the shortening/strengthening of bonds that is generally observed in cationic fluorides.[15] Consequently, the formal addition of F^+ may occur in two steps, involving the initial formation of a radical intermediate, $Ph_2S(O)F^\bullet$, followed by the transfer of $F^\bullet$, from $FXe^\bullet$ or XeF_2, as outlined in Scheme 7.

The mechanism of Scheme 7 explains why some oxidations, but not others, are carried out in the presence of fluoride ion. A fluoride ion allows the formation of anions, which are then oxidized to radicals. But radicals can be formed without the anionic intermediates because many oxidizing agents are themselves sources of free radicals, e.g. $SO_3F^\bullet$ from $S_2O_6F_2$,[133] or $CF_3O^\bullet$ from CF_3OOCF_3.[123] More vigorous reaction conditions of heating or irradiation may, however, be required if radicals are generated directly from oxidizing agents because bonds of moderate strength must be broken, e.g. RO-OR, Cl-Cl, F-XeF, whereas only very weak bridging bonds, i.e. $[S\text{--}F\text{--}Xe]^\bullet$, are cleaved if oxidation occurs in the presence of fluoride ion.

Such a mechanistic analysis can be extended to other well-known oxidations. For example, the Reed reaction, i.e. the chlorosulfonation of organic compounds with chlorine and SO_2, generally includes the following steps.[134]

$$[66] \quad R\bullet \xrightarrow{SO_2} R\text{-}SO_2\bullet \xrightarrow{Cl_2} R\text{-}SO_2Cl\bullet$$

By analogy with the cleavage of $[S\text{--}F\text{--}Xe]^\bullet$ bonds in Scheme 7, oxidation of sulfur(IV) compounds in the Reed reaction may involve cleavage of the $[S\text{--}Cl\text{--}Cl]^\bullet$ bond, as proposed in eq [67]

$$[67] \quad R\text{-}SO_2\bullet \xrightarrow{Cl_2} [R\text{-}SO_2\text{--}Cl\text{--}Cl]\bullet \longrightarrow R\text{-}SO_2Cl\bullet \; + \; Cl\bullet$$

3.3.2.2.3 Intermediates and molecular orbital calculations

The mechanism of Scheme 6 postulates that F^-, rather than Cl^-, forms an anionic $Ph_2S(O)X^-$ intermediate. In an attempt to uncover any differences between the reactivity of F^- and Cl^- ions, or $F^\bullet$ and $Cl^\bullet$ radicals, we carried out *ab initio* calculations of several anionic and radical species **19-22** using the GAUSSIAN92 program[19] with a fixed phenyl ring of standard geometry at the 3-21G* level. The calculated structures are shown in Figure 32. Phenyl substituents in **19-20** have been replaced with fluoro substituents in **21-22** in order to simplify the calculations. Experimental structural data are available for compounds such as **23-25**, as shown in Figure 33, and our analysis is based on a simple comparison between calculated and experimental structures. S-X bond lengths are also known for related compounds such as SOF_2 (158.0 pm), $SOCl_2$ (207.0 pm), and SO_2Cl_2 (199.0 pm).[135]

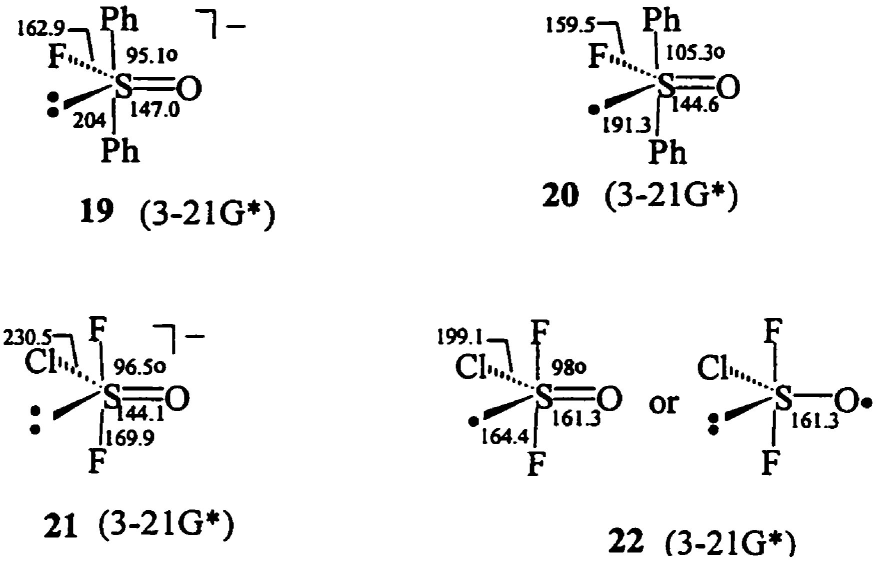

19 (3-21G*) **20** (3-21G*) **21** (3-21G*) **22** (3-21G*)

Figure 32. Calculated geometries of some anionic and radical species.

The calculated structures of fluoroanion **19** and chloroanion **21** reveal a significant difference in S-X bond length. The S-F bond length in **19** is 162.9 pm, which may be compared with experimental S-F bond lengths of 153.9-159.6 pm in **23-25**, for an average lengthening of 3.9%. On the other hand, the chloroanion **21** has a calculated S--Cl bond length of 230.5 pm, which is 12.6% longer than the experimental S-Cl bond length of 204.7 pm in **25**. The lengthened/weakened S--Cl bond in **21** implies a short-lived intermediate of low concentration, which makes further oxidation to a chloro radical less likely. The relatively short/strong S-F bond in fluoroanion **19**, $Ph_2S(O)F^-$, however, implies a more stable intermediate of greater concentration, which favours subsequent oxidation to the fluoro radical **20**, $Ph_2S(O)F^{\bullet}$. Such an interpretation can explain the unique role of fluoride ion in **6**, and is consistent with catalysis of oxidation reactions by CsF and KF.[136]

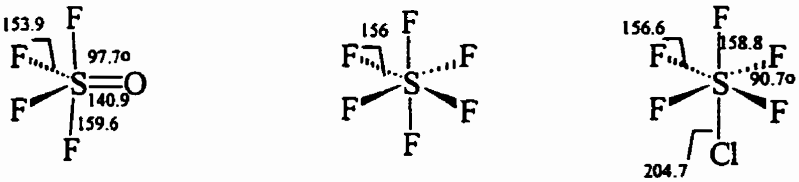

23 (exp) **24** (exp) **25** (exp)

Figure 33. Experimental structural data of some sulfur (VI) halides

Quite a different conclusion is reached on the basis of the calculated structures of radical species **20** and **22**. The S-F bond length in **20** is 159.5 pm, which may be compared with experimental S-F bond lengths of 153.9-159.6 pm in **23-25**. The chloroanion **22** has a calculated S-Cl bond length of 199.1 pm, which is compared with the experimental S-Cl bond length of 204.7 pm in **25**. Both S-F and S-Cl bond lengths are shorter/stronger in the radicals than in the anions and, most significantly, both S-F and S-Cl bonds in the radicals are comparable in length to those in stable compounds **23-25**. These results suggest that both fluoro and chloro radicals are reasonable intermediates. According to this interpretation, fluorosulfur(V) radical $Ph_2S(O)F^{\bullet}$ may be formed from sources of $F^{\bullet}$, or by oxidation of fluoroanion $Ph_2S(O)F^{-}$, whereas chlorosulfur(V) radical $Ph_2S(O)Cl^{\bullet}$ can only be formed from sources of $Cl^{\bullet}$. It is interesting to speculate whether the behaviour of the F^--$F^\cdot$ system in the oxidation reaction, as discussed above, is shared by the closely related OH^--$HO^\cdot$ system.

3.3.2.3 Synthesis of diphenylsulfur(VI) cation, $Ph_2S(O)F^+$

Reaction pathways change abruptly in the presence of Lewis acid. Addition of boron trifluoride, BF_3, to $Ph_2S(O)F_2$ produced the diphenylsulfur(VI) cation, $Ph_2S(O)F^+$, in essentially quantitative yield according to eq 68. This cation is stable in ptfe equipment for months and can be characterized by ^{19}F and ^{13}C NMR (Table 6 and Figure 34-35).

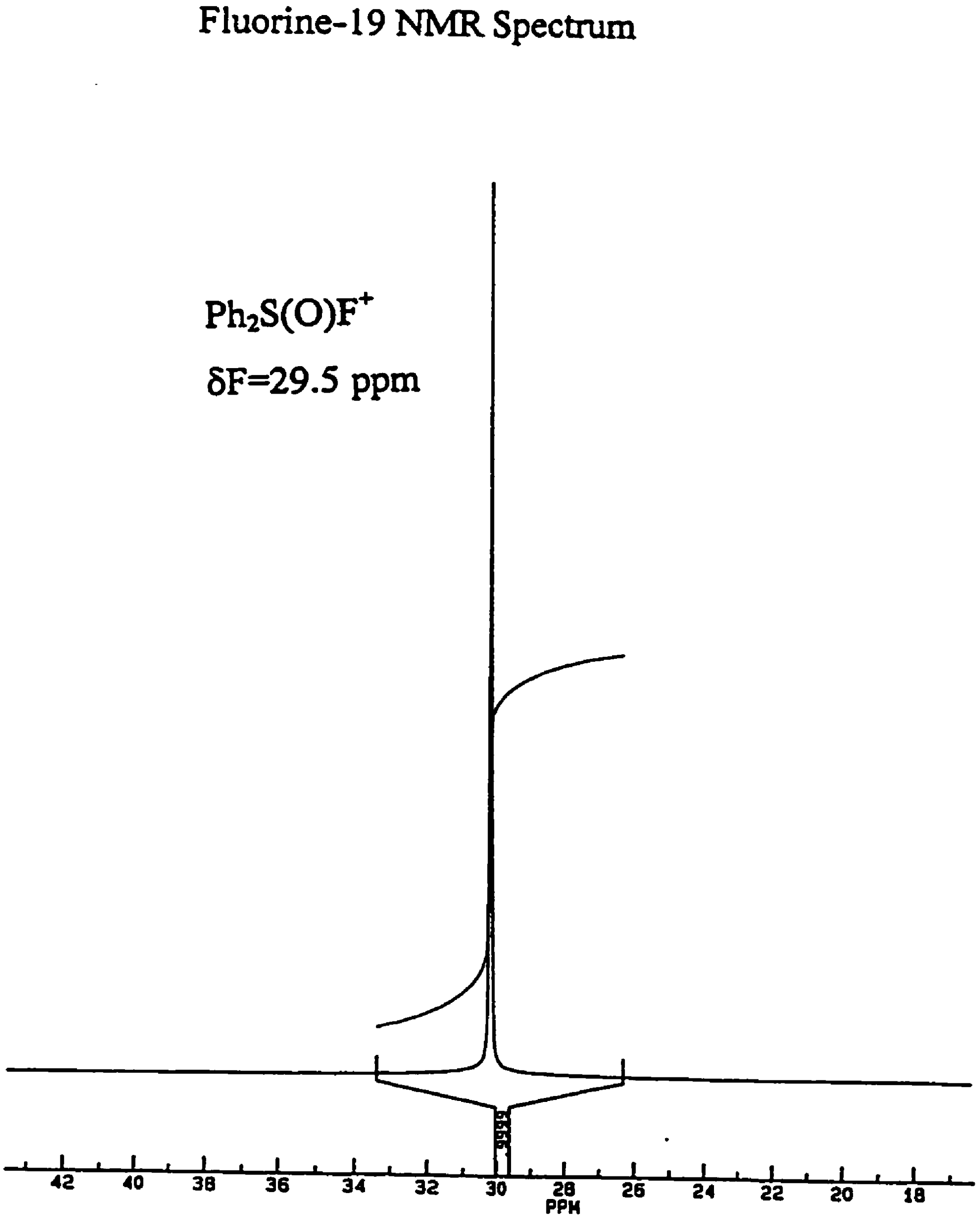

Figure 34. ^{19}F NMR spectrum of $Ph_2S(O)F^+BF_4^-$ in CD_2Cl_2.

Carbon-13 NMR Spectrum

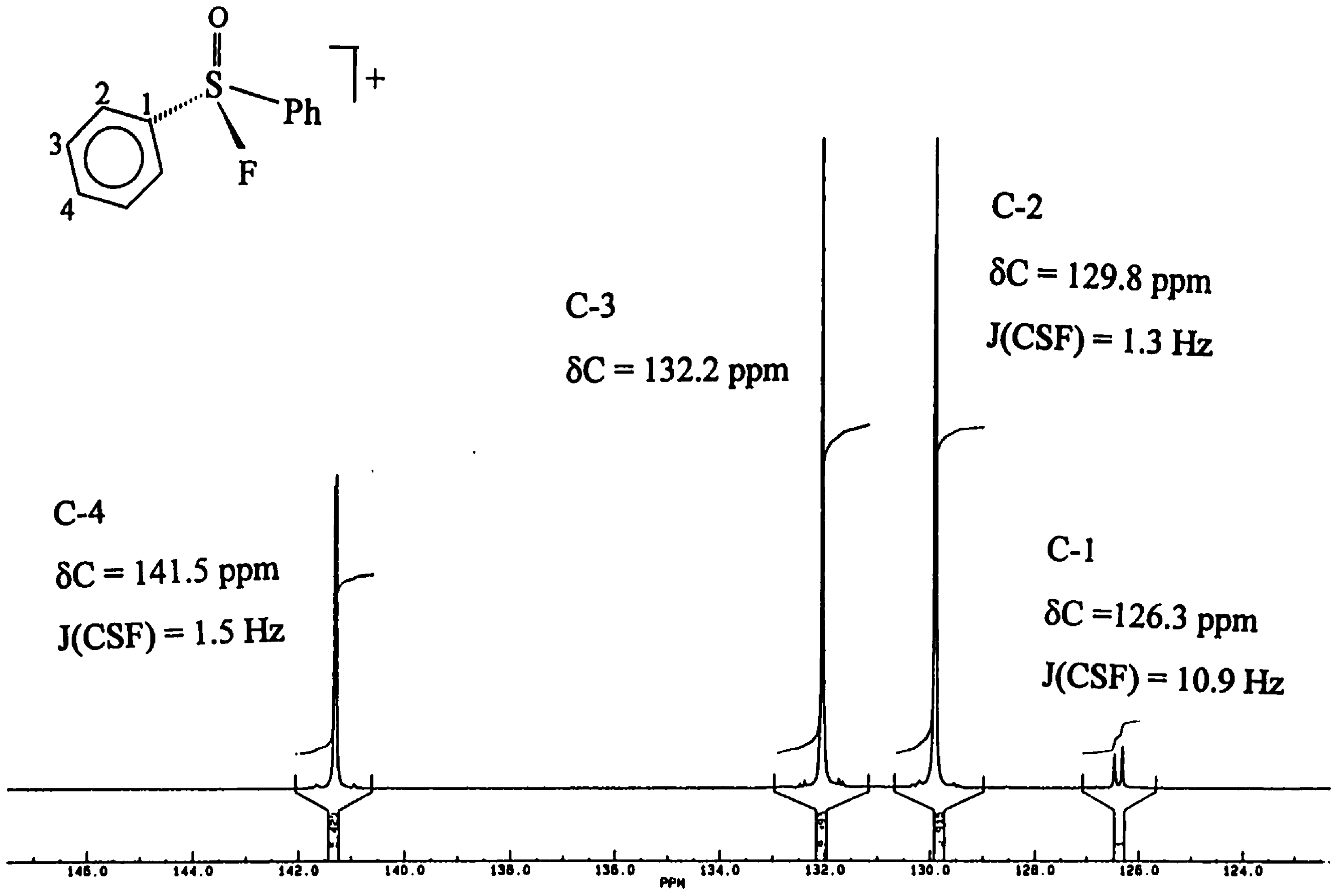

Figure 35. ^{13}C NMR spectrum of $Ph_2S(O)F^+BF_4^-$ in CD_2Cl_2.

The ^{19}F NMR spectrum in Figure 34 shows a singlet at 29.5 ppm, as only one fluorine is left in the molecule, and the ^{13}C NMR examination of $Ph_2S(O)F^+$ in Figure 35 revealed the equivalence of the two phenyl substituents. The presence of one fluorine atom in the molecule is proven by the doublet splitting of the ipso carbon C1 and ortho carbon C2.

[68] 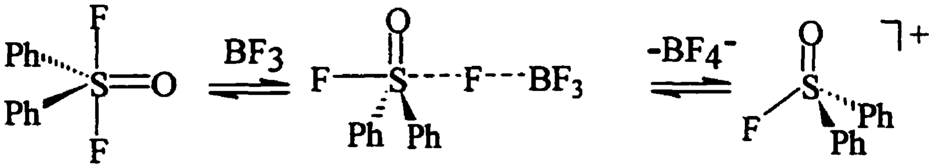

Reaction [68] is written as an equilibrium, but this equilibrium lies completely to the right and it does not provide a pathway of rapid fluorine exchange, as demonstrated by the ^{13}C NMR spectrum in Figure 34, which shows retention of C-S-F coupling in all samples of purified $Ph_2S(O)F^+BF_4^-$. Since C1-F and C2-F coupling is clearly visible, there cannot be any fluorine exchange in the cation which is rapid in the NMR time scale. Rapid exchange does occur on mixing $Ph_2S(O)F^+BF_4^-$ and $Ph_2S(O)F_2$ at room temperature, as will be discussed in the following section.

3.3.2.4 Fluorine exchange in the $Ph_2S(O)F_2$-$Ph_2S(O)F^+$ system and preparation of diphenyldichlorosulfur(VI) oxide

3.3.2.4.1 Fluorine exchange in the $Ph_2S(O)F_2$-$Ph_2S(O)F^+$ system

The fluorine exchange studies were carried out for a mixture of $Ph_2S(O)F_2$ and $Ph_2S(O)F^+$ cation. A symmetrical intermediate with a weak bridging S--F--S bond may be postulated, as shown in Scheme 8.

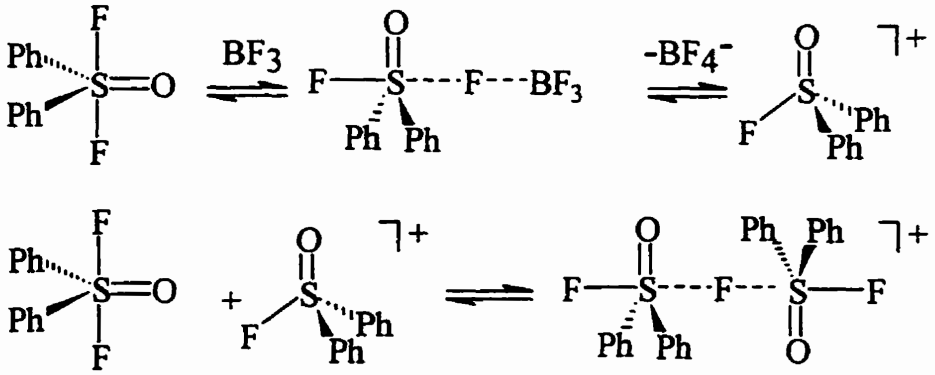

Scheme 8. Proposed mechanism of fluorine exchange in the $Ph_2S(O)F_2$-$Ph_2S(O)F^+$ system

In support of the mechanism of Scheme 8, it may be noted that related cations of S(VI), Se(VI) and Te(VI) are stable[137] e.g. OSF_3^+, OSF_2Cl^+, $RN{=}SF_3^+$, RSF_4^+, $Me_2NSF_4^+$ and $FS[C_6H_4C(CF_3)_2O]_2^+$. Rapid fluorine exchange between cationic and neutral tellurium(VI) fluorides has been discussed for the Ph_3TeF_2X-Ph_3TeFX^+ (X=F, Cl, OH) systems[9], and fluorine-bridged intermediates are postulated in each case. Fluorine exchange and isomerization in octahedral sulfur(VI) and tellurium(VI) fluorides undoubtedly involves cationic species because the processes are catalyzed by Lewis acids such as SbF_5, PF_5, and BF_3. In some cases, Lewis acids are not deliberately added, but the H_2O-HF-glass system may inadvertently provide boron- or silicon- containing Lewis acids.[3]

Mixtures of $Ph_2S(O)F_2$ and $Ph_2S(O)F^+$ were prepared in two ways, either by mixing a sample of $Ph_2S(O)F_2$ and $Ph_2S(O)F^+BF_4^-$, or by adding less than an equivalent of BF_3 to $Ph_2S(O)F_2$. The latter method is generally more convenient because it reduces the handling of moisture sensitive compounds. The ^{13}C NMR chemical shift of C1 moves downfield by 21.5 ppm, as $Ph_2S(O)F_2$ is converted to $Ph_2S(O)F^+$, in agreement with the trend established for a variety of main group fluorides, in which C1 shifts downfield by 16 to 26 ppm as F^- is removed. (See Section 3.3.2.5 for more details). Rapid fluorine exchange in the $Ph_2S(O)F_2$-$Ph_2S(O)F^+$ system can be monitored and studied by either ^{19}F or ^{13}C NMR at room temperature (300 K) as shown in Figure 36 and Figure 37.

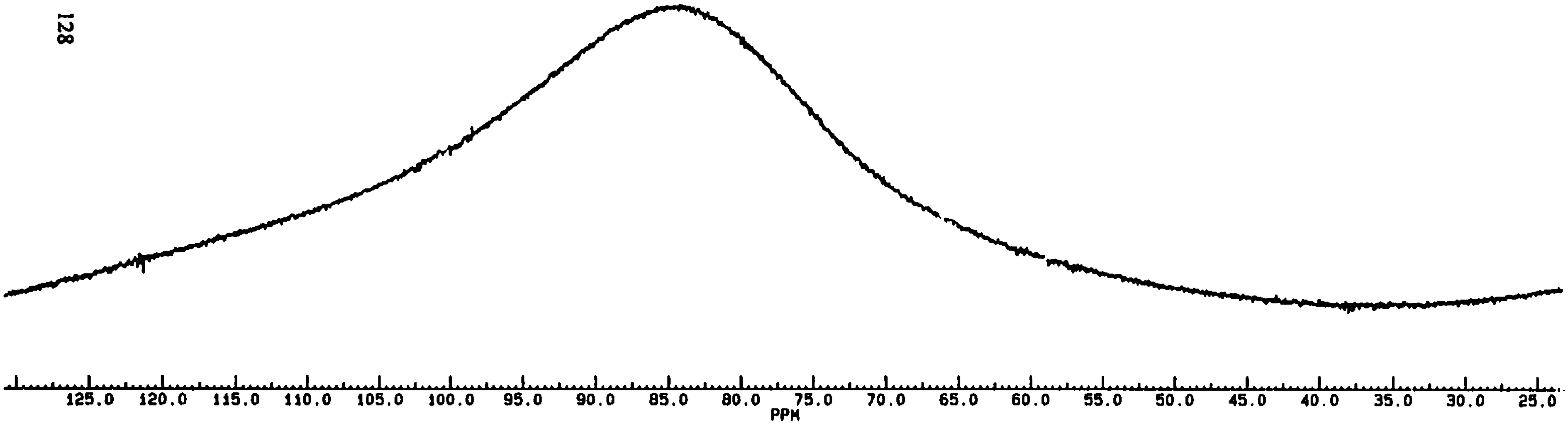

Figure 36. ^{19}F NMR spectrum of a 3:1 mixture of $Ph_2S(O)F_2$ and $Ph_2S(O)F^+BF_4^-$ in CD_2Cl_2 at room temperature.

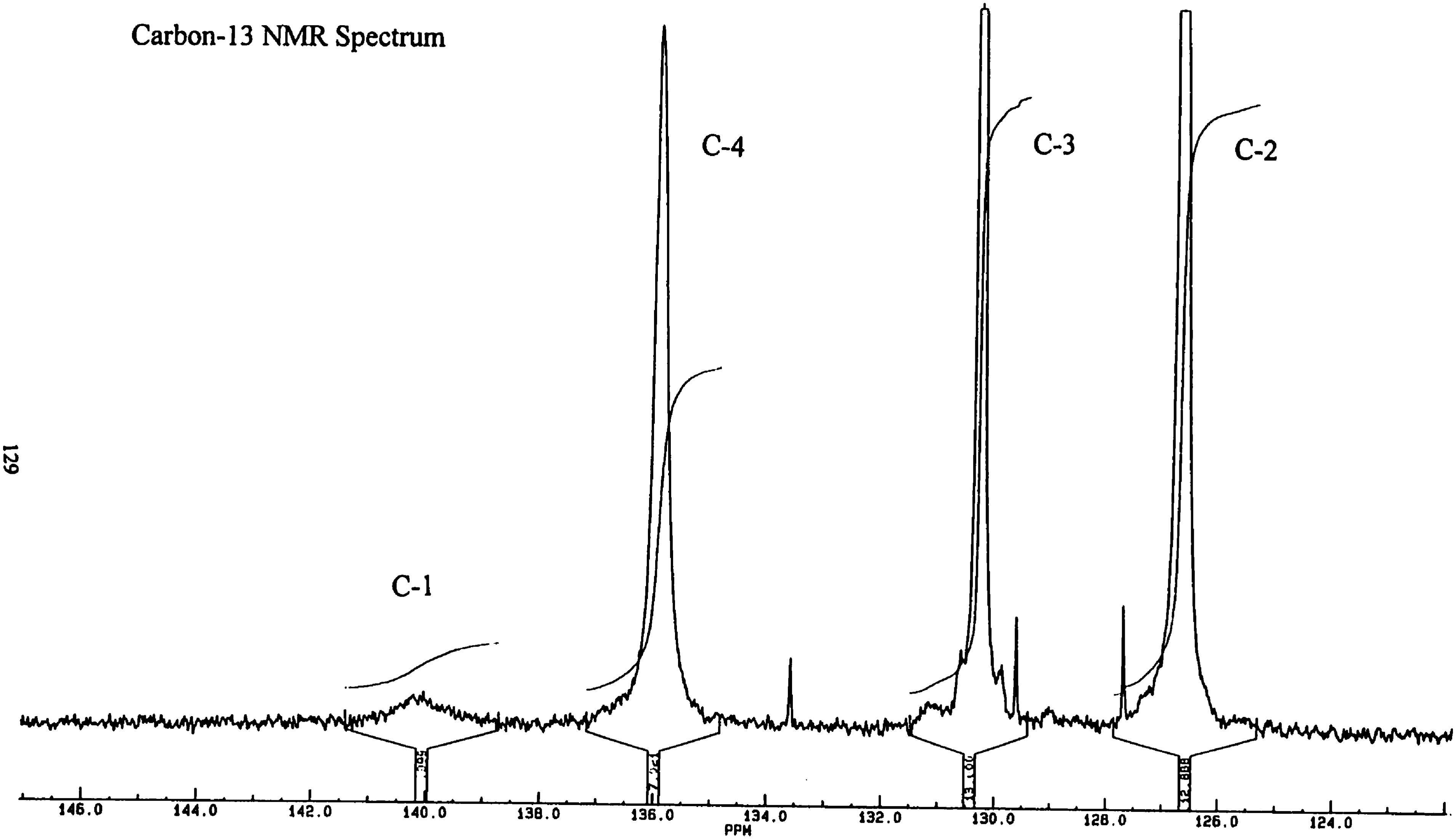

Figure 37. ^{13}C NMR spectrum of a 3:1 mixture of $Ph_2S(O)F_2$ and $Ph_2S(O)F^+BF_4^-$ in CD_2Cl_2 at room temperature.

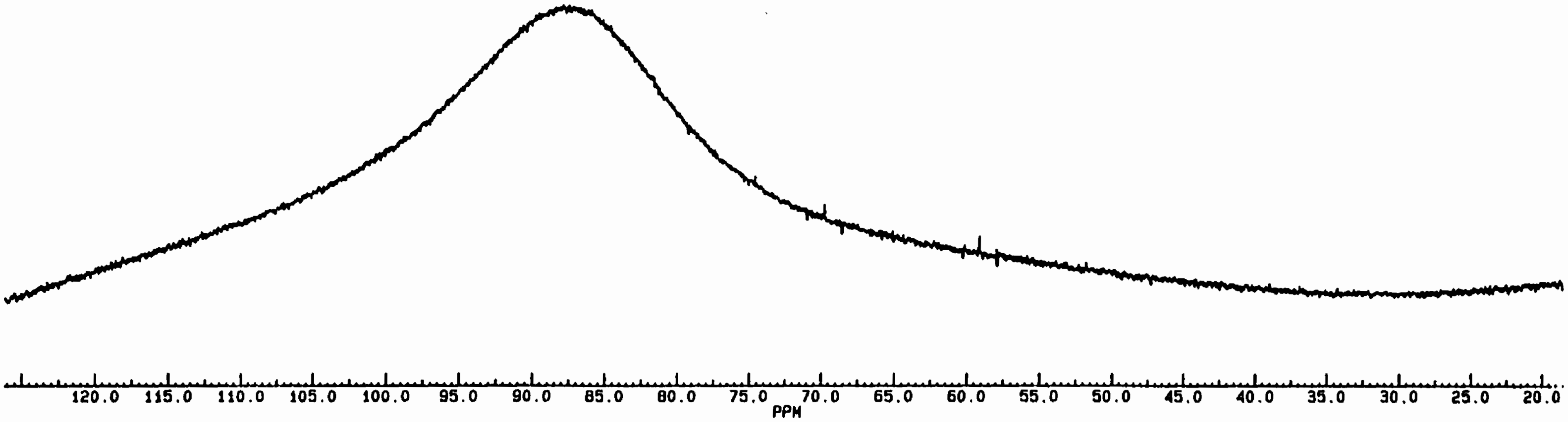

Figure 38. ^{19}F NMR spectrum of a 6:1 mixture of $Ph_2S(O)F_2$ and $Ph_2S(O)F^+BF_4^-$ in CD_2Cl_2 at room temperature.

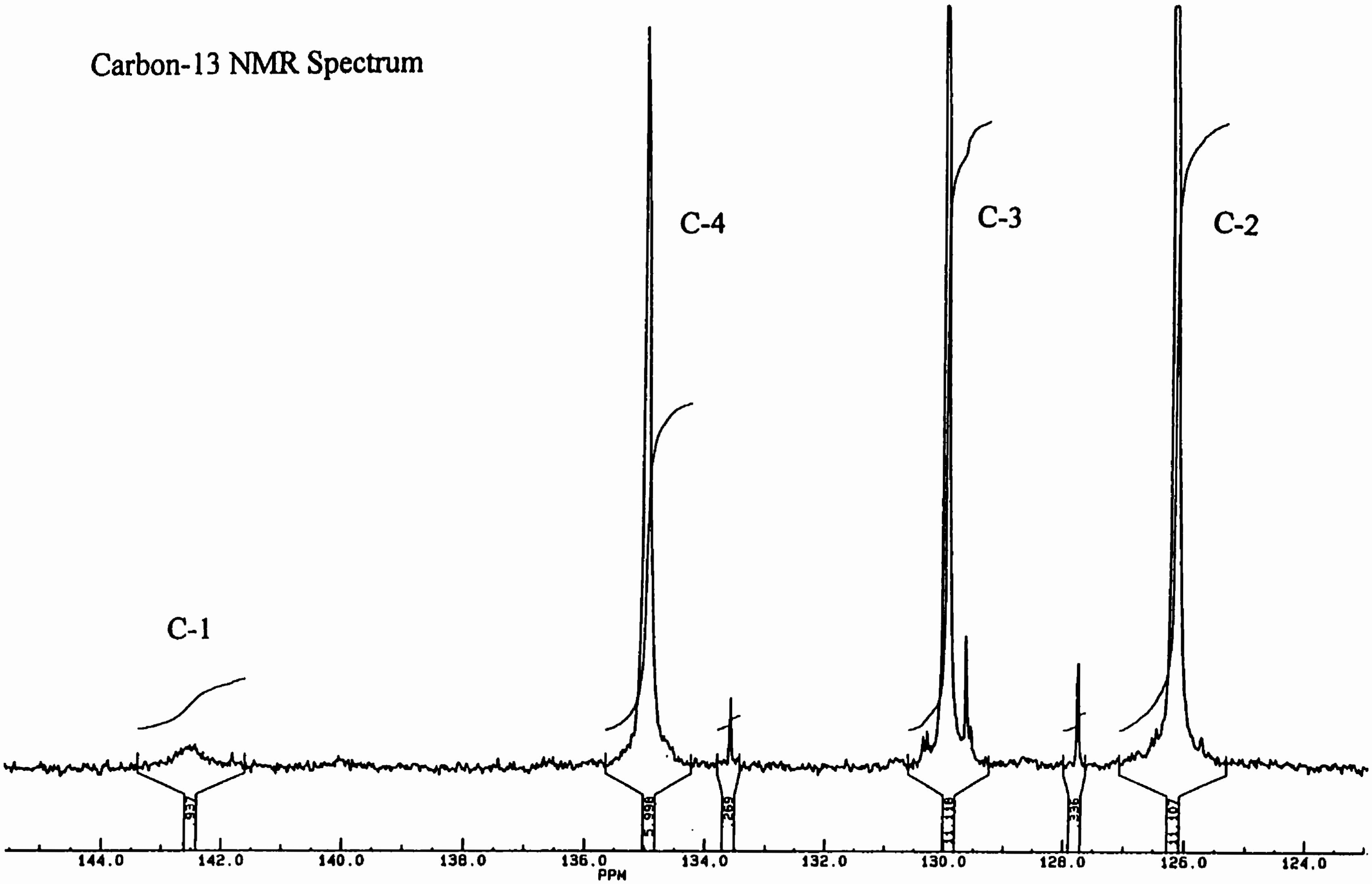

Figure 39. ^{13}C NMR spectrum of a 6:1 mixture of $Ph_2S(O)F_2$ and $Ph_2S(O)F^+BF_4^-$ in CD_2Cl_2 at room temperature.

The ^{13}C NMR of the mixture shows that the J_{C-F} coupling in both $Ph_2S(O)F_2$ and $Ph_2S(O)F^+$ is lost, and the ^{13}C NMR resonances for phenyl groups in both $Ph_2S(O)F_2$ and $Ph_2S(O)F^+$ were not observed, instead, only the weighted average and broadened peaks of C1-C4 of the phenyl group were observed at ambient temperature because of rapid fluorine exchange.

The ^{19}F NMR peaks for both $Ph_2S(O)F_2$ and $Ph_2S(O)F^+$ also disappeared and only one very broadened peak between $\delta F[Ph_2S(O)F_2]$ and $\delta[Ph_2S(O)F^+]$ was obtained. ^{19}F and ^{13}C NMR spectra with different concentrations of reactants are shown in Figure 38 and 39.

Variable temperature ^{19}F NMR experiments on a mixture of $Ph_2S(O)F_2$ and $Ph_2S(O)F^+$ were carried out in CD_2Cl_2 solution from 300 K down to 200 K. Figure 40 illustrates the temperature-dependent ^{19}F NMR spectra observed in the $Ph_2S(O)F_2$ and $Ph_2S(O)F^+$ system. At 300 K, fluorine exchange occurs at an intermediate rate. A very broad peak was observed. The chemical shift of the mixture is very close to the weighted average chemical shifts of $Ph_2S(O)F_2$ and $Ph_2S(O)F^+$. As the temperature decreases to 270 K, the fluorine exchange moves to slow exchange range, and two broad separated peaks appear. Successive sharpening of the single peak occurs with decreasing rate constant (on decreasing the temperature), and eventually at 200 K the fluorine exchange is essentially stopped. Two very sharp peaks corresponding to the "rigid" compounds $Ph_2S(O)F_2$ and $Ph_2S(O)F$ were obtained, and integration of this low temperature spectrum gives a direct measure of the ratio of $Ph_2S(O)F_2$ and $Ph_2S(O)F^+$, which is consistent with the ratio obtained from the room temperature ^{13}C NMR spectrum and the weighted

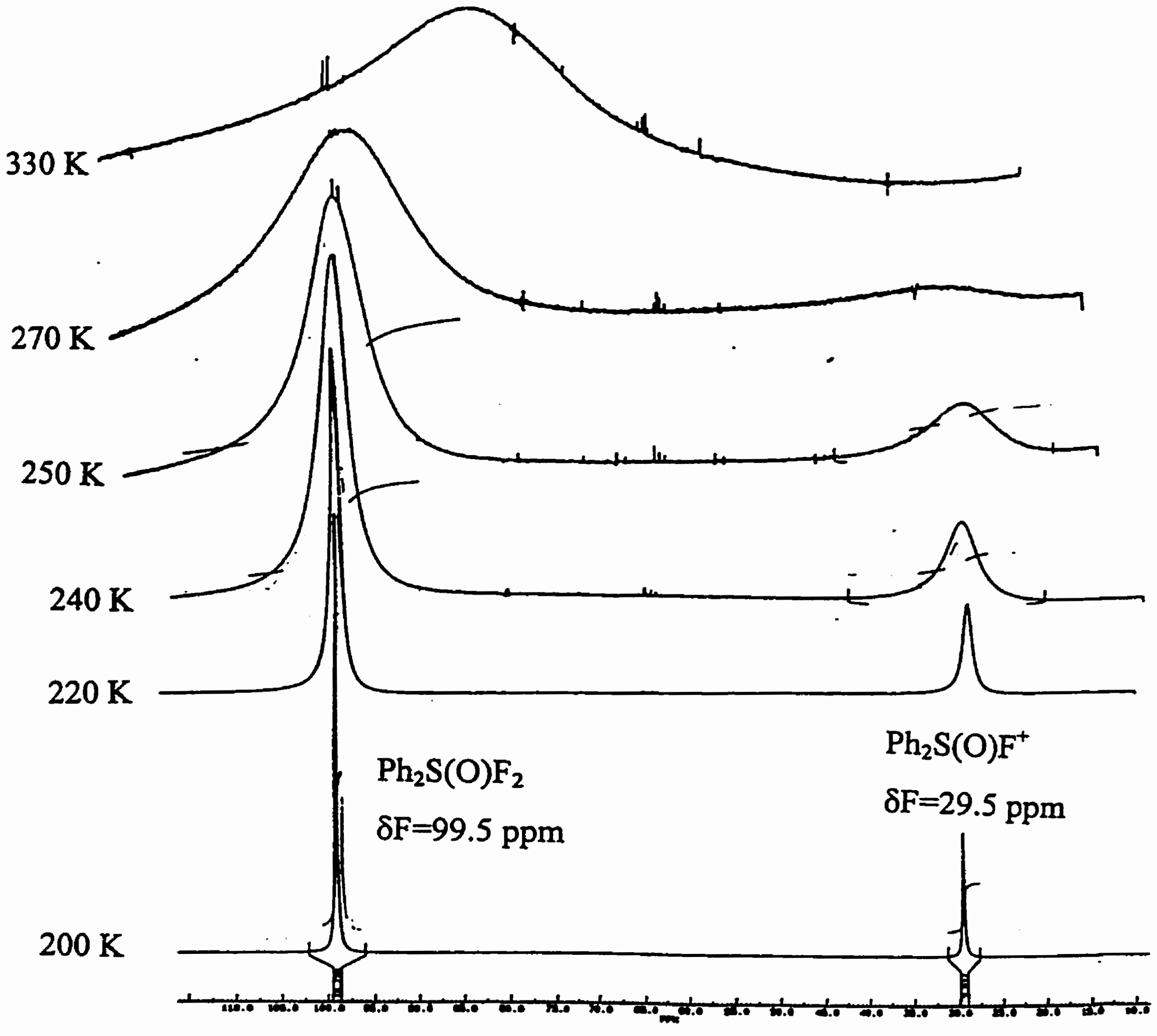

Figure 40. Variable-temperature ^{19}F NMR spectra of a 3:1 mixture of $Ph_2S(O)F_2$ and $Ph_2S(O)F^+BF_4^-$ in CD_2Cl_2.

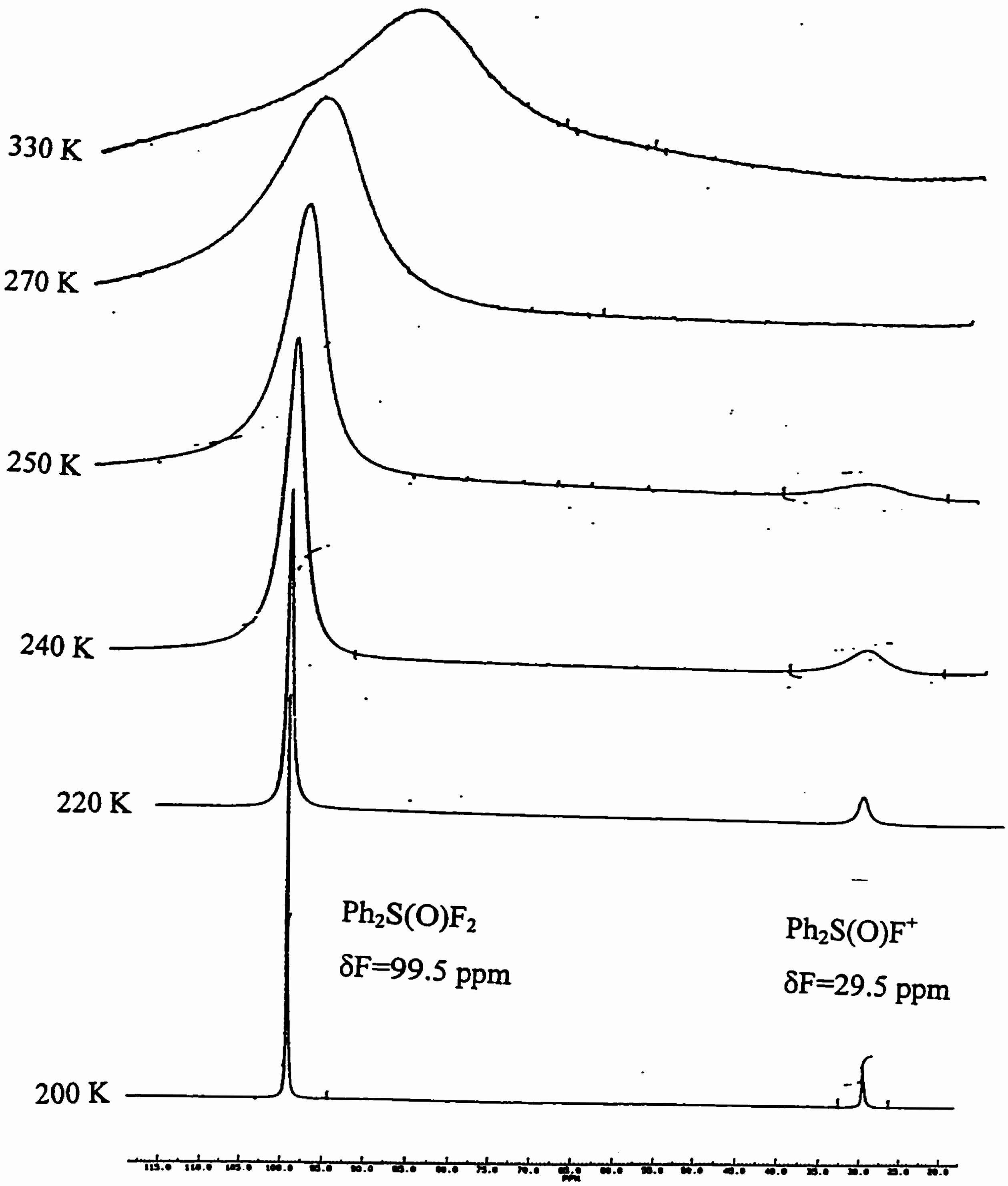

Figure 41. Variable-temperature ^{19}F NMR spectra of a 6:1 mixture of $Ph_2S(O)F_2$ and $Ph_2S(O)F^+BF_4^-$ in CD_2Cl_2.

average of the C1-C4 chemical shifts. The temperature-dependent ^{19}F NMR spectra shown in Figure 40 and 41 clearly display these effects.

That bridged S--F--S bonds are indeed longer/weaker than terminal S-F bonds in typical sulfur fluorides, as required by the mechanism of Scheme 6, is apparent from the calculated S--F--S bridge bond of 193.7 pm in **26**. An experimental value of 211.7 ppm has been found for the S--F--S bridge bond in **27**.[58] Calculated and experimental terminal S-F bond lengths in **26-27** are considerably shorter, in the range 150-173 pm.

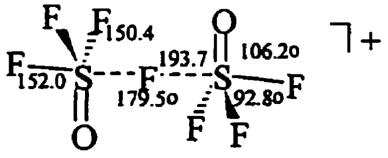

26 (3-21G*)

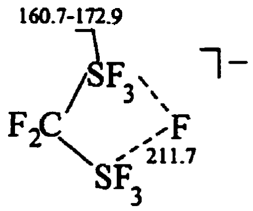

27 (exp)

Figure 42. Calculated and experimental structures for bridged S--F--S Compounds.

3.3.2.4.2 Preparation of diphenyldichlorosulfur(VI) oxide

The mechanism of fluorine exchange in the $Ph_2S(O)F_2$-$Ph_2S(O)F^+$ system can be generalised and applied to the synthesis of $Ph_2S(O)Cl_2$, as proposed in Scheme 9. Both mechanisms of Scheme 8 and Scheme 9 involve cleavage of [S--F--B] $^+$ and [S--F--S] $^+$ bridging bonds.

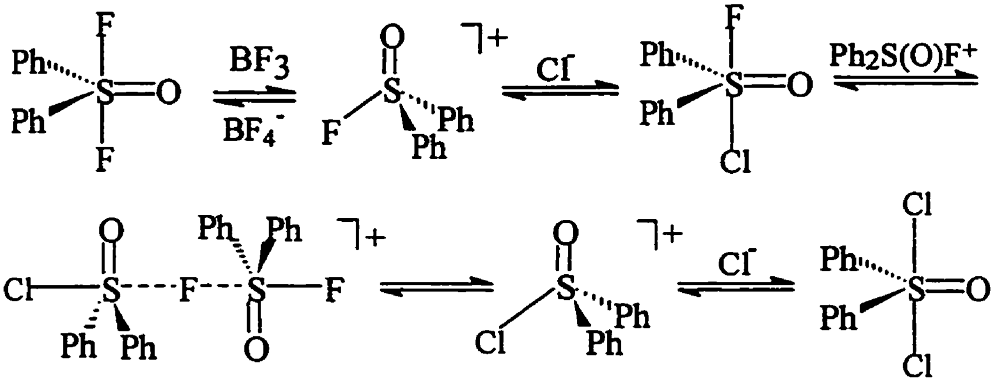
BF3
BF4-
Cl-
Ph2S(O)F+
Cl-

Scheme 9. Proposed mechanism of formation of $Ph_2S(O)Cl_2$.

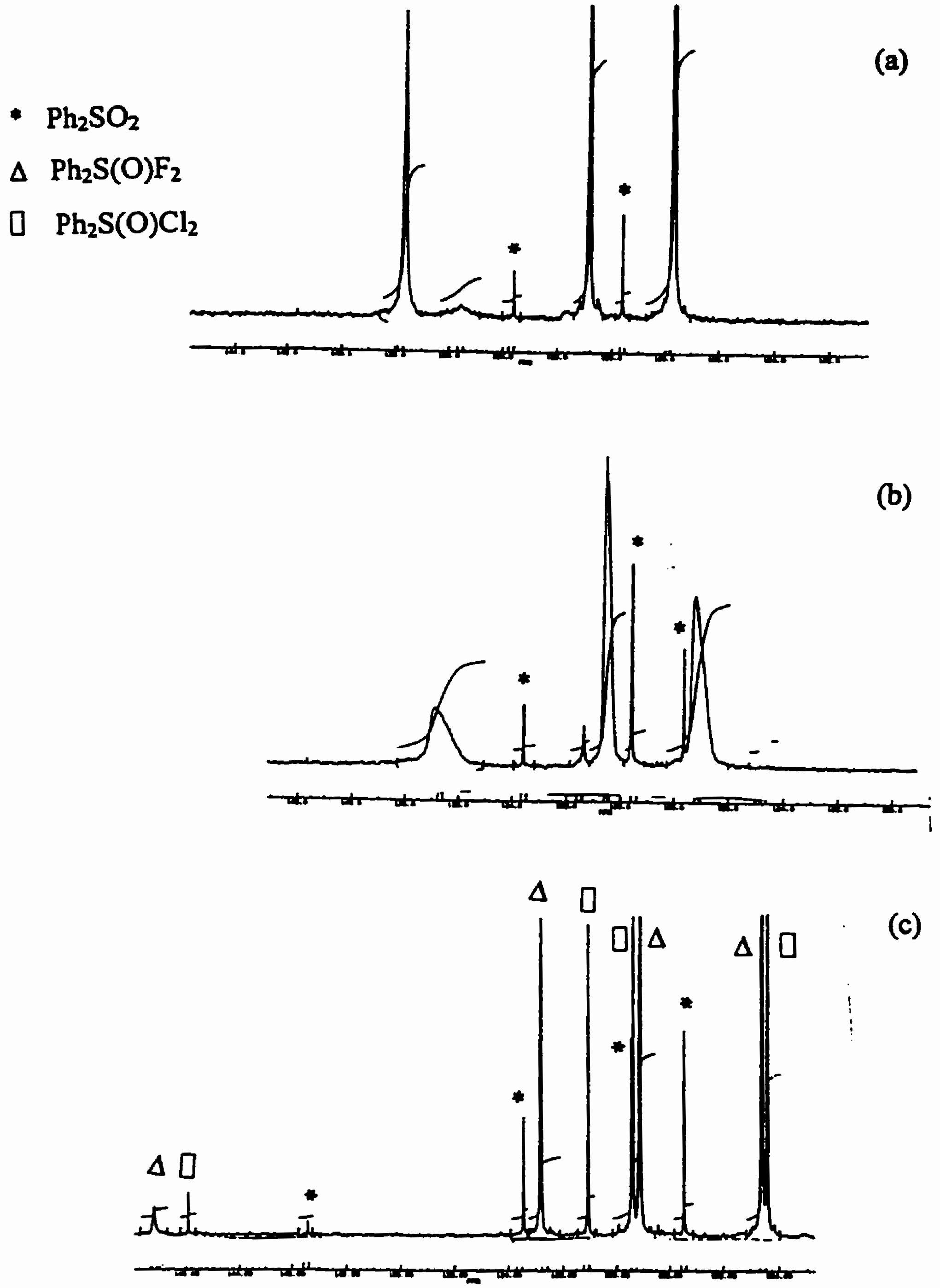

Figure 43. (a) The ^{13}C NMR spectrum of a 45:55 (0.297 mmol in total) mixture of $Ph_2S(O)F^+$ and $Ph_2S(O)F_2$ in a ptfe-lined NMR tube in CD_2Cl_2 solution. (b) The same sample after addition of 18 mg (0.12 mmol) of Et_4NCl, showing that all species in solution are undergoing rapid halogen exchange. (c) The ^{13}C NMR spectrum after addition of another 50 mg (0.32 mmol) of Et_4NCl to b, showing that halogen exchange is stopped. Eight carbon peaks expected for a mixture of "rigid" $Ph_2S(O)Cl_2$ and $Ph_2S(O)F_2$ are observed. The C1-C4 peaks of the hydrolysis product Ph_2SO_2 are marked with an asterisk.

$Ph_2S(O)Cl_2$ was prepared by adding an excess of tetraethylammonium chloride to a solution containing $Ph_2S(O)F^+$, and identified by ^{13}C NMR and by its hydrolysis to $Ph_2S(O)Cl_2$. The C1-C4 chemical shifts of $Ph_2S(O)Cl_2$ are very similar to those of $Ph_2S(O)F_2$, as seen in Table 6 and Figure 42, and the absence of C1-F and C2-F coupling confirms that no S-F bonds are present. The possibility that an exchange process is responsible for lack of C1-F or C2-F coupling was ruled out through preparation of a sample containing a mixture of $Ph_2S(O)Cl_2$ and $Ph_2S(O)F_2$. This mixture showed eight ^{13}C NMR peaks, as expected for a mixture of "rigid" $Ph_2S(O)Cl_2$ and $Ph_2S(O)F_2$. As shown in Figure 43c, hydrolysis of this mixture gave only Ph_2SO_2, eq [69], as confirmed by ^{13}C NMR.

$$[69] \quad Ph_2S(O)F_2 \; + \; Ph_2S(O)Cl_2 \xrightarrow{H_2O} Ph_2SO_2 \; + \; HX\,(X{=}F, Cl)$$

Some evidence for the stoichiometry and mechanism of scheme 9 was obtained by adding varying amounts of Cl^- to a solution containing $Ph_2S(O)F_2$ and $Ph_2S(O)F^+$. If the amount of Cl^- is less than that of $Ph_2S(O)F^+$, the ^{13}C NMR spectrum shows only four broadened and averaged C1-C4 peaks (seen in Figure 42b), as all species in solution undergo rapid halogen exchange in the presence of excess cation $Ph_2S(O)F^+$. If the amount of Cl^- (a large excess) exceeds that of cation $Ph_2S(O)F^+$, then halogen exchange is stopped and the ^{13}C NMR spectrum shows eight carbon peaks as expected for a mixture of "rigid" $Ph_2S(O)Cl_2$ and $Ph_2S(O)F_2$. Integration of the ^{13}C NMR spectrum shows that each mole of cation $Ph_2S(O)F^+$ produced half a mole of $Ph_2S(O)Cl_2$ and half a mole of $Ph_2S(O)F_2$, consistent with the stoichiometry of Scheme 9.

Brief investigation by ^{13}C NMR showed that no fluorine exchange occurs in a mixture of $Ph_2S(O)F_2$ and Ph_2SO_2, nor in a mixture of Ph_2SO_2 and $Ph_2S(O)F^+$.

The reaction of Et_4NCl with $Ph_2S(O)F^+$ was studied separately and the reaction was monitored by ^{13}C NMR. When 18 mg (0.12 mmol) of Et_4NCl was added to a mixture of $Ph_2S(O)F_2$ and $Ph_2S(O)F^+$ in CD_2Cl_2, only the average broadened peaks of C1-C4 of phenyl were observed (indicating a much slower exchange rate) in its ^{13}C NMR spectrum, as shown in Figure 43. When another 50 mg (0.32 mmol) of Et_4NCl was added to the reaction mixture, ^{13}C NMR revealed that the exchange was completely stopped and two types of "rigid" phenyl derivatives of sulfur compounds, were formed as characterised in Figure 43c and Table 6, with very similar chemical shifts of C1-C4 of the phenyl rings. Hydrolysis of the reaction products by adding excess of water into the reaction mixture produced Ph_2SO_2 as the only hydrolysis product.

TABLE 6 ^{19}F and ^{13}C NMR chemical shifts (ppm) and C-F coupling constants (Hz) of some diphenylsulfur oxyhalides

Compound	δF	δC1	δC2	δC3	δC4
$Ph_2S(O)F^+BF_4^-$	29.5	126.3 (10.8 Hz)	129.8 (1.3 Hz)	132.2	141.5 (1.2 Hz)
$Ph_2S(O)F_2$	99.0	147.8 (17.1 Hz)	124.9 (6.1 Hz)	129.2	132.9
$Ph_2S(O)Cl_2$	- - -	145.9	124.4	129.4	131.1

3.3.2.5 ^{13}C NMR study of phenyl derivatives of B, Si, Sn, P, Te and S fluorides

The above and previous NMR studies of fluorine exchange in silicon, phosphorus, and tellurium fluorides in our laboratory have found that intermolecular fluorine exchange is rapid in systems such as $Ph_2S(O)F_2$-$Ph_2S(O)F^+$, $MeSiF_3$-$MeSiF_4^-$, SiF_5^--SiF_6^{2}, $PhPF_4$-$PhPF_5^-$, and $Ph_3TeF_2^+$-Ph_3TeF_3, through fluorine-bridged intermediates. This intermolecular exchange, sometimes initiated by common impurities, may complicate spectral identification if ^{19}F NMR is used to monitor fluorine site exchange. ^{13}C NMR spectroscopy is particularly useful for confirming the geometry since it reveals the equivalence of the non-labile phenyl substituent in both exchanging species.

Ten published ^{13}C NMR spectra of phenyl-element fluorides are collected, along with $Ph_2S(O)F^+$ and $Ph_2S(O)F_2$ for comparison purpose. The same numbering system was used for all compounds. For those molecules which have two types of phenyl substituents, e.g. *mer*-Ph_3TeF_3, two sets of carbons C1-C4 and C1'-C4' are used (seen in Scheme 10). The distribution of the chemical shifts of all 12 compounds is shown in Table 7. As we can see from the table, the ^{13}C NMR chemical shift of ipso carbon C1 moves consistently downfield by 15.6 to 25.7 ppm as F^- is added to various phenyl-element fluorides. There is an opposite effect on carbons C2-C4, which move upfield as F^- is added, with the exception of C2 of $PhSiF_3$. C4 has the largest upfield chemical shift change, C2 has a modest change, while C3 has hardly changed although it indeed moved slightly upfield.

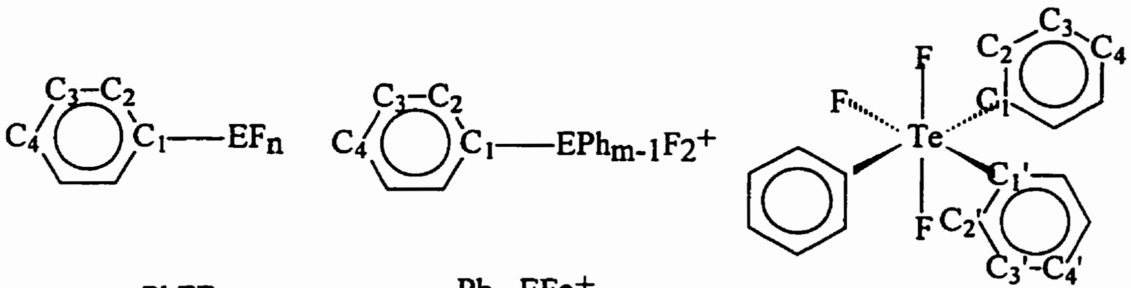
C3–C2
C4
C1——EFn
C3–C2
C4
C1——EPhm-1F2+
F
F
Te
F
C2
C3
C4
C1
C1'
C2'
C3'-C4'

PhEFn

E=B, C, Si, P, S(O)

n=2-5

$Ph_mEF_2^+$

E=Te, S(O)

m=2-3

mer-Ph_3TeF_3

Scheme 10. Atom numbering for phenyl-element fluorides.

Table 7. ^{13}C NMR chemical shifts (ppm) and C-F coupling constants (in Hz, in parenthesis) of some phenyl derivatives of B, C, Si, P, Te, and S fluorides.

Compound	δC1	δC2	δC3	δC4
$PhBF_2$	124.8 (36.3)	136.9 (4.8)	129.1 (0)	134.8 (1.2)
$PhBF_3^-$	150.1 (49.2)	131.8 (1.6)	126.8 (0)	125.6 (0.7)
$PhCF_2^+$	112.2 (8.2)	145.5 (10.7)	134.1 (1.0)	159.5 (5.7)
$PhCF_3$	131.0 (32.2)	125.2 (3.9)	128.8 (--)	131.8 (1.4)
$PhSiF_3$	120.8 (25.6)	134.8 (1.3)	128.9 (0.8)	133.6 (0.4)
$PhSiF_4^-$	141.8 (34.9)	137.7 (3.2)	127.2 (0)	128.8 (0)
$PhPF_4$	125.9 (20.0)	137.4	129.8	133.6
$PhPF_5^-$	151.6 (46.2 F_{eq}) (0 F_{ax})	131.1 (4.8 F_{eq}) (0 F_{ax})	126.8 (2.2 F_{eq}) (0 F_{ax})	126.6 (0 F_{eq}) (0 F_{ax})
$Ph_3TeF_2^+$	129.6	133.3	133.2	137.6
Ph_3TeF_3	151.2	129.7	130.8	129.9
C1' to C4'	145.2	131.6	131.9	132.2
$Ph_2S(O)F^+$	126.3 (10.8)	129.8 (1.3)	132.2	141.5
$Ph_2S(O)F_2$	147.8 (17.1)	124.9 (6.1)	129.2	132.9

A similar qualitative behavior in the $Ph_2S(O)F^+$-$Ph_2S(O)F_2$ system has also been observed. The ^{13}C chemical shift of C1 shifts downfield by 21.5 ppm, C4 moves upfield by 8.6 ppm, C2 shifts upfield by 4.9 ppm, and C3 moves upfield only by 0.6 ppm as demonstrated in Figure 44. In mixtures of $Ph_2S(O)F_2$ and $Ph_2S(O)F^+$, only the weighted average ^{13}C shifts can be observed at ambient temperature because of rapid fluorine exchange, as illustrated in Figure 44 for a 45:55 mixture.

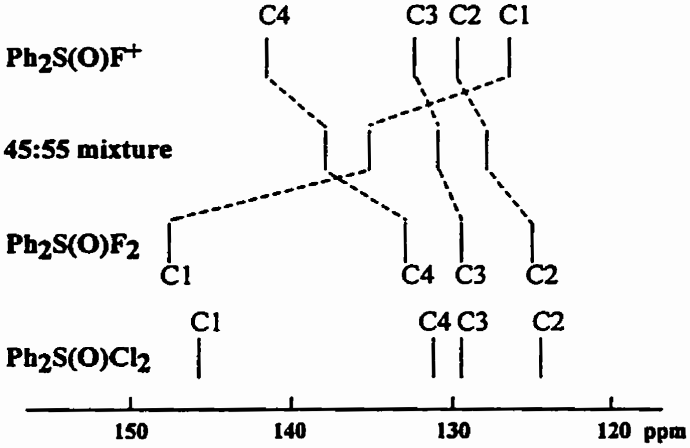

Figure 44. Distribution of ^{13}C NMR chemical shifts of the $Ph_2S(O)F^+$ and $Ph_2S(O)F_2$ system. The 45:55 mixture of $Ph_2S(O)F^+$ and $Ph_2S(O)F_2$ was prepared by adding BF_3 to a solution of $Ph_2S(O)F_2$ in CD_2Cl_2. Also shown for comparison is the ^{13}C NMR spectrum of $Ph_2S(O)Cl_2$.

3.3.2.6 $Ph_2S(O)F_2$ and the H_2O-HF-glass system

The hydrolysis of difluorosulfurane oxides, $R_2S(O)F_2$, and reactions with glass, alcohols, and other reagents, has been reported.[67,114,119] Our study of fluorine exchange in the $Ph_2S(O)F_2$-$Ph_2S(O)F^+$ system described above suggested a method of monitoring the effects of the H_2O-HF-glass system. The latter system often interferes with synthetic and mechanistic studies of reactive fluorinated compounds. The detection method depends on the ^{13}C NMR spectrum of the "rigid" hydrolysis product Ph_2SO_2, eq [70], and on the weighted average of the ^{13}C NMR spectrum of rapidly exchanging $Ph_2S(O)F_2$ and $Ph_2S(O)F^+$ in eq [72]. In addition, the ratio of fluorinated products can be determined either by integration of the low temperature ^{19}F NMR spectrum where all exchange is stopped, or at room temperature by means of the weighted average ^{13}C NMR chemical shifts, as described earlier in this chapter. Therefore, if the concentration of the cation is known, then an estimate can be made of the amount of Lewis acid in solution. Another convenient feature about this system is that the hydrolysis product of $Ph_2S(O)F_2$, i.e. Ph_2SO_2, is not involved in the exchange process, but it can be readily detected by ^{13}C NMR.

[70] $Ph_2S(O)F_2 + H_2O \longrightarrow Ph_2SO_2 + 2HF$

[71] $Ph_2S(O)F_2 + HF \rightleftharpoons Ph_2S(O)F^+ + FHF^-$

[72] $Ph_2S(O)F_2 + Ph_2S(O)F^+ \rightleftharpoons Ph_2F(O)S\text{--}F\text{--}S(O)FPh_2^+$

Experiments were carried out with dry and wetted glass in order to distinguish between water on the surface of glass and water that arises as a result of a chemical reaction of glass with hydrogen fluoride, as in eq [73]

$$[73] \quad \text{Borosilicate glass} \xrightarrow{HF} H_2O + BF_3 + SiF_4 + \cdots$$

First, the ^{13}C NMR spectrum of $Ph_2S(O)F_2$ is recorded in a ptfe-lined NMR tube in CD_2Cl_2 solution as shown in Figure 45(a). The coupling of C1-S-F, as well as C2-S-F is clearly seen, hence there is no S-F bond cleavage in $Ph_2S(O)F_2$.

Next, a small dried capillary of borosilicate glass[138] was added to $Ph_2S(O)F_2$ solution. The ^{13}C NMR spectrum was recorded immediately, and again after several hours. The spectrum shown in Figure 45(b) was recorded after 18 hr, and it is identical to that of unreacted $Ph_2S(O)F_2$, as shown in Figure 45(a). Coupling of C1-S-F, as well as C2-S-F is retained, and this demonstrates that dry glass does not react with $Ph_2S(O)F_2$ within 18 hr.

Finally, a small capillary of borosilicate glass was dipped into water and then added to the above sample. As seen in Figure 45(c), four new C1-C4 peaks of the hydrolysis product Ph_2SO_2 are clearly visible. The hydrolysis product Ph_2SO_2 does not participate in any exchange process, and its C1-C4 peaks can be uniquely identified by comparison with an authentic sample. There is a significant change in the C1-C4 chemical shifts of $Ph_2S(O)F_2$, and the C1 triplet (and C2 triplet) has been replaced by a single averaged peak. These four averaged C1-C4 peaks in Figure 45(c) are due to an equilibrium between $Ph_2S(O)F_2$ and $Ph_2S(O)F^+$, Scheme 8, which has been discussed in the previous section of this chapter.

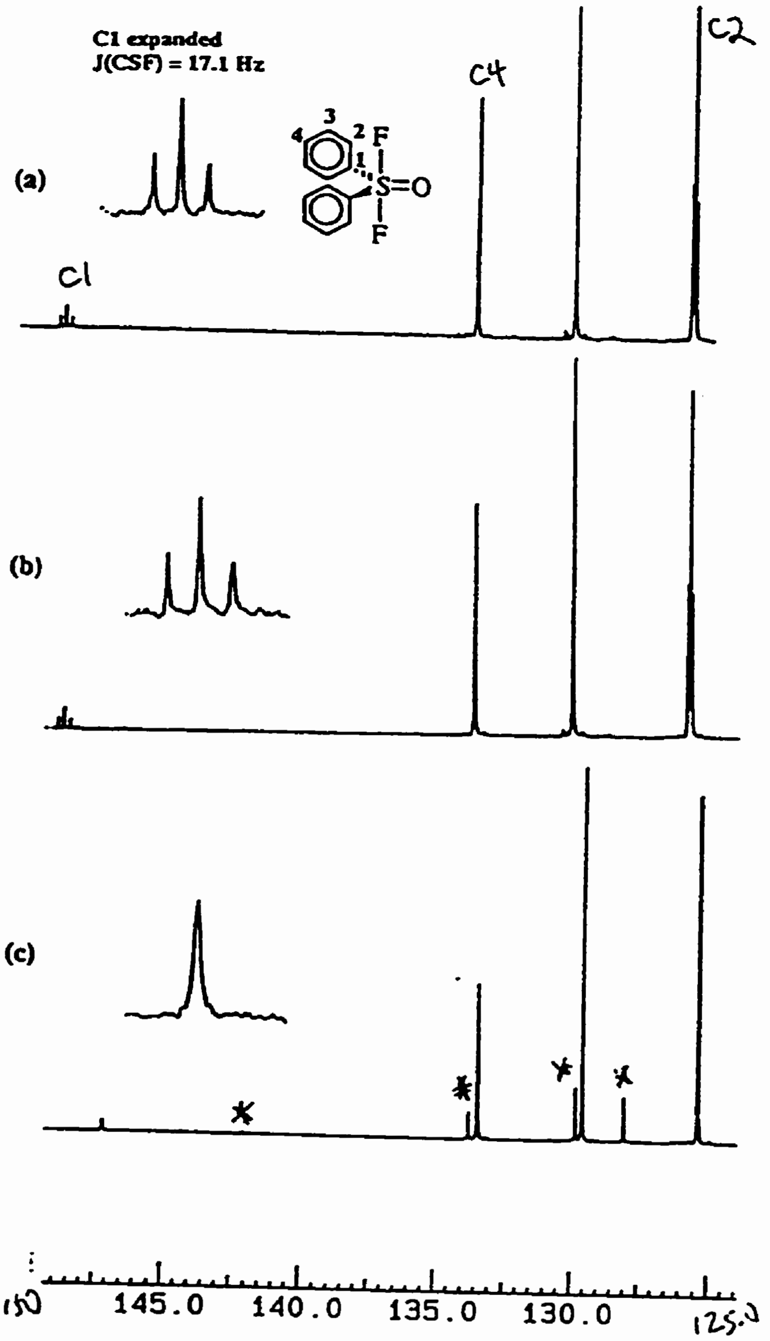

Figure 45 (a) The ^{13}C NMR spectrum of $Ph_2S(O)F_2$ (0.297 mmol) in a ptfe-lined NMR tube in CD_2Cl_2 solution. The expanded C1 region shows a triplet due to C-S-F coupling. (b) The same sample after addition of a dry capillary of borosilicate glass. This spectrum was recorded after 18 hr. The expanded C1 region shows a triplet due to C1-S-F coupling, $^2J(CSF) = 17.1$ Hz, which is identical to that in a. (c) The ^{13}C NMR spectrum after addition of a wetted capillary of borosilicate glass to b, showing loss of C1-S-F (and C2-S-F) coupling, and changes in the chemical shifts of C1-C4 peaks. The C1-C4 peaks of the hydrolysis product Ph_2SO_2 are marked with an asterisk.

It has been demonstrated in section 3.3.2.5 of this chapter that the ^{13}C NMR spectra of phenyl-substituted main group fluorides are sensitive indicators of the formation of cations. In Figure 46, the ^{13}C NMR chemical shifts of authentic $Ph_2S(O)F^+$ and $Ph_2S(O)F_2$ are compared with those of the averaged C1-C4 peaks observed in Figure 45c, i.e., after addition of wetted glass to $Ph_2S(O)F_2$. As seen in Figure 46, the averaged C1-C4 peaks are intermediate between those of $Ph_2S(O)F^+$ and $Ph_2S(O)F_2$, as expected if only these species are involved in the rapid equilibrium of eq [72]

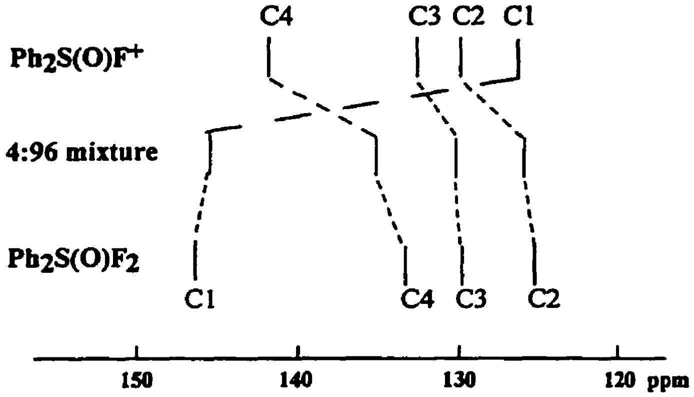

Figure 46. Comparison of the ^{13}C NMR spectra of $Ph_2S(O)F^+$ and $Ph_2S(O)F_2$ with that of the 4:96 mixture of $Ph_2S(O)F^+$ and $Ph_2S(O)F_2$ of Figure 45c.

It is possible to estimate how much water is present on the glass surface. Integration of the Ph_2SO_2 peak in Figure 45c, relative to that of the average $Ph_2S(O)F_2$-$Ph_2S(O)F^+$ peaks, shows 12.4% of hydrolysis product Ph_2SO_2. By subtraction, the sample contains 87.6% of a combined mixture of $Ph_2S(O)F_2$ and $Ph_2S(O)F^+$. The sample in Figure 45c contains a 96:4 ratio of $Ph_2S(O)F_2$ and $Ph_2S(O)F^+$. The ratio was determined by comparison of the experimental average chemical shifts of C1-C4; i.e. C1 146.96, C2 125.16, C3 129.37, C4 133.23, with the chemical shifts that are calculated for a 96.0:4.0 mixture of $Ph_2S(O)F_2$ and $Ph_2S(O)F^+$; i.e. C1 146.95, C2 125.12, C3 129.35, C4 133.21. Since the original sample in Figure 45 was made up from 0.297 mmol of $Ph_2S(O)F_2$, therefore, the sample in Figure 45c contains 0.250 mmol of $Ph_2S(O)F_2$ (0.297 x 87.6% x 96%), and 0.010 mmol of cation $Ph_2S(O)F^+$ (0.297 x 87.6% x 4%), plus 0.037 mmol of hydrolysis product Ph_2SO_2 (0.297 x 12.4%). According to the stoichiometry of eq [70], the wetted glass surface must have contained 0.037 mmol of water. On hydrolysis, 0.074 mmol of HF is released.

Hydrogen fluoride reacts with glass. After standing for 5 days, the sample of Figure 46c contained 23% of sulfone Ph_2SO_2, and a 83:17 ratio of $Ph_2S(O)F_2/Ph_2S(O)F^+$. This slow reaction must correspond to reaction of $Ph_2S(O)F_2$ with water that is slowly released as a result of the reaction of glass with HF. The amount of water liberated in this way is again proportional to the amount of sulfone Ph_2SO_2 in solution. The concentration of cation $Ph_2S(O)F^+$ can be estimated from weighted average of C1-C4 peaks, but a variety of anions may now be present in solution, e.g., FHF^-, BF_4^-, SiF_5^-, and SiF_6^{2-}.

$$[74]\quad Ph_2S(O)F_2 \xrightleftharpoons{\text{Lewis acid (HF, BF}_3\text{, SiF}_4\text{)}} Ph_2S(O)F^+ + FHF^-, BF_4^-, SiF_5^-, SiF_6^{2-}$$

Thus the hydrolysis of $Ph_2S(O)F_2$ to sulfone Ph_2SO_2 allows detection of water on the glass surface by means of a rapid initial reaction, eq [70], whereas a much slower reaction detects water that is derived from the reaction of glass with HF (eq [73]).

3.3.2.7 Reaction of $Ph_2S(O)F_2$ with alcohols

The reactions with hydrogen fluoride and water demonstrate that $Ph_2S(O)F_2$ is a good fluoride ion donor with a high affinity for oxygen, and these properties might be useful for the fluorination of alcohols. Some alcohols were fluorinated according to eq [75].

$$[75]\quad Ph_2S(O)F_2 + ROH \longrightarrow Ph_2SO_2 + RF + HF$$

$$R{=}CH_3, C_2H_5, Ph(CF_3)CH, Me_3Si$$

Reactions of $Ph_2S(O)F_2$ with alcohols have been carried out with similar reaction conditions. Products from these reactions were characterised by ^{13}C NMR spectra, and Table 8 summarises the ^{13}C NMR data of these reaction products.

Table 8 ^{13}C data of fluorinated products of the reaction of $Ph_2S(O)F_2$ with alcohols (chemical shift in ppm and C-F coupling constants in Hz, in parenthesis).

Compound	δC1 (Ph)	δC2 (Ph)	δC3 (Ph)	δC4 (Ph)	δCH_2F (or δCF)	δCH_3F (or δCF_3)
EtF					80.7 (d, 160.2)	16.2 (d, 21.3)
Et_3SiF					5.2 (d, 14.1)	6.2 (d, 1.7)
$PhCF(CF_3)$	---	127.5 (d, 6.6)	129.1	130.8	122.8 (q,d,2 9.2, 281.4)	89.2 (q,d, 34.7 184.50)

3.3.3 Preparation of phenylchalogen (VI) fluorides

3.3.3.1 Synthesis of Ph_2SF_4

The preparation of Ph_2SF_4 was first reported by Denny and co-workers,[108] who treated diphenyl sulfide with a large excess of trifluoromethyl hypofluorite CF_3OF at -78 °C as shown in eq [76]. The reaction was very slow and only *trans*-Ph_2SF_4 was obtained. Under their conditions, warming a solution of the product to room temperature led to extensive decomposition to unidentified products.

$$[76]\quad CF_3OF + Ph_2S \xrightarrow[-78^{o}C]{\text{Large excess } CF_3OF} Ph_2SF_2 \longrightarrow \textit{trans}\text{-}Ph_2SF_4$$

Ruppert[114] reported direct F_2 liquid-phase fluorination of Ph_2S at -78 °C in CF_3Cl to give a 1:2 mixture of *cis*- and *trans*-diphenylsulfur tetrafluoride via isolable Ph_2SF_2. Both *cis*- and *trans*-Ph_2SF_4 were uniformly hydrolyzed in $CHCl_3$ with a little NEt_3 to give Ph_2SO_2.

Lagow and co-workers[117] studied the reaction of *neo*-$C_6H_{11}SH$ with elemental fluorine at -120 °C, and a yield of 24 % *neo*-$C_6H_{11}SF_5$ was obtained.

Early study of the oxidative fluorination of Ph_2SF_2 with xenon difluoride, XeF_2 in this laboratory[142] indicated that no reaction occurred when Ph_2SF_2 was mixed with XeF_2.

The oxidative fluorination of Ph_2S with a stoichiometric amount of XeF_2, was completed within ~5 minutes at -5 °C to give Ph_2SF_2 in essentially quantitative yield. However, further oxidative fluorination of Ph_2SF_2 with excess of xenon difluoride did not occur even after one month. When a small amount of tetraethylammonium chloride,

Et_4NCl, was added to this reaction mixture in CD_2Cl_2, the oxidation occurred immediately to give both *cis*- and *trans*-Ph_2SF_4. As shown in Figure 47, *trans*-Ph_2SF_4 is characterised by a singlet ^{19}F NMR peak, while *cis*-Ph_2SF_4 shows two triplets (A_2B_2 system).

$$[77] \quad Ph_2S + XeF_2 \longrightarrow Ph_2SF_2 \xrightarrow[CH_2Cl_2]{XeF_2/Et_4NCl} \textit{cis} \text{ and } \textit{trans}\text{-}Ph_2SF_4$$

Along with *cis*- and *trans*-Ph_2SF_4, a product resulting from the loss of one phenyl group, *trans*-$PhSF_4Cl$ was also found, as well as fluorinated by-products such as FDF^-, CD_2F_2 and CDF_3. The mechanism of the oxidative fluorination of Ph_2SF_2 will be discussed in a later section.

The *cis* isomer slowly undergoes *cis*-to-*trans* isomerization in solution. On standing for 1 month, almost all *cis*-Ph_2SF_4 was converted to *trans*-Ph_2SF_4.

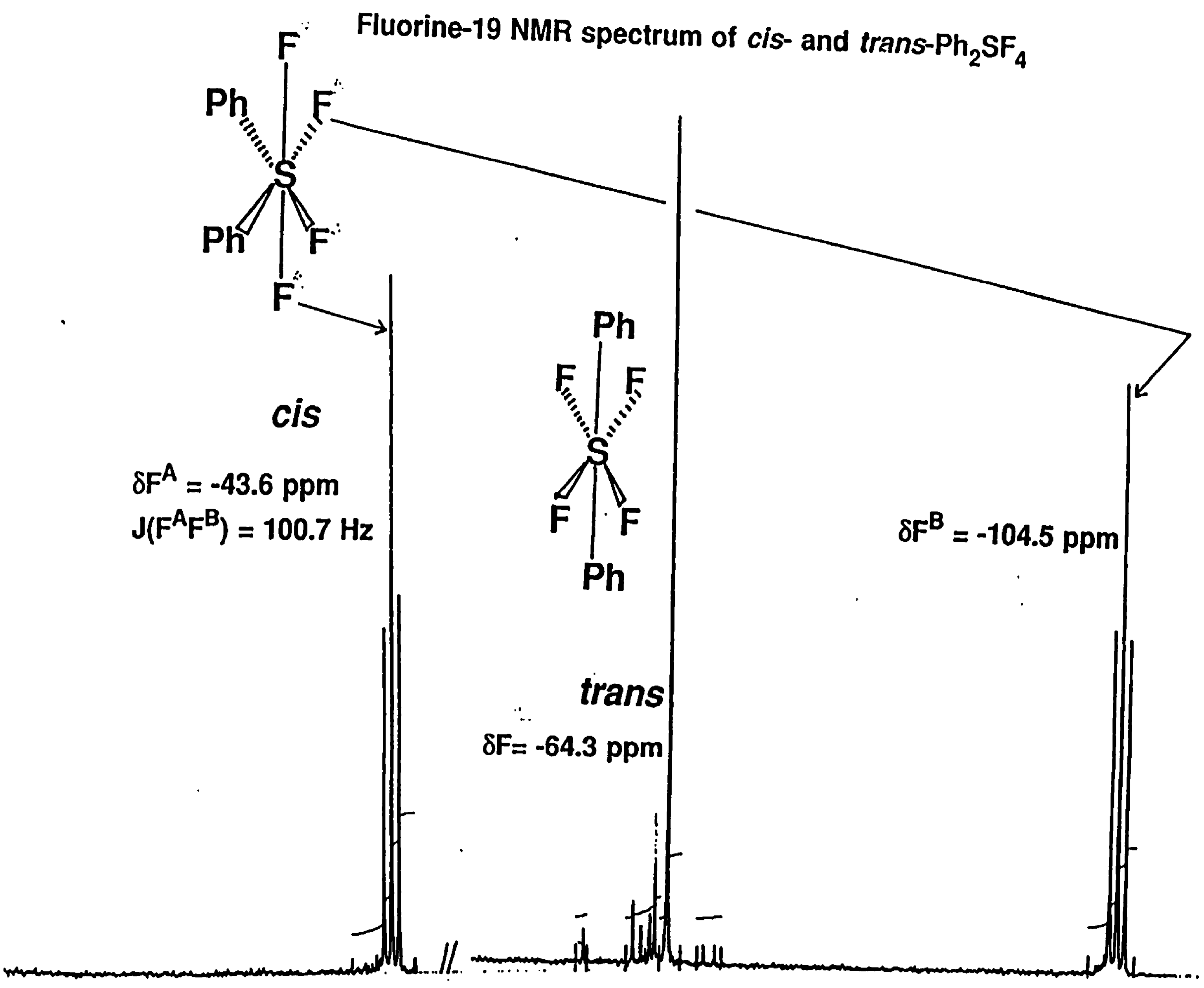

Figure 47. ^{19}F NMR spectrum of *cis*- and *trans*-Ph_2SF_4 in CD_2Cl_2.

3.3.3.2 Synthesis of $PhEF_5$ (E = S, Se, Te)

Oxidative fluorination of Ph_2Te_2 with a stoichiometric amount of xenon difluoride gives $PhTeF_5$, which was first prepared by Alam[143] in this laboratory. The reaction with xenon difluoride was so sluggish that it required about 10 hours to complete the oxidation giving about 50% crude yield of $PhTeF_5$.

$$[78]\quad Ph_2Te_2 + XeF_2 \longrightarrow PhTeF_3 \xrightarrow[\text{Slow}]{XeF_2} PhTeF_5$$

This method was modified by adding a catalytic amount of tetraethylammonium chloride, Et_4NCl. When a catalytic amount of Et_4NCl were added to the reaction mixture of XeF_2 and Ph_2Te_2 (or $PhTeF_3$), the oxidative reaction occurred immediately to give $PhTeF_5$ in essentially quantitative crude yield. In general, the reaction is completed within 10 minutes at room temperature.

$$[79]\quad Ph_2Te_2\ (\text{or } PhTeF_3) + XeF_2 \xrightarrow[\text{10 minutes}]{Et_4NCl} PhTeF_5$$

Sheppard[102] prepared the first phenylsulfur(VI) pentafluoride by the reaction of the corresponding disulfide with solid silver difluoride via a two step reaction as shown in eq [80], and reported a yield of 5-14%. The reaction required a temperature of 120-130 °C and 2-3 hour reaction time.

$$[80]\quad Ar_2S_2 + AgF_2 \longrightarrow ArSF_3 \xrightarrow[130\ oC]{AgF_2} ArSF_5$$

The synthesis of arylsulfur(VI) pentafluoride can be achieved under mild

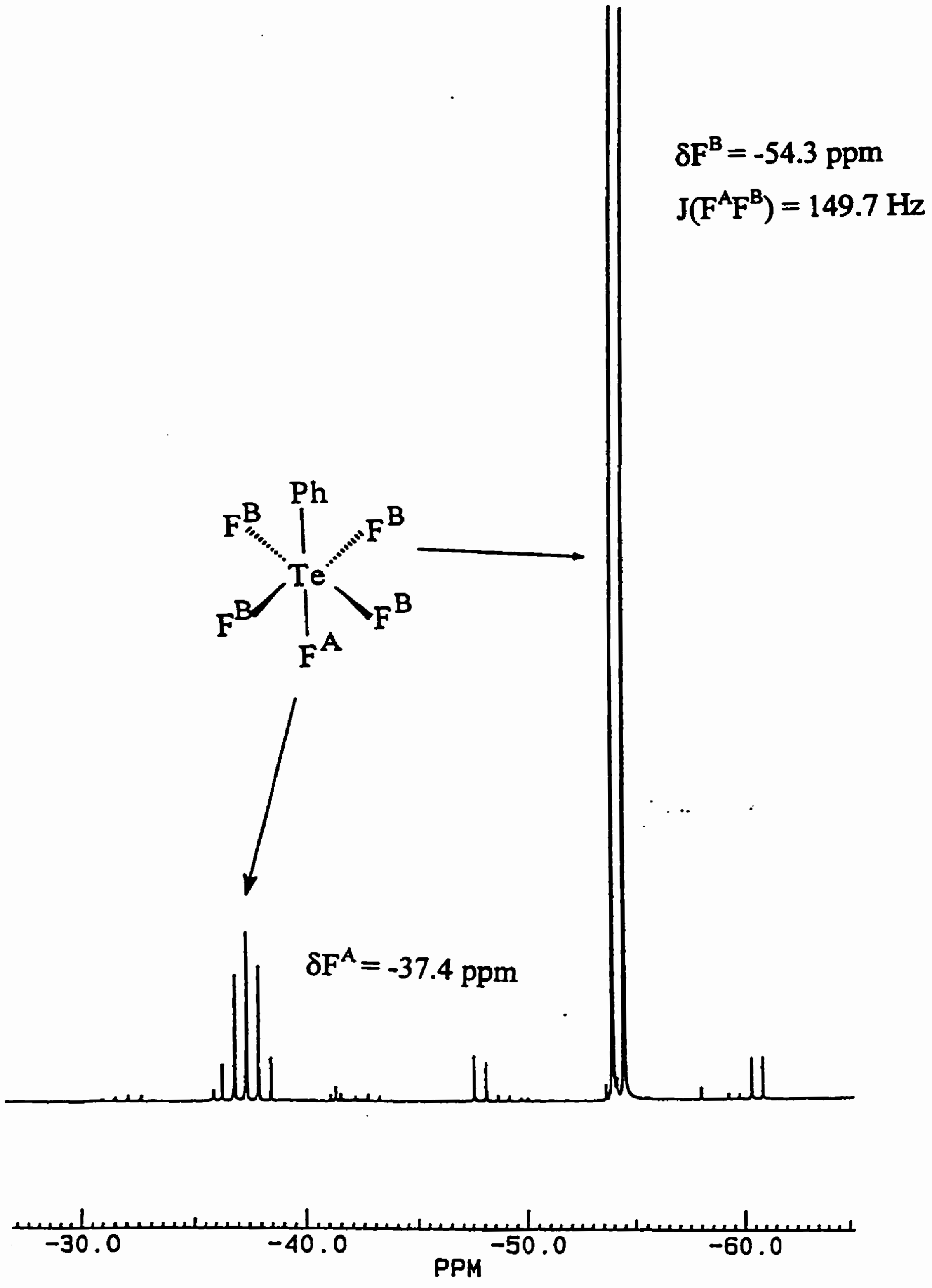

Figure 48. ^{19}F NMR spectrum of $PhTeF_5$ in CD_3CN. The small satellite peaks arise from ^{123}Te isotope.

conditions by using xenon difluoride as a fluorinating reagent in the presence of catalytic amount of tetraethylammonium chloride.

Diphenylsulfur pentafluoride, Ph_2S_2, reacts with xenon difluoride in the presence of catalytic amount of Et_4NCl at ambient temperature to give $PhSF_3$ in essentially qualitative yield as seen in eq [81].

$$[81] \quad Ph_2S_2 + XeF_2 \xrightarrow{\text{catalytic amount of } Et_4NCl} PhSF_3$$

An excess of XeF_2 and a small amount of Et_4NCl were added to the reaction mixture of xenon difluoride and $PhSF_3$, and $PhSF_5$ is produced in 5 minutes according to eq [82] in a crude yield of ~25%.

$$[82] \quad PhSF_3 + XeF_2 \xrightarrow{Et_4NCl} PhSF_5$$

A new compound, $PhSeF_5$, was prepared by exactly the same method as described above, as confirmed from its ^{19}F NMR spectrum in Figure 50, with a crude yield of ~25%.

$$[83] \quad Ph_2Se_2 + XeF_2 \xrightarrow{Et_4NCl} PhSeF_5$$

Table 9 shows the comparison of ^{19}F NMR data for $ClEF_5$ and $PhMF_5$ (E = S, Se, Te).

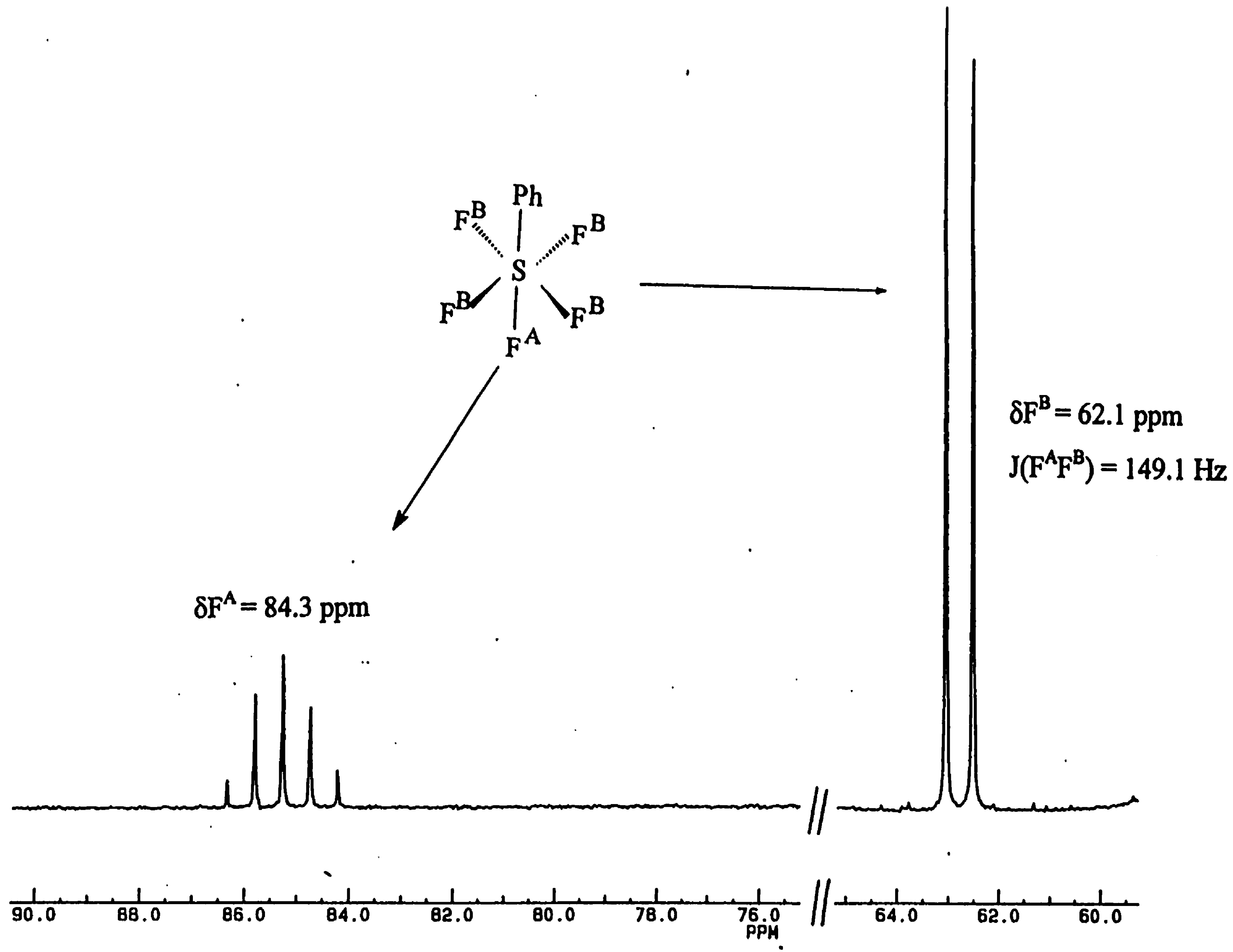

Figure 49. ^{19}F NMR spectrum of $PhSF_5$ in CD_2Cl_2.

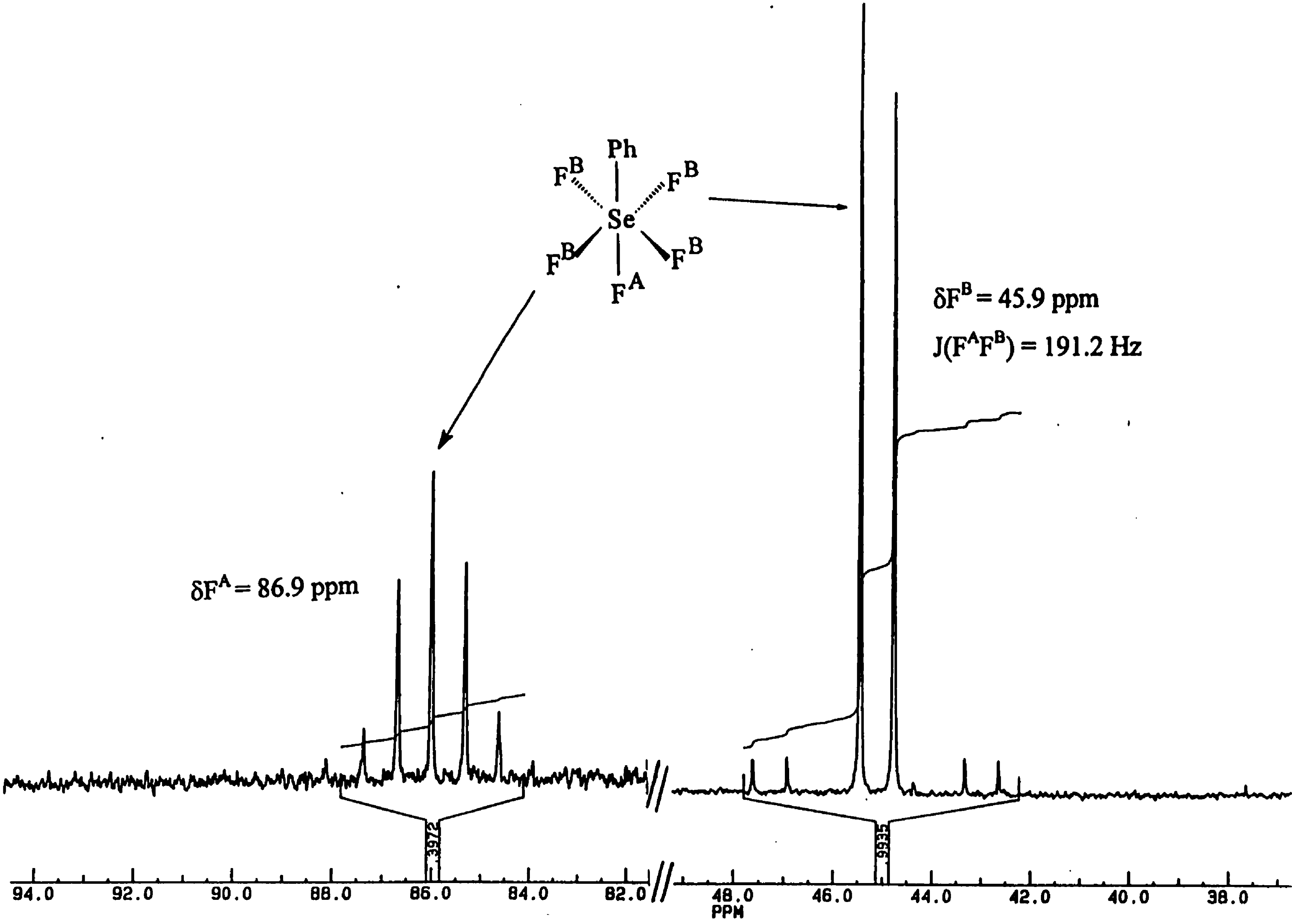

Figure 50. ^{19}F NMR spectrum of $PhSeF_5$ in CD_3CN.

TABLE 9 ^{19}F NMR data for $ClEF_5$ and $PhEF_5$ (E=S, Se, Te)

Compound	spin system	$\delta F^A{}_{ax}$ (ppm)	$\delta F^B{}_{eq}$ (ppm)	$J_{F^A{}_{ax}-F^B{}_{eq}}$ (Hz)
$ClSF_5$[a]	AB_4	63.7 (d)	125.3 (q)	152.2
$ClSeF_5$[b]	AB_4	71.3 (d)	132.0 (q)	---
$ClTeF_5$[c]	AB_4	-42.7 (d)	-4.0 (q)	173
$PhSF_5$[a]	AB_4	84.3 (d)	62.1 (q)	149.1
$PhSeF_5$[a]	AB_4	86.9 (d)	45.9 (q)	191.2
$PhTeF_5$[a,d]	AB_4	-37.4 (d)	-54.3 (q)	149.7

[a] This work.

[b] Ref. 144

[c] Ref. 145

[d] Only first order effects are considered.

3.3.3.3 Proposed mechanism of oxidative fluorination of diphenylsulfur difluoride

It has been demonstrated in the previous discussions that oxidative fluorination of organochalcogen(IV) to organochalcogen(VI) by XeF_2 was very slow or did not take place at all, except in the presence of Et_4NCl. Oxidative fluorination and/or chlorination of sulfur(IV), selenium(IV) and tellurium(IV) compounds such as diphenyl sulfoxide, diphenyl sulfide, diaryl disulfide, diphenyl diselenium, diphenyl ditellurium, etc., occurs very rapidly and smoothly under mild conditions by xenon difluoride in the presence of Et_4NCl. In most cases, the sulfur(VI) and tellurium(VI) products are formed in high yield within a few minutes at room temperature.

As described in the previous discussion, the oxidative addition reaction of main group compounds resulting in six-coordinated compounds may lead to the formation of *cis-* or *trans-*isomers or isomeric mixtures. *Cis* and *trans* isomers of six-coordinated sulfur,[151] and tellurium[146,151] are known, but the stereochemical outcome of a reaction is difficult to predict because of the mechanistic complexity of competing oxidative-addition, isomerization and ligand exchange processes. Complexity also arises from the H_2O-HF-glass system because of the potential introduction of BF_3 or SiF_4, and strong Lewis acids are known to isomerize six-coordinate sulfur(VI) and tellurium(VI) fluorides via cationic intermediates.

The reaction of diphenyl sulfoxide with XeF_2 in the presence of Et_4NCl has been described in Section 3.3.1 of this Chapter, and a very similar reaction mechanism can also be proposed for this oxidative fluorination reaction as shown in Scheme 11.

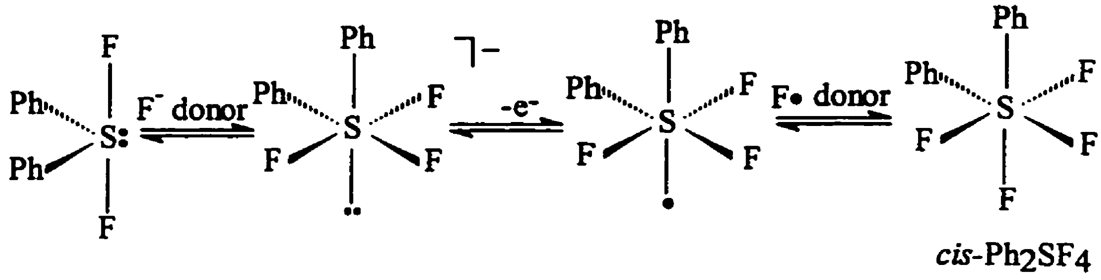

Scheme 11. Proposed mechanism of oxidative fluorination of diphenylsulfur difluoride.

Again, the first step of the reaction is the addition of fluoride ion to the starting compound, Ph_2SF_2. Fluoride anion F^- is produced by the reaction of XeF_2 with Et_4NCl, as discussed before. This could be the reason why the oxidative fluorination is very slow or does not occur at all if no Et_4NCl is present.

3.3.3.3.1 The intermediate diphenylsulfur(IV) trifluoride anion $Ph_2SF_3^-$

Once fluoride ion is produced in the solution of Ph_2SF_2 in common solvents, the intermediate phenylsulfur(IV) trifluoride, $Ph_2SF_3^-$, may be formed as an equilibrium mixture of Ph_2SF_2 and $Ph_2SF_3^-$. The square pyramidal structure of $Ph_2SF_3^-$ can exist as three possible structures as shown in Figure 51.

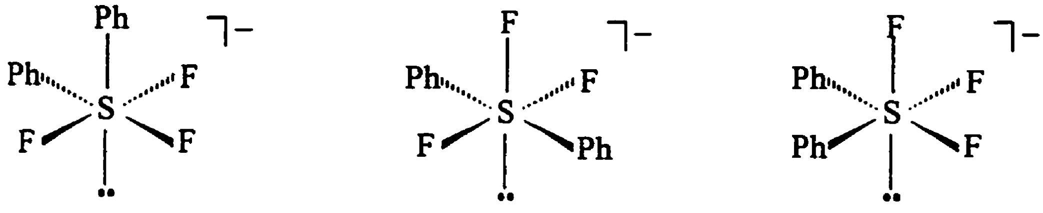

28a **28b** **28c**

Figure 51. Three possible isomeric structures of sulfur(IV) anion $Ph_2SF_3^-$.

In Figure 51, the two phenyl substituents are in the cis position for the first two structures **28a** and **28c**, while phenyl substituents are in the trans position for the third structure **28b**. The intermediate structure should be either **28a** or **28c** for $Ph_2SF_3^{\cdot}$, i.e., *cis-* phenyl substituents, if *cis*-Ph_2SF_4 is the kinetically favoured product. On the other hand, intermediate structure **28b** for $Ph_2SF_3^{\cdot}$ is predicted if *trans*-Ph_2SF_4 is the kinetically favoured product. However, our results and results from our previous study[11] of oxidation of Ph_2TeF_2 to Ph_2TeF_4, and results from the literature for the oxidation of $(C_6F_5)_2TeF_2$ to $C_6F_5)_2TeF_4$,[146] have shown that the *cis*-isomer is the kinetically favoured product. It is also agree with the concepts and conventions like Bent's rule, hybirdization schemes, etc..

The first key intermediate, $Ph_2SF_3^{\cdot}$, must adopt the structure of **28a** in which the bulky phenyl group is *trans* to the lone pair of electrons, thus ensuring that two phenyl substituents occupy cis positions during oxidative-fluorination, rather than **28c**, in which both bulky phenyl substituents are cis to the lone pair electrons and F substituent is trans to the lone pair electrons. Structure **28a** is supported by *ab initio* calculations and analogous structures in the literature.

(1) *Ab initio* MO calculation results

Figure 52 shows the *ab initio* molecular orbital calculation results for all three possible structures of $Ph_2SF_3^{\cdot}$. It is clearly seen that **29a**, in which the bulky phenyl substituent is *trans* to the lone of pair electrons, has the lowest energy, followed by **29b**, which has a relative energy 66.7 kJ/mol higher, and **29c** which has the highest energy of 72.0 kJ/mol higher than **29a**. Therefore, structure **29a** is a more resonable structure for the key intermediate $Ph_2SF_3^{\cdot}$.

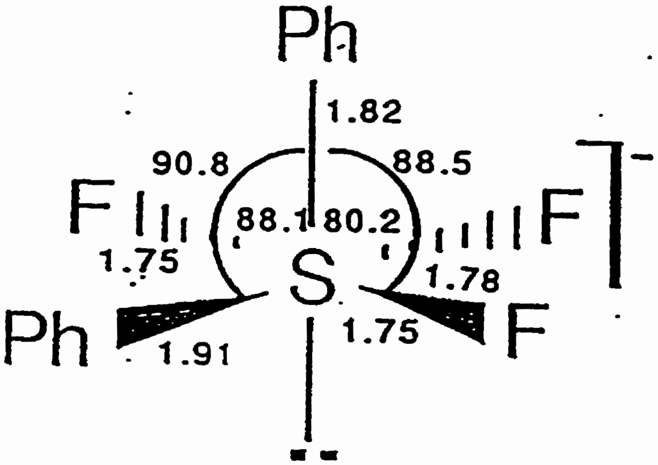
Ph
1.82
90.8
88.5
F
88.1
80.2
F
1.75
S
1.78
Ph
1.91
1.75
F

29a

RELATIVE ENERGY = 0

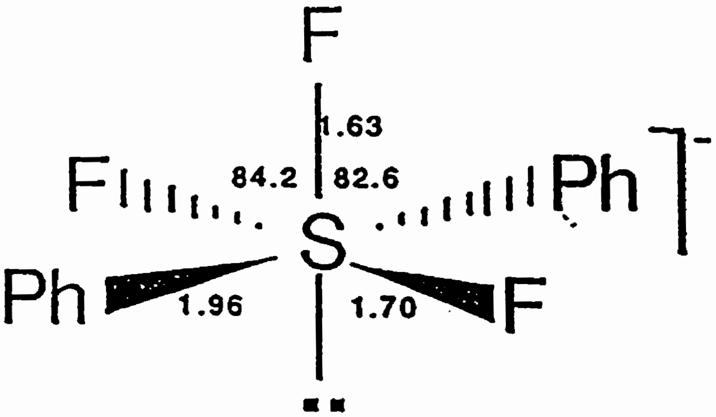
F
1.63
F
84.2
82.6
Ph
S
Ph
1.96
1.70
F

29b

RELATIVE ENERGY = +66.7 kJ

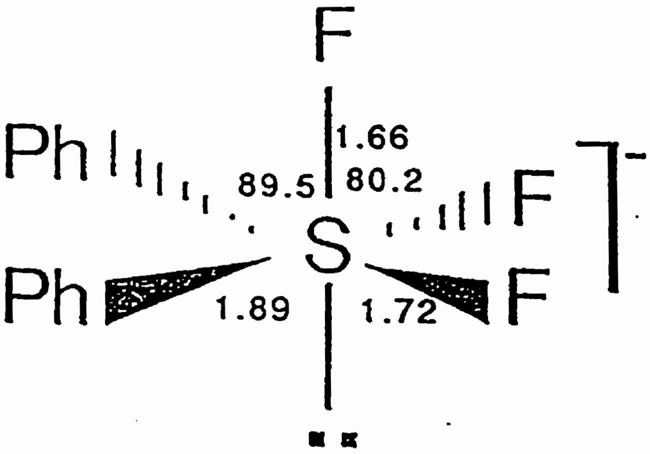
F
1.66
Ph
89.5
80.2
F
S
Ph
1.89
1.72
F

29c

RELATIVE ENERGY = +72.0 kJ

Figure 52. Optimised geometries for three possible structures of $Ph_2SF_3^-$.

(2) Structure of 5-coordinated sulfur(IV) anion

The variable temperature ^{19}F NMR spectra of alkylsulfur(IV) tetrafluoride,[104, 128d] RSF_4^- [$R = CF_3$, $CF(CF_3)_2$] revealed that RSF_4^- has a square pyramidal geometry with the "bulky" alkyl group R preferentially occupying the axial position and trans to the lone pair electrons.

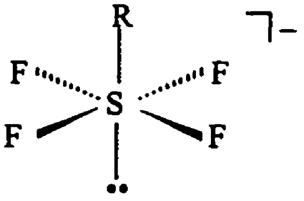

$R=CF_3$, $CF(CF_3)_2$

(3) Structure of 5-coordinate selenium(IV) anion

The structure of $Cs^+C_2F_5SeF_4^-$(IV)[147] has a square pyramidal geometry and the "bulky" C_2F_5 substituent appears to have the *trans* confirmation with respect to the lone pair electrons.

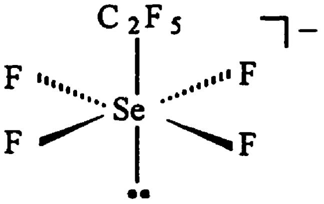

(4) $Ph_3Te^+PhTeX_4^-$ (X=Cl, Br, I)

It has been demonstrated that tetrahalophenyl tellurates (IV) of the type $Ph_3Te^+PhTeX_4^-$ (X=Cl, Br, I)[148] adopt a square pyramidal structure with a phenyl substituent trans to the lone pair electrons.

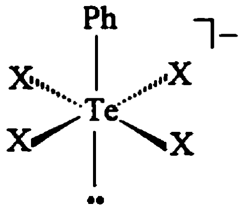

(5) $Y^+ArTeCl_4^-$ ($Y=MePh_3P$, C_7H_7, and Me_4N)

Petragnani and co-workers[149] found that tetrachloroaryl tellurates(IV) of the type $Y^+ArTeCl_4^-$ ($Y=MePh_3P$, C_7H_7, and Me_4N) adopt a square pyramidal structure, with the aryl substituent always *trans* to the lone pair electrons.

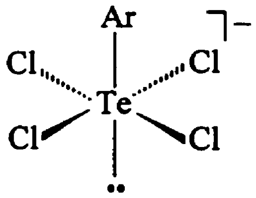

(6) $Me_3Te^+MeTeI_4^-$

Tetraiodomethyl tellurate(IV), $Me_3Te^+MeTeI_4^-$, has been shown[150] to have a square pyramidal geometry, with the methyl substituent *trans* to the lone pair electrons.

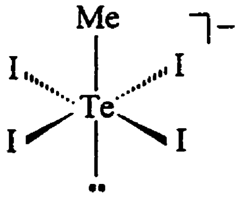

3.3.3.3.2 The intermediate diphenylsulfur(V) trifluoride radical $Ph_2SF_3^{\cdot}$

After the formation of $Ph_2SF_3^-$, the next step in the mechanism of oxidative fluorination of Ph_2SF_2 is the loss of one electron from $Ph_2SF_3^-$ to give a radical intermediate $Ph_2SF_3^{\cdot}$. Again there are three possible structures for $Ph_2SF_3^{\cdot}$ as shown in Figure 53.

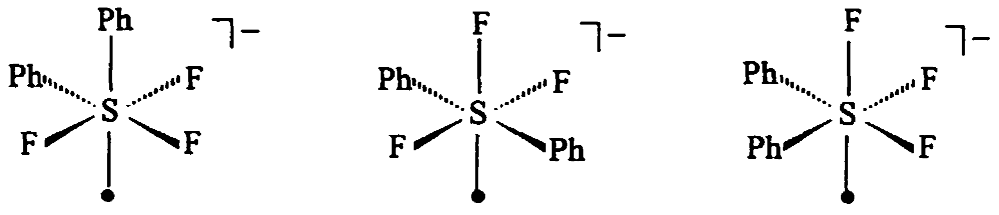

30a **30b** **30c**

Figure 53. Three possible structures of sulfur(V) radical $Ph_2SF_3^{\cdot}$

In Figure 53, the two phenyl substituents are in the *cis* position for the first two structures **30a** and **30c**, while phenyl substituents are in the *trans* position for the third structure **30b**. The intermediate structure should prefer either **30a** or **30c** for $Ph_2SF_3^{\cdot}$ because *cis*-Ph substituents give kinetically favoured *cis*-Ph_2SF_4. In other words, if the intermediate prefers structure **30b** for $Ph_2SF_3^{\cdot}$, then *trans*-Ph_2SF_4 would be expected to be the kinetically favoured product. However, our experimental results have shown that the *cis*-isomer is the kinetically favoured product.

The structure of intermediate **30a** has the bulky phenyl group *trans* to the lone electron, thus ensuring that two phenyl substituents occupy cis positions during oxidative-fluorination, whereas **30c**, has both bulky phenyl substituents cis to the single electron, and F substituent is trans to the single electron. Again, *ab initio* MO calculations were used to calculate the geometry of intermediate $Ph_2SF_3^{\cdot}$. Figure 54 shows the *ab initio* molecular orbital calculation results for all three possible structures of $Ph_2SF_3^{\cdot}$. It is clearly indicated that **31a**, in which the bulky phenyl substituent is *trans* to the single electron has the lowest energy, followed by **31b**, which has a relative energy 33.6 kJ/mol higher than **31a**, and **31c** has a relative energy of 66.6 kJ/mol higher than **31a**, suggesting that the preferred intermediate structure of $Ph_2SF_3^{\cdot}$ is structure **31a**.

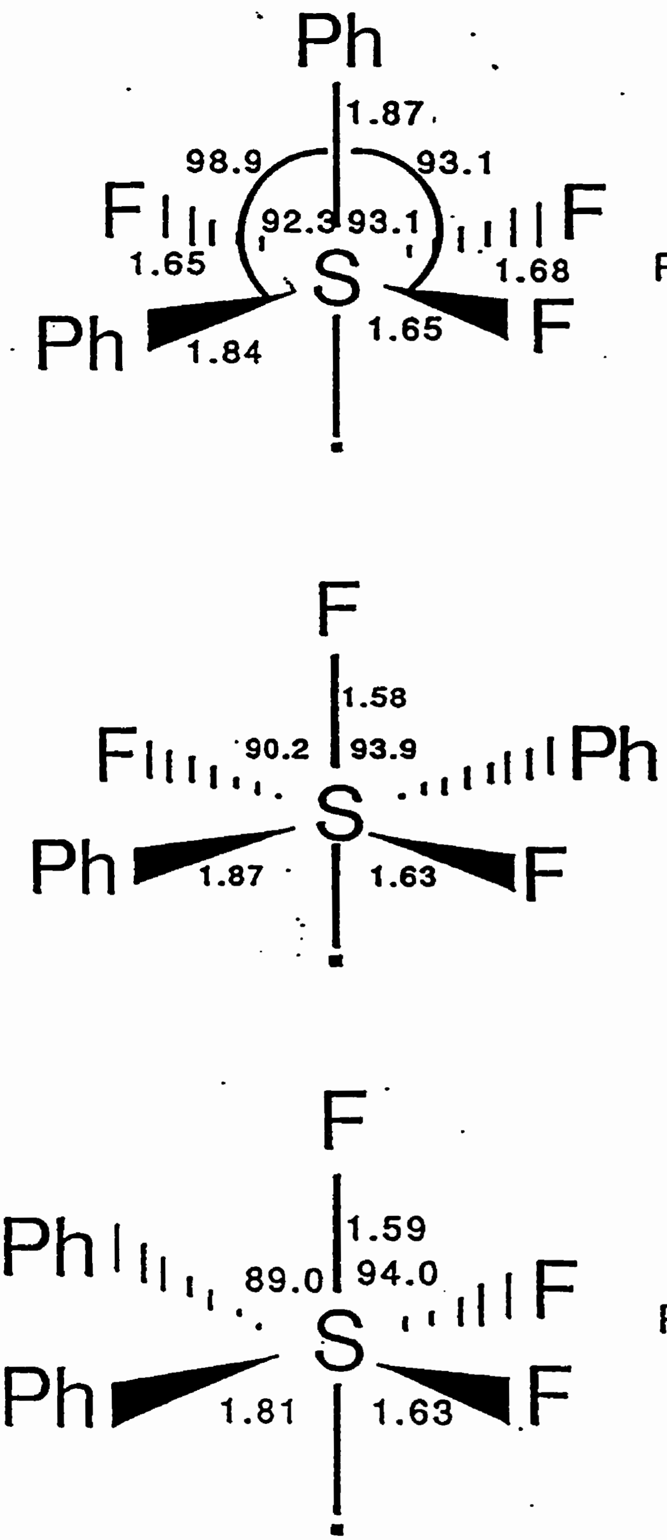
Ph
1.87
98.9
93.1
F
F
92.3
93.1
1.65
S
1.68
Ph
1.84
1.65
F
F
1.58
F
90.2
93.9
Ph
S
Ph
1.87
1.63
F
F
1.59
Ph
89.0
94.0
F
S
Ph
1.81
1.63
F

31a

RELATIVE ENERGY = 0

31b

RELATIVE ENERGY = 33.6 kJ mol^{-1}

31c

RELATIVE ENERGY = 66.6 kJ mol^{-1}

Figure 54. Optimised geometries for three possible structures of $Ph_2SF_3^{\cdot}$, **31**.

3.3.3.4 Proposed mechanism of isomerization of *cis*-Ph_2SF_4 to *trans*-Ph_2SF_4

The fact that there is always more *cis*-Ph_2SF_4 than *trans*-Ph_2SF_4 in the products of oxidative fluorination of Ph_2SF_2 by XeF_2, and the fact that the amount of *cis*-Ph_2SF_4 decreases while the amount of *trans*-Ph_2SF_4 increases on standing, as discussed previously, indicates that Lewis acids, which may be generated from glass apparatus, might catalyze the isomerization of *cis*- to *trans*-Ph_2SF_4. As proposed in Scheme 12, in the presence of Lewis acids such as BF_3 or SiF_4, often originating from glass apparatus, the kinetically favoured cis isomer is converted to the thermodynamically more stable trans isomer via a five-coordinate cation, $Ph_2SF_3^+$ (as the chain carrier), followed by formation and cleavage of a $[S{-}{-}F{-}{-}S]^+$ bridging bond.

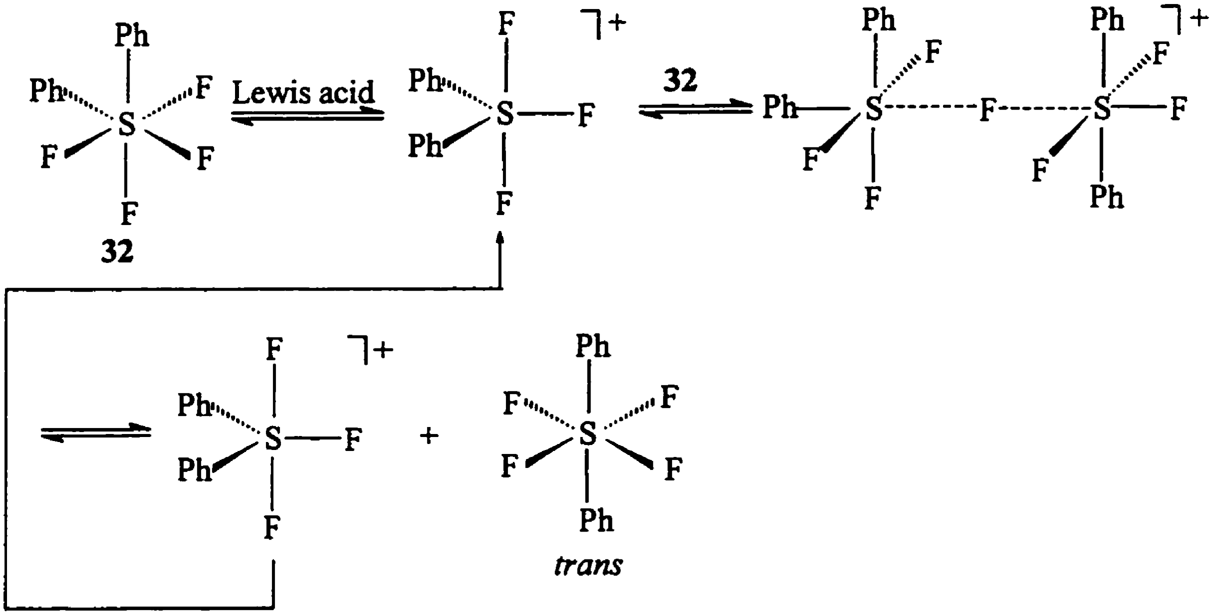

Scheme 12. Proposed mechanism of isomerization of *cis*- to *trans*-Ph_2SF_4.

Octahedral cis and trans isomers of a variety of main group chalcogen fluorides have been reported, including tellurium fluorides, e.g. *cis*- and *trans*-$F_2Te(OTeF_5)_4$[152] and *cis*-$(C_6F_5)_2TeF_4$,[146] *cis* and *trans*-sulfur(VI) fluorides,[153,154] and related derivatives.[115,155,143,156] The isomerization of geometrical isomers is catalysed by Lewis acids, as demonstrated by the SbF_5 catalysed isomerization of *trans*- to *cis*-$F_2Te[C_6H_4C(CF_3)_2O]_2$,[151] or SbF_5, PF_5 and BrF_3 catalysed isomerization of *trans*- to *cis*-$F_2S[C_6H_4C(CF_3)_2O]_2$.[115] A similar reaction mechanism was also found previously for the catalysed isomerization of *cis*- to *trans*-Ph_2TeF_4[11] in this laboratory.

The most likely structure of intermediate $Ph_2SF_3^+$ is **33a**, in which the electronegative fluorines occupy axial sites in TBP molecules and ions.[170] Another possibility is structure **33b**, in which both phenyl substituents are in axial positions. As shown in Figure 55, our *ab initio* molecular calculation clearly indicates that **33b** has relative energy of 197.1 kJ/mol higher than **33a**, indicating that the structure of **33a** would be a much more reasonable candidate for the key intermediate $Ph_2SF_3^+$. Interaction of **33a** and **32** gives a fluorine-bridged intermediate which then leads to the formation of *trans*-Ph_2SF_4 and **33a**, as shown in Scheme 12.

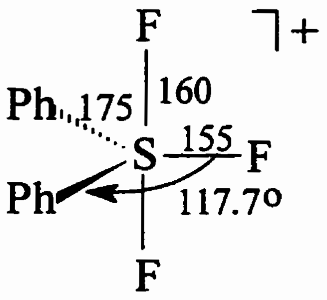
F
Ph
175
160
155
F
Ph
117.7°
F
+

32a

Relative Energy = 0

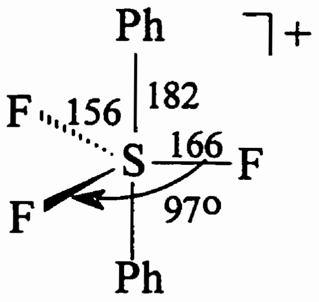
Ph
F
156
182
166
F
F
97°
Ph
+

32b

Relative Energy = 197.1 kJ/mol

Figure 55. Optimised geometries for two possible structures of $Ph_2SF_3^+$.

3.3.4 Stereoselective synthesis and isomerization of *cis*- and *trans*-aryltetrafluorosulfur(VI) chloride, $ArSF_4Cl$ (Ar = Ph, *p*-MeC_6H_4, *p*-$O_2NC_6H_4$)

Among all the sulfur(VI) fluorides, SF_5X (X = Cl, Br) and R_fSF_4Cl have the richest chemistry. Addition to olefins and electrochemical fluorination are two routes to a large family of SF_5- or R_fSF_4-substituted compounds.

Sulfur chloride pentafluoride has been prepared by electrolysis of a sulfur dichloride-hydrogen fluoride mixture, by chlorination of disulfur decafluoride, by the reaction of sulfide dichloride and fluorine, by addition of chlorine monofluoride to sulfur tetrafluoride, and by the reaction of sulfur tetrafluoride, chlorine, and cesium fluoride, as shown in eq [84-85], but only the following two methods are of value[101,168] from a preparative point of view.

[84] $SF_4 + ClF \longrightarrow ClSF_5$

[85] $SF_4 + Cl_2 + CsF \xrightarrow{130\ ^oC} ClSF_5 + CsCl$

Organosulfur(VI) chloride tetrafluoride, RSF_4Cl, can exist as two geometrical isomers with respect to the phenyl ring and chlorine substituents, i.e. *cis*- and *trans*-RSF_4Cl, as illustrated in Figure 56.

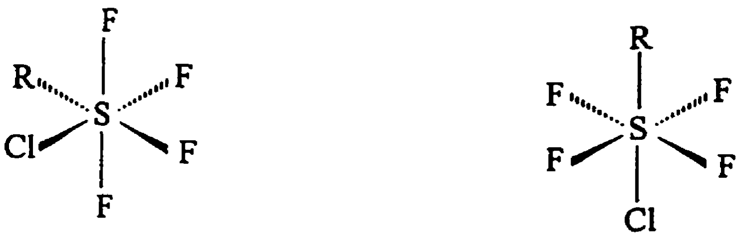

cis *trans*

Figure 56. Two geometrical isomers of RSF_4Cl.

Although the trans isomer, *trans*-RSF_4Cl ($R=R_f=CF_3$, C_2F_5, C_3F_7, C_4F_9), has been extensively studied,[103,109,116] as far as we are aware the cis chlorofluoride of composition RSF_4Cl has never been reported.

Using chlorine monofluoride as a primary chlorinating and fluorinating reagent in the reaction with perfluoroalkylsulfenyl chloride (R_fSCl) and perfluoroalkyl disulfides (R_fSSR_f') at 25 °C, a series of *trans*-perfluoroalkylsulfur(VI) chloride tetrafluorides, *trans*-R_fSF_4Cl, were prepared by Shreeve and co-workers,[109,116] as shown in eq [86].

$$[86]\quad RSCl\,(\text{or } R_fSSR_f') + ClF \xrightarrow[10\ \text{hours}]{25\ ^oC} trans\text{-}R_fSF_4Cl + RSF_5$$

$R_f = CF_3,\ C_2F_5,\ C_3F_7,\ C_4F_9$ yield: 42%

$R_f = R_f' = CF_3$

$R_f = CF_3,\ R_f' = C_2F_5$ yield: 13%

In this type of reaction, a modest yield was achieved, and small amounts of perfluoroalkylsulfur pentafluoride, R_fSF_5, were also obtained.

In 1969, Darragh and Sharp[103] reported the synthesis of *trans*-trifluoromethylsulfur(VI) chloride tetrafluoride, *trans*-CF_3SF_4Cl, from the reaction of chlorine with trifluoromethylsulfur trifluoride in the presence of cesium fluoride according to eq [87] , but the yield was not reported.

$$[87]\quad CF_3SF_3 + Cl_2 \xrightarrow{CsF} trans\text{-}CF_3SF_4Cl + CsCl$$

In this case, no trace of the cis-isomer of *cis*-RSF_4Cl was detected.

3.3.4.1 Synthesis of *cis*- and *trans*-$ArSF_4Cl$ (Ar=Ph, *p*-MeC_6H_4, *p*-$O_2NC_6H_4$)

Oxidative-fluorination of S(IV) to S(VI), or Te(IV) to Te(VI), by XeF_2 is catalysed by the presence of Cl^-, as described earlier in this thesis for the oxidative fluorination of Ph_2SO to $Ph_2S(O)F_2$, Ph_2SF_2 to *cis*- and *trans*-Ph_2SF_4[67], and Ph_2TeF_2 to *cis*- and *trans*-Ph_2TeF_4.[11]

Similar reaction conditions have now been used for the stereoselective synthesis of *cis*- and *trans*-$ArSF_4Cl$ (Ar = Ph, *p*-MeC_6H_4, *p*-$O_2NC_6H_4$).

Both *cis*- and *trans*-$ArSF_4Cl$ can be prepared in high yield by oxidative fluorination of ArSSAr, or directly from its corresponding arylsulfur(IV) trifluorides, $ArSF_3$, as illustrated in eq [89] and [90].

[89]

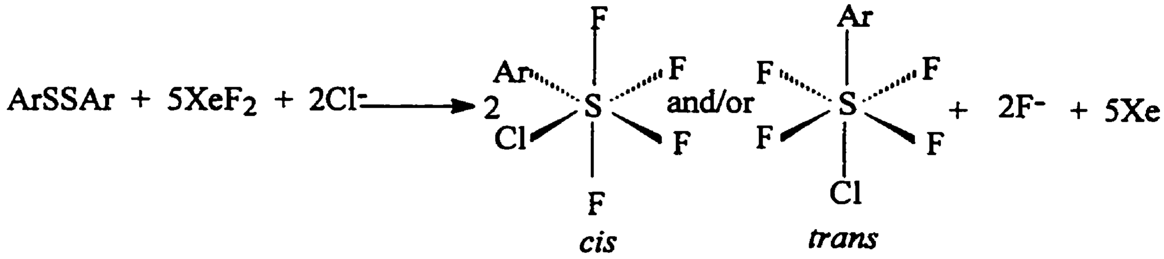
ArSSAr + 5XeF2 + 2Cl-
2
Ar
F
F
S
Cl
F
F
and/or
Ar
F
F
S
F
F
Cl
+ 2F- + 5Xe
cis
trans

[90]

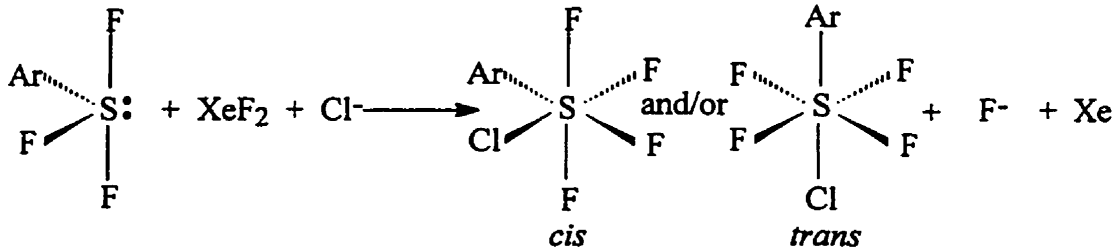
Ar
F
S:
F
F
+ XeF2 + Cl-
Ar
F
F
S
Cl
F
F
and/or
Ar
F
F
S
F
F
Cl
+ F- + Xe
cis
trans

The oxidative fluorination of ArSSAr or $ArSF_3$ with XeF_2 was carried out on a ~0.06 mmol scale in a polytetrafluoroethylene-lined tube in either CH_2Cl_2 or CH_3CN solution. The reaction proceeds very rapidly at room temperature to give *cis*- and/or *trans*-$ArSF_4Cl$. Typical reaction conditions for the reaction of ArSSAr or $ArSF_3$, XeF_2, and Et_4NCl in CH_2Cl_2 or CH_3CN are summarized in Table 11. All products were characterised by ^{19}F and ^{13}C NMR spectroscopy as shown by example in Figure 57-60. The ^{13}C and ^{19}F NMR spectra data are listed in Tables 10 and 12. For comparison purposes, the fluorine chemical shifts were estimated by the method of Dean and Evans,[158] with adjustable parameters determined from the measured chemical shifts of $ClSF_5$ and $PhSF_5$ (will be discussed in the following section).

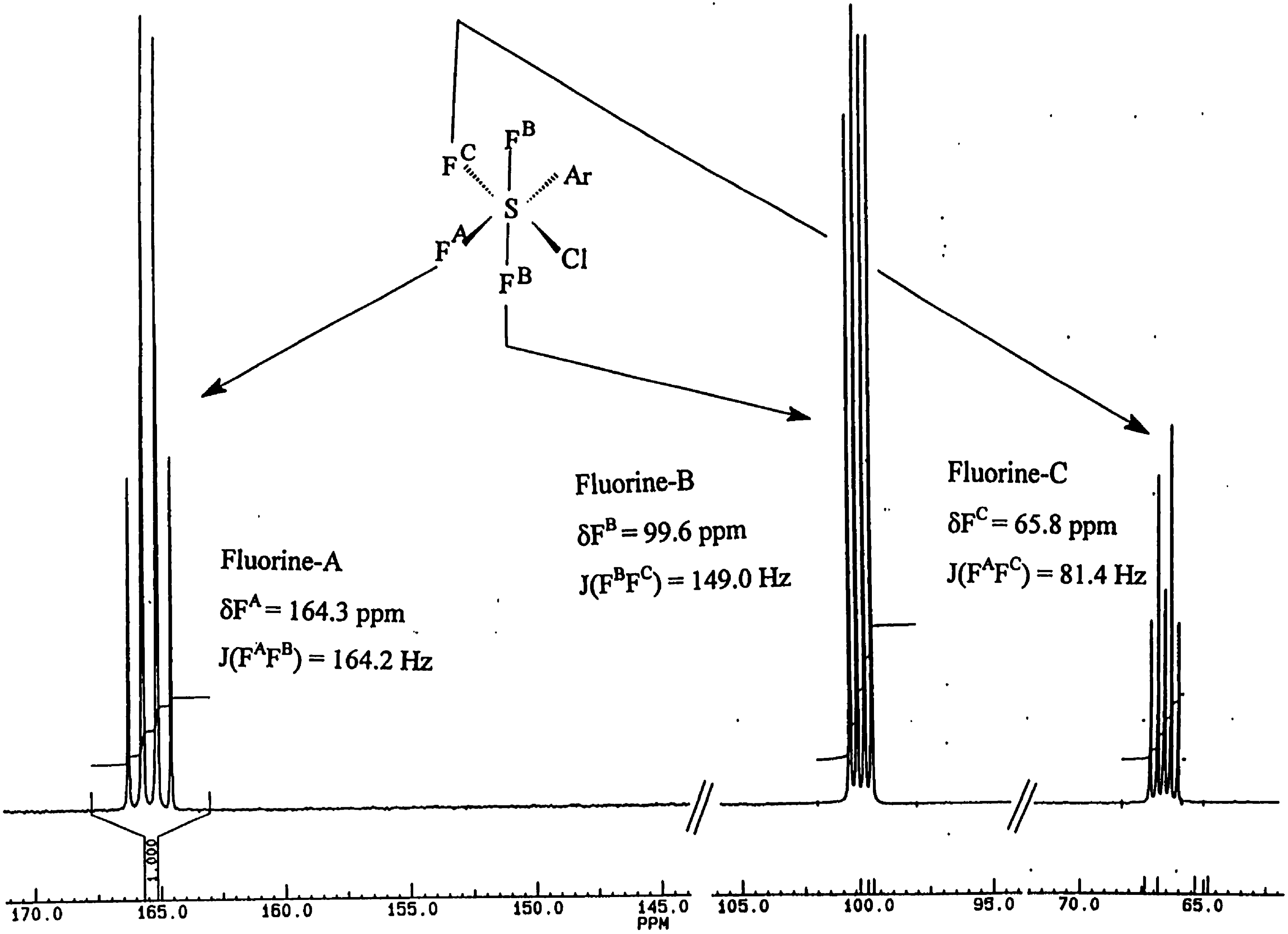

Figure 57. ^{19}F NMR spectrum of *cis*-$ArSF_4Cl$ (Ar = *p*-MeC_6H_4) in CD_2Cl_2 showing an AB_2C spin system. Dean and Evan's method was used for the assignment of Fluorines A and C.

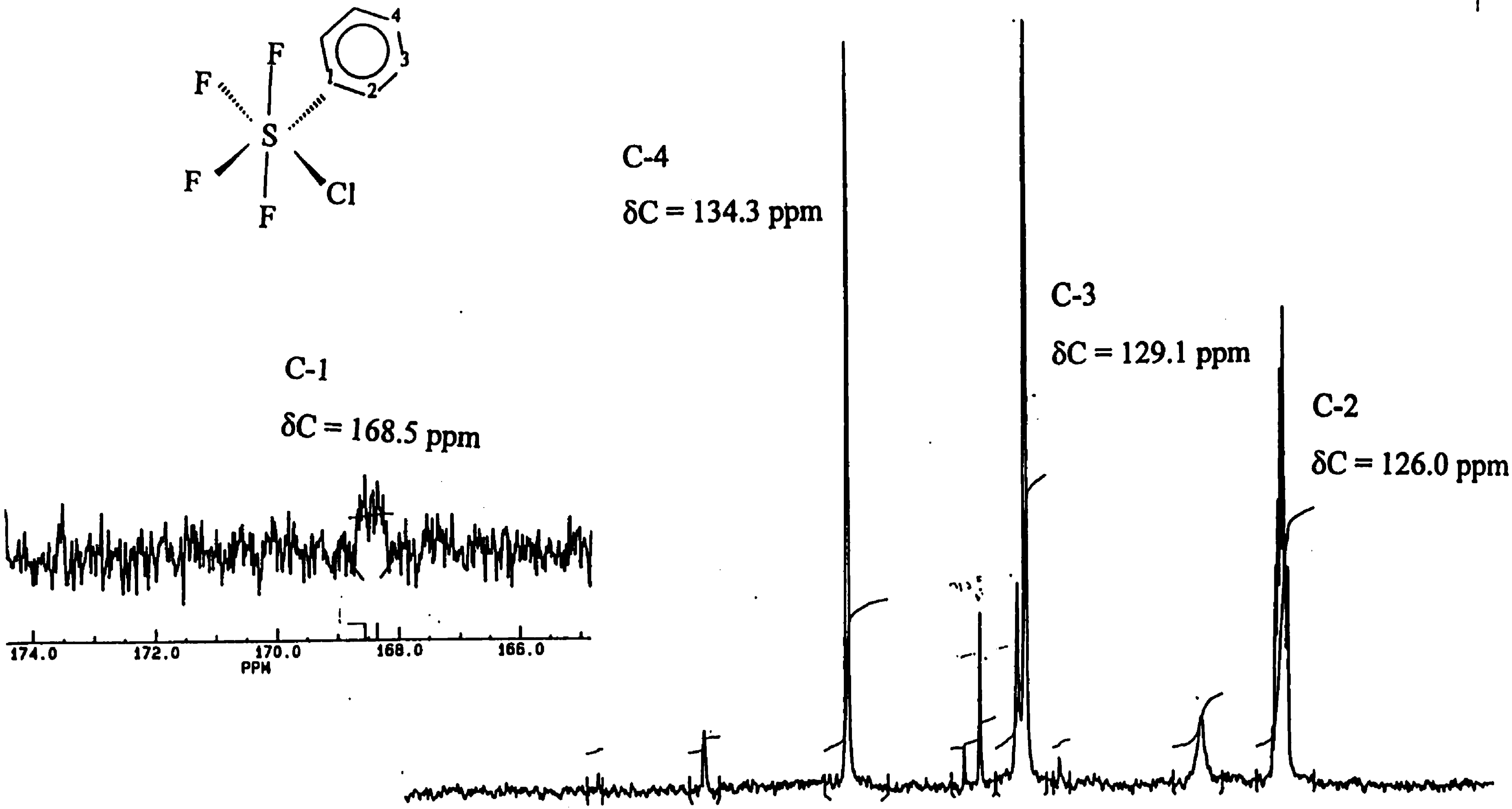

Figure 58. ^{13}C NMR spectrum of *cis*-$ArSF_4Cl$ (Ar = Ph) in CD_2Cl_2 showing an AB_2C spin system.

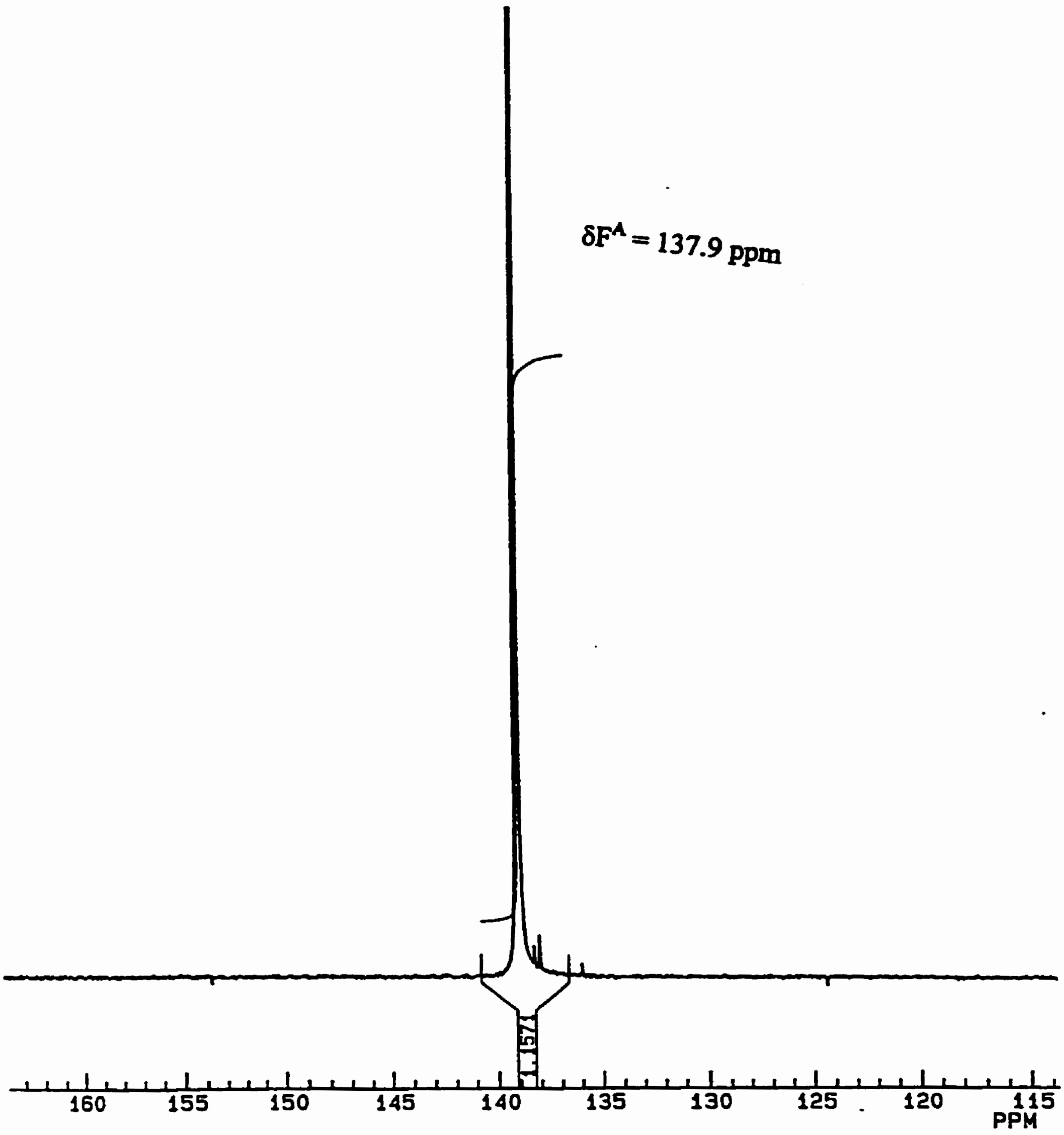

Figure 59. ^{19}F NMR spectrum of *trans*-$ArSF_4Cl$ (Ar = *p*-MeC_6H_4) in CD_3CN showing an A_4 spin system.

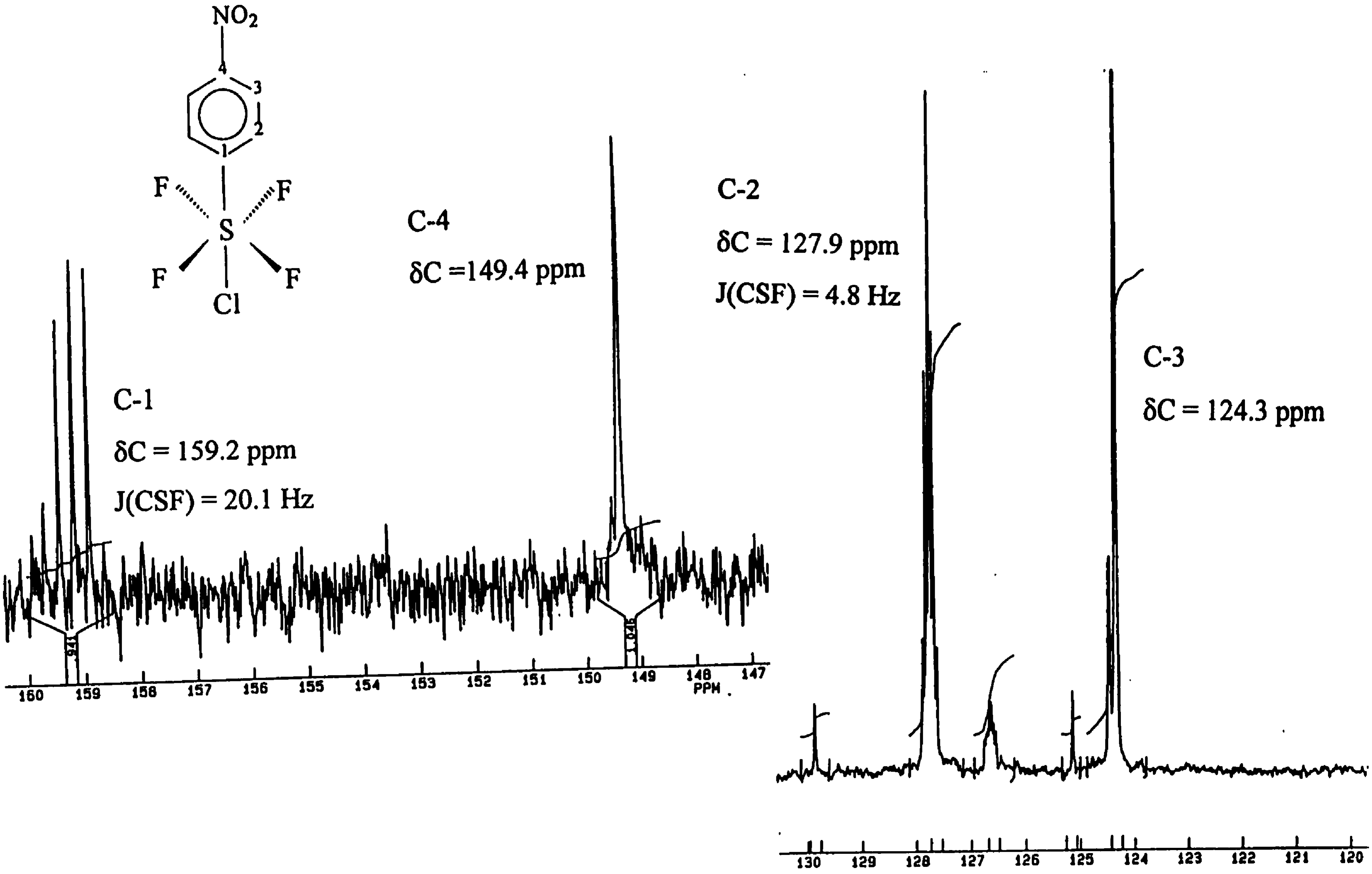

Figure 60. ^{13}C NMR spectrum of *trans*-ArSF$_4$Cl (Ar = *p*-O$_2$NC$_6$H$_4$) in CD$_2$Cl$_2$ showing an A$_4$ spin system.

TABLE 10. ^{13}C NMR data of *cis*- and *trans*-ArSF$_4$Cl in CD$_2$Cl$_2$.[a]

Compound	δC1	δC2	δC3	δC4	δCH$_3$
cis-PhSF$_4$Cl	168.5 (m)	126.0 (m)	129.1	134.3	—
cis-*p*-MeC$_6$H$_4$SF$_4$Cl	167.5 (m)	124.4 (m)	129.1	142.6	20.8
cis-*p*-O$_2$NC$_6$H$_4$SF$_4$Cl	170.3 (m)	125.9 (m)	124.4	148.9	—
trans-PhSF$_4$Cl	155.4 (q, 17.5 Hz)	125.9 (q, 4.7 Hz)	129.1	132.1	—
trans-*p*-MeC$_6$H$_4$SF$_4$Cl	153.3 (q, 17.7 Hz)	125.8 (q, 4.7 Hz)	129.2	143.0	21.1
trans-*p*-O$_2$NC$_6$H$_4$SF$_4$Cl	159.2 (q, 20.1 Hz)	127.9 (q, 4.8 Hz)	124.3	149.4	—

[a] q = quintet, m = multiplet, chemical shifts in ppm

The identity of *cis*-$ArSF_4X$ is established by its ^{19}F NMR AB_2C spin pattern as shown in Figure 57, and the characteristic ^{13}C NMR spectrum of the aromatic substituent is seen in Figure 58. Similarly, the identity of *trans*-$ArSF_4Cl$ is confirmed by the equivalence of all fluorines (a singlet) in the ^{19}F NMR spectrum as illustrated in Figure 59, and by C1 and C2 quintets in the ^{13}C NMR spectrum as shown in Figure 60.

Diaryl disulfides, ArSSAr, also react step-by-step with XeF_2 to give *cis*- and/or *trans*-$ArSF_4Cl$, as illustrated in eq [91].

$$[91]\quad \mathrm{ArSSAr} + \mathrm{XeF_2} \xrightarrow{\text{catalytic amount of } \mathrm{Cl^-}} \mathrm{ArSF_3} \xrightarrow{\mathrm{XeF_2}\ +\ \mathrm{Cl^-}} \textit{cis} \text{ and } \textit{trans}\text{-}\mathrm{ArSF_4Cl}$$

The oxidative fluorination of Ar_2S_2 with a stoichiometric amount of XeF_2 is slow and only gives a modest yield of $ArSF_3$. If a catalytic amount of Et_4NCl is added initially, then the reaction could be completed within 10 minutes to give $ArSF_3$ in an essentially quantitative crude yield. However, further oxidative fluorination of $ArSF_3$ with addition of an equivalent of XeF_2 (without Et_4NCl) did not occur even after 24 hours. When an equivalent amount of tetraethylammonium chloride, Et_4NCl, was added to this reaction mixture, a rapid reaction occurred within 5 minutes to give *cis-/trans*-$ArSF_4Cl$ in high yield. Reactions are accompanied by the evolution of xenon gas and a colour change from colourless to deep yellow and back to colourless.

TABLE 11. Experimental conditions for the synthesis of *cis*- and *trans*-$ArSF_4Cl$ at 25 °C in CD_2Cl_2 and CD_3CN.[a]

Entry	Molar ratio of reactants	Reaction Cond	*cis*-$ArSF_4Cl$	*trans*-$ArSF_4Cl$	$ArSF_5$	other products identified
	Stoichiometric, or less XeF_2 in CD_2Cl_2					
1	$(p\text{-}O_2NC_6H_4)_2S_2:Et_4NCl:XeF_2$ /1:2:6	CD_2Cl_2, ~24 h	83%	11%	nil	$ArSOF_3$, CD_2F_2, CD_2FCl, DF_2^-/DF
2	$Ph_2S_2:Et_4NCl:XeF_2$/1:4:5	CD_2Cl_2, ~24 h	75%	14%	nil	$PhSOF_3$, CD_2F_2, CD_2FCl, DF_2^-/DF
3	$Ph_2S_2:Et_4NCl:XeF_2$/1:2:5	CD_2Cl_2, ~24 h	54%	26%	<1%	$PhSF_3$, CD_2F_2, CD_2FCl, DF_2^-/DF
		~1 week	59%	12%		
4	$PhSF_3:Et_4NCl:XeF_2$/1:1:1	CD_2Cl_2, ~24 h	54%	37%	3.1%	$PhSOF_3$, CD_2F_2, CD_2FCl, DF_2^-/DF
		~1 week	79%	12%		
5	$Ph_2S_2:Et_4NCl:XeF_2$/1:2:4	CD_2Cl_2, ~24 h	39%	19%	nil	$PhSF_3$,$PhSOF_3$, DF_2^- /DF, CD_2F_2, CD_2FCl
		~1 week	44%	6%		
6	$Ph_2S_2:Et_4NCl:XeF_2$/1:2:6	CD_2Cl_2, ~24 h	38%	53%	<1%	$PhSOF_3$, CD_2F_2, CD_2FCl, DF_2^-/DF^-
		~1 week	72%	11%		
7	$(p\text{-}MeC_6H_4)_2S_2:Et_4NCl:XeF_2$/1:2:5	CD_2Cl_2, ~24 h	38%	35%	nil	$PhSF_3$, $ArSOF_2$, DF_2^-/DF, CD_2F_2, CD_2FCl
		~1 week	46%	13%		
8	$PhSF_3:Et_4NCl:XeF_2$/1:0.3:1	CD_2Cl_2, ~24 h	<1%	<1%	46%	XeF_2, $PhSF_3$, DF_2^-/DF, CD_2F_2, CD_2FCl
		~1 month	<1%	34%	20%	
	Excess XeF_2 in CD_2Cl_2					
9	$(p\text{-}O_2NC_6H_4)_2S_2:Et_4NCl:XeF_2$/1:2:8	CD_2Cl_2, ~24 h	14%	80%	nil	XeF_2, $ArSOF_3$, DF_2^-/DF, CD_2F_2, CD_2FCl
10	$PhSF_3:Et_4NCl:XeF_2$/1:1:2	CD_2Cl_2, ~24 h	<1%	82%	<1%	XeF_2, $PhSOF_3$, DF_2^-/DF, CD_2F_2, CD_2FCl
11	$(p\text{-}MeC_6H_4)_2S_2:Et_4NCl:XeF_2$/1:2:8	CD_2Cl_2, ~24 h	nil	83%	2%	XeF_2, $ArSOF_3$, DF_2^-/DF, CD_2F_2, CD_2FCl
12	$Ph_2S_2:Et_4NCl:XeF_2$/1:2:8	CD_2Cl_2, ~24 h	1%	89%	2%.	XeF_2, $PhSOF_3$, DF_2^-/DF, CD_2F_2, CD_2FCl

	Solvent CD_3CN					
13	Ph_2S_2:Et_4NCl:XeF_2/1:3:5	CD_3CN, ~24 h	77%	7%	nil	$PhSOF_3$, DF_2^-/DF, CD_2F_2, CD_2FCN
14	Ph_2S_2:Et_4NCl:XeF_2/1:2:4.7	CD_3CN, ~24 h	69%	<1%	nil	$PhSF_3$, $PhSOF_3$, DF_2/DF, CD_2FCN
15	Ph_2S_2:Et_4NCl:XeF_2/1:3:5	CD_3CN, ~24 h	55%	25%	<1%	XeF_2, $PhSOF_3$, DF_2^-/DF, CD_2FCN
16	Ph_2S_2:Et_4NCl:XeF_2/1:2:6	CD_3CN, ~24 h	27%	60%	trace	XeF_2, $PhSOF_3$, DF_2^-/DF, CD_2FCN
17	Ph_2S_2:Et_4NCl:XeF_2/1:2:7	CD_3CN, ~24 h	12%	75%	trace	XeF_2, $PhSOF_3$, DF_2^-/DF, CD_2FCN
18	Ph_2S_2:Et_4NCl:XeF_2/1:2:8	CD_3CN, ~24 h	4%	84%	trace	XeF_2, $PhSOF_3$, DF_2^-/DF, CD_2FCN

[a] Reactions were complete within 10 minutes. ^{19}F NMR spectra were recorded after reaction time of ~24h. Yields based on integration of ^{19}F NMR signals of all sulfur fluoride compounds.

Attempts were made to optimise the yield of *cis*- and *trans*-$ArSF_4Cl$ and, as seen in Table 11, either cis or trans isomers can be prepared in high yield exclusively, for example, some reactions give 89% *trans*-$PhSF_4Cl$ (reaction 12 in Table 11) and others give 83% *cis*-$PhSF_4Cl$ (reactions 10,18 in Table 11).

The cis/trans ratio of products appears to depend mainly on the amount of XeF_2, with a large excess of XeF_2 giving exclusively trans isomer, as illustrated by reactions 9-12, while less XeF_2 favours the cis isomer, e.g., reactions 1, 2 and 4. Excess of Et_4NCl also favours the cis isomer.

The yields given in Table 11 were determined after 24 hrs. On standing for one week, or longer, the yield of cis isomer slowly increases at the expense of trans isomer, as indicated in the footnotes for reactions 4, 5 and 6.

A small amount of $ArSF_5$ is produced in some reactions, e.g. 4, 6, 8, 11, and 12. Its presence appears to be inversely related to Cl^-, and it was shown in a separate experiment that as the ratio of Cl^- decreases, i.e. $PhSF_3$:Et_4NCl:XeF_2/1:0.3:1, the yield of $PhSF_5$ increases to 20%.

Generally, ArSSAr was the starting compound of choice, because of its ease of preparation and commercial availability. We assume, however, that $ArSF_3$ is formed *in situ* in all reactions of ArSSAr. This assumption was tested by carrying out reactions in two stages. In the first stage, $ArSF_3$ was prepared from ArSSAr and XeF_2 and a catalytic amount of Et_4NCl, and identified by ^{19}F NMR spectroscopy. In the second stage, more XeF_2 and Et_4NCl was added to give *cis*- and *trans*-$ArSF_4Cl$, e.g., reactions 4 and 10. If reactions of ArSSAr are carried out with a stoichiometric deficiency of XeF_2, then unreacted $ArSF_3$ can be identified at the completion of the reaction, e.g., 5 and 7.

Also listed in the last column of Table 11 are the products CD_2F_2, CD_2FCl, and CD_2FCN, identified by ^{19}F NMR spectroscopy.

As described above, the cis/trans ratio of products appears to depend mainly on the amount of XeF_2 and Et_4NCl, with an excess of XeF_2 favouring the *trans* isomer, while less XeF_2 and excess Et_4NCl favours the *cis* isomer. It was also found in some reactions that a mixture of *cis*- and *trans*-$ArSF_4Cl$ was obtained, with the ^{19}F NMR resonance of *trans*-$ArSF_4Cl$ being a broader peak suggesting a rapid fluorine exchange reaction, while the ^{19}F NMR resonances of *cis*-$ArSF_4Cl$ remained sharp. After one week or longer, the yield of *cis* isomer slowly increases at the expense of the *trans* isomer. *Trans*-$ArSF_4Cl$ is stable if there is an excess amount of XeF_2 in the solution. However, on standing, as XeF_2 slowly reacts with impurities in the solution or attacks the solvent, excess XeF_2 is used up and then all the *trans*-$ArSF_4Cl$ is gradually converted to the thermodynamically more stable cis isomer.

When a small amount of Et_4NCl was added to a solution containing *trans*-$ArSF_4Cl$ in CD_3CN or CD_2Cl_2, isomerization occurs to give the thermodynamically more stable cis isomer. The isomerization process was monitored by measuring the relative areas of the fluorine resonances of both cis and trans isomers in the ^{19}F NMR spectra. To a sample that had originally contained a 2:1 ratio of *trans-/cis*-$PhSF_4Cl$ with excess XeF_2 in the solution, there was added a small amount of tetraethylammonium chloride, Et_4NCl. The ^{19}F NMR spectrum after 16 hours revealed that the singlet sharp peak of *trans*-$ArSF_4Cl$ became very broad at almost the same chemical shift, and its relative integration decreased significantly. However, the position of all peaks from *cis*-$PhSF_4Cl$ remained unchanged, although their relative intensities increased significantly. The molar ratio of *trans*-$PhSF_4Cl$ to *cis*-$PhSF_4Cl$ changed from ~2:1 to a ratio of ~1:2. After 64 hours, the ratio of *trans/cis*-$PhSF_4Cl$ was about 1:4. After 5 days, the ratio of *trans/cis* changed to ~1:8, and finally after two weeks, almost all *trans*-$PhSF_4Cl$ were converted to *cis*-$PhSF_4Cl$. Figure 62 clearly shows this isomerization process i.e. the composition changes of *trans*- and *cis*-$PhSF_4Cl$ as time elapses, as monitored by ^{19}F NMR spectroscopy.

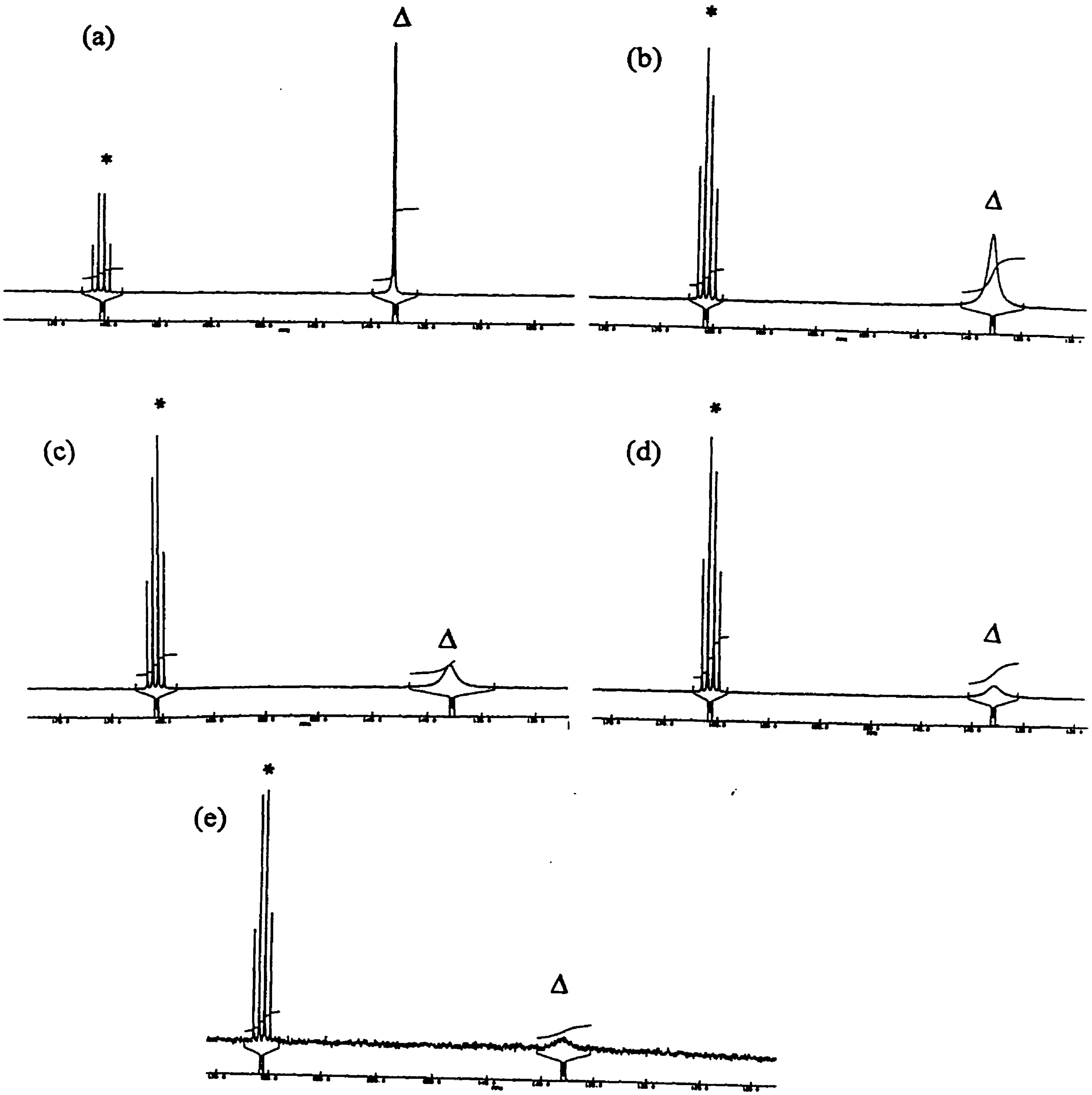

Figure 61. ^{19}F NMR spectrum of a mixture *trans*- and *cis*-$PhSF_4Cl$ on standing after Et_4NCl was added: (a) original 2:1 mixture; (b) after 16 hrs; (c) after 64 hrs; (d) after 5 days; (e) after more than two weeks. The cis isomer is marked by asterisk, and the trans isomer is marked by a triangle. In each spectrum, only part of the fluorine spectrum is shown for the cis and trans isomers.

Reaction in both CD_2Cl_2 and CD_3CN solution was accompanied by attack on solvent. Reaction with the solvent is more serious in CD_2Cl_2 than in CD_3CN. A large amount of CD_2F_2 and CD_2FCl was identified in all reactions when CD_2Cl_2 was used as the solvent, and CFD_2CN was found when CD_3CN was used as the solvent. Such Cl/F interchange is consistent with the presence of anhydrous fluoride ion[124] and radical processes.[125] An exchange-broadened ^{19}F NMR peak at ~ -153 ppm is seen in all samples and is assigned to a mixture of FDF^-, FHF^-, DF and HF.

The solvent (CD_2Cl_2 or CD_3CN) does not appear to have a large effect on the oxidative fluorination of ArSSAr and/or $ArSF_3$. The fact that this reaction occurs very similarly in CD_3CN solvent excludes the possibility that the reactions might proceed by virtue of the use of the CD_2Cl_2 (without adding Et_4NCl as a Cl^- source).

In most reactions, but not all, some $ArS(O)F_3$ can be identified by ^{19}F and ^{13}C NMR, and this hydrolysis product serves as an indicator of our experimental technique. Careful purification of reactants and solvents avoids completely the appearance of $ArS(O)F_3$, whereas the deliberate introduction of water to typical reaction mixtures leads to conversion of $ArS(O)F_3$ to $ArS(O)_2F$.

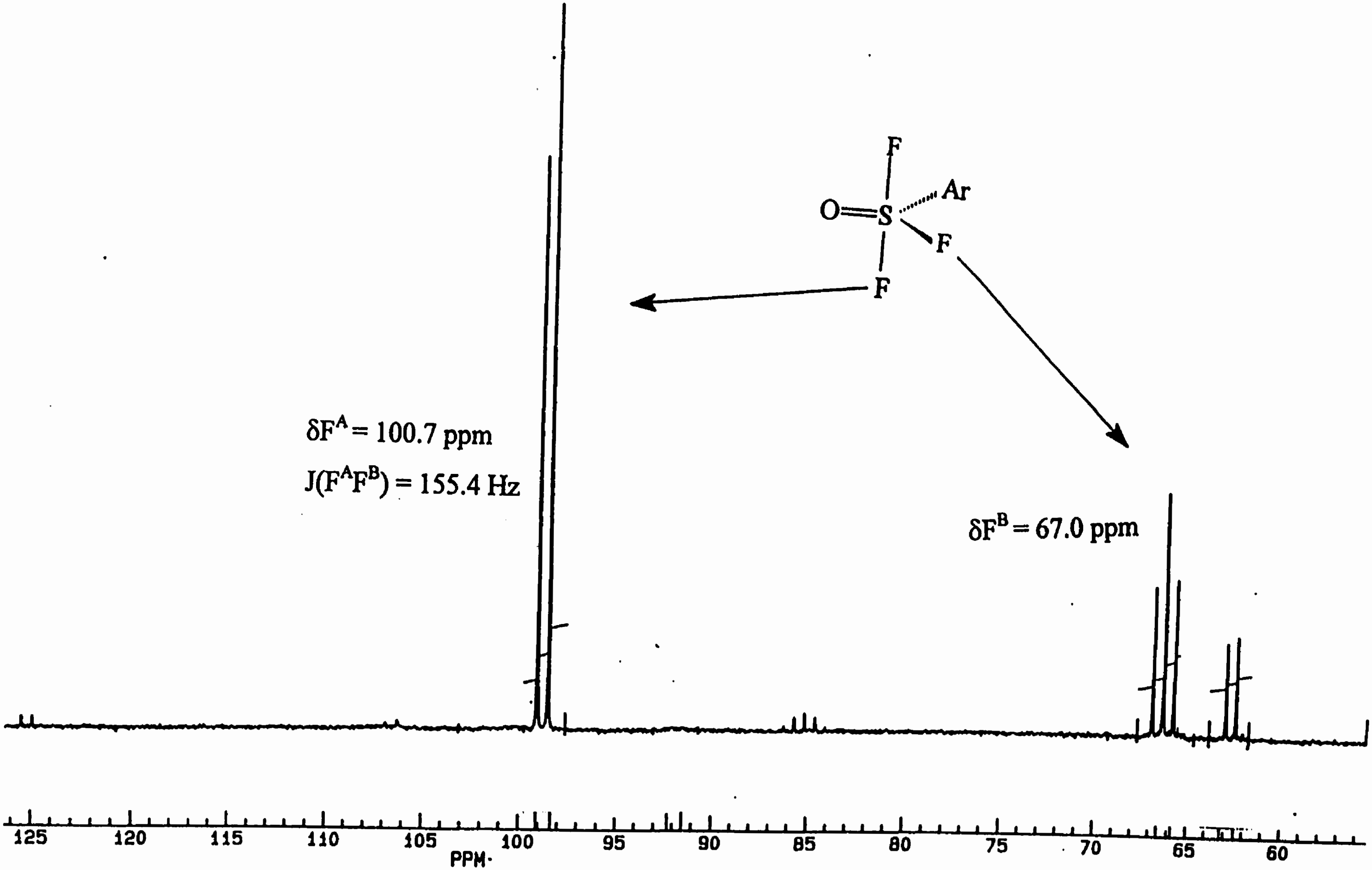

$\delta F^A = 100.7$ ppm

$J(F^AF^B) = 155.4$ Hz

$\delta F^B = 67.0$ ppm

Figure 62. ^{19}F NMR spectrum of *p*-$MeC_6H_4S(O)F_3$.

TABLE 12. ^{19}F NMR data of $ArS(O)F_3$ in CD_2Cl_2 or CD_3CN.

Compound	δF_{ax} (ppm)	δF_{eq} (ppm)	$J_{Fax-Feq}$ (Hz)
$PhS(O)F_3$	102.0 (d)	65.9 (t)	157.8
$p\text{-}MeC_6H_4S(O)F_3$	100.7 (d)	67.0 (t)	155.4
$p\text{-}O_2NC_6H_4S(O)F_3$	103.1 (d)	66.2 (t)	162.4

Note: d = doublet, t = triplet

3.3.4.2 Empirical correlations of NMR parameters of *cis*- and *trans*-$ArSF_4Cl$

Simple ^{19}F NMR spectra sometimes do not yield definitive structural information for compounds of the type $ArSF_4Cl$. For such molecules, the trans geometry has equivalent fluorines and thus will display a single fluorine resonance, however, direct assignment of fluorine resonances for cis-isomer from the line patterns is difficult without additional information.

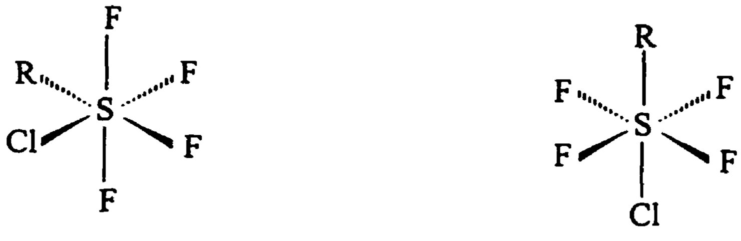

cis *trans*

Figure 63. Two geometrical isomers of RSF_4Cl.

Attempts have been made to overcome the above difficulties by empirical correlation of spectroscopic parameters. It has been demonstrated for a number of octahedral fluoro-species MX_nF_{6-n} (n=1-6) that the ^{19}F NMR chemical shifts relative to MF_6 may be correlated in terms of a linear function. This function is given by eq [92],

$$[92] \qquad \Delta(^{19}F) = pC + qT$$

where C and T are adjustable constants characteristic of the substituent, while p and q are the number of substituents in a position *cis* and *trans*, respectively, to the resonating fluorine ligand. The value for q is either zero or one, while p ranges from zero to four. This empirical method was first employed by Dean and Evans[158] to assign the ^{19}F NMR spectra of a range of fluorostannate(IV) species, $[SnX_nF_6]^{2-}$, where, for example, X = Cl, Br, I, OR, NCO, and N_3. Since then the same procedure has been successfully applied to a number of analogous systems, e.g. $[PtX_nF_{6-n}]^{2-}$ (X=OH, Cl), $(CH_3O)_nWF_{6-n}$, $SbClF_{6-n}^-$, and $AsCl_nF_{6-n}^-$, $(HO)_nTeF_{6-n}$, $(RO)_nTeF_{6-n}$, CH_3OTeF_4Cl, and $(HO)_nTeF_{5-n}Cl$.[158]

In the present work, the assignment of resonances arising from $ArSF_4Cl$ was carried out by comparison with literature ^{19}F NMR data (chemical shifts, resonance multiplicities, and relative integration intensities).

Empirical constants for the phenyl substituent trans (labeled as T_{Ph}) and cis (labeled as C_{Ph}) to the resonating fluorine in $ArSF_5$ are calculated from the known chemical shifts of $ArSF_5$ from the present work (A_4B system) and SF_6.[159]

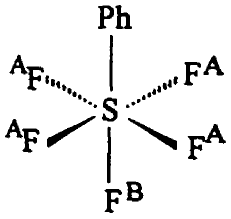

Figure 64. Structure of $PhSF_5$

In the above structure (Figure 64), the chemical shift of the F^B fluorine is 62.1 ppm and that of F^A is 84.3 ppm with respect to $CFCl_3$, from the present work. These chemical shifts relative to SF_6 (+57.0 ppm)[159] are then +5.1 ppm and +27.3 ppm for F^B and F^A fluorines, respectively. Fluorines F^B and F^A are in the *cis* and *trans* position to phenyl, respectively. Therefore, from eq [92], the following values are obtained:

$$5.1 = 62.1 - 57.0 = \Delta(^{19}F) = pC_{Ph} + qC_{Ph} = 1xC_{Ph} + 0xT_{Ph} = C_{Ph}$$

$$27.3 = 84.3 - 57.0 = \Delta(^{19}F) = pC_{Ph} + qC_{Ph} = 0xC_{Ph} + 1xT_{Ph} = T_{Ph}$$

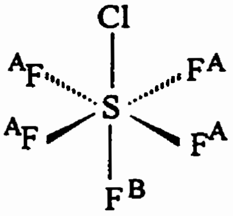

Figure 65. Structure of $ClSF_5$.

Empirical constants for chlorine ligand trans (labelled as T_{Cl}) and cis (labelled as C_{Cl}) to the resonating fluorine in $ClSF_5$ have been calculated from the measured chemical shifts of $ClSF_5$ from the present work (B_4X system) and SF_6.[159] The chemical shifts of F^A and F^B (Figure 65) are 125.3 ppm and 63.7 ppm, respectively, since F^A and F^B are in the position of *cis* and *trans* with respect to the chlorine ligand. Hence,

$$68.3 = 125.3 - 57.0 = \Delta(^{19}F) = pC_{Cl} + qC_{Cl} = 1xC_{Cl} + 0xT_{Cl} = C_{Cl}$$

$$6.7 = 63.7 - 57.0 = \Delta(^{19}F) = pC_{Cl} + qC_{Cl} = 0xC_{Cl} + 1xT_{Cl} = T_{Cl}$$

With these values of T_{Ph}, C_{Ph}, T_{Cl}, and C_{Cl}, the empirical chemical shifts of fluorine in *cis*- and *trans*-$PhSF_4Cl$ have been calculated as follows:

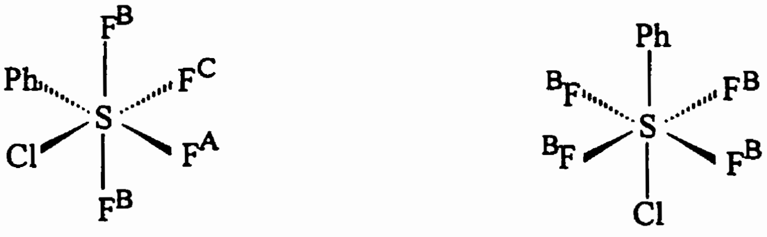

cis *trans*

Figure 66. Structure of *cis*- and *trans*-$PhSF_4Cl$.

cis-$PhSF_4Cl$:

$\Delta(F^A) = T_{Ph} + C_{Cl} = 27.3 + 68.3 = 95.6$ (ppm)

$\Delta(F^B) = C_{Ph} + C_{Cl} = 5.1 + 68.3 = 73.4$ (ppm)

$\Delta(F^C) = C_{Ph} + T_{Cl} = 5.1 + 6.7 = 11.8$ (ppm)

trans-$PhSF_4Cl$:

$\Delta(F^B) = C_{Ph} + C_{Cl} = 5.1 + 68.3 = 73.4$ (ppm)

Therefore, the ^{19}F chemical shifts of fluorines in *cis*- and *trans*-$PhSF_4Cl$ with respect to $CFCl_3$ are :

cis-$PhSF_4Cl$:

$\delta(F^A) = \Delta(F^A) + \delta SF_6 = 95.6 + 57.0 = 152.6$ ppm

$\delta(F^B) = \Delta(F^B) + \delta SF_6 = 73.4 + 57.0 = 130.4$ ppm

$\delta(F^C) = \Delta(F^C) + \delta SF_6 = 11.8 + 57.0 = 68.8$ ppm

trans-$PhSF_4Cl$:

$\delta(F^B) = \Delta(F^B) + \delta SF_6 = 73.4 + 57.0 = 130.4$ ppm

The observed ^{19}F NMR chemical shifts for *cis*- and *trans*-$PhSF_4Cl$ are listed as follows:

cis-$PhSF_4Cl$:

$\delta(F^A) = 164.3$ ppm

$\delta(F^B) = 99.6$ ppm

$\delta(F^C) = 68.5$ ppm

trans-$PhSF_4Cl$:

$\delta(F^B) = 136.8$ ppm

The same method can be applied to *cis*- and *trans*-*p*-$MeC_6H_4SF_4Cl$, and *cis*- and *trans*-*p*-$O_2NC_6H_4SF_4Cl$. The calculated values of the chemical shifts are summarised in parentheses in Table 13, and it can be seen that the agreement is good for δF^A, and acceptable for δF^C, thus providing a reasonable basis for the assignment of F^A versus F^C. Agreement with experimental values for δF^B is much poorer, however, the assignment of F^B is not in doubt.

TABLE 13. ^{19}F NMR data of *cis*- and *trans*-PhSF$_4$Cl in CD$_2$Cl$_2$ (and chemical shifts calculated by the method of Dean and Evans[158]).

Comound	Spin system	δF^A	δF^B	δF^C	$J(F^AF^B)$	$J(F^AF^C)$	$J(F^BF^C)$
cis-PhSF$_4$Cl	AB$_2$C	164.3(152.6)	99.6 (130.4)	65.8 (68.8)	164.2	81.4	149.0
cis-*p*-MeC$_6$H$_4$SF$_4$Cl	AB$_2$C	165.4(153.5)	100.2(131.0)	66.5(69.4)	165.5	81.2	149.8
cis-*p*-O$_2$NC$_6$H$_4$SF$_4$Cl	AB$_2$C	159.5(149.1)	100.6(130.5)	66.7(69.9)	163.3	84.9	153.6
trans-PhSF$_4$Cl	B$_4$		136.8(130.4)				
trans-*p*-MeC$_6$H$_4$SF$_4$Cl	B$_4$		137.9(131.0)				
trans-*p*-O$_2$NC$_6$H$_4$SF$_4$Cl	B$_4$		135.1(130.5)				

[a] Numbers in parentheses are calculated chemical shifts by the method of Dean and Evans.

[b] Dean and Evans constants: C=68.3 T =6.7 for Cl, C=5.1 T=27.3 for Ph, C=5.7 T=28.2 for *p*-MeC$_5$H$_4$, C = 5.2 T=23.8 for *p*-O$_2$NC$_6$H$_4$. See text for details.

3.3.4.3 $^{37}Cl/^{35}Cl$ isotope shifts on the ^{19}F NMR spectrum of *trans*-$ArSF_4Cl$

To verify that $ArSF_4X$ contains a chlorine substituent, we carried out the $^{37}Cl/^{35}Cl$ isotope shift measurements* on the ^{19}F NMR spectra for all *trans*-$ArSF_4Cl$. The $^{37}Cl/^{35}Cl$ isotope shifts for all *cis*-$ArSF_4Cl$ were also observed, but the resolution was never good enough to show two separated peaks. Figure 67 shows a typical ^{19}F NMR spectrum of *trans*-$ArSF_4Cl$ at 282.363 MHz. The ^{19}F NMR peak of *trans*-$ArSF_4Cl$ contained an additional single peak with about 1/3 the intensity of the more intense peak, which corresponds to the ratio of the natural abundances of ^{37}Cl and ^{35}Cl (75.53% and 24.47%, respectively).

A similar ratio of peak intensities was also observed for $^{34}S^{37}Cl$ and $^{34}S^{35}Cl$ (natural abundance of ^{32}S and ^{34}S are 95.0% and 4.22%, respectively). The results of $^{37}Cl/^{35}Cl$ isotope effects for all three *trans*-$ArSF_4Cl$ (Ar = Ph, *p*-O_2N-C_6H_4, p-MeC_6H_4) are given in Table 14. As we can see from the table, the values obtained for $\Delta^{19}F(^{37}Cl/^{35}Cl)$ are almost identical, suggesting that this parameter is invariable to the substituent group in the para position of the phenyl ring.

---

* in collaboration with Mr. Guy Bernard of this department

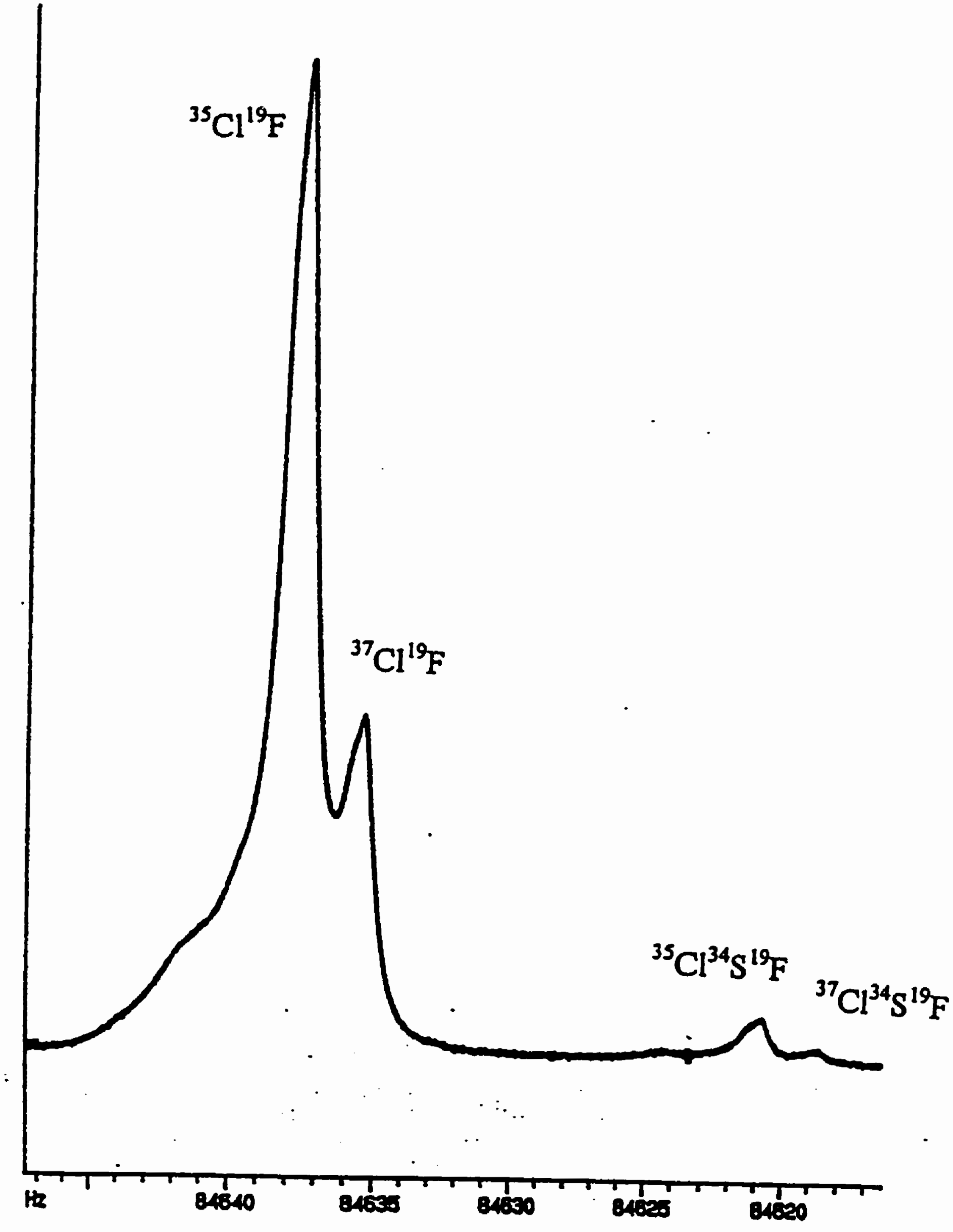

Figure 67. ^{19}F NMR spectrum at 282.363 MHz of *trans*-$ArSF_4Cl$ in CD_3CN.

TABLE 14. ^{19}F NMR chemical shift of *trans*-ArSF$_4$Cl and chlorine ^{37}Cl/^{35}Cl and sulfur ^{34}S/^{32}S isotope effects.[a,b]

Compound	δ^{19}F(ppm)	$^2\Delta$F(^{37}Cl/^{35}Cl)	$^1\Delta$F(^{34}S^{37}Cl/^{34}S^{35}Cl)	^{3}J(F,H$_{ortho}$)
trans-PhSF$_4$Cl	136.85(2)	-2.09(6) Hz -7.4(2) ppb	-16.7(2) Hz -59.1(7) ppb	decoupled
trans-*p*-MeC$_6$H$_4$SF$_4$Cl	139.13(3)	-1.96(9) Hz -6.9(3) ppb	not resolved	decoupled
trans-*p*-O$_2$NC$_6$H$_4$SF$_4$Cl	135.21(1)	-2.04(3) Hz -7.2(1) ppb	-16.7(1) Hz -59.1(4) ppb	0.89(2) Hz

[a] Numbers in parentheses are the uncertainty in the last digit.

[b] A negative sign implies increased shielding as a result of substitution with the heavier isotope, i.e. $^2\Delta$F(^{37}Cl/^{35}Cl) = δ^{19}F(^{37}Cl)- δ^{19}F(^{35}Cl)

3.3.4.4 Synthesis of *cis*- and *trans*-$PhTeF_4Cl$, and $PhTeF_3Cl_2$

Phenyltellurium tetrafluoride chloride, $PhTeF_4Cl$, can exist as two geometrical isomers with respect to phenyl and chlorine substituents, i.e. *cis*- and *trans*-$PhTeF_4Cl$, as illustrated in Figure 68.

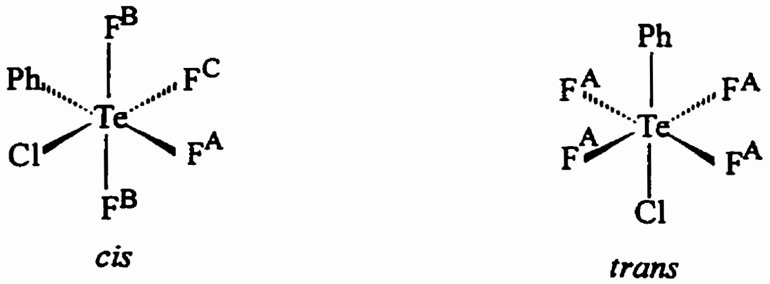

Figure 68. Two possible structures of $PhTeF_4Cl$.

However, if the number of chlorine substituents increases, the number of possible geometrical isomers increases. Three possible isomers for $PhTeF_3Cl_2$ as illustrated in Figure 69.

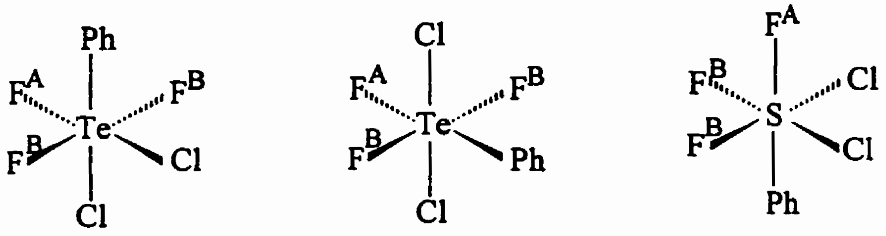

33a *cis, mer*-$PhTeF_3Cl_2$

33b *trans, mer*-$PhTeF_3Cl_2$

33c *cis, fac*-$PhTeF_3Cl_2$

Figure 69. Three possible structures of $PhTeF_3Cl_2$ with *mer*- and *fac*- arrangement of three fluorine substituents, and *cis*- and *trans*- arrangement of two chlorine substituents.

When three fluorine substituents retain their mer arrangement, $PhTeF_3Cl_2$ can exist as two geometrical isomers with respect to two chlorine substituents, i.e., *cis*, *mer*-

$PhTeF_3Cl_2$ **34a** and *trans*, *mer*-$PhTeF_3Cl_2$ **34b**. When fluorine substituents have the *fac*-arrangement, only one isomer is possible, i.e. *cis, fac*-$PhTeF_3Cl_2$ **34c**.

The oxidative fluorination and chlorination of Ph_2Te_2 or $PhTeF_3$ were carried out on a 0.06 ~0.12 mmol scale in a ptfe bottle in CH_3CN/CD_3CN solution with a slight stoichiometric deficiency of XeF_2. If an excess of XeF_2 is used, then the final product is predominantly $PhTeF_5$. The reaction proceeds very rapidly at room temperature to give a mixture of *cis*- and *trans*-$PhTeF_4Cl$. The ^{19}F and ^{125}Te NMR provide evidence that compounds in Figure 68, i.e., *cis* and *trans*-$PhTeF_4Cl$, as well as $PhTeF_3Cl_2$ **34**, are formed. Their ^{19}F and ^{125}Te NMR data are listed in Table 15. Evidence for the *trans* isomer, *trans*-$PhTeF_4Cl$, comes from the observation of a singlet (A_4 spin system) in the ^{19}F NMR spectrum at δ -39.4 ppm, as shown in Figure 70, and a quintet (A_4X spin system) with the same Te-F coupling constant in the ^{125}Te NMR spectrum as in its ^{19}F NMR spectrum. In the same ^{19}F NMR spectrum (Figure 70), three resonances with multiplet fine structure were also observed. These are in accord with the expected A_2BC system for *cis*-$PhTeF_4Cl$. Its ^{125}Te NMR spectrum showed an A_2BCX spin system, as expected. Evidence for the new species with the formula $PhTeF_3Cl_2$ was also provided by the observation of three types of doublets and triplets in the ^{19}F NMR. Both doublet and triplet peaks in the ^{19}F NMR are flanked by ^{125}Te satellites. Three isomeric configurations are possible for $PhTeF_3Cl_2$, *cis, mer*-$PhTeF_3Cl_2$ **34a**, *trans,mer*-$PhTeF_3Cl_2$ **34b** and *cis, fac*-$PhTeF_3Cl_2$ **34c**, as shown in Figure 69. All three isomers are expected to give rise to the same AB_2 splitting patterns in the ^{19}F and ^{125}Te NMR spectra and consequently the splitting pattern does not afford a means of determining which isomer is present. Further identification was not carried out.

TABLE 15. ^{19}F NMR data of $PhTeF_4Cl$, and $PhTeF_3Cl_2$ in CD_3CN

Comound	Spin system	δF^A	δF^B	δF^C	$J(F^AF^B)$	$J(F^BF^C)$	$J(F^AF^C)$
cis-$PhTeF_4Cl$[a, b]	A_2BC	-46.5	-33.7	-24.1	120.1	150.9	120.7
trans-$PhTeF_4Cl$	A_4	-39.4					
$PhTeF_3Cl_2$ I[a]	AB_2	-40.1 (d)	-38.1 (t)		89.7		
$PhTeF_3Cl_2$ II[a]	AB_2	-4.3 (d)	34.5 (t)		127.3		
$PhTeF_3Cl_2$ III[a]	AB_2	-26.7 (d)	-41.5 (t)		60.1		

[a] The assignment of F^B versus F^C in *cis*-$PhTeF_4Cl$ is arbitrary.

[b] δTe 23.1 ppm; $J(TeF^A)$=3281 Hz.

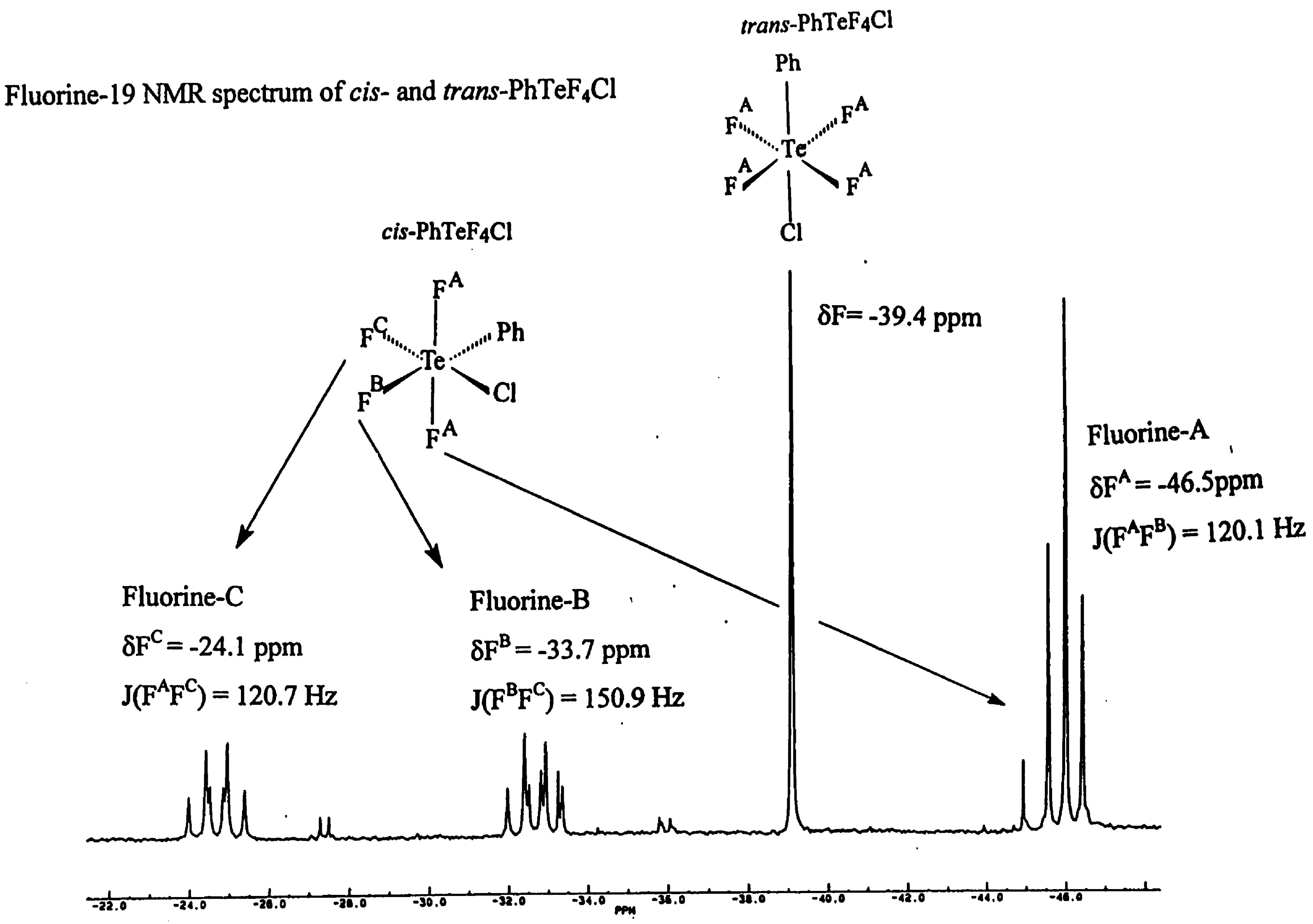

Figure 70. ^{19}F NMR spectrum of *cis* and *trans*-$PhTeF_4Cl$ in CD_3CN.

3.3.4.5 Proposed mechanism of oxidative-halogenation

Due to the difficulty of identifying and eliminating trace impurities, and the difficulty of identifying reactive intermediates in solution, no simple generalization about the mechanisms of oxidative fluorination and chlorination reactions of main group compounds can be found in the literature.

The oxidative addition reaction of ArSSAr or $ArSF_3$ has been discussed previously in Section 4.1. In general, when ArSSAr was used as the starting compound for the synthesis of *cis*- and/or *trans*-$ArSF_4Cl$, we assume that $ArSF_3$ is formed *in situ* in all reactions of ArSSAr. This assumption was tested by carrying out the reaction in two stages. In the first stage, $ArSF_3$ was prepared from ArSSAr, XeF_2 and Et_4NCl, and confirmed by ^{19}F NMR. In the second stage, more XeF_2 and Cl^- was added to give *cis*- and/or *trans*-$ArSF_4Cl$. If reactions of ArSSAr are carried out with a stoichiometric deficiency of XeF_2, then unreacted $ArSF_3$ can be identified at the completion of the reaction. Therefore, our mechanism of oxidative fluorination and chlorination of ArSSAr will be restricted to oxidation of $ArSF_3$. Ph_3CCl does not catalyse this type of reaction, presumably because it does not function as a convenient source of Cl^-. Furthermore, we assume that XeF_2 and Cl^- can produce HF-free and anhydrous F^-, according to eq [90], as proposed previously in section 3.3.1.

In order to account for the experimental results of Table 11, a mechanism of oxidation of $ArSF_3$ in the presence of fluoride ion can then be proposed which accounts for the formation of *trans*-$ArSF_4Cl$ and $ArSF_5$, as shown in Scheme 13.

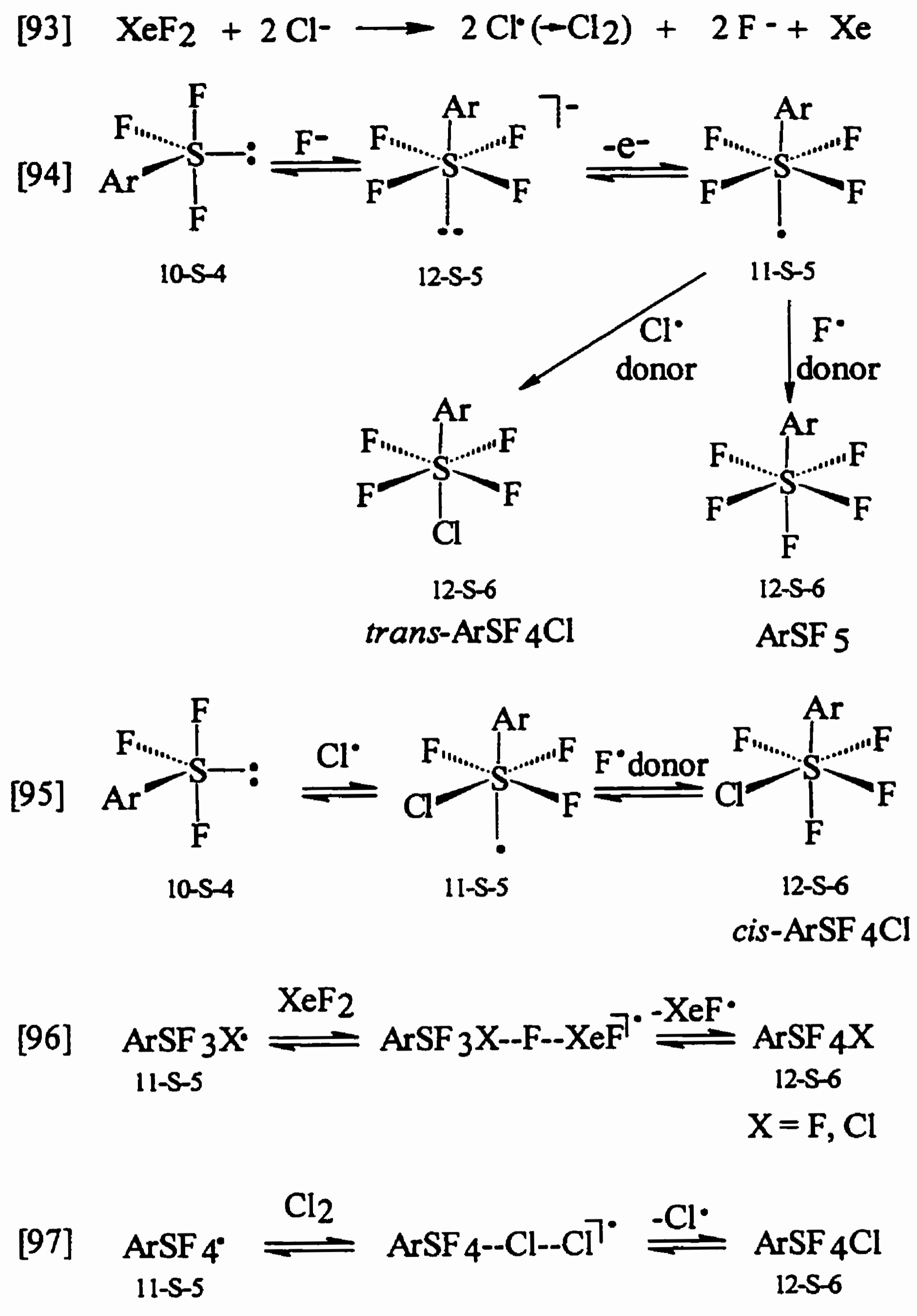
[93] XeF2 + 2 Cl- → 2 Cl•(→Cl2) + 2 F- + Xe
[94]
F-
-e-
10-S-4
12-S-5
11-S-5
Cl• donor
F• donor
12-S-6
trans-ArSF4Cl
12-S-6
ArSF5
[95]
Cl•
F•donor
10-S-4
11-S-5
12-S-6
cis-ArSF4Cl
[96] ArSF3X• XeF2 ArSF3X--F--XeF]• -XeF• ArSF4X
11-S-5
12-S-6
X = F, Cl
[97] ArSF4• Cl2 ArSF4--Cl--Cl]• -Cl• ArSF4Cl
11-S-5
12-S-6

Scheme 13. Proposed mechanism of formation of *cis*- and *trans*-$ArSF_4Cl$ and $ArSF_5$.

The N-X-L notation of Perkins *et al.*,[48] is used again to specify the valence electron count and coordination number of sulfur-containing compounds and intermediates. The mechanism is portrayed as a sequence of steps involving species containing 10-S-4, 12-S-5, 11-S-5, and 12-S-6 sulfur. It may be noted that fluorinated analogues of these sulfur species have been identified experimentally, i.e. SF_4, SF_5^-, $SF_5^{\cdot}$[160] and SF_6, respectively. A cationic species containing 10-S-5 sulfur, e.g. $ArSF_4^+$,[161] is also known, but considered unlikely because the formation of chalcogen(VI) cations generally requires the presence of strong Lewis acids, which were avoided in this work.

Some of the proposals in Scheme 13 have been discussed previously in this thesis, including the reaction of XeF_2 and Cl^- to give $Cl^{\cdot}$ and F^- in eq [93], the *trans* arrangement of aryl substituents and non-bonding electrons in eq [94]-[95], anion-to-radical oxidation in eq [94], and cleavage of oxidizing agents such as XeF_2 and Cl_2 via bridged $[S{-}{-}F{-}{-}Xe]^{\cdot}$ and $[S{-}{-}Cl{-}{-}Cl]^{\cdot}$ intermediates in eq [96]-[97].

It is postulated in eq [94] that addition of F^- to $ArSF_3$, followed by anion-to-radical oxidation, gives the radical $ArSF_4^{\cdot}$. Further addition of $Cl^{\cdot}$ then leads to *trans*-$ArSF_4Cl$. The experimental finding that excess XeF_2 favours the synthesis of *trans*-$ArSF_4Cl$ (Table 11) is consistent with eqs [93] and [94] since excess XeF_2 favours the synthesis of F^- and $Cl^{\cdot}$, eq [93], and the latter species are required for the synthesis of *trans*-$ArSF_4Cl$, eq [94].

It is also postulated in eq [94] that interaction of radical $ArSF_4^{\cdot}$ with a F^- donor leads to $ArSF_5$. A competition thus exists for radical $ArSF_4^{\cdot}$, and the yield of $ArSF_5$

should increase as the concentration of $Cl^{\cdot}$ donor decreases, which is consistent with our experimental results (Table 11, entry 8). However, the overall synthesis of $ArSF_5$ still requires a catalytic amount of Cl^- because of the role of Cl^- in the production of F^-, $ArSF_4^-$ and $ArSF_4^{\cdot}$ according to eq [93]-[94].

Fluoride-catalyzed oxidation of sulfur(IV) compounds in eq [94] thus follows the sequence: 10-S-4 → 12-S-5→ 11-S-5 → 12-S-6. If the same sequence is adopted by the F^--catalyzed oxidation of SF_4, then the following pathway is predicted: $SF_4 \rightarrow SF_5^- \rightarrow SF_5^{\cdot} \rightarrow SF_6$. In the absence of F^- (and SF_5^-), the mechanism of oxidation is presumably simplified to $SF_4 \rightarrow SF_5^{\cdot} \rightarrow SF_6$, and the latter sequence of 10-S-4→11-S-5→12-S-6 is proposed in eq [95] for the stereospecific synthesis of *cis*-$ArSF_4Cl$.

It is postulated in eq [96]-[97] that oxidizing agents such as XeF_2 and Cl_2 interact with radicals $ArSF_4^{\cdot}$ and $ArSF_3Cl^{\cdot}$, with bond cleavage occurring via bridged $[S\text{--}F\text{--}Xe]^{\cdot}$. and $[S\text{--}Cl\text{--}Cl]^{\cdot}$ intermediates. Bridged bonds are expected to be very weak, and the role of F^- in the formation of these weak bonds provides an explanation for the catalytic role of F^- in oxidative addition reactions. In the absence of F^-, the oxidizing agents XeF_2 or Cl_2 would have to function as sources of free radicals, and that would require the cleavage of bonds in the oxidizing agents themselves, perhaps under more drastic conditions of heat, or photochemically. Indeed, free radical reactions with oxidizing agents such as $FO_2SO\text{-}OSO_2F$ or $F_5SO\text{-}OSF_5$ generally require elevated temperatures.[162]

Scheme 13 is necessarily vague in several respects. Oxidation of ArSSAr is not discussed. Instead, we assume that $ArSF_3$ is a common sulfur(IV) intermediate in all reactions. Our experimental results do not allow us to identify the electron acceptor that converts $ArSF_4^-$ to $ArSF_4^{\cdot}$, eq [94]. However, anion-to-radical oxidations are known for related fluorinated species, e.g. $PhSiF_5^{2-}$ to $PhSiF_5^{-}$, and numerous one-electron acceptors can be used for this oxidation, including halogen compounds, tetracyanoethylene, metal ions, etc. .[40,87] It is also not possible to identify with certainty the halogen donors in Scheme 13. While Cl_2, $Cl^{\cdot}$, XeF_2, and $XeF^{\cdot}$ are sources of halogen atoms, it is likely that $ArSF_4^{\cdot}$, $ArSF_3Cl^{\cdot}$, and other intermediates, can also function as halogen donors. An evaluation of the relative importance of various halogen donors is not possible and specific halogen donors are not identified in eq [94]-[95]. We do not attempt to explain why Cl^- and excess XeF_2 favours the slow isomerization of *trans*-$ArSF_4Cl$ to *cis*-$ArSF_4Cl$, although it may be noted that Michalak and Martin reported previously that the stereochemical outcome of oxidative-fluorination depends on the ratio of oxidizing agent, with 2/3 mole of BrF_3 favouring the synthesis of *trans*-$F_2S[OC(CF_3)_2C_6H_4]_2$ whereas more than 2/3 mole of BrF_3 favours the *cis* isomer[115] as shown in Scheme 4.

3.3.4.6 *Ab initio* calculations

The mechanism of Scheme 13 assumes that only F^- forms an anionic intermediate $ArSF_4^-$, but not Cl^-, whereas both fluoro and chloro radical intermediates are postulated, i.e., $ArSF_4^{\cdot}$, and $ArSF_3Cl^{\cdot}$. A difference between the catalytic role of F^- and Cl^- was discussed previously and attributed, on the basis of *ab initio* calculations of optimised geometries, to the reduced stability and lower concentration of chloro anions in solution.

Experimental support for this view is based on ion-molecule reactions which show that SF_4 readily abstracts a fluoride ion to produce SF_5^-, but SF_4Cl^- is formed much more slowly and more drastic reaction conditions are required, and SF_4Br^- is not observed.[163] Calculations based on density functional theory shows a relatively long S-Cl bond in SF_4Cl^-, 223-241 pm, but a shorter S-Cl bond in radical $SF_4Cl^{\cdot}$, 207-219 pm.[164] Calculations also reveal a shorter S-F bond length in radical $SF_5^{\cdot}$, 156.2 pm, than in anion SF_5^-, 163.3 pm.[164]

Ab initio calculations were carried out for species **35-38**. Of these, **35**, **36**, **38** are postulated intermediates in Scheme 13, but not chloro anion **37**. The calculated (3-21G*) structure of chloro anion **37** shows a very long S-Cl bond of 313.8 pm which approaches the sum of van der Waals radii of 330-370 pm,[165] implying that $PhSF_3Cl^-$ is probably unimportant in oxidation reactions because of its short lifetime and low concentration. On the other hand, fluoro anion **35** shows four approximately equal S-F bonds in the range 171-172.5 pm.

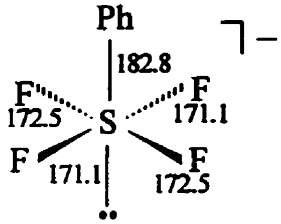
Ph
182.8
F
172.5
S
F
171.1
F
171.1
F
172.5
−

∠CSF=84.5-87.5°

1 (3-21G*)

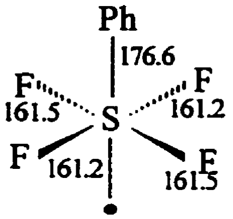
Ph
176.6
F
161.5
S
F
161.2
F
161.2
F
161.5

∠CSF=94.3-94.4°

2 (3-21G*)

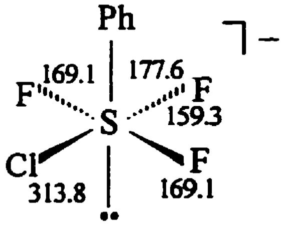
Ph
169.1
177.6
F
S
F
159.3
Cl
313.8
F
169.1
−

∠CSF=88.8, 89.5, 100.5°

∠CSCl=84.9°

3 (3-21G*)

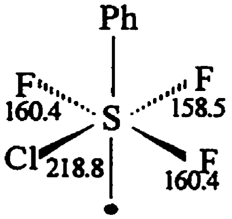
Ph
F
160.4
S
F
158.5
Cl
218.8
F
160.4

∠CSF=91.9, 91.9, 95.7°

∠CSCl=99.7°

4 (STO-3G*)

Figure 71. Calculated structures of anionic and radical sulfur fluorides.

All S-F bonds in fluoro radical **36**, 161.2-161.5 pm, are shorter than those of anion **35**, in fact, the bonds in **36** approach those of SF_4, 154-165 pm,[140] and SF_6, 156.22 pm.[166] The S-Cl bond in radical **38** is significantly shorter and stronger than in anion **37**, and the S-Cl bond length in **38**, 218.8 pm, is only 6.9% longer than in SF_5Cl, 204.7 pm[141]. These calculations thus support the mechanism of Scheme 13 which postulates that fluoro anion $ArSF_4^-$ and fluoro and chloro radicals $PhSF_4^{\cdot}$ and $PhSF_3Cl^{\cdot}$, but not chloro anion $ArSF_4Cl^-$, are intermediates in the oxidation of S(IV) to S(VI) compounds.

It is assumed in scheme 13 that a *trans* arrangement is adopted by aryl substituents and non-bonded electrons. A similar geometry has been assumed for related anions $CF_3SF_4^-$ and $(CF_3)_2CFSF_4^-$.[104, 128d] *Ab initio* calculations (3-21G*) were carried for an isomer of **35** in which phenyl and fluorine substituents were interchanged such that fluorine was trans to a non-bonded electron pair, but the energy of this isomer is calculated to be 29.3 kJ/mol higher than **35**.

3.3.5. Preparation of alkyl and arylchalcogen(IV) trifluorides.

The synthesis of alkyl and arysulfur(IV) trifluorides have been accomplished previously by the reaction of R_fSSR_f with various oxidative-fluorinating agents such as CF_3OF, ClF_3, F_2 and AgF_2. However, these reactions involve handling extremely corrosive compounds and are difficult to control unless low temperature is used. The fluorination with metal fluoride, AgF_2, leaves a reaction residue as a by-product.

Generally, long reaction times are also required and only modest yields were achieved for all those reactions.

In the course of synthesis of organosulfur(VI) fluorides, we have found a very convenient laboratory method for direct fluorination of RSSR with XeF_2 in the presence of catalytic amount of Et_4NCl. In a typical reaction, diphenyl disulfide on a ~0.06 mmol scale was dissolved in CH_2Cl_2 at room temperature, and XeF_2 was then introduced into this solution. If no Et_4NCl was added into the reaction mixture, $PhSF_3$ (~50%) and various other unidentified compounds were found after 24 hours as shown by its ^{13}C NMR spectrum in Figure 72. However, if a catalytic amount of Et_4NCl was added into the reaction mixture of ArSSAr and XeF_2 in CH_2Cl_2, a rapid reaction occurred very smoothly to give an essentially quantitative yield of $PhSF_3$, as illustrated by its ^{13}C NMR spectrum in Figure 73. Using the same procedure, several new organochalcogen (IV) trifluorides such as $PhSF_3$, t-Me_3CSF_3, and $PhSeF_3$ have been synthesised. The ^{19}F NMR spectrum of one of these products p-$MeC_6H_4SF_3$, is displayed in Figure 74. The NMR data have been summarised in Table 16.

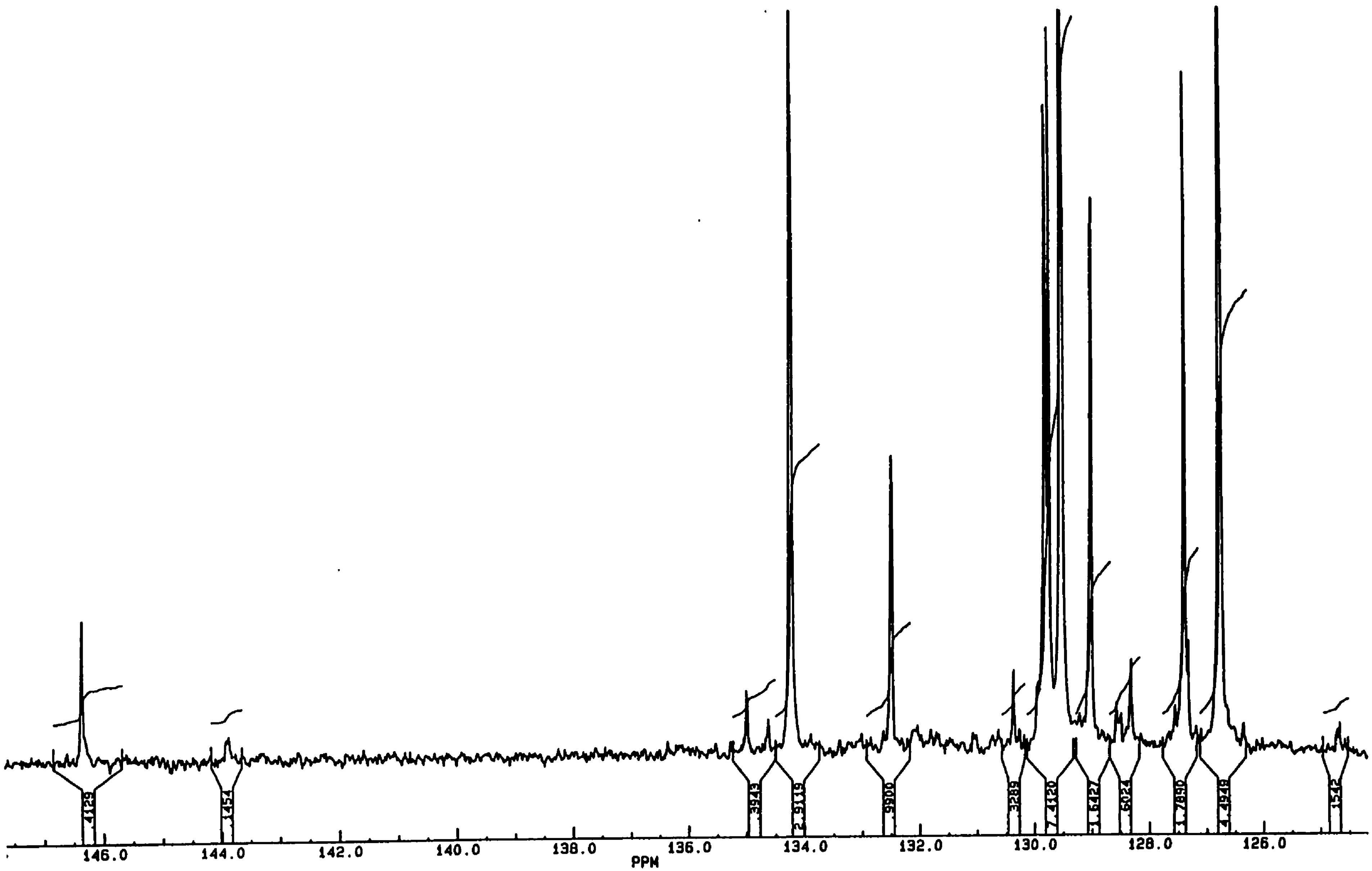

Figure 72. ^{13}C NMR spectrum of reaction product of Ph_2S_2 with XeF_2 in the absence of catalyst, Et_4NCl.

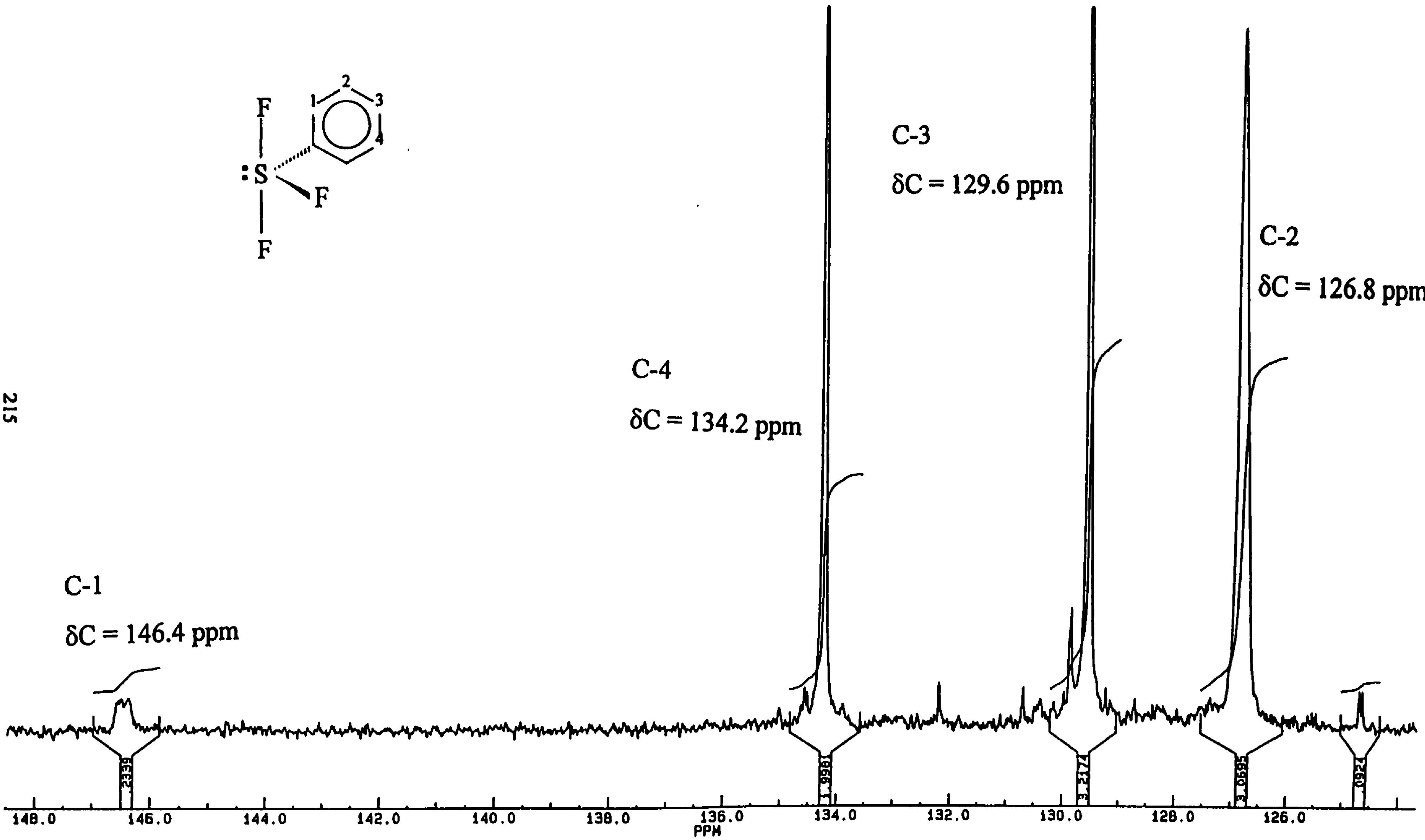

Figure 73. ^{13}C NMR spectrum of reaction product of Ph_2S_2 with XeF_2 in the presence of catalyst, Et_4NCl.

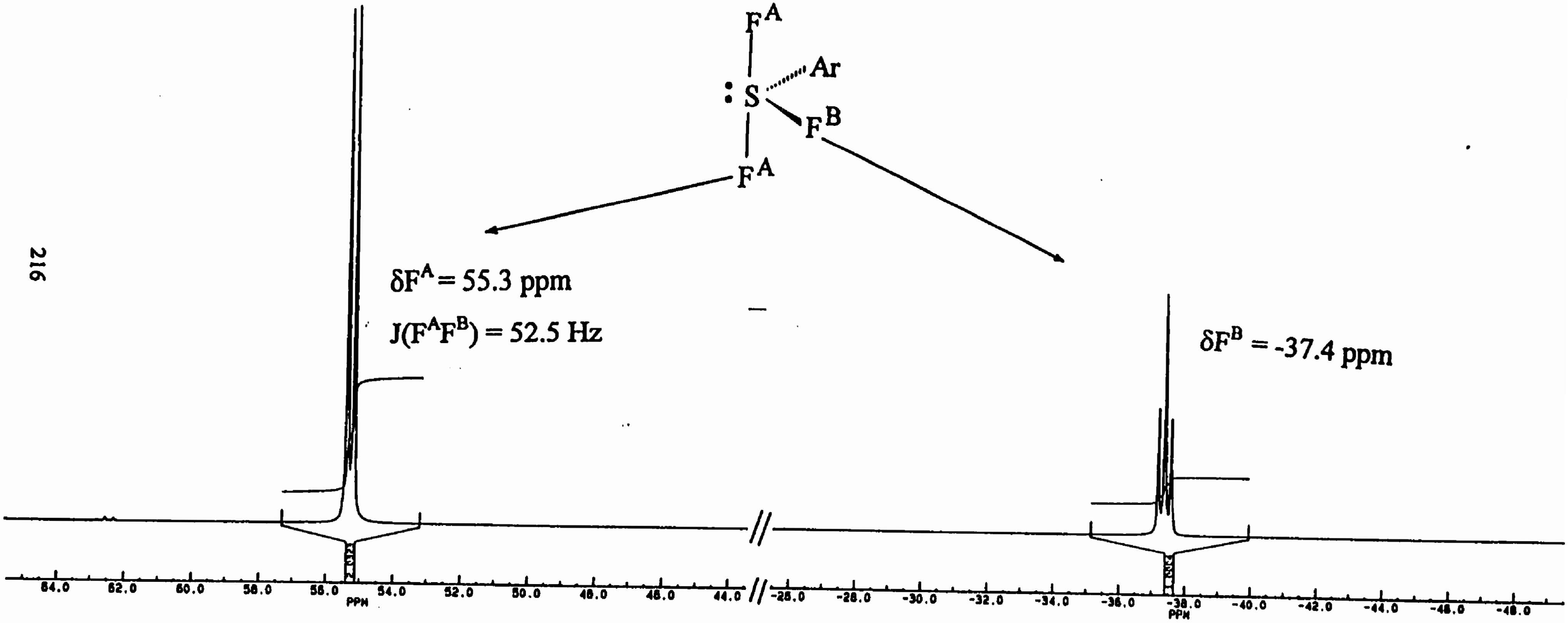

$\delta F^A = 55.3$ ppm

$J(F^AF^B) = 52.5$ Hz

$\delta F^B = -37.4$ ppm

Figure 74. ^{19}F NMR spectrum of p-$MeC_6H_4SF_3$.

TABLE 16. ^{19}F NMR data of some alkyl and arylsulfur(IV) fluorides.

Compound	δFax (ppm)	δFeq (ppm)	$J_{Fax\text{-}Feq}$ (Hz)
$PhSF_3$	-40.2 (t)	57.5 (d)	58.7
$p\text{-}MeC_6H_4SF_3$	-37.4(t)	55.3 (d)	54.3
$t\text{-}Me_3CSF_3$	-63.7(t)	32.5 (d)	52.5

GENERAL CONCLUSIONS

1. The mechanism of reaction of boron trifluoride with amines, dialkyl ethers, and pyridine has been analyzed on the basis of the Coordination Model of Reaction Mechanisms. This model is tested mathematically by carrying out kinetic simulation of pathways P(X,C), accompanied by the calculation of structures of postulated intermediates by GAUSSIAN92 or GAUSSIAN86 methods. The calculated concentration v.s. time curves are in general agreement with experimental results for the BF3-base system and may be applied to synthetic problems.

2. Reaction mechanisms of silicon-fluorine and silicon-carbon bond cleavage in organofluorosilicates, and the rapid equilibrium between five- and six-coordinate phosphorus fluorides, and the exchange of axial and equatorial fluorines in PF_5, are also analyzed on the basis of the Coordination Model of Reaction Mechanisms and with the aid of molecular orbital calculations. These calculations support the view that cleavage of Si-F bonds occurs by way of fluorine-bridged Si--F--Si intermediates (intermolecular). Cleavage of a Si-C bond in $PhSiF_3$ is catalysed by fluoride ion. Cleavage of Si-C occurs by the formation of $PhSiF_4^-$ and $PhSiF_5^{2-}$, followed by oxidation to a radical anion $PhSiF_5^{-\cdot}$. The calculations are also in agreement with the view that axial and equatorial fluorines in PF_5 undergo intramolecular ligand exchange as a result of bond formation, +C, whenever PF_5 interacts with a donor molecule such as NH_3, OH_2, CH_3F and PF_6^-. In the absence of reliable thermodynamic and kinetic data of reactive intermediates, the calculated bond lengths may serve as a simple criterion of bond cleavage, -C, and the

generalisation, "the longer the bond, the faster it breaks" is therefore applied to these reactive intermediates.

3. Oxidative halogenation of sulfur compounds under mild conditions can be achieved by a new route: XeF_2/Et_4NCl. This method has been successfully applied in

a) Oxidative fluorination of Ph_2SO and fluorine exchange in the $Ph_2S(O)F_2$-$Ph_2S(O)F^+$ system: oxidative fluorination of diphenyl sulfoxide with xenon difluoride occurs under mild conditions in the presence of a catalytic amount of chloride ion to give $Ph_2S(O)F_2$ in essentially quantitative yield. Addition of BF_3 to $Ph_2S(O)F_2$ produced the cation $Ph_2S(O)F^+$ in essentially quantitative yield. Addition of cationic $Ph_2S(O)F^+$ to $Ph_2S(O)F_2$ initiates rapid fluorine exchange, and this exchange process has been studied by ^{13}C and variable temperature ^{19}F NMR spectroscopy. In the presence of chloride ion, $Ph_2S(O)Cl_2$ is formed and can be identified by ^{13}C NMR and by its hydrolysis to Ph_2SO_2.

b) Syntheses of *cis*- and *trans*-Ph_2SF_4, $PhEF_5$ (E = S, Se, Te): the synthesis of *cis*-Ph_2SF_4 and *trans*-Ph_2SF_4 can be achieved by adding a mixture of XeF_2 and Et_4NCl at room temperature, and the results are comparable to the synthesis of *cis*- and *trans*-Ph_2TeF_4. The same method can also be used for the syntheses of $PhSeF_5$ and $PhTeF_5$.

c) Stereoselective oxidation and isomerization of *cis*- and *trans*-$ArSF_4Cl$: either *cis*- or *trans*-$ArSF_4Cl$ (Ar = Ph, *p*-MeC_6H_4, *p*-$O_2NC_6H_4$) can be exclusively synthesized by varying the ratio of starting material: Ar_2S_2, XeF_2, and Et_4NCl. Adding a mixture of Et_4NCl and XeF_2 to *trans*-$ArSF_4Cl$ results in isomerization of *trans*-$ArSF_4Cl$ (Ar = Ph, *p*-MeC_6H_4, *p*-$O_2NC_6H_4$) to its corresponding *cis*-isomer. This method has also been extended to the synthesis of *cis*- and *trans*-$PhTeF_4Cl$. Products were characterised by ^{19}F, ^{13}C, and ^{125}Te NMR spectroscopy, and by the $^{37}Cl/^{35}Cl$ and $^{34}S/^{32}S$ isotope effects on ^{19}F NMR chemical shifts.

4. A mechanism of oxidative halgenation of organsulfur (IV) to organosulfur (VI) is proposed, involving anionic and free radical intermediates. Chloride ion appears to react with xenon difluoride to generate fluoride ion. Evidence has been presented to support the following mechanism: the first step of the reaction mechanism is the addition of a fluoride ion to the starting compound to give a anionic organsulfur (IV), then fluoroanion is oxidized to the organosulfur (V) radical intermediate, followed by cleavage of weak $[S\text{--}F\text{--}Xe]^{\cdot}$ bridging bonds. The radical intermediate further reacts with XeF_2 or $XeF^{\cdot}$ or $Cl^{\cdot}$ to give the final product and regenerates the $XeF^{\cdot}$ radical etc.. *Ab initio* molecular orbital calculations (GAUSSIAN92) were carried out for some of the postulated intermediates. Both experiment data, and the literature dealing with these systems are consistent with the mechanism proposed for this process.

REFERENCES

1. (a) Larson, J.W. and McMahon, T.B. J. Am. Chem. Soc. 1985, 107, 766; (b) Hehre, J.W.; Radon, L.; Schleyer, P.v.R.; Pople, J.A. Ab inito molecular orbital theory, Wiley-interscience: N.Y., **1986.**
2. (a) Janzen, A.F.; Jang, M. Can. J. Chem. **1989**, 67, 71; (b) Ref 53.
3. Nguyen, T.Q.; Qu, F.; Huang, X.; Janzen, A.F. Can. J. Chem. **1992**, 70, 2089.
4. Janzen, A.F.; Sowa, M.G. J. Fluorine. Chem. **1991**, 54, 179.
5. Marat, R.K.; Janzen, A.F. Can. J. Chem. **1977**, 55, 3845.
6. Marat, R.K.; Janzen, A.F. Inorg. Chem. **1980**, 19, 798.
7. Wang, C.; Janzen A.F. Can. J. Chem. **1984**, 62, 1563.
8. Nguyen, T.Q. M. Sc. Thesis, The University of Manitoba, **1988.**
9. (a) Secco, A.S.; Alam, K.A.; Blackburn, B.J.; Janzen, A.F. Inorg. Chem. **1986**, 25, 2125; (b) Janzen, A.F.; Alam, K.; Jang, M; Blackburn, B.J.; Secco, A.S. Can. J. Chem. **1988**, 66, 1308.
10. Jang, M.; Janzen, A.F. J. Fluorine Chem. **1994**, 66, 129.
11. Jang, M.; Janzen, A.F. J. Fluorine Chem. **1991**, 52, 45.
12. Kistiakowsky, G.B.; Williams, R. J. Chem. Phys. **1955**, 23, 334.
13. Rutenberg, A.C.; Palko, A.A.; Drury, J.S. J. Am. Chem. Soc. **1963**, 85, 2702.
14. Hartman, J.S.; Miller, J.M. Adv. Inorg. Chem. Radiochem. **1978**, 21, 147.
15. Farquharson, M.J.; Hartman, J.S. Can. J. Chem. **1989**, 67, 1711.
16. (a) Massey, A.G. Adv. Inorg. Chem. Radiochem. **1967**, 10, 1; (b) Gmelin handbook of inorganic chemistry, boron compounds. 2nd Suppl. Vol. 2, Springer-Verlag: Berlin, **1982**, pp 18-29; Vol. 37, **1976**, pp 114-125; Vol. 46, **1977**; pp 75-170.

17. Benton-Jones, B.; Miller, J.M. Inorg. Nuclear Chem. Letters. **1972**, 8, 485.

18. (a) Hartman, J.S.; Schrobilgen, G.J. Inorg. Chem. **1974**,13, 874; (b) Hartman, J.S.; Stilbs, P. J. Chem. Soc, Dalton Trans. **1980**, 1142.

19. Wiberg, N.; Buchler, J.W. Chem Ber. **1963**, 96, 3000.

20. Brown, H.C.; Singaram, B. Inorg. Chem. **1979**, 18, 53.

21. Stanton, R.G. Numerical methods for science and engineering. Prentice-Hall, Englewood Cliffs: N.J., **1961.**

22. MathSoft User's Journal. Vol. 4, Number 2, Spring **1990**, p 4.

23. Perkins, P.G.; Stewart, J. J. Inorg. Chim. Acta. **1970**, 4, 40.

24. Bishop, D.M.; Laidler, K.J. J. Chem. Phys. **1965**, 42, 1688.

25. Brown, H.C.; Stehle, P.F.; Tierney, P.A. J. Amer. Chem. Soc. **1957**, 79, 2020.

26. (a)Hartman, J.S.; Stilbs, P. J. Chem. Soc., Chem. Comm. **1975**, 566; (b) Brownstein, S.; Paasivirta, J. Can. J. Chem. **1965**, 43, 1645.

27. Brownstein, S.; Eastham, A.M.; Latremouille, G.A. J. Phys. Chem. **1963**, 67, 1028

28. Bauer, S.H.; McCoy, R.E.; J. Phys. Chem. **1956**, 60, 1529.

29. Cotton, F.A.; Wilkinson, G. Advanced inorganic chemistry, 5th ed. John Wiley & Sons: N.Y., **1988**; p 46.

30. Westheimer, F.H. Acc. Chem. Res. **1968**, 1, 70.

31. Schomburg, D.; Stelzer, O.; Weferling, N.; Schmutzler, R.; Sheldrick, W.S. Chem Ber. **1980**, 113, 1566; (b) Janzen, A.F.; Lemire, A.E.; Marat, R.K.; Queen, A. Can. J. Chem. **1983**, 61, 2264.

32. Frisch, M.J.; Binkley, J.S.; Schlegel, H.B.; Raghavachari, K.; Melius, C.F.; Martin, R.L.; Stewart, J.J.P.; Bobrowicz, F.W.; Rohlfing, C.M.; Kahn, L.R.; Defrees, D.J.;

Seeger, R.A.; Whiteside, R.A.; Fox, D.J.; Fleuder, E.M.; Pople, J.A. GAUSSIAN86, Camegie-Mellon Quantum Chemistry Publishing Unit, Pittsburgh PA, **1984.**

33. Katalnikov, S.G.; Pisarev, V.E.; Frantskevichute, D.I. Russ. J. Phys. Chem. **1969**, 43, 671.
34. Graham, W.A.G.; Stone, F.G.A.; J. Inorg. Nucl. Chem. **1956**, 3, 164.
35. Pimentel, G.C.; McClelland, A.L. The hydrogen bond. W.H. Freeman and Company: San Francisco and London, **1960**, p.360.
36. Kollman, P.A.; Allen, L.C. J. Am. Chem. Soc. **1971**, 93, 4991.
37. Gay-Lassac, J.L.; Thenard, L.J. Memorives de physique et de chimie de la societed arcueil, **1809**, 2, 317.
38. Davy, J. Phil. Trans. Roy. Soc. London **1812**, 102, 352.
39. Tansjoe, L. Acta Chem. Scand. **1961**, 15, 1583.
40. Muller, R. Z. Chem. **1984**, 24, 41.
41. Kumada, M.; Tamao, K.; Yoshida, J. J. Organomet. Chem. **1982**, 239, 115.
42. Marat, R.K.; Janzen, A.F. J. Chem. Soc. Chem. Commun. **1977**, 671.
43. Tamao, K.; Akita, M.; Kato, H.; Kumada, M. J. Organomet. Chem. **1988**, 341, 165.
44. Yoshida, J.; Tamao, K.; Kumada, M.; Kawamura, T. J. Am. Chem. Soc. **1980**, 102, 3269.
45. Dixon, D.; Farnham W.; Heileman, W.; Mews, R. Heteroatom Chem. **1993**, 4, 287.
46. Huheey, J.E.; Keiter, E.A.; Keiter, R.L. Inorganic chemistry: principles of structure and reactivity, 4th ed; Harper Collins: New York, **1993**; p 30.
47. Ou, X.; Wallace, R.; Janzen, A.F. Can. J. Chem. **1993**, 71, 51.

48. Perkins, C.W.; Martin, J.C.; Arduengo, A.J.; Lau, W.; Alegria, A.; Kochi, J.K. J. Am. Chem. Soc. **1980**, 102, 7753.

49. Tamao, K.; Kayashi, T.; Ito, Y.; Yosiro, M. J. Am. Chem. Soc. **1990**, 112, 2422.

50. Tamao, K.; Kayashi, T.; Ito, Y.; Yosiro, M. J. Am. Chem. Soc. **1992**, 114, 2029.

51. Bubnov, N.N.; Solodovnikov, S.P.; Prokofev, A.I.; Kabachnik, M.I. Russ. Chem. Rev. (Engl. transl.) **1978**, 47, 549.

52. Chuit, C.; Corriu, R.J.P.; Reye. C.; Young, J.C. Chem. Rev. **1993**, 93, 1371 and reference therein.

53. Janzen, A.F. Coord. Chem. Rev. **1994**, 130, 355.

54. Pople, J.A. Faraday Discuss. Chem. Soc. **1982**, 73, 7.

55. McDowell, R.S.; Reisfeld, M. J.; Patterson, C.W.; Krohn, B.J.; Vasquez, M.C.; Laguna, G.A. J. Chem. Phys. **1982**, 77, 4337.

56. Schomburg, D.; Krebs, R. Inorg. Chem. **1984**, 23, 1387.

57. Hamilton, W.C. Acta Cryst. **1962**, 15, 353.

58. Viets, D.; Heilemann, W.; Waterfied, A.; Mews, R.; Besser, S.; Herbst-Irmer, R.; Sheldrich, G.M.; Stohrer, W. D. J. Chem. Soc. Chem. Commun. **1992**, 1017.

59. Kata, H.E. J. Am. Chem. Soc. **1985**, 107, 1420.

60. Licht, K.; Peuker, C.; Dathe, C. Z. Anorg. Allg. Chem. **1971**, 380, 293

61. Ref 46, p 292.

62. Tamao, K.; Yoshida, J.; Kumada, M. J. Am. Chem. Soc. **1980**, 102, 3267.

63. Tamao, K.; Hayashi, T.; Ito, Y; Shiro, M. Organometallics **1992**, 11, 2099.

64. (a) Hodge, H.C.; Smith, F.A. Fluorine chemistry, Ed. Simons, J.H; Academic Press, New York, **1965**, Vol. IV (b) Craig, P.J. Comprensive organometallic chemistry,

Eds. Wilkinson, G.; Stone, F.G.A.; Abel. E.W.; Pergamon Press: New York, **1982**, 2, 979.

65. (a) Ho, P. and Melius, C.F. J. Phys. Chem. **1990**, 94, 5120; (b) Gutsev, G.L. Russian Chem. Bulletin, **1993**, 42, 36 (c) Marsden, C.J.J. Chem. Phys. **1987**, 6626 (d) Dixon, D.A. J. Phys. Chem. **1988**, 92, 86.
66. Ou, X.; Janzen, A.F. Inorg. Chem. **1997**, 83, 27.
67. (a) Ou, X.; Janzen, A.F. Can. J. Chem. **1996**, 74, 2002; (b) Janzen, A.F.; Ou, X. J. Fluorine Chem. **1995**, 71, 207.
68. Holmes, R.R. Chem. Rev. **1990**, 90, 17.
69. Storzer, W.; Schomburg, D.; Röschenthaler, G. V.; Schmutzler, R. Chem. Ber. **1983** 116, 367.
70. Gibson, J.A.; Ibbott; D. G.; Janzen, A. F. Can. J. Chem. **1973**, 51, 3203.
71. Kant, M.; Meisel, M. Z. Anorg. Allg. Chem. **1994**, 620, 1937.
72. Kolditz, L.; Röhnsch, W. Z. Anorg. Allg. Chem. **1957**, 293, 168.
73. Wharf, I.; Onyszchuk, M. Can. J. Chem. **1970**, 48, 2250.
74. Calves, J.-Y.; Gillespie, R.J.; J. Am. Chem. Soc. **1977**, 99 1788.
75. Musher, J.I. Tetrahedron Lett. **1973**, 1093.
76. Brownstein, S.; Bornais, J. Can. J. Chem. **1968**, 46, 225.
77. Kölmel, C.; Palm, G.; Ahlrichs, R.; Bär M.; Boldyrev, A.I. Chem. Phys. Lett. **1990**, 173, 151.
78. a) Dean, P.A.W.; Gillespie, RJ.; Hulme, R; Humphreys, D.A. J. Chem. Soc. A, **1971**, 341; (b) Davies, C.G.; Gillespie, R. J.; Ireland, P.R.; Sowa, J.M. Can. J. Chem. **1974** 52, 2048.

79. a) Clifford, A.F.; Kongpricha, S. J. Inorg. Nucl. Chem. **1961**, 20, 147; (b) Gut, R.; Gantschi, K. J. Inorg. Nucl. Chem. Supplement, **1976**, 95.

80. Kawashima, Y.; Cox, A.P. J. Mol. Spectros. **1977**, 65 , 319.

81. Christe, K.O.; Dixon, D.A.; Mercier, H.P.A.; Sanders, J.C.P.; Schrobilgen, G.J.; Wilson, W.W. J. Am. Chem. Soc. **1994**, 116, 2850.

82. Cramer, C.J.; Lim, M. H. J. Phys. Chem. **1994**, 98, 5024.

83. Hansen, K.W.; Bartell, L.S. Inorg. Chem. **1965**, 4, 1775.

84. Rhyne, T.C.; Dillard, J.G. Inorg. Chem. **1971**, 10, 730.

85. Goldberg, I.B.; Crowe, H.R.; Pilipovich, D. Chem. Phys. Lett. **1975**, 33, 347.

86. Wilson, J. N. J. Am. Chem. Soc. **1958**, 80, 1338.

87. Tamao, K.; Yoshida, J.; Yamamoto, H.; Kakui, T.; Matsumoto, H.; Takahashi, M.; Kurita, A.; Murata, M.; Kumada, M. Organometallics, **1982**, 1, 355.

88. Dillon, K.B.; Platt, A.W.G.; Schmidpeter, A.; Zwaschka, F.; Sheldrick, W.S. Z. Anorg. Allg. Chem. **1982**, 488, 7.

89. a) Gutsev, G.L. Chem. Phys. **1994**, 179, 325; (b) Kokoszka, G.F.; Brinckman, F.E. J. Am. Chem. Soc. **1970**, 92, 1199.

90. Frisch, M.J.; Trucks, G.W.; Head-Gordon, M.; Gill, P.M.W.; Wong, M.W.; Foresman, J.B.; Johnson, B.G.; Schlegel, H.B.; Robb, M.A.; Replogle, E.S.; Gomperts, R.; Andres, J.L.; Raghavachari, K.; Binkley, J.S.; Gonzalez, C.; Martin, R. L.; Fox, D.J.; Defrees, D.J.; Baker, J.; Stewart, J. J. P.; Pople, J.A. GAUSSIAN 92 Revision C. Gaussian, Inc., Pittsburgh PA, **1992**.

91. Huzinaga, S.; Andzelm, J.; Klobukowski, M.; Radzio-Andzelm, E.; Sakai, Y.; Tatewaki, H. Gaussian basis sets for molecular calculations, Elsevier, Amsterdam, **1984**.

92. Schmidt, M. W.; Boatz, J. A.; Baldridge, K. K.; Koseki, S.; Gordon, M. S.; Elbert, S. T.; Lam, B. GAMESS, QCPE Bulletin **1987**, 7, 115.

93. Boys, S.F.; Bernardi, F. Mol. Phys. **1970**, 19, 553.

94. Shreeve, J.M.; Cady, G.H. J. Am. Chem. Soc. **1961**, 83, 4521.

95. Duncan, L.C.; Cady, G.H. Inorg. Chem. **1964**, 3, 850.

96. Hohorst, F.A.; DesMarteau, D.D.; Anderson, L.R.; Could, D.E.; Fox, W.B. J. Am. Chem. Soc. **1973**, 95, 3866.

97. O'Brien, B.A.; DesMarteau, D.D.; Inorg. Chem. **1984**, 23, 644.

98. Clifford, F.; El-Shamy, H.K.; Emeleus, H.J.; Haszeldine, R.N. J. Chem. Soc. **1953**, 2372.

99. Martin, L.D.; Perozzi, E.F.; Martin, J.C. J. Am Chem. Soc. **1979**, 101, 3595.

100. Silvey, G.; Cady, G.H. J. Am. Chem. Soc. **1950**, 72, 3624.

101. Tullock, C.W.; Coffman, D.D.; Muetteries, E.L. J. Am. Chem. Soc. **1964**, 86, 357.

102. Sheppard, W.A. J. Am, Chem. Soc. **1962**, 84, 3058, *ibid,* 3064.

103. Darragh, J.I.; Sharp, W.A. J. Chem. Soc., Chem. Commun. **1969**, 864.

104. Minkwitz, R.; Werner, A. J. Fluorine Chem. **1987**, 37, 397.

105. Darragh, J.L.; Haran, G.; Sharp, D.W.A.; J Chem. Soc. Dalton Trans **1973**, 2289.

106. Pass, G.; Roberts, H.L. Inorg. Chem. **1963**, 2, 1016.

107. Leonard, C.D.; Cady, G.H. Inorg. Chem. **1964**, 3, 1045.

108. Denny, D.B.; Denny, D.Z.; Hus, Y.F. J. Am. Chem. Soc. **1973**, 95, 8191.

109. Abe, T.; Shreeve, J.M. J. Fluorine Chem. **1973/74**, 3, 187.

110. Abe, T.; Shreeve, J.M. Nucl. Chem. Lett. **1973**, 9, 465.

111. Glemser, O.; Hofer, R. Angew. Chem., Int. Ed. Eng, **1973**, 12, 1000.

112. Sauer, D.T.; Shreeve, J.M. Z. Anorg. Allg. Chem. **1971**, 385, 113.

113. Ruppert, I. J. Fluorine Chem. **1979**, 13, 81.

114. Ruppert, I. Angew. Chem., Int. Ed. Engl. **1979**, 18, 880.

115. Michalak, R.S.; Martin, J.C. J. Am. Chem. Soc. **1982**, 104, 1683.

116. Alam, K.; Shreeve, J.M. J. Molecular Structure **1988**, 178, 207.

117. Huang, H.; Lagow, R.J. Chem. Mater. **1990**, 2, 477.

118. (a) Drago, R.S.; Physical methods for chemists, 2nd Ed., Saunders, **1992**, Chapt. 8. (b) L.M. Jackman and F.A. Cotton (Ed), Dynamic Nuclear magnetic Resonance Spectroscopy, Academic Press: New York, **1975**.

119. Zupan, M.; Zajc, B. J. Chem. Soc., Pekin Trans. I. **1978**, 965.

120. Wilson, I.L. J. Fluorine Chem. **1975**, 5, 13.

121. Drabowicz, J.; Mikolajczyl, M. Synthesis, **1980**, 32.

122. Maxwell, W.M.; Wynne, K.J. Inorg. Chem. **1981**, 20, 1707.

123. Morton, J.R.; Preston, K.F. Chem Phys. Lett. **1973**, 18, 98.

124. Christe, K.O; Wilson, W.W. J. Fluorine Chem. **1990**, 47, 117.

125. Dukat, W.W.; Holloway, J.H.; Hope, E.G.; Townson, P.J. J. Fluorine Chem. **1993**, 62, 293.

126. Shaw, M.J.; Holloway, J.H.; Hyman, H.H. Inorg. Nucl. Chem. Letters, **1970**, 6, 321.

127. Moody, G.J.; Tomas, J.D.R. Rev. Pure Appl. Chem. **1966**, 16, 1.

128. (a) Seel, F.; Riehl, L. Z. Anorg. Allg. Chem. **1955**, 282, 293; (b) Ref 101 (c) Christe, K.O.; Curtis, E.C.; Schack, C.J.; Pilipovich, D. Inorg. Chem. **1972**, 11, 1679; (d) Heilemann, W.; Mews, R. Pohl, S.; Saak, W. Chem. Ber. **1989**, 122, 427.

129. (a) De Marco, R.A.; Shreeve, J.M. Adv. Inorg. Chem. Radiochem. **1974**, 16 109; (b) Morton, J.R.; Preston, K.F. J. Chem. Phys. **1973**, 58, 2657.

130. (a) Filler, R. Israel J. Chem. **1978**, 17, 71; (b) Patrick, T.B.; Khazaeli, S.; Nadji, S.; Hering-Smith, K.; Rief, D. J. Org. Chem. **1993**, 58, 705.

131. (a) Malm, J.G.; Selig, H.; Jortner, J.; Rice, S.A. Chem. Rev. **1965**, 65, 199; (b) Zerza, G.; Sliwinski, G.; Schwenter, N.; Hoffman, G.J.; Imre, D.G.; Apkarian, V.A. J. Chem. Phys. **1993**, 99, 8414.

132. Cartwright B.; Woolf, A.A. J. Fluorine Chem. **1981**, 19, 101.

133. Dudley, F.B.; Cady, G.H. J. Am. Chem. Soc. **1963**, 85, 3375.

134. March, J. Advanced organic chemistry, 4th Ed.; John Wiley & Sons: New York, **1992**; p 711.

135. Derflinger, G.; Polamsky, O.E. Theor. Chim. Acta (Berl.) **1963**, 1, 316.

136. (a) Ref 101; (b) Ruff, J.K.; Lustig, M. Inorg. Chem. **1964**, 3, 1422; (c) Ref 106; (d) Schack, C.J.; Wilson, R.D.; Muirhead, J.S.; Cohz, S.N. J. Am. Chem. Soc. **1969**, 91, 2907; (e) Smith, J.E.; Cady, G.H. Inorg. Chem. **1970**, 9, 1442; (f) Seppelt, K. Z. Anorg. Allg. Chem. **1977**, 428, 35.

137. (a) Lau, C; Lynton, H.; Passmore, J.; Siew, P. J. Chem. Soc. Dalton Trans. **1973**, 2535; (b) Dunphy, R.F.; Lau, C.; Passmore, J. J. Chem. Soc. Dalton Trans. **1973**, 2533; (c) Wessel, J.; Kleemann, G.; Seppelt. K. Chem. Ber. **1983**, 116, 2399; (d) Meier, T.; Mews, R. Angew. Chem., Int. Ed. **1985**, 24, 344.

138. A standard test tube made of borosolicate glass (Pyrex No. 9800) was drawn into a capillary, and a small segment of dimensions 4mm x 1mm was removed and dried overnight at 110 °C.

139. Hedberg, L.; Hedberg, K. J. Phys. Chem. **1982**, 86, 598.

140. Cotton, F.A.; Wilkinson, G. Advance inorganic chemistry, 5th ed., John Wiley & Sons, N.Y.: **1988**; p 509.

141. Marsden, C.J.; Bartell, L.S. Inorg. Chem. **1976**, 15, 3504.

142. Marat, R.K.; Janzen, A.F. J. Can. Chem. **1977**, 55, 3031.

143. Alam, K.; Janzen, A.F. J. Fluorine Chem. **1985**, 27, 467.

144. Schack, C.J.; Wilson, R.D.; Hon, J.F. Inorg. Chem. **1972**, 11, 208.

145. Fraser, G.W.; Peacock, R.D.; Watkins, P.M. J. Chem. Soc., Chem. Commun. **1968**, 1257.

146. Klein, G.; Naumann, D. J. Fluorine Chem. **1985**, 30, 259.

147. Lau, C.; Passmore, J. J. Fluorine Chem. **1976**, 7, 261.

148. Petragnani, N.; Comasseto, J.V.; Kawano, Y. Inorg. Nucl. Chem. **1976**, 38, 608.

149. Petragnani, N.; Castellanos, J. J. Organomet. Chem. **1973**, 55, 295.

150. Mellor, J.W. A Comprehensive treatise on inorganic and theoretical chemistry; Longmans Green and Co.: London. **1948**.

151. Michalak, R.S.; Wilson, S.R.; Martin, J.C. J. Am. Chem. Soc. **1984**, 106, 7529.

152. Lentz, D.; Pritzkow, H.; Seppelt, K. Inorg. Chem. **1978**, 17, 1926.

153. Marsden, H.M.; Shreeve, J.M. Inorg. Chem. **1986**, 25, 4021.

154. O'Brien B.A.; DesMarteau, D.D. Inorg. Chem. **1984**, 23, 2188.

155. Janzen, A.F.; Alam, K.; Blackburn, B.J. J. Fluorine Chem. **1989**, 42, 173

156. Gelmboldt, V.O.; Dyachkov, P.N. Zh. Neorg. Khim. **1989**, 34, 840.

157. Ahmed, L.; Morrison, J.A. J. Am. Chem. Soc. **1990**, 112, 7411.

158. Dean, P.A.W.; Evans, D.F. J. Chem. Soc.(A) **1968**, 1154.

159. Marlow, M.G.; Dean, R.R.; Lee, J. Trans Faraday Soc. **1965**, 65, 321.

160. (a) Morton, J.R.; Preston, K.F. Chem. Phys Lett. **1973**, 18, 98; (b) Gawlowski, J.; Herman, A. Can. J. Chem. **1974**, 52, 3631; (c) Ref 132a; (d) Ref 132b; (e) Gara, W.B.; Roberts, B.P.; Kirk, C.M.; Gilbert, B.C.; Norman, R.O.C. J. Magn. Res. **1977**, 27, 509.

161. Neier, T.; Mews, R. Angew. Chem. Int. Ed. **1985**, 24, 344.

162. (a) Merrill, C.I.; Cady, G.H. J. Am. Chem. Soc. **1963**, 85, 909; (b) Ref 136.

163. Babcock, L.M.; Streit, G.E. J. Chem. Phys. **1981**, 75, 3864.

164. Ziegler, T.; Gutsev, G.L. J. Chem. Phys. **1992**, 96, 7623.

165. Huheey, J.E.; Keiter, E.A.; Keiter, R.L.; Inorganic chemistry, principle of structure and reactivity. 4th ed. HarperCollins, N.Y.: **1993**; p 292.

166. Miller, B.R.; Fink, M. J. Chem. Phys. **1981**, 75, 5326.

167. Marsden, C.J.. Inorg. Chem. **1976**, 15, 3004.

168. Nyman, F.; Roberts, H.L. J. Chem. Soc. **1962**, 3180.

169. (a) Jones, P.G.; Kirby, A.J. J. Chem. Soc. Chem Commun. **1979**, 288. (b) Kirby, A.J. Adv. Phys. Org. Chem. **1994**, 29, 87.

170. Gillespie, R.J.; Hargitta, I. The VSEPR model of molecular geometry; Allyn-Bacon: Boston, **1991.**

171. (a) Lentz, D.; Pritzkow, H.; Seppelt, K. Inorg. Chem. **1978**, 17, 1926; (b) Zupan, M. J. Fluorine Chem. **1976**, **8**, 305.

VITA

NAME	Xiaobo Ou
DATE OF BIRTH	September, 1965
EDUCATION	B. Sc. (Chemistry), 1987 Wuhan University Wuhan, P.R.C.
	M. Sc. (Chemistry), 1990 Wuhan University Wuhan, P.R.C.
	Ph. D. (Chemistry), 1991-1998 Department of Chemistry University of Manitoba
AWARDS	University of Manitoba Graduate Fellowship
PUBLICATIONS	X. Ou, G. Bernard and A.F. Janzen "Oxidative addition and isomerization reactions. The synthesis of *cis* and *trans*-ArSF$_4$Cl, and *cis* and *trans*-ArTeF$_4$Cl", Can. J. Chem. 75, **1997**, 1878.

A.F. Janzen, X. Ou and M.G. Sowa "Reaction mechanisms of phosphorus fluorides: An ab initio study", J. Fluorine Chem. 83, **1997**, 27.

X. Ou and A.F. Janzen "Silicon-fluorine and silicon-carbon bond cleavage in organofluorosilicates: A molecular orbital study", Inorg. Chem. 36, **1997**, 392

A.F. Janzen and X. Ou "Oxidative fluorination in the Ph_2SO-XeF_2-Cl^- system", Can. J. Chem. 74, **1996**, 2002.

X. Ou and A.F. Janzen "Oxidative fluorination of sulfur(IV) compounds by XeF_2", J. Fluorine Chem., 71, **1995**, 207.

X.Ou, R. Wallace and A.F. Janzen "The boron trifluoride-base system: application of the Coordination Model of Reaction Mechanisms". Can. J. Chem., 71, **1993**, 51.

CONFERENCE PAPERS

A.F. Janzen and X. Ou "Stereoselective synthesis of sulfur(VI) and tellurium(VI) fluorides", (invited paper). 52nd ACS Northwest Regional Meeting, Moscow, Idaho, U.S.A., June 18-21, **1997**

A.F. Janzen and X. Ou "Mechanism of silicon-fluorine bond cleavage and the interaction of fluorides with the H_2O-HF-glass system", (invited paper). 29th ACS Central Regional Meeting,Midland, Michgan, U.S.A., May 27-30, **1997**.

J.S. Hartman, A.F. Janzen and X. Ou "Difluoroboron cations: Towards systematic synthesis of ionization isomers of boron trifluoride adducts". 79th CSC Conference, St. John's, Newfoundland, Canada, June 23-26, **1996**.

A.F. Janzen and X. Ou "Mechanism of silicon-fluorine and silicon-carbon bond cleavage in organofluorosilicates: A molecular orbital study". 12th Winter Fluorine Conference, St. Petersburg, Florida, U.S.A., Jan. 22-27, **1995**.

X. Ou and A.F. Janzen "Silicon-fluorine and silicon-carbon bond cleavage in organofluorosilicates: An ab initio study". 77th CSC Conference, Winnipeg, Canada, May 30-June 2, **1994**.

A.F. Janzen and X. Ou "Oxidative fluorination of sulfur(IV) compounds by XeF_2", 207th ACS National Meeting, San Diego, CA, U.S.A., March 13-18, **1994**.

A.F. Janzen and X. Ou "Stereoselective synthesis of organosulfur (VI) compound with xenon difluoride", 76th CSC Conference, Sherbrooke, Quebec, Canada, May 30- June 3, **1993**.

A.F. Janzen and X. Ou "Stereoselective synthesis of *cis* and *trans*-Ph_2SF_4", 11th Winter Fluorine Conference, St. Petersburg, Florida, U.S.A., Jan. 25-30, **1993**.

A.F. Janzen and X. Ou "Reactions of phosphorus fluorides with water, ammonia and hydrogen sulfide: *ab initio* calculations and kinetic simulations", 75th CSC Conference, Edmonton, Alberta, Canada, June 1-4, **1992**.

A.F. Janzen and X. Ou "Analysis and predication of reaction mechanisms in fluorine chemistry", 203rd ACS National Meeting, San Francisco, U.S.A., April 5-10, **1992**.

IMAGE EVALUATION TEST TARGET (QA-3)

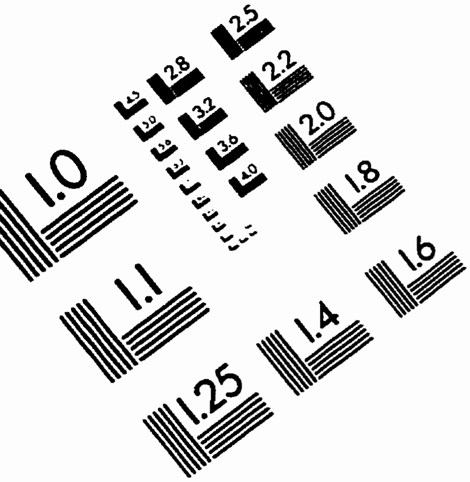
1.0
1.1
1.25
1.4
1.6
1.8
2.0
2.2
2.5
2.8
3.2
3.6
4.0

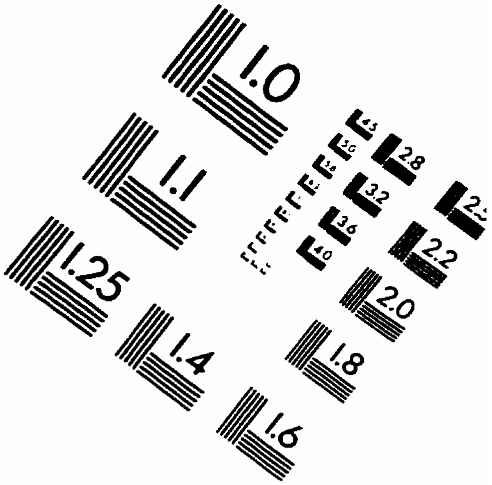
1.0
1.1
1.25
1.4
1.6
1.8
2.0
2.2
2.8
3.2
3.6
4.0

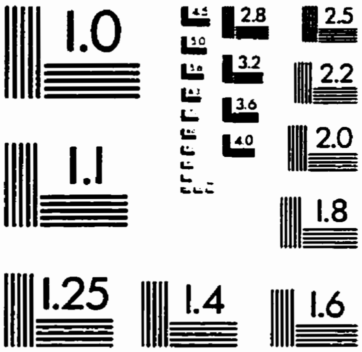
1.0
2.8
2.5
3.2
2.2
3.6
4.0
2.0
1.1
1.8
1.25
1.4
1.6

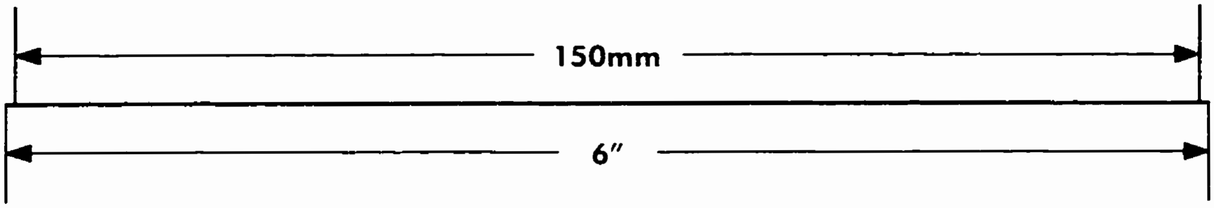

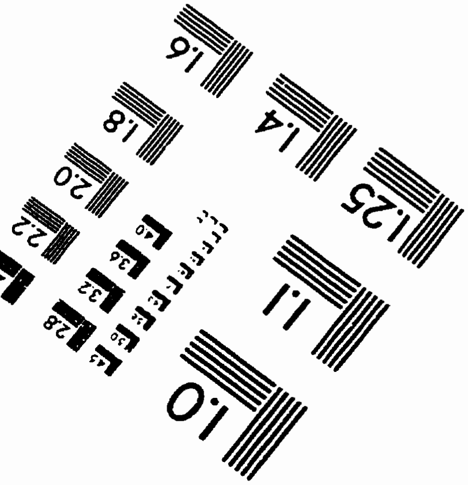
1.6
1.8
1.4
2.0
1.25
2.2
4.0
3.6
1.1
3.2
2.8
1.0

APPLIED IMAGE . Inc
1653 East Main Street
Rochester, NY 14609 USA
Phone: 716/482-0300
Fax: 716/288-5989

© 1993, Applied Image, Inc., All Rights Reserved

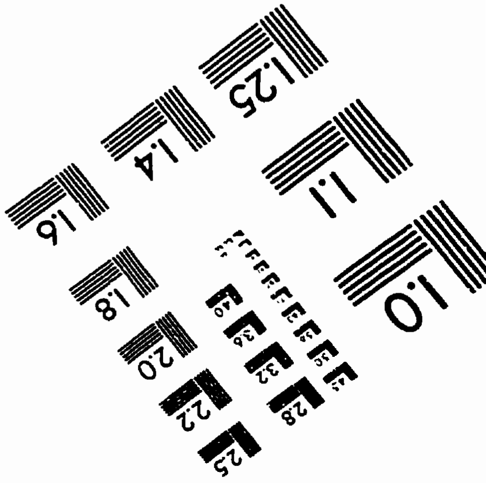
1.25
1.4
1.1
1.6
1.8
1.0
4.0
3.6
2.0
3.2
2.2
2.8
2.5